PREDICTING HUMAN INTESTINAL ABSORPTION USING CHROMATOGRAPHY AND SPECTROSCOPY

Dina Shokry

A thesis submitted in partial fulfilment of the requirements for the degree of Doctor of Philosophy

Under supervision of

Dr Laura J Waters **Dr Gareth M Parkes**

School of Applied Sciences

The University of Huddersfield

2017

Dedication

This thesis is dedicated to my dear loving parents, you were, still are and always will be my backbone in life. Without your love, support and belief in me none of this would have been possible.

Acknowledgement

I would like to praise God for his countless blessings and giving me the strength and power to complete my work and achieve my goals. Also I would like to show my deep and sincere appreciation to my main supervisor **Dr Laura Waters** for her endless support, understanding and concern on both the professional and personal level. Without her scientific and technical guidance, her patience and continuous encouragement, none of this would have been possible. I would also like to express my profound gratitude to my second supervisor **Dr Gareth Parkes** for his help, valuable advice, guidance and support.

I would also like to thank **Professor John C. Mitchell** for his valuable guidance throughout the publishing of one of the thesis papers.

Also I would like to thank the **University of Huddersfield Graduate Centre** for providing me with the needed conference presentation funds during the time of my PhD.

I must also extend my thanks to the **technical staff** of Huddersfield University, School of applied sciences for their great help throughout the duration of my PhD and to my **friends and colleagues** who made my PhD time an enjoyable time.

I would like to thank **my parents** for their unconditional love and genuine concern and always believing in me and making me feel I am not alone. Thank you for always pushing me forward, supporting and helping me, no words can thank you enough, I am really blessed to have you as my parents.

Finally, I would like to thank **my sisters** who have always been there for me whenever I needed their support, encouragement and wise advice. Also I thank my **nephew and niece**, the two little angels, who always put a smile on my face.

Abstract

New drug entities (NDE) are constantly being developed with most of them intended for oral administration. For this reason, there is a need to estimate their absorption in order to save time and money that would be lost if the drug enters the clinical stage and is then found to exhibit poor absorption. For many years, the use of animals was the most abundant method for studying pharmacokinetics to predict parameters such as intestinal absorption. However, these methods are time consuming, and expensive as well as being ethically unfavourable. As a result, developing other methods to evaluate a drug's pharmacokinetics is crucial. The aim of this work was to develop *in vitro* methods for estimation of human intestinal absorption (%HIA) to replace the use of the aforementioned, less favourable methods involving the use of animals. Among the developed methods in this thesis is a unique type of chromatography known as micellar liquid chromatography (MLC) using biosurfactants such as bile salts as a mobile phase. Furthermore, studies investigated the effect of a change in the stationary phase in addition to investigating the effect of the change in temperature on the elution of the analysed compounds. It was found that R^2_{PRED} for the developed MLC methods was in the range of 43.3 % - 91.12 %. Another developed method was a spectrophotometric method based on the use of the solubilising effects of bile salts, as well as their binding to compounds. Therefore, two spectrophotometric methods were developed, a solubilisation method and a double reciprocal method, and used in the prediction of %HIA. It was found that the solubilisation method had a better predictability for %HIA than that of the double reciprocal method where R^2_{PRED} was found to be 82.32 % and 61.90 % respectively. Finally, a permeation method was developed using the ability of NaDC to form a hydrogel under specific conditions and applying the investigated drugs in an infinite dose to the prepared hydrogels. This facilitated the determination of permeability coefficients (K_p) that were then used in the prediction of %HIA using the obtained model. The two developed permeation methods were found to have close values of R^2_{PRED} for % HIA where R^2_{PRED} of the permeation method using flow through cells was found to be 79.8 % while that of the permeation method using Franz cells was found to be 79.67 %. In summary, this work reports several unique models for the *in vitro* prediction of human intestinal absorption, potentially removing the need for animal testing to predict %HIA.

List of Abbreviations

Abbreviation	Full term
IAMs	Immobilised Artificial Membranes.
ILC	Immobilised Liposome Chromatography.
CMC	Critical Micellar Concentration.
HPLC	High performance liquid chromatography
TLC	Thin layer chromatography
GC	Gas chromatography
MLC	Micellar Liquid Chromatography
IP	Ion Pairing.
BMC	Biopartitioning Micellar Chromatography
QSAR	Quantity structure activity relationship
NaDC	Sodium deoxycholate
NaTDC	Sodium taurodeoxycholate
NaC	Sodium cholate
NaTC	Sodium taurocholate
SIFsp	Simulated Intestinal Fluid sine pancreatine
CM	Micellar concentration
%HIA	% Human Intestinal Absorption
CE	Capillary electrophoresis
MEKC	Micellar electrokinetic chromatography
MEEKC	Microemulsion electrokinetic chromatography
CCC	Counter current chromatography
PSA	Polar Surface Area
nHA	Number of hydrogen bond acceptors
nHD	Number of hydrogen bond Donors
FRB	Free Rotatable bonds
MLR	Multiple linear regression
MLP	Molecular lipophilicity potentials
$K_{o/w}$	octanol-water partition coefficient
SEM	Scanning Electron Microscopy
FT-IR	Fourier Transform Infrared

List of Contents

List of Figures

List of Tables

CHAPTER 1

Introduction & Literature Review

Chapter 1: Introduction and Literature Review

1. Introduction

1.1. Drug development and Intestinal permeability:

Most emerging drug compounds are formulated as orally administered medicines due to the convenience of this route. However, the properties of some compounds can be incompatible with oral administration. In fact, the pharmaceutical industry suffers from major financial losses because of the poor bioavailability of some new drugs after their oral administration, only discovered once in the clinical development stage [1-4].

Therefore, poor drug candidates with poor biopharmaceutical properties, such as poor oral bioavailability, and aqueous solubility should be identified as soon as possible before entering the clinical development stage in which the cost of research performed for a compound is significantly high.

In the past few years, drug discovery programs have been developed that help in the generation of a large number of lead compounds, however these compounds (compared with conventional drugs) tend to have high lipophilicity, low aqueous solubility, and high molecular weight. These are all unfavourable characteristics that decrease the success rates of such compounds in clinical development [5]. As a result, there has been a growing interest in the early prediction of biopharmaceutical properties by means of experimental and theoretical models.

The two main properties that influence drug absorption from the intestinal lumen are drug solubility and permeation [6-8]. Low intestinal permeability of a drug has less possibility for improvement when compared with poor solubility, since drug solubility can be altered by choosing a suitable formulation. This is the main reason why synthesis of compounds with structures of reasonably high permeability during the early stages of drug development is considered as a very important and vital step.

First, it is crucial to describe the mechanisms by which drug molecules cross the intestinal barrier to reach systemic circulation, and subsequently site of action.

1.2. Mechanisms of permeation of compounds across intestinal membrane:

Solutes encounter a number of barriers during their passage from intestine to systemic circulation. There are two main routes for the transport of molecules across the intestinal membrane: 1) the transcellular route in which the intestinal membrane is

penetrated by the drug molecule by the aid of channels and transporters, hence it is a carrier mediated route, 2) the paracellular route, in which the drug molecules cross the intestinal epithelium through aqueous pores in between the cells by means of a diffusion process that is not carrier mediated [9].

As described in the fluid mosaic model, the construction of the cell membrane of a double phospholipid bilayer with various lipids and embedded proteins is what gives it its unique characteristics [10, 11] (Figure (1)). An example of these unique characteristics is the difference in the permeability properties between the apical and basolateral sides of the intestinal membrane due to the difference in the lipid and protein compositions between the two sides. Also the cell membrane structure has a sieving effect on the diffusion of molecules.

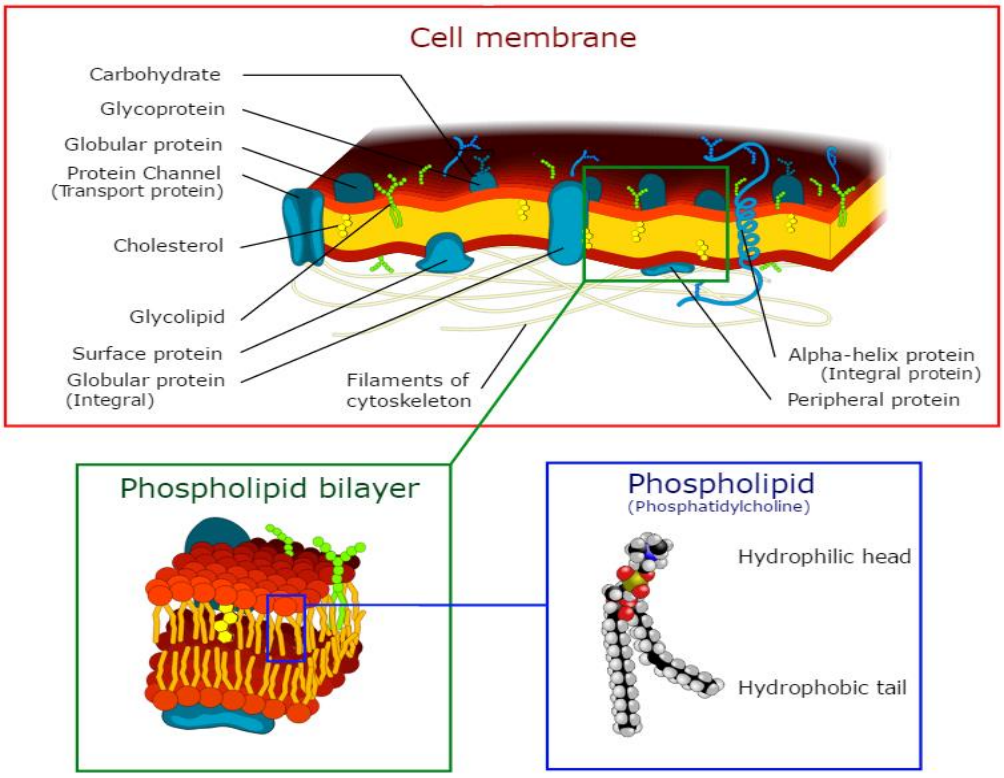

Figure 1: Intestinal cell membrane structure (reference [12]).

1.2.1. Passive transcellular diffusion:

This mode of transport mainly requires molecules of reasonable lipophilicity and size as it occurs by the apical membrane penetration by the drug molecules followed by their diffusion into the cell cytoplasm, which is the rate limiting step of passive transcellular permeability [13].

Most of the drug molecules which are well absorbed across the intestinal membrane take this mode of transport [14-16].

1.2.2. Paracellular passive transport:

This is the mode of transport favoured by hydrophilic molecules which are incapable of penetrating the intestinal epithelial cell membrane. It takes place by means of aqueous pores in between the cells which form a small portion of the total surface area of the intestine [17-20].

1.2.3. Carrier-mediated transport:

1.2.3. a. Active and facilitated transport:

Nutrients and other essential compounds are extracted by the embedded proteins in the cell membrane through different carrier-mediated mechanisms. This mode of transport is only limited to a small number of drugs which structurally resemble the original substrates of cell membrane protein transporters[21].

Specificity, saturability, and regional variability are considered to be the three main properties of carrier–mediated transport of such drugs [21].

1.2.3. b. Receptor-mediated transcytosis:

Receptor-mediated transcytosis is a subtype of transcellular transport where the drug molecule binds to a receptor found on the surface of the cell then crosses to the other membrane surface within an endocytic vesicle formed by endocytosis. This mode of transport is not abundant and is limited to highly potent macromolecular drugs [22].

1.2.3. c. Efflux mechanism:

Carrier-mediated mechanisms help to enhance transcellular transport of drugs into the cell interior whereas efflux mechanisms carried out by efflux proteins (e.g. P-gp) help pump drugs in the opposite direction therefore decreasing the overall permeability of these drugs [23-25]. The efflux systems main role is to avoid toxic compound uptake or help in the excretion of such compounds across the intestinal mucosa [26].

An overall summary of transport across the intestinal membrane is shown in Figure (2).

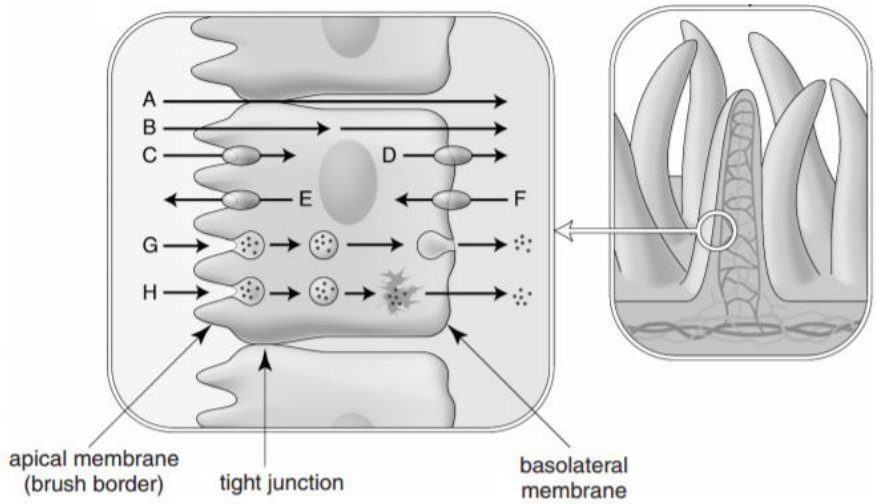

Figure 2: Mechanisms of transport across the intestinal membrane (reference [27]). Pathways of the intestinal barrier. A: paracellular passive diffusion, B: transcellular passive diffusion, CF: influx/efflux facilitated transport facilitated by membrane proteins, G: transcytosis, and H: endocytosis.

Over the years, the prediction of the biopharmaceutical properties of new drug entities (NDE) has received growing attention where a large number of experimental (*in vitro* and *in situ*) and theoretical (statistical) models have been developed. These developed models contribute in saving money and time by helping screen for the best drug candidates and exclude poor candidates during drug discovery and development [28]. As drug intestinal permeability is one of the major biopharmaceutical properties it is worth investigating and predicting using these models. A brief description of some of the methods used in determination and measuring of intestinal permeability is given below:

1.3. Methods for determination of intestinal permeability:

1.3.1. Cell culture based models: e.g. (Caco-2 cells)

For almost forty years Caco-2 cells have been used as an *in vitro* model for investigation of drug absorption. Caco-2 cells originating from the isolation of human colon tumour cells (adenocarcinoma) possess some of the main and important structure and function related characteristics of the small intestine. Therefore, this model is considered to be one of the most commonly used among cell culture based models in the study of the transport of already available and newly synthesised drugs. This is especially used in the drug discovery process for example, reducing the use of

animals for identification of pharmaceutical compounds with optimised properties [29]. A schematic representation of Caco-2 is shown in Figure (3).

Caco-2 cells present some advantages such as:[30]

- Human origin, i.e. a closer *in vivo* mimic
- Less use of animals in studies.
- No bioanalysis.
- Good screening model.
- Evaluation of absorption enhancing strategies, toxicity of compounds and transport mechanisms.
- Availability of techniques to improve biorelevance of model.

Limitations include:[30]

- Very expensive.
- Time consuming with a long differentiation period.
- Laboratory intensive.
- Inter and intra-laboratory variability of permeability data.
- Low uptake transporters expression.

Caco-2 cells have also been used in other applications involving [31]:

1- Evaluation of the bioactivity of plant extracts: The bioavailability of these extracts is usually unclear, as they are often composed of a complicated mixture of molecules. Furthermore, they are metabolised to some extent before reaching their destination inside the body. It is possible to use these extracts in the formation of new functional foods, therefore Caco-2 has proven to be a suitable method for investigation of bioactivity by co-culturing of Caco-2 with the desired cells**.**

2- Study of cell matrix interactions and wound healing in intestinal cells: A co-culture system of Caco-2 cells and myofibroblasts was found to be efficient for studying the process of intestinal epithelium wound healing and its regulation. This is because Caco-2 cells have the capability of producing and releasing extracellular components responsible for controlling the ability (power) and rate of intestinal epithelium cells wound healing and repair.

3- Genotoxicity of food contaminants: Human Caco-2 cells have been described by Erlejman *et al.* as a popular method for studying food contaminants crossing the intestinal barrier to get to systemic circulation.

Figure 3: Schematic representation of Caco-2 on a microporous filter (reference [32]).

1.3.2. Membrane based models:

For over almost four decades, synthetic membranes have been used in studying diffusion processes. Parallel artificial membrane permeation assay (PAMPA) is one of the most common membrane based models used since it was introduced by Kansy *et al.* in 1998 [33]. PAMPA is a method where the donor and the acceptor compartments are placed on top of each other in a microtiter plate with a lipid infused membrane hence called a 'sandwich' assembly. This lipid membrane system is made of a phospholipid 'cocktail' supported on a filter in an organic solvent (Figure 4) [34].

PAMPA presents some advantages such as: [30]

- Relatively low cost.
- Good predictability.
- Availability of various lipid compositions.
- High throughput.

Limitations include: [30]

- The obtained value depends on pH and lipid composition.
- Membrane retention of lipophilic drugs.
- Prediction is limited only to a part of the overall absorption process.

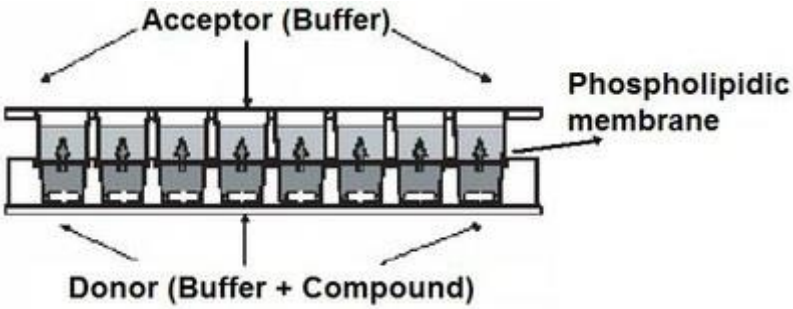

Figure 4: Schematic representation of PAMPA model (reference [35]).

1.3.3. Ex Vivo models:

In 1951, “Ussing chambers” were first developed by Ussing and Zerahn [36]. These were initially used for studies related to ion and water transport. However, modifications were further introduced by Grass and Sweetana to include determination of drug absorption across the intestine [37].

In the Ussing set up, a tissue of an animal, usually rat, is fixed in between the two parts of a diffusion cell (Figure 5) [38]. This model differs from ordinary diffusion cells in that both compartments of the Ussing diffusion cell are supplied with bicarbonate buffer in which an oxygen/carbon dioxide mixture is bubbled through continuously to keep the excised segment viable [39].

Furthermore, when electrodes are fitted to the Ussing chambers, they become a useful model for investigating how some compounds affect the electrical characteristics of intestinal membrane physiology, as well as, to check the viability of the excised tissue [40].

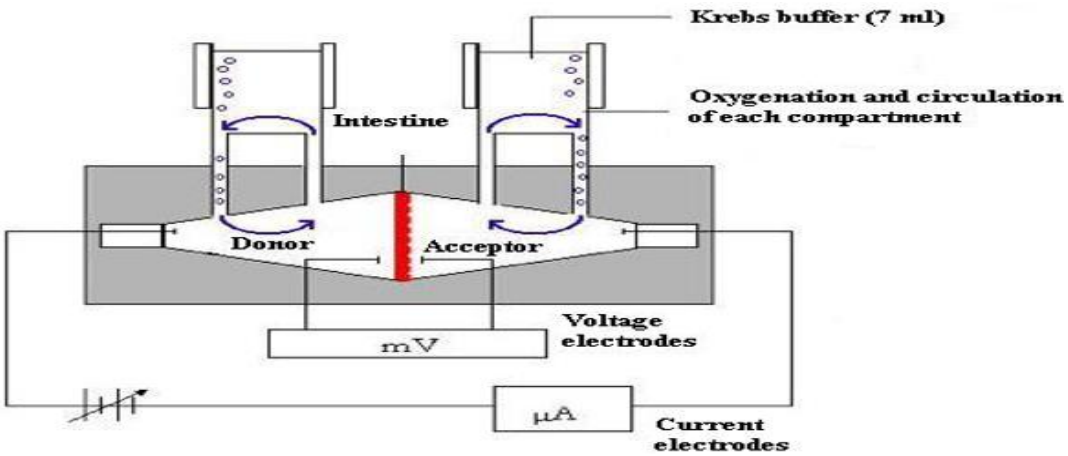

Figure 5: Schematic diagram of an Ussing chamber (reference [41]).

Applications of Ussing chambers:

This technique is useful for various purposes including the study of transepithelial drug transport and intestinal metabolism simultaneously [42-44].

Furthermore, it appears to be particularly useful in the assessment of the effect of surface active agents or additives on tissue integrity and on the transport of compounds [45-47]. Another important application for this technique is investigation of the effect of different diseases which cause changes in the intestinal membrane function with subsequent changes in permeability e.g. inflammatory bowel disease (IBD) and Crohn’s disease [48].

Among its advantages, are [30]:

- Permeability data obtained from this method correlates well with that obtained from *in vivo* experiments [49].
- Good oxygenation.
- No bioanalysis.

Limitations, include [30, 50]:

- Underestimation of drug transport due to membrane retention.
- Viability and integrity of tissues used which is time dependant.
- Surfactants can only be used at low concentrations especially in set ups fitted with gas lifts due to foaming in chambers.
- Difficulty in obtaining suitable tissues.

1.3.4. *In Situ* intestinal perfusion models

In this approach, the small intestine of an anaesthetised rat is either chronically removed (open loop) or initially removed then may be returned to the intestine during perfusion (closed loop) by laparotomy which is an approach including a large incision in the abdominal wall giving access into the abdominal cavity (Figure 6) [32].

The blood supply in this approach remains intact allowing multiple sampling therefore, studying the kinetics of the drug introduced into the intestinal segment.

Among its advantages, are [32]:

- The rat *in situ* model shows good correlation with *in vivo* human data [51].
- Avoids exposure of the investigated drug to the stomach acidic conditions that lead to the precipitation or the breakdown of some drugs.
- First pass effect by the liver can be studied if sampling from the hepatic vein is carried out.

Limitations include:

- Use of anaesthesia might affect the drug intestinal absorption [52].
- Use of animal in this approach [53].

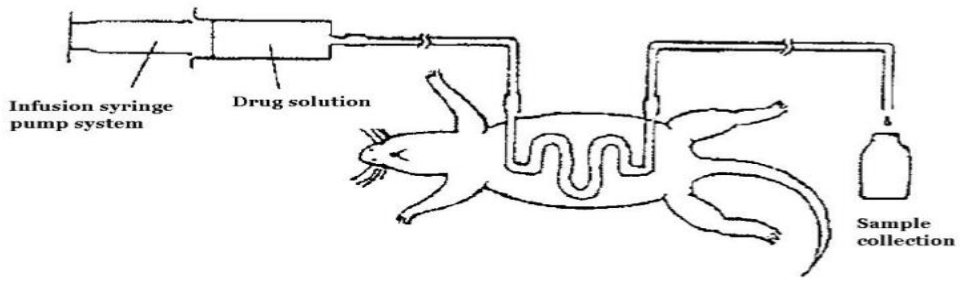

Figure 6: Schematic representation of *in situ* intestinal perfusion (reference [54]).

1.3.5. Everted intestinal ring/sac

Intestinal segments used in this approach are tied from both sides (everted or not) forming sacs and can therefore be used for measuring drug transport out or into the sacs (Figure 7). These sacs are placed in oxygenated buffer [41].

Among its advantages are [41, 53]:

- Fast and inexpensive.
- Measures permeability in all intestinal cell types and the mucus layer
- Useful method for classifying compounds with high or low permeability according to the Biopharmaceutical Classification System (BCS).

Some of its limitations are [54, 55]:

- Enzymatic activity is lost within the experiment conditions.
- The viability of the intestinal tissue is lost within the experiment conditions which leads to limited sampling points.
- Absence of nervous response upon exposure to drug.

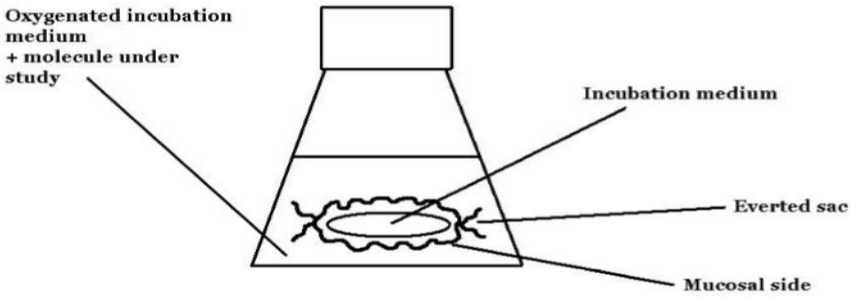

Figure 7: Schematic representation of the everted gut technique (reference [54]).

1.3.6. *In silico* models for prediction of intestinal permeability through *in vitro-in vivo* correlation

An alternative method for prediction of intestinal absorption of drugs intended for oral administration is through the use of physiologically based *in silico* models.

In literature, a large number of publications describe many mathematical models generated for prediction of the intestinal absorption that involve the use of coefficients of permeability obtained either from *in vitro* models such as Caco-2 [56-61] and PAMPA [62-65] or from *in situ* models [66-68] in combination with some physicochemical parameters such as log P, number of hydrogen bonds or aqueous solubility.

Among all of the previously mentioned physicochemical parameters, log P is considered to be one of the most important and widely investigated parameters in the field of prediction of drug pharmacokinetics such as prediction of intestinal absorption of pharmaceutical compounds.

Among the advantages of this method are [69]:

- Money and time saving as it decreases the number of molecules synthesised and tested.
- Contribution to the decrease in animal use.
- Reliable prediction of the pharmacokinetic and pharmacodynamic properties of pharmaceutical compounds.

Some of its limitations are [69]:

- Training in modelling and informatics is required.
- Lack of the presence of a computer programme that can completely model a biological systems complexity.

1.4. Importance of lipophilicity in medicinal chemistry and drug discovery:

Pre-formulation is considered as the first learning phase where the main physicochemical properties of a drug are determined prior to its development into a dosage form. Determination of such properties is essential for selection of the drug candidate itself and selection of the optimum delivery system to ensure its delivery to the site of action [70, 71].

Since drug lipophilicity is considered as a key descriptor that controls permeation across biological membranes [72], the evaluation or determination of the lipophilicity of a drug is important for its characterisation to ensure its potential to penetrate lipid barriers and subsequently be absorbed [73, 74].

Among the most important pre-formulation studies, is determination of drug lipophilicity which reflects the ability of a compound to dissolve in lipids or nonpolar solvents, and it is generally expressed as a partition coefficient (log P). A partition coefficient is defined as, the ratio of the unionised drug distributed between organic and aqueous phases at equilibrium [70]. It is very useful in the prediction of various biological properties of chemicals.

In the case of ionisable compounds partitioning is known to be a function of pH, this relationship is called the distribution coefficient (log D) and is pH dependant [75]. Log D is defined as the ratio of the concentration of a compound in the lipid phase to the

concentration of all species in the aqueous phase at a given pH (organic phase is assumed to contain only unionised species). Therefore, log P is the partitioning of the unionised form of a compound (in the case of neutral compounds) while log D is the net partition of ionised and unionised forms of a compound.

log D can be estimated from log P and pK_a [75]:

$$\text{Log D acids} = \text{Log P} + \text{Log}\ \frac{1}{1+10^{(pH-pKa)}} \qquad \text{Eq. (1)}$$

$$\text{Log D bases} = \text{Log P} + \text{Log}\ \frac{1}{1+10^{(pKa-pH)}} \qquad \text{Eq. (2)}$$

When the compound is largely unionised, log P is assumed to be approximately equal to log D, then:

$$\text{Log D} \cong \text{Log P}$$

A correlation is known between the oil-water partition coefficient of simple organic compounds and their biological activity [76]. For biological purposes, long chain esters or alcohols are often selected as the organic phase for partition coefficient determination.

An octanol-water system is traditionally used in most biological correlation work as n-octanol was found to be an appropriate oil phase for biological applications.

The octanol-water partition coefficient was also found to be used for the correlation of structural changes of drugs with biological, biochemical, and toxic effects [77]. Log P values have been determined for a diverse set of compounds creating a large dataset of octanol-water partition coefficient (K_{ow}) values. It has been widely used as a hydrophobicity parameter in pharmacological and toxicological modelling.

Methods for determination of partition coefficient are summarised in Figure 8.

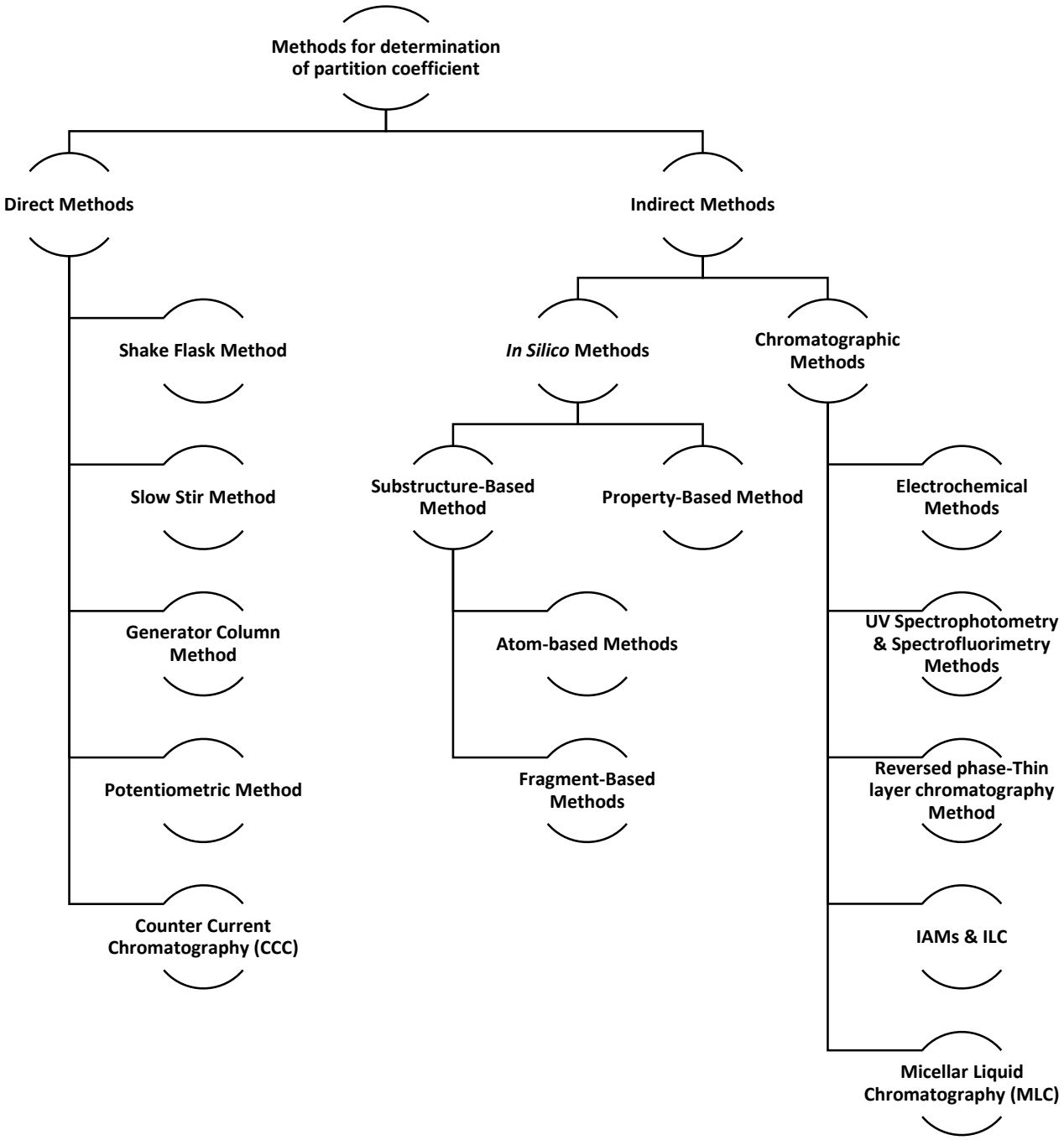

Figure 8: A schematic diagram illustrating methods for determination of a partition coefficient. (**IAMs**: Immobilised artificial membranes, **ILC**:Immobilised liposome chromatography).

1.5. Methods for determination of a partition coefficient:

Being the oldest parameter in physicochemical profiling, log P has been determined by a vast number of well-established experimental methods. These methods have been classified into two groups (direct and indirect).

1.5.1. Direct methods:

1.5.1. a. Shake Flask Method:

It is generally regarded as the most reliable method for log P determination. The idea of this method is mainly based on an extraction procedure, where a solute is allowed to partition between a two liquid system (octanol-water) followed by determination of the concentration of that solute in each layer after equilibrium using either UV/Vis spectroscopy, fluorimetry, high performance liquid chromatography (HPLC), thin layer chromatography (TLC), gas chromatography (GC) or other detection techniques such as radiometry in the case of radioactive solutes [78, 79].

Among its advantages, are:

- Application to a wide range of solutes.
- Accurate and precise.

Limitations include:

- Tedious and time consuming method.
- Large amount of solute is required.
- Pure solutes must be used as interference from impurities of the solute used will also partition into the liquid phases which may lead to inaccurate and erratic results [78].
- This method is not suitable for compounds of poor solubility in any of the solvent phases used as concentration will be difficult to quantify by any of the detection techniques used.

1.5.1. b. Slow Stir Method:

The “slow stir” method is similar to the “shake flask” method, it only differs in the procedure of the method where slow stirring under rigid temperature control is applied instead of vigorous shaking thus avoiding microemulsion formation [80, 81].

Advantages:

- Avoids microemulsion formation.
- Reliable for relatively all compounds.
- Does not require expensive equipment.
- Relatively fast.

Limitations:

- Strict experimental conditions should be applied with slow stirring and close temperature monitoring to avoid formation of a microemulsion.

1.5.1. c. Generator column method:

To overcome the previous limitations of the “shake flask” method, a “generator column” method was developed. In this method, the generator column is packed with a solid support coated with an organic stationary phase, when water is pumped through the column an aqueous solution is generated which is in equilibrium with the stationary phase. The concentration of the solute eluted with the aqueous phase is measured by HPLC or solvent extraction followed by GC [82-85].

Advantages:

- Avoids microemulsion formation.
- Colloidal dispersion formation can be avoided by a slow flow rate.
- Rapid equilibration by the large interfacial area.
- No loss of volatile solutes as well as no errors from adsorption as it is a continuous and closed flow system.
- Easy and requires no special skill of the operator.

Limitation:

- The requirement of sophisticated and expensive equipment.

1.5.1. d. Potentiometric method:

In dual phase potentiometric titrations, the tested compound is titrated twice, firstly in the absence of the partitioning solvent to measure its aqueous pK_a then secondly, in the presence of a partitioning solvent (octanol) with stirring until the pH is measured. The partitioning of the unionised form of the compound in to octanol will cause a shift in titration curves. Log P is calculated from a difference in pK_a values [86, 87].

Advantages:

- Accurate and precise
- Used for ionisable compounds.

Limitation:

- Limited capacity as compounds with a pK_a out of the measurable pH range cannot be used in this method.

1.5.1. e. Counter current chromatography method (CCC):

In this method, both the mobile phase and the stationary phase are liquid where the stationary phase has no solid support. These two phases are immiscible with each other and the only physicochemical interaction that controls the retention of solutes is liquid-liquid partitioning. Also, the centrifugal field keeps both immiscible phases together. This method is considered as a direct method for determination of log P as it directly relates the distribution volume to the partition coefficient of the solute as both phases present are only liquid and there is no chemical reaction, ionisation or complexation taking place in the mobile phase or stationary phase to be considered so the distribution ratio D= K_D [88]

Advantage:

- CCC provides the D ratio of compounds directly and in any biphasic liquid system.

Limitation:

- The restriction over the range of the measurable D ratios where large D values need prohibitive times and mobile phase volumes to be determined.

1.5.2. Indirect methods:

1.5.2. a. *In silico* methods:

Since the octanol-water partition coefficient was introduced by Hansch *et al.* [89, 90], it has been vastly used in quantitative structure activity relationship (QSAR) studies as a hydrophobicity descriptor. Lately, log P has proved to be a key descriptor for modelling and evaluation of absorption, distribution, metabolism, and excretion-toxicity (ADMET) properties through a large number of developed approaches which help detect unsatisfactory pharmacokinetic properties and the toxicity of drugs at the early stages of drug discovery therefore reducing the cost of these drugs failing at later stages [91].

Since the 1970's several computational methods have been developed for calculation or prediction of log P. These methods are classified in to two main classes:

1.5.2. a. 1. Substructure-based Method:

The substructure-based method is divided into two types: atom-based & fragment based. [92]

- **Atom-based Methods**

  The overall molecular log P is computed by this method through the additive contribution of individual atoms in the molecule.

- **Fragment-based Method**

  This method determines log P through the contribution of the sum of non-overlapping fragments and functional groups attached to the molecule.

  This latter method is better than the former because it includes corrections that account for electronic and steric effects.

Both types of contributions are fitted on experimentally determined log P values leading to the generation of a molecular lipophilicity map.

The main advantage of atom-based methods is the avoidance of ambiguities [93] therefore it provides good estimation results compared to the fragment-based methods which are considered to be very accurate methods [94].

Limitations:

For atomic-based log P calculation methods [92]:

- Ambiguity in the classification system.
- Large number of atom types.
- Unrealistic values of some atom contributions.
- Perceived failure at prediction and bias towards underestimation of log P.

For fragment-based log P calculation methods:

- The inability to predict log P for molecules with unusual functional groups as a result of lack of experimental data for molecules containing such functional groups [95, 96].

1.5.2. a. 2. Property-based (Whole molecule) method:

Log P calculation is based on physicochemical properties of the molecule under investigation such as volumes, partial charges, molecular surfaces or different topological and electrostatic indices. These can be used as parameters for log P quantification or molecular lipophilicity potentials (MLP) [97].

Advantages:

- Substructure based methods are normally validated on a large group of data so they give more reliable and accurate results than the whole molecule approach so that is why they are more popular and more widely used [98, 99].

Limitations:

- Many of these methods are validated based on small groups of organic compounds so the feasibility of their application to a larger chemical space is not known. Despite the correlation of many physicochemical properties to log P, there is still no clear explanation for the combination of certain physicochemical properties used to compute log P [97].

1.5.2. b. Chromatographic methods

With chromatographic methods , log P determination is through a simple correlation of the obtained chromatographic data (retention or mobility time) characteristic of solutes with similar compounds of known log P [100].

A calibration graph of standard reference compounds with known log P values is plotted against their retention or migration times. Therefore, knowing the retention or migration time of the solute of interest, its log P can be easily calculated.

Among these methods are reversed phase high performance liquid chromatography (RP-HPLC) [100], reversed phase thin layer chromatography (RP-TLC) [100], immobilised artificial membrane (IAM), micellar liquid chromatography (MLC), counter current chromatography (CCC), electrochemical chromatography (capillary electrophoresis (CE), micellar electrokinetic chromatography (MEKC) and microemulsion electrokinetic chromatography (MEEKC)).

Advantages:

- Fast and ease of automation.
- Simultaneous determination of log P for more than one solute in a mixture.
- Applicable for a wide range of analytes of different lipophilicity.
- High precision, accuracy and reproducibility.

1.5.2. b. 1. Electrochemical methods:

CE has been widely used in the determination of partition coefficients where MEKC [101-103] and MEEKC [104-107] are commonly used types of CE for this purpose. These are rapid screening electrochemical methods that study and examine the transfer of charged species from one phase to another according to the type of the medium selected; one of the three previously mentioned methods is used. The introduction of micelles into CE for separation of neutral compounds according to their micelle affinity is a method called micellar electrokinetic chromatography (MEKC)

which allows the calculation of the partition coefficient for the solute of interest by relating the solute partitioning within the micelle to its log P. The use of a microemulsion instead of micelles as a mobile phase is known as MEEKC where the solutes of different lipophilicity are allowed to partition into the small oil droplets in the microemulsion and the aqueous phase with different mobility allowing both the separation and the calculation of the log P of more than one solute at the same time.

Advantages:

- These methods overcome the direct methods limitations.
- Less time consuming, swift analysis and high automation.

Limitations:

- Its limitations are related to the method development as the need for internal standard incorporation to overcome poor injection precision [108].

1.5.2. b. 2. UV spectrophotometry and spectrofluorimetry:

A partition coefficient can also be determined by means of spectroscopic methods such as spectrophotometry and spectrofluorimetry and then the obtained log P can be used as a tool for prediction of different biological activities [109, 110].

1.5.2. b. 3. RP-TLC method:

TLC is a rapid and easy tool for estimation of log P [111-114]. This method is similar to RP-LC where the Retention factor (K) and lipophilicity parameter (R_m) of a certain compound analysed are linearly plotted against log P.

Advantages:

- Samples used are of very small amounts and are not required to be pure.
- Cheap and simple.

Limitation:

- Restriction of its application to mainly small data sets of compounds of similar properties.

1.5.2. b. 4. Immobilised artificial membranes (IAMs) and Immobilised Liposome Chromatography (ILC):

These previously mentioned methods are considered fast and reliable methods to predict biological properties such as drug distribution, absorption and transport across biological membranes including intestinal membranes [115-117], blood brain barriers [118, 119], and skin [120, 121] through chromatographic retention measurement [122]. IAMs were first introduced as HPLC packaging materials by Pidgeon and Venkataram

[123]. The IAMs structure is composed of synthetic phospholipid analogues linked covalently to silica propylamine particles, while in immobilised liposome chromatography (ILC), liposomes are stably immobilised in the pores of gel beads. Both methods are useful in the early profiling of drug candidates in the drug discovery process [124, 125].

The structure of these chromatographic surfaces are prepared in such a way to mimic the fluid phospholipid bilayers chemically and physically supporting drug-membrane partitioning based on lipophilicity and electrostatic interactions, thus the retention factors obtained on IAMs or liposomal columns are used for determination of the solute partition coefficient where the solute capacity factors K'_m are measured in liposome systems [124, 126].

In addition to their ability to predict drug membrane interactions, distribution, absorption, and transport across various biological membranes, IAMs appear to have other applications as purification of membrane proteins[127-130], immobilising enzymes [131, 132], obtaining enzyme ligand binding constants for drugs and obtaining hydrophobic parameters [133].

Advantages of ILC [134]:

- Electrostatic interactions are involved when partitioning into liposomes which is important especially when considering lipophilicity for ionisable compounds.
- Good correlation between lipophilicity determined by ILC and Caco-2 drug permeability and absorption of orally administered drugs in humans.

Limitations of ILC:

- Limited stability of liposomes [135].
- Preparation of identical columns is difficult.
- Unavoidable column to column variation because of the methods used to entrap liposomes [136].
- Laborious and very time consuming.

Therefore, IAMs appear to be a simple, rapid and reproducible method for measuring partition coefficients and better for the prediction of drug transport than ILC and other conventional expensive, time consuming and laborious methods such as Caco-2 permeability tests.

1.5.2. b. 5. Micellar Liquid Chromatography (MLC):

The use of micelles in HPLC was first introduced by Armstrong and Henry in 1980 [137], this technique is called micellar liquid chromatography (MLC) and was used to enhance retention and selectivity of various solutes that would be inseparable or poorly resolved.

Micellar liquid chromatography is a reversed phase liquid chromatographic (RP-LC) mode which uses mobile phases containing a surfactant (ionic or non-ionic) above its critical micellar concentration (CMC). The stationary phase is modified with approximately constant amounts of surfactant monomers so the presence of micelles alters the solubilising capability of the mobile phase leading to diverse interactions (hydrophobic, ionic and steric) [138] with major implications in retention and selectivity. The basic and very important parts of MLC are the surfactants, the stationary phase and the micellar mobile phase.

Surfactants used in MLC:

Surfactants possess both hydrophobic and hydrophilic moieties where the hydrophobic moiety is represented by the tail of the molecule and the hydrophilic moiety is represented by the polar head group (as shown in Figure (9)). Surfactants are classified in to different classes: anionic, cationic, zwitterionic or nonionic.

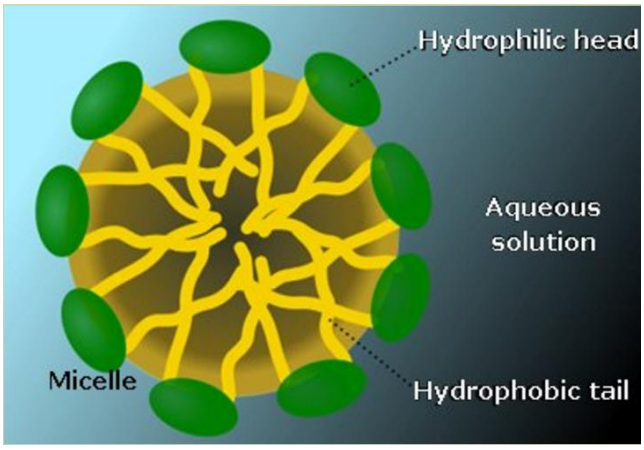

Figure 9: Structure of a Micelle (reference [139]).

Because of the dual nature of surfactants, they have the ability for self-organisation in solution. When the surfactant concentration reaches the critical micellar concentration (CMC) or more, aggregates of monomers which are called micelles are formed. Selection of the most appropriate surfactant to be used in MLC depends upon different properties, such as CMC, Krafft point, cloud point and aggregation number (AN).

CMC: Surfactants with a low CMC are the most appropriate type of surfactants to be used in MLC as those with a high CMC result in a viscous solution giving undesirable high system pressure and background noise in UV detectors. Sodium dodecyl sulphate (SDS), cetyltrimethyl ammonium bromide (CTAB), and Brij-35 are the most commonly used surfactants in MLC as they have low CMC values. CMC values are affected by the addition of organic modifiers to reduce retention in MLC from modification in the structure of the micelle [140].

Krafft point: In the case of ionic surfactants, the Krafft point is the temperature at which the solubility of an ionic surfactant monomer becomes equal to the CMC [141, 142].

If the solubility is very low, then no micelles are present below the Krafft point temperature. Therefore, chromatographic work should always be carried out above this temperature to avoid surfactant precipitation.

Cloud point: In the case of non-ionic surfactants, the cloud point is the temperature above which phase separation takes place therefore chromatographic work using non-ionic surfactants should be carried out below this temperature.

Micellar Mobile Phase: The mobile phase used in MLC consists of surfactants at a concentration above their CMC, where any increase in the surfactant concentration is translated into an increase in the concentration of micelles in solution while the number of the surfactant monomers in the mobile phase remains constant. Micelles provide hydrophobic and electrostatic sites (for ionic surfactants) of interaction [143].

Micelles have three sites of solubilisation:

- The core, which is hydrophobic in nature.
- The surface, which is hydrophilic in nature.
- The palisade layer which is the region between the core and the surfactant head group (Figure 10).

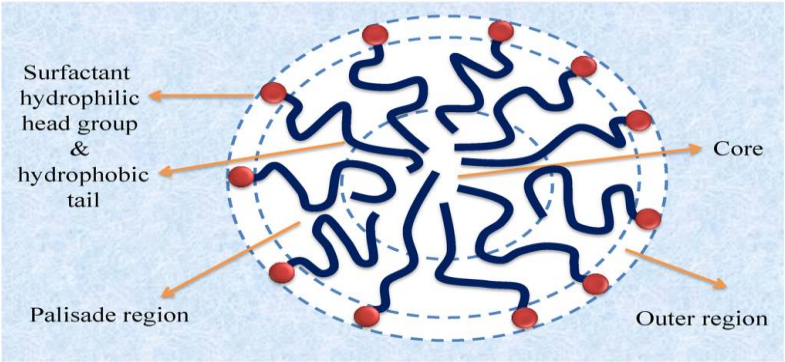

Figure 10: Structure of the palisade region of the micelle (reference [144])

A non-polar stationary phase and a polar aqueous mobile phase are the common basic components of MLC and RPLC however in conventional RPLC the hydro-organic mobile phase is homogenous, but in MLC the micellar mobile phase is microscopically heterogeneous as it is composed of two different media: the amphiphilic micellar aggregates (micellar pseudophase) and the aqueous-organic solvent containing surfactant monomers concentration (approximately equal to the CMC).

Organic solvents may be added to the micellar mobile phase for modification of the eluent strength [145], peak efficiency improvement and retention time reduction (via changing the micelle structure) and lowering the polarity of the aqueous solution resulting in the so-called “Hybrid micellar mobile phase” containing micelles, surfactant monomers, molecules of organic solvent and water.

The choice of the best organic solvent used in MLC depends on the polarity of the analytes. The maximal allowable organic solvent concentration used depends on the type of organic solvent and the surfactant, where a high concentration of organic solvent leads to the disaggregation of micelles and sweeping completely the adsorbed surfactant molecules from the bonded phase thus only free surfactant molecules remain in the mobile phase [139].

Modified Stationary Phase: The alkyl bonded C_{18} column is the most widely used stationary phase in MLC, other columns (e.g. C_8 and cyanopropyl) are also used [146]. Surfactant monomers incorporated in the mobile phase adsorb on the porous RPLC packing altering the various surface properties of the stationary phase, such as surface area, polarity, structure, and pore volume which majorly influences chromatographic retention. The stationary phase pores are also coated by the surfactant molecules which results in decreasing their volume [147].

For most surfactants and stationary phases, the amount of the surfactant adsorbed remains constant after equilibrium between mobile and stationary phase is reached. The adsorption of a surfactant on a silica-bonded stationary phase can occur in two ways:

Hydrophobic Interaction: The hydrophobic alkyl tail of the surfactant is adsorbed on the stationary phase while the ionic head is projected outwards which gives the stationary phase some ion exchange ability with charged analytes.

Silanophilic Interaction: The ionic head group of the surfactant is adsorbed on the stationary phase giving the stationary phase more hydrophobic character.

Competition between surfactant and analyte may possibly take place on the stationary phase. Owing to the number of interactions which are possible in MLC, factors affecting chromatographic separations for example electrostatic, hydrophobic or steric interactions plus surfactant monomers adsorbing on the stationary phase may lead to its modification. Therefore, the MLC system is more complex than conventional RP-HPLC with hydro-organic solvents [148].

For buffering of pH and ionic strength adjustment, ionic compounds are commonly added to the micellar mobile phases in MLC. A change in the amount of the adsorbed ionic surfactant may occur by salt addition by decreasing surfactant CMC, electrostatic repulsion and hydrophobic interactions [149].

Retention Behaviour:

The separation behaviour in MLC is explained by taking three phases into consideration which are: stationary phase, micellar pseudophase, and bulk solvent. According to the analytes differential partitioning between micelles and bulk solvent either in the mobile phase or in surfactant-coated stationary phase, separation of analytes takes place. As a result, three coefficients explain the partitioning behaviour in MLC:

P_{sw} ➡ Partition coefficient between aqueous solvent and stationary phase.

P_{mw} ➡ Partition coefficient between aqueous solvent and micelles.

P_{ms} ➡ Partition coefficient between micelles and stationary phase.

An outline of the interactions taking place between the three phases is shown in Figure (11).

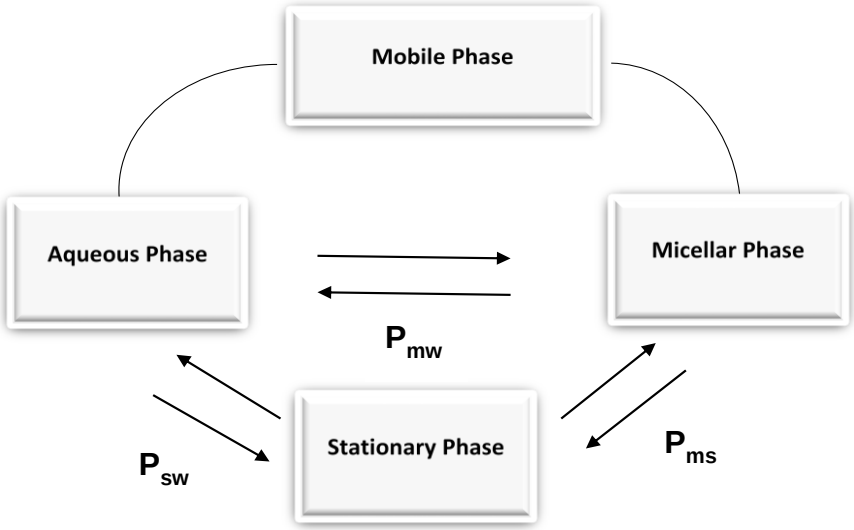

Figure 11: Summary of interactions in MLC

P_{sw} and P_{mw} have opposite effects on solute retention. P_{sw} represents solute affinity with the stationary phase, thus as P_{sw} increases, the retention increases, whereas when P_{mw} increases, a decrease in retention is observed from the greater association with micelles as P_{mw} represents solute affinity with micelles.

Nature of interactions:

The retention behaviour of solutes in MLC depends on the interactions between the solute and the surfactant modified stationary phase and between the solute and micelles.

The elution of neutral analytes with non-ionic and ionic surfactants and the elution of charged analytes with non-ionic surfactants is only influenced by dipole-dipole, nonpolar and proton donor acceptor interactions[150, 151].

In addition to the previously mentioned interactions, charged analytes interact electrostatically with ionic surfactants which form charged micelles and a charged surfactant layer on the stationary phase.

According to the charges of the analyte and that of the ionic surfactant, repulsion or attraction may occur.

In the case of electrostatic repulsion, unless significant hydrophobic interaction with the modified bonded layer exists, the charged analytes cannot be retained by the stationary phase and elute early at the dead time. On the other hand, in the case of combined electrostatic attraction and hydrophobic interactions with the modified stationary phase, strong retention may be achieved in MLC.

Solutes are classified according to their elution behaviour into three categories, which are binding, non-binding and antibinding solutes:

- **Binding solutes:** solutes that bind or associate to micelles, they show decreased retention when the micelle concentration is increased.
- **Non-Binding solutes:** solutes that do not bind or associate to micelles, they show unaltered retention by changing the micelle concentration.
- **Antibinding solutes:** solutes that show increased retention with increasing the concentration of micelles; it should be noted that antibinding behaviour is not very common.

Electrostatic repulsion is an important issue in antibinding behaviour, where the antibinding behaviour has never been observed between a charged solute and an oppositely charged surfactant.

Antibinding behaviour has not been observed with C_8 or C_{18} bonded phases modified by adsorption of ionic surfactants since repulsion between solutes and the charged surfactant layer on the stationary phase tend to result in elution in the void volume region.

On the other hand, when using stationary phases which do not adsorb large amounts of surfactant (C_1) or cyanobonded phases where the surfactant charge is buried close to the bonded phase, antibinding behaviour is observed, this is a consequence of a compound being strongly excluded or repelled from the micelle which forces the solute on to the stationary phase where it is retained as a result of hydrophobic interactions [152].

Retention behaviour in micellar mobile phases:

Retention behaviour of binding solutes as a function of the micellar concentration [M] (concentration of surfactant monomers forming micelles equal to total surfactant concentration minus the CMC) has been explained by many proposed theoretical approaches [153].

- Armstrong & Nome partitioning model:

The model proposed by Armstrong and Nome [148] considers transitions among three environments in a micellar chromatographic system i.e. water, micelles and stationary phase.

$$\frac{V_e - V_o}{V_s} = \frac{K}{\Phi} = \frac{P_{sw}}{1 + v\,(P_{mw} - 1)[M]} \qquad \text{Eq. (3)}$$

Where:

V_e: The total volume of mobile phase needed to elute a given solute from the column.

V_o: The column void volume.

V_s: The volume of the active surface of the stationary phase.

Φ: V_s/V_o phase ratio.

v: Partial specific volume of monomers of surfactant in the micelle.

- Arunyanarat & Cline-Love model:

Arunyanarat and Cline-Love [154] assumed association equilibrium of solute in bulk aqueous solvent (A) with the stationary phase binding sites (S) and with monomers of surfactant in the micelle (M) governed by the binding constants K_{AS} and K_{AM} respectively.

$$K=\Phi\frac{[AS]}{[A]+[AM]}=\frac{\Phi K_{AS}[AS]}{1+K_{AM}[M]} \qquad \text{Eq. (4)}$$

- Foley model:

This model is based on the idea that the association between solute and micelle is a secondary equilibrium affecting the retention in the absence of micelles (K_o). Foley put forward the idea of treating the retention factor as an apparent parameter.

$$K=K_o\frac{1}{1+K_{AM}[M]} \qquad \text{Eq. (5)}$$

This model resembles the previous two models as the retention factor of free solute (K_o) coincides with P_{sw} in the Armstrong and Nome model and (K_{AS}) in the Arunyanarat and Cline-Love model whereas (K_{AM}) coincides with (K_{AM}) in the Arunyanarat and Cline-Love model.

A comparison of the pros and cons of the MLC method in general are listed in Table (1).

Table 1: A summary of the advantages and disadvantages of the micellar liquid chromatography method

Advantages	Limitations
- It is an interesting technique for green chemistry because it uses a mobile phase containing 90 % or more water, these micellar mobile phases have low toxicity, are non-flammable and do not produce hazardous waste [139]. - The incorporation of surfactants in the mobile phase leads to altering of the interactions formed inside the column which reduces the amount of organic solvent in the mobile phase compared with that in conventional RPLC [147]. - It provides an alternative to conventional RPLC as it confers analytical procedures of greater accuracy and at a lower cost [155-158]. - It allows direct injection of real biological samples (for example urine, plasma, serum) for analysis of untreated physiological fluids as micelles have the ability to solubilise proteins therefore no sample extraction or preparation is required prior to analysis proving to be time saving compared with other analytical methods such as HPLC and ion pairing (IP) [159]. - Analysis of various pharmaceutical compounds.	- One of the major drawbacks of MLC systems is the reduced chromatographic efficiency compared with conventional RPLC with an aqueous organic mobile phase, this decrease in chromatographic efficiency results from an increase in the resistance of solute mass transfer from the mobile phase to the stationary phase and poor wetting of the stationary phase by the mobile phase [170, 171]. Also, the increase in the thickness of the stationary phase (by the adsorbed surfactant) has a major effect on MLC efficiency [149, 172, 173]. - The reduced chromatographic efficiency of MLC can be improved by: - Addition of small amounts of an organic modifier to the mobile phase causing surfactant desorption out of the stationary phase, therefore improving efficiency[170, 174]. - Increasing the working temperature[175]. - Working with low flow rates and low surfactant concentrations. To obtain efficiency in MLC similar to that obtained in conventional RPLC with aqueous organic mobile phase it is essential the eluent strength of the micellar

- Excessive peak tailing that is observed in (IP) seen for basic drugs is reduced by the use of MLC. - It is used in the separation of hydrophilic drugs that are usually unretained in HPLC. - A novel application of MLC is separation and analysis of inorganic compounds (mostly simple ions) [160]. - It is considered as a superior technique to ion pairing and ion exchange for separation of charged molecules and mixtures of charged and neutral species [161]. - Micelles can be considered as chemical models for biomembranes, which enable the application of MLC to hydrophobicity estimation of organic compounds [145] where partition coefficients can be calculated by plotting their capacity factors obtained from MLC against micellar concentration of surfactant used. - Micellar liquid chromatography is the same as biopartitioning micellar chromatography (BMC) but they differ in the composition of the micellar mobile phase. In BMC, a C_{18} stationary phase and polyoxyethylene (23) lauryl ether (Brij 35) mobile phase are used for the prediction of biological behaviour of drugs [162]. BMC is useful in obtaining many models for the prediction of various biological behaviours of different drugs for example BBB penetration[163], ocular tissue permeability [164], skin	mobile phase is very small. Despite that the eluent strength of purely micellar eluents increases with the increase in the micelle concentration in the mobile phase, the increase in the micelle concentration in the mobile phase causes a loss of efficiency. The eluent strength of a micellar mobile phase can be increased by addition of alcohols such as methanol, propanol or butanol [145].

permeability[165], drug absorption [166], and mutagenicity of aromatic amines [167]. Similar to BMC, MLC has also been used in the prediction of biological behaviour such as skin permeability[168], and oral drug absorption[169].	

1.6. Bile Salts:

One particular type of surfactants is the naturally occurring biosurfactants such as (bile salts) which have a distinguished shape and unusual micellar properties compared with conventional head and tail synthetic surfactants.

Bile salts (Figure (12)) are metabolic products of cholesterol [176, 177]. They are derived from cholic acid, comprised of a rigid and slightly curved tetracyclic steroid ring based structure [176, 178, 179]. Hydrophilic groups are attached to the hydrophobic ring, these hydrophillic groups are one to three hydroxyl (OH)-groups and an acidic group. Bile salts are conjugated to either taurine or glycine amino acid. Because of their distinct structure, where the hydroxyl groups are oriented towards the concave side of the rigid steroid ring backbone so the hydrophilic part of the bile salt structure is its concave side while, the hydrophobic part is represented by the convex side. It appears that as a result of the rigid structure of the steroid ring there is no complete separation between hydrophilic and hydrophobic parts in micelles [176].

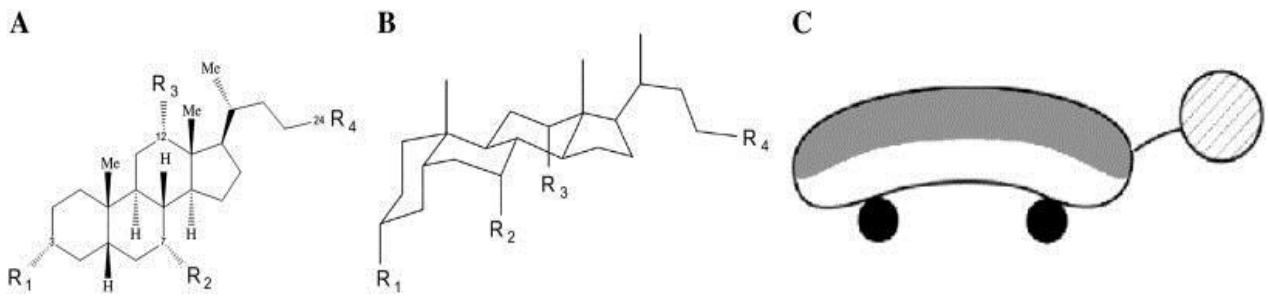

Figure 12: Structure of bile salts. (A): Structural formula, (B): 3D structure, (C): Schematic representation of a dihydroxy bile salt (reference [176]).

According to the type of the bile salt, positions R_1 to R_3 can be hydroxylated. R_4 is the acidic group that can be conjugated with taurine or glycine.

Based on their unique structure, there are different assumptions for explaining the micellisation process in bile salts as shown in Figure (13) where (A and B) are different primary micelles, (C) is a disclike micelle and (D) is a hellical micelle [176].

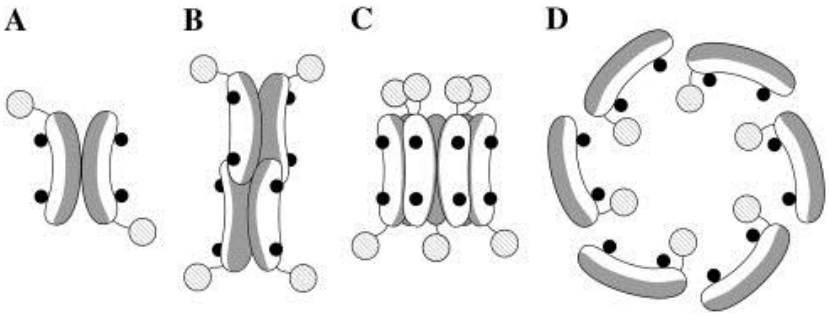

Figure 13: Schematic representation of different models for a bile salt micellar structure (reference [176]).

Bile salts have both hydrophobic and hydrophilic sides; they form micelles in water by means of hydrophobic association of their hydrophobic sides. A variety of models have been proposed to describe bile salt aggregation (micellisation). Among the popular models for bile salt aggregation are:

- **Small's model:** This model suggested the formation of primary aggregates through hydrophobic association between the hydrophobic parts of (2-9) monomers of bile salts followed by further aggregation of the primary aggregates via hydrogen bonding between the hydroxyl groups. Furthermore, the model proposed that the primary aggregates are a globular shape while the secondary aggregates are oblate ellipsoidal in shape [180].
- **Oakenfull and Fisher's model:** This model proposed that the bile salts form dimers while in water via a hydrophobic interaction. The dimers are claimed to be rod-like in structure [181].
- **Kawamura *et al.* model:** This model proposed that the secondary aggregates are disc-shaped in structure, in which the hydrophobic sides are facing each other towards the inside while the hydrophilic sides are facing outwards towards the solvent molecules [182].
- **Warren *et al.* model:** According to this model the bile salt aggregates are formed by polar interactions between the bile salt molecules. The formed aggregates are proposed to be helical in shape which is based on the crystalline state rather than the liquid state. This model has since been discounted and the

so disc-shaped hypothesis of bile salt aggregates has become widely recognised [183].

Aims of the work

In this work MLC is used in the prediction of human intestinal absorption through the use of **'biological surfactants'** to form the micellar mobile phase, the biosurfactants used are bile salts. Biosurfactants are used in this work as an attempt to mimic or simulate the human inner intestinal environment for prediction of intestinal absorption via a study of the retention behaviour of a diverse group of drugs as bile salts are very prominent components of intestinal fluid. This method will also be compared with other methods commonly used in the prediction of intestinal absorption, alongside spectroscopic predictive analysis.

Overall, the aim of this work is to investigate the development of *in vitro* methods to predict *in vivo* performance for pharmaceutical compounds. This can be considered through the following objectives:

1- Investigate the application of MLC for predicting human intestinal absorption.
2- Investigate the effect of changing the type of the chromatographic column used in MLC.
3- Investigate the effect of changing column temperature throughout MLC experiments.
4- Investigate the application of spectroscopy for predicting human intestinal absorption.
5- Develop a novel hydrogel to be considered as a predictor of human intestinal absorption.

Chapter 2: Materials and Methods

2.1. Materials and reagents

Sodium deoxycholate (NaDC) (97 %), sodium taurodeoxycholate (NaTDC) (95 %), sodium taurocholate (NaTC) (≥ 97 %), sodium cholate (NaC) (97 %), Sodium glycocholate (GC) (≥ 97 %), sodium glycodeoxycholate (GDC) (≥ 97 %) and L-α-phosphatidylcholine from dried egg yolk (≥ 50 %) were used as purchased from Sigma Aldrich, Dorset, UK for preparation of stock solutions of mobile phase. Analytical grade, sodium chloride (NaCl), sodium dihydrogen orthophosphate dihydrate ($NaH_2PO_4.2H_2O$), disodium hydrogen orthophosphate anhydrous (Na_2HPO_4) were purchased from Fisher Scientific, Loughborough, UK also 4-(2-hydroxyethyl)-1-piperazineethanesulfonic acid (HEPES buffer) was purchased from Sigma Aldrich, Dorset, UK. The compounds considered in this work were caffeine 97 % (Sigma Aldrich, Dorset, UK), fenoprofen 97 % (Fluka, Dorset, UK), quinine 96 % (Fluka, Dorset, UK), acetaminophen 99 % (Sigma Aldrich, Dorset, UK), haloperidol 99 % (Sigma Aldrich, Dorset, UK), leflunomide 98 % (Sigma Aldrich, Dorset, UK), linezolid >98 % (Sigma Aldrich, Dorset, UK), ketoprofen 98 % (Sigma Aldrich, Dorset, UK), lidocaine 98 % (Sigma Aldrich, Dorset, UK), indomethacin 99 % (Sigma Aldrich, Dorset, UK), propranolol 98 % (Sigma Aldrich, Dorset, UK), phenylbutazone 99 % (Sigma Aldrich, Dorset, UK), fluconazole 98 % (Sigma Aldrich, Dorset, UK), alprenolol 98 % (Sigma Aldrich, Dorset, UK), amitriptyline 98 % (Sigma Aldrich, Dorset, UK), carbamazepine 99 % (Sigma Aldrich, Dorset, UK), cimetidine (Sigma Aldrich, Dorset, UK), mannitol 98 % (Sigma Aldrich, Dorset, UK), moexipril >98 % (Sigma Aldrich, Dorset, UK), naproxen 98 % (Sigma Aldrich, Dorset, UK), piroxicam 98 % (Sigma Aldrich, Dorset, UK), terbutaline 96 % (Sigma Aldrich, Dorset, UK), zolmitriptan >98 % (Sigma Aldrich, Dorset, UK), salicylic acid 99 % (Fisher Scientific, Loughborough, UK), ibuprofen 98 % (BASF, Cheshire, UK), acetyl salicylic acid 99% (Acros Organics, Geel, Belgium), diclofenac 98 % (TCI Europe, Zwijndrecht, Belgium), diphenhydramine 98 % (TCI Europe), flurbiprofen 98 % (TCI Europe), gemfibrozil 98 % (TCI Europe), lornoxicam >98 % (TCI Europe), nicotinic acid >98 % (Sigma Aldrich, Dorset, UK), theophylline 98 %, (TCI, Oxford, UK), meloxicam 98 % (TCI Europe). 2,7-dichlorofluorescein was purchased from BDH chemicals Ltd, Poole, Dorset, UK for

CMC determination experiments and methanol was used as a solvent for preparation of the dye stock. The utilised Dialysis membrane was a high retention seamless cellulose tubing with an average flat width of 23 mm (0.9 in.) and molecular weight cut off (MWCO) of 12400.

The bile salts and compounds used in the thesis are summarised in Table (2).

Table 2: General properties of bile salts and drugs under study.

Sodium Deoxycholate (NaDC)		**Structure**
Molecular weight	414.6 g/mol[184]	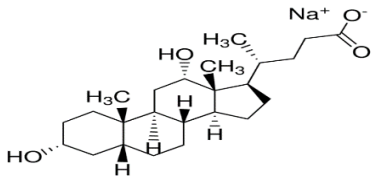
Charge	Anionic	
CMC	4-6 mM[185]	
Aggregation number (AN)	5.1-7.1 [186]	
Sodium Taurodeoxycholate (NaTDC)		
Molecular weight	521.7 g/mol[184]	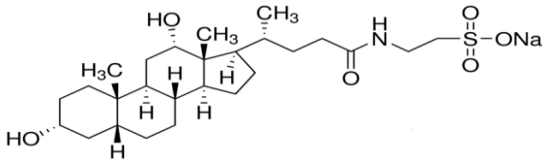
Charge	Anionic	
CMC	2-6 mM[185]	
Aggregation number (AN)	2-3[187]	
Sodium Cholate (NaC)		
Molecular weight	430.6 g/mol[184]	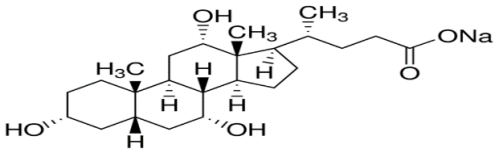
Charge	Anionic	
CMC	9-15 mM[188]	
Aggregation number (AN)	2-4[185]	
Sodium Taurocholate (NaTC)		
Molecular weight	537.7 g/mol[184]	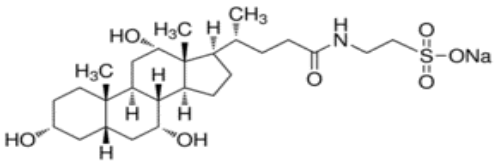
Charge	Anionic	
CMC	3-11 mM[189]	
Aggregation number (AN)	5[185]	
Sodium glycocholate (GC)		
Molecular weight	487.6 g/mol[184]	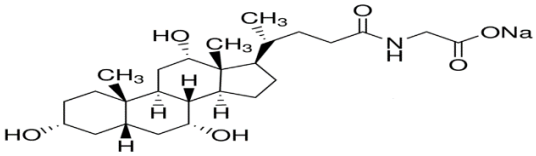
Charge	Anionic	
CMC	13 mM[190]	
Aggregation number (AN)	6[191]	
Sodium glycodeoxycholate (GDC)		
Molecular weight	471.6 g/mol[184]	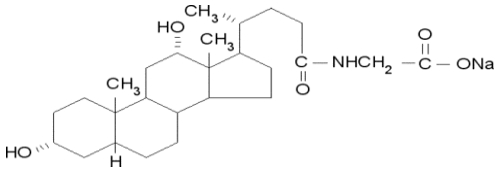
Charge	Anionic	
CMC	2.12 mM[192]	
Aggregation number (AN)	26[191]	

L-α-Phosphatidylcholine		**Structure**
Molecular weight	758.1 g/mol[184]	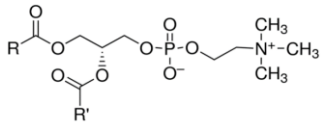 R, R' = fatty acid residues
Charge	Zwitterionic	
Acetaminophen (APAP)		
Molecular weight	151.2 g/mol[184]	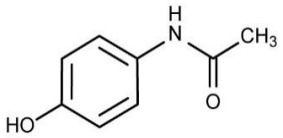
Charge	Neutral	
Log $P_{o/w}$	0.46[184]	
λ_{max}	243 nm[193]	
Acetylsalicylic acid (ASA)		
Molecular weight	180.2 g/mol[184]	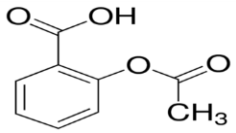
Charge	Anionic	
Log $P_{o/w}$	1.19[184]	
λ_{max}	295 nm[193]	
Alprenolol (Alp)		
Molecular weight	249.3 g/mol[184]	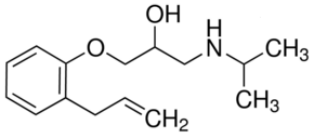
Charge	Anionic	
Log $P_{o/w}$	3.10[184]	
λ_{max}	270 nm[193]	
Amitriptyline (AMI)		
Molecular weight	277.4 g/mol[184]	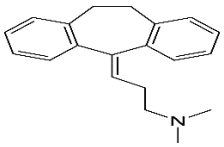
Charge	Anionic	
Log $P_{o/w}$	4.92[184]	
λ_{max}	240 nm[193]	
Caffeine (CAF)		
Molecular weight	194.2 g/mol[184]	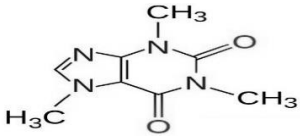
Charge	Neutral	
Log $P_{o/w}$	- 0.07[184]	
λ_{max}	273 nm[193]	
Carbamazepine (CBZ)		
Molecular weight	236.3 g/mol[184]	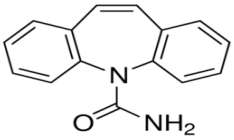
Charge	Anionic	
Log $P_{o/w}$	2.45[184]	
λ_{max}	284 nm[193]	
Cimetidine (CIMET)		
Molecular weight	252.3 g/mol[184]	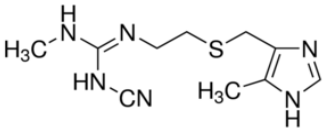
Charge	Neutral	
Log $P_{o/w}$	0.40[184]	
λ_{max}	218 nm[193]	
Diclofenac (dicl)		
Molecular weight	296.1 g/mol[184]	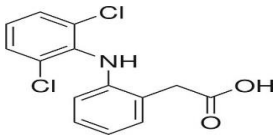
Charge	Anionic	
Log $P_{o/w}$	4.51[184]	
λ_{max}	276 nm[193]	

Diphenhydramine (DIPHEN)		**Structure**
Molecular weight	255.4 g/mol[184]	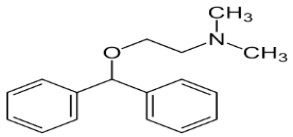
Charge	Cationic	
Log $P_{o/w}$	3.27[184]	
λ_{max}	221 nm[193]	
Fenoprofen (FEN)		
Molecular weight	242.3 g/mol[184]	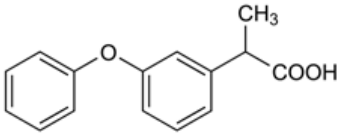
Charge	Anionic	
Log $P_{o/w}$	3.10[184]	
λ_{max}	271 nm[193]	
Fluconazole (Fluc)		
Molecular weight	306.3 g/mol[184]	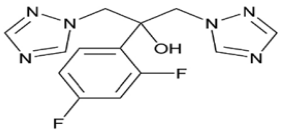
Charge	Neutral	
Log $P_{o/w}$	0.40[184]	
λ_{max}	260 nm[193]	
Flurbiprofen (FBP)		
Molecular weight	244.3 g/mol[184]	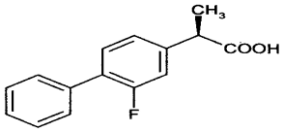
Charge	Anionic	
Log $P_{o/w}$	4.16[184]	
λ_{max}	247 nm[193]	
Fosinopril (FOS)		
Molecular weight	563.3 g/mol[184]	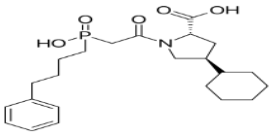
Charge	Anionic	
Log $P_{o/w}$	6.30[184]	
λ_{max}	208 nm[193]	
Gemfibrozil (Gem)		
Molecular weight	250.3 g/mol[184]	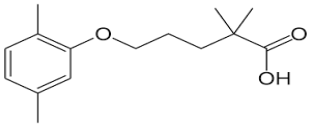
Charge	Anionic	
Log $P_{o/w}$	3.40[184]	
λ_{max}	274 nm[193]	
Haloperidol (Halo)		
Molecular weight	375.9 g/mol[184]	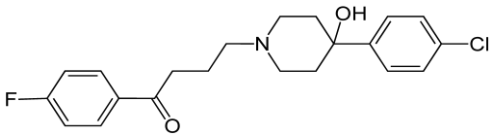
Charge	Cationic	
Log $P_{o/w}$	4.30[184]	
λ_{max}	248 nm[193]	
Ibuprofen (IBU)		
Molecular weight	206.3 g/mol[184]	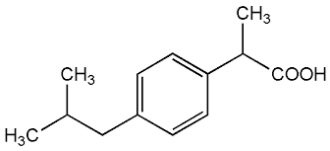
Charge	Anionic	
Log $P_{o/w}$	3.97[184]	
λ_{max}	272 nm[193]	
Indomethacin (Indo)		
Molecular weight	357.8 g/mol[184]	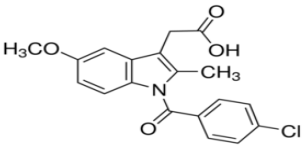
Charge	Anionic	
Log $P_{o/w}$	4.27[184]	
λ_{max}	320 nm[193]	

Ketoprofen (Keto)		**Structure**
Molecular weight	254.3 g/mol[184]	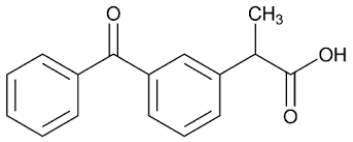
Charge	Anionic	
Log $P_{o/w}$	3.12[184]	
λ_{max}	261 nm[193]	
Leflunomide (LEF)		
Molecular weight	270.2 g/mol[184]	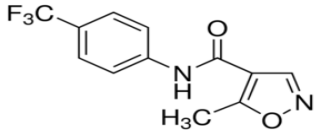
Charge	Neutral	
Log $P_{o/w}$	2.80[184]	
λ_{max}	258 nm[193]	
Lidocaine (LDC)		
Molecular weight	234.3 g/mol[184]	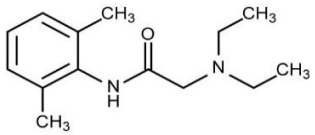
Charge	Cationic	
Log $P_{o/w}$	2.44[184]	
λ_{max}	262 nm[193]	
Linezolid (lzd)		
Molecular weight	337.3 g/mol[184]	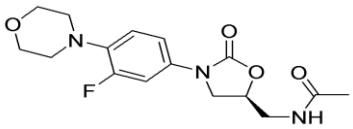
Charge	Neutral	
Log $P_{o/w}$	0.90[184]	
λ_{max}	251 nm[193]	
Lornoxicam (LORN)		
Molecular weight	371.8 g/mol[184]	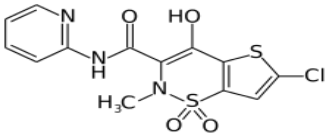
Charge	Anionic	
Log $P_{o/w}$	2.62[184]	
λ_{max}	381 nm[193]	
Mannitol (MAN)		
Molecular weight	182.2 g/mol[184]	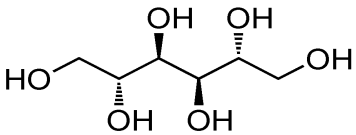
Charge	Neutral	
Log $P_{o/w}$	-3.10[184]	
λ_{max}	295 nm[193]	
Meloxicam (MEL)		
Molecular weight	351.4 g/mol[184]	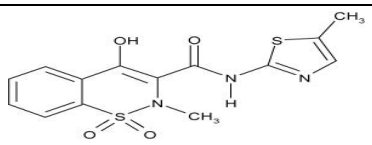
Charge	Anionic	
Log $P_{o/w}$	3.43[184]	
λ_{max}	362 nm[193]	
Moexipril (MOEX)		
Molecular weight	498.6 g/mol[184]	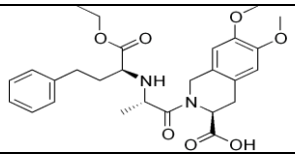
Charge	Anionic	
Log $P_{o/w}$	2.70[184]	
λ_{max}	282 nm[193]	
Naproxen (NAP)		
Molecular weight	230.3 g/mol[184]	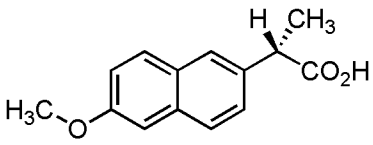
Charge	Anionic	
Log $P_{o/w}$	3.18[184]	
λ_{max}	230 nm[193]	

Nicotinic acid (NIC)		**Structure**
Molecular weight	123.1 g/mol[184]	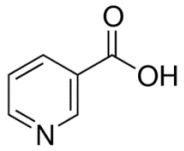
Charge	Anionic	
Log $P_{o/w}$	0.36[184]	
λ_{max}	262 nm[193]	
Phenylbutazone (PBZ)		
Molecular weight	308.4 g/mol[184]	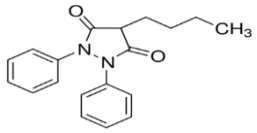
Charge	Anionic	
Log $P_{o/w}$	3.16[184]	
λ_{max}	264 nm[193]	
Piroxicam (PRX)		
Molecular weight	331.3 g/mol[184]	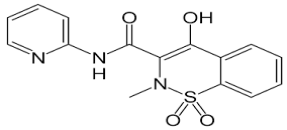
Charge	Anionic	
Log $P_{o/w}$	3.06	
λ_{max}	355 nm[193]	
Propranolol (PROP)		
Molecular weight	259.3 g/mol[184]	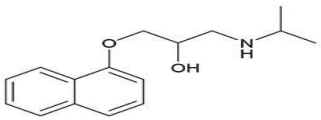
Charge	Anionic	
Log $P_{o/w}$	3.48[184]	
λ_{max}	292 nm[193]	
Quinine (QN)		
Molecular weight	324.4 g/mol[184]	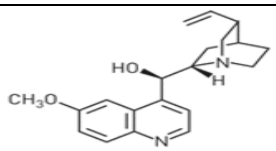
Charge	Cationic	
Log $P_{o/w}$	3.44[184]	
λ_{max}	332 nm[193]	
Salicylic acid (SA)		
Molecular weight	138.1 g/mol[184]	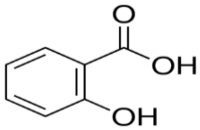
Charge	Anionic	
Log $P_{o/w}$	2.26[184]	
λ_{max}	296 nm[193]	
Terbutaline (Terb)		
Molecular weight	225.3 g/mol[184]	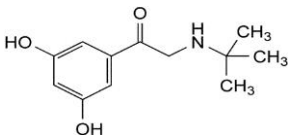
Charge	Cationic	
Log $P_{o/w}$	0.90[184]	
λ_{max}	280 nm[193]	
Theophylline (Theo)		
Molecular weight	180.2 g/mol[184]	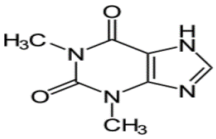
Charge	Neutral	
Log $P_{o/w}$	-0.02[184]	
λ_{max}	273 nm[193]	
Zolmitriptan (ZMT)		
Molecular weight	287.4 g/mol[184]	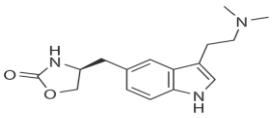
Charge	Cationic	
Log $P_{o/w}$	1.60[184]	
λ_{max}	283 nm[193]	

2.2. Methods

This thesis includes data from a number of methods, mainly involving micellar liquid chromatography (MLC) and spectroscopy. Two separate methods for studying permeation of compounds through prepared gels using Franz diffusion cells and flow through cells are discussed in Chapter 5. Also scanning electron microscopy (SEM) and Fourier transform infrared (FT-IR) techniques were used for the characterisation of the prepared gels.

2.2.1. Micellar Liquid Chromatography

Micellar mobile phase stock solutions and dilutions preparation

- **Preparation of stock solutions of NaDC, NaTDC, NaC and NaTC in water or 0.15 M NaCl or (SIFsp)**

20 mM stock solutions for NaDC, NaTDC and NaTC and 35 mM stock solutions for NaC bile salts in water or 0.15 M NaCl were prepared by transferring an accurately weighed amount of each bile salt to a 250 mL volumetric flask and completing to the mark with deionised water (for NaDC, NaTDC and NaC) or 0.15 M NaCl (for NaDC and NaTC) or SIFsp (for NaTC).

- **Preparation of bile salt dilutions in water or 0.15 M NaCl or (SIFsp)**

Preparation of bile salt solutions over the concentration range of (5-20 mM for NaDC), (6-20 mM for NaTDC), (19-35 mM for NaC) and (3-20 mM for NaTC) was carried out by serial dilution of the stock solution of each bile salt to give the different micellar mobile phase concentrations. Accurately measured aliquots were transferred from the stock solution in water or 0.15 M NaCl to 50 mL volumetric flasks; solutions were completed to the final volume with deionised water or 0.15 M NaCl.

- **Preparation of stock solution of mixed micellar mixture simulating the physiological bile salt mixture**

17 mM stock solution of a mixed micellar system was prepared by transferring accurately weighed amounts equivalent to 2.71 mM, 2.00 mM, 2.08 mM, 2.08 mM, 4.70 mM and 3.43 mM of NaTC, NaTDC, NaDC, NaC, NaGC and NaGDC bile salts respectively and 0.75 mM of egg phosphatidylcholine (PC) to a 250 mL volumetric flask and completing to the mark with a buffer solution of 10 mM HEPES, pH of 6.5, in 0.15 M NaCl. The solution was then sonicated for 30 minutes and stored for 12 hours before use to allow the formation of stable mixed micelles.

- **Preparation of a mixed micellar solution for dilution**

Different concentrations of the micellar mixture were prepared over the range of (5-17 mM) by diluting the stock mixture solution (17 mM) using a 2 mM mixture solution. The 2 mM mixture solution contained the same six bile salts and lecithin used in the preparation of the stock mixture solution in the same molar ratios. The 2 mM diluting mixture was prepared by transferring accurately weighed amounts equivalent to 0.32 mM, 0.25 mM, 0.24 mM, 0.24 mM, 0.55 mM, 0.4 mM of NaTC, NaTDC, NaDC, NaC, NaGC and NaGDC bile salts respectively and 0.75 mM of egg phosphatidylcholine (PC) to a 250 mL volumetric flask and completing to the mark with a buffer solution of 10 mM HEPES, pH of 6.5, in 0.15 M NaCl. The resultant solution was then sonicated for 30 minutes then stored for 12 hours before use. Dilution was carried out in this way as the 2 mM mixture is considered to be the monomer bile salt concentration that is required to be kept constant in each solution in order to keep the size of the micelle constant while its concentration is being changed.

In unbuffered MLC experiments, samples solutions were prepared each at a concentration of 0.2 mM. All the solutions used were freshly prepared. The pH of the medium was measured before each experiment and it was found to be in the range of 6.4 to 8 (for NaDC), 5.2 to 6.1 (for NaTDC) and 7.1 to 9.6 (for NaC).

Instrumentation and measurement

Experiments were carried out with a chromatographic system consisting of a Severn Analytical SA 6410B pump, a Rheodyne injector through which 20 µL samples were injected in to the system and a UV detector (Perseptive Biosystems UVIS-205), set at a wavelength appropriate for each drug producing a peak via Picolog software indicating the retention of the solute within the column as a function of time. The mobile phase was filtered through a 0.45 µm Nylon filter and degassed in an ultrasonic bath. Data were recorded and then analysed to obtain capacity factors and each run was repeated three times to ensure that reasonable accuracy and precision were achieved. Analytical separation was accomplished using a reversed phase cyanopropyl column (Spherisorb 5 µm, 15 cm × 4.6 mm i.d., WATERS) using different mobile phases and conditions or an aminopropyl column (APS) (Hypersil 5µm, 15 cm x 4.6mm, Thermo Scientific) using different mobile phases and conditions (Table (3)). The flow rate used was 1.34 mL/min with all assays carried out at room temperature (25 ºC -methods A, B and C) or (37 ºC -methods D, E and F) or over the temperature range of (30-45 ºC)

(method G) using the column chiller (Jones Chromatography model 7950). During the course of this study the Severn Analytical SA 6410B pump was replaced with an Agilent1100 Series Binary Pump.

Determination of dead time t_0

The dead time (t_0) is defined as the time taken by the solvent front to reach the detector. According to literature, dead time in MLC is measured by the injection of water [194] or an organic solvent e.g. acetonitrile or methanol [195, 196] and observing the base line for the appearance of the first major perturbation while recording the retention time of the first peak that appeared. In this work, dead time was determined by injecting distilled water or acetonitrile in to the system and recording the retention time of the first peak that appeared after injection (solvent front). The same method was repeated for each of the bile salt concentrations used and dead time was recorded. A reliable value of the dead time used in the calculation of capacity factor (K') for all the experiments (using Equation 4) was determined from an average of at least ten recordings.

Calculation of log P_{mw}

Retention time of each drug was recorded for each bile salt concentration. The capacity factor for each retention time was calculated using the following equation:

$$K' = \frac{(\text{Retention time} - \text{dead time})}{\text{dead time}} \qquad \text{Eq. (6)}$$

The reciprocal of each capacity factor was obtained (1/K') with the average plotted against the micellar concentration (C_M) that was calculated according to the following equation:

$$(C_M) = \text{Total surfactant concentration} - \text{Critical micellar concentration (CMC)} \qquad \text{Eq. (7)}$$

The partition coefficient (log P_{mw}) was obtained from the slope and intercept of the line obtained from the plot of (C_M) against (1/K').

$$\text{Log } P_{mw} = \log[\text{intercept}/\text{slope}] \qquad \text{Eq. (8)}$$

Table 3: Micellar Liquid Chromatography (MLC) Methods.

MLC Method	Mobile Phase	Column Used	Column Temperature	Drugs Used
Method A "Use of NaDC as mobile phase with RP-CN column"	Sodium deoxycholate (NaDC) in **water** used over concentration Range (5-20 mM).	Reversed phase cyanopropyl column (Spherisorb 5 µm, 15 cm × 4.6 mm i.d., WATERS)	25 ^{o}C	Acetaminophen, acetyl salicylic acid, diclofenac, diphenhydramine, fenoprofen, fluconazole, gemfibrozil, ibuprofen, indomethacin, ketoprofen, lidocaine, nicotinic acid, phenylbutazone, piroxicam, propranolol and theophylline.
	Sodium deoxycholate (NaDC) in **0.15 M** NaCl used over concentration Range (5-20 mM).			Trials for method development with acetaminophen and caffeine.
Method B "Use of NaTDC as mobile phase with RP-CN column"	Sodium taurodeoxycholate (NaTDC) in used water over concentration Range (6-20 mM).			Acetaminophen, acetyl salicylic acid, caffeine, diclofenac, diphenhydramine, fenoprofen, fluconazole, gemfibrozil, ibuprofen, ketoprofen, lidocaine, phenylbutazone, propranolol, salicylic acid, theophylline.

Method C **"Use of NaTC as mobile phase with RP-CN column"**	Sodium taurocholate (NaTC) in **0.15 M NaCl** over concentration range (5-20 mM). Sodium taurocholate (NaTC) in **SIFsp** (pH 6.8) over concentration range (5-20 mM).	Reversed phase cyanopropyl column (Spherisorb 5 µm, 15 cm × 4.6 mm i.d., WATERS)	25 ºC	Acetaminophen, caffeine and ketoprofen.
				Caffeine, ibuprofen, ketoprofen and theophylline.
Method D **"Use of NaC as mobile phase with RP-CN column"**	Sodium cholate (NaC) in water used over concentration range (17-35 mM).		37 ºC	Acetaminophen, caffeine, diclofenac, fenoprofen, fluconazole, gemfibrozil, ibuprofen, indomethacin, ketoprofen, lidocaine, meloxicam, phenylbutazone, salicylic acid and theophylline.
Method E **"Physiological Mixture Method"**	A 17 mM stock of mixed micellar system of 2.71 mM Sodium taurocholate, 2 mM Sodium taurodeoxycholate, 2.08 mM			Acetaminophen, aspirin, caffeine, carbamazepine, cimetidine, diclofenac, fenoprofen, fluconazole, flurbiprofen, ibuprofen, ketoprofen, naproxen,

Method E "Physiological Mixture Method" (cont.)	Sodium deoxycholate, 2.08 mM Sodium cholate, 4.7 mM Sodium glycocholate, 3.43 mM Sodium glycodeoxycholate and 0.75 mM egg PC in 10 mM HEPES (pH 6.5) and 0.15 M NaCl used over the concentration range (5-17mM). A 2 mM mixture of the same ratios of bile salts used in the stock mixture was used in the preparation of different mixture concentrations by dilution of the stock mixture.	Reversed phase cyanopropyl column (Spherisorb 5 µm, 15 cm × 4.6 mm i.d., WATERS)	37 ^{o}C	nicotinic acid, phenylbutazone, salicylic acid, terbutaline, theophylline and zolmitriptan.

Method F **"Effect of Change in Column Type"**	Sodium deoxycholate (NaDC) in water used over concentration Range (5-20 mM).	Aminopropyl column (APS) (Hypersil 5µm, 15 cm x 4.6mm, Thermo Scientific)	37 ^{o}C	Acetaminophen, aspirin, caffeine, carbamazepine, cimetidine, diclofenac, fenoprofen, fluconazole, flurbiprofen, gemfibrozil, ibuprofen, indomethacin, ketoprofen, lidocaine, lornoxicam, meloxicam, naproxen, nicotinic acid, phenylbutazone, piroxicam, salicylic acid, terbutaline and theophylline.
Method G **"Effect of Change of Temperature"**	Sodium deoxycholate (NaDC) in water used over concentration Range (5-20 mM).	Reversed phase cyanopropyl column (Spherisorb 5 µm, 15 cm × 4.6 mm i.d., WATERS)	Runs were carried out at different temperatures (30, 35, 40 and 45 ^{o}C).	Acetaminophen, caffeine, ibuprofen, ketoprofen and theophylline.

2.2.2. UV-Vis Spectrophotometry

For all spectrophotometric experiments an Agilent Model Cary 60 UV-Vis was fitted with a Cary single cell Peltier accessory to keep the samples in the sample compartment at a specified temperature. A quartz cuvette of 10 mm internal thickness was used in all measurements. Samples were scanned over the wavelength range of (200-400 nm) or (400-800 nm) depending on the aim of the experiment.

2.2.2. a. Critical Micelle Concentration (CMC) determination

Stock and working solution preparation

- **Dye stock solution preparation:**

A stock solution of 10^{-3} M of the dye was prepared by dissolving an accurately weighed amount of dye in a certain volume of methanol. A 10^{-5} M concentration was then used for CMC determination tests.

- **Bile salt stock solution preparation**

A 20 mM and 35 mM stock solution of NaDC and NaC respectively were prepared by transferring accurately weighed amounts of each bile salt to two volumetric flasks then completing to the mark with deionised water. Dilutions from each stock solution were then prepared and scanned with the sample compartment thermostat set to each of the temperatures at which CMC is required to be determined.

Measurement

Temperatures studied were 30, 35, 40, 45 ºC for NaDC CMC determination and at 37 ºC for NaC CMC determination. Each dilution was scanned over the wavelength range from 400-800 nm and absorbance of the dye was recorded at its wavelength of maximum absorbance (λ_{max}) (503 nm).

For NaDC the absorbance at each temperature (30, 35, 40, 45 ºC) was recorded and plotted against the corresponding NaDC concentration for determination of CMC. For NaC the absorbance at 37 ºC was recorded and then plotted against the corresponding NaC concentration for determination of CMC.

The sample compartment thermostat was set to each temperature at which CMC was required to be determined.

2.2.2. b. Solubilisation method

Standard and sample solution preparation

- **Bile salt stock solutions preparation**

Since a calibration plot was required for each drug at different concentrations of the bile salt used (NaDC), a stock solution of the drug at each bile salt concentration over the range (7-

20 mM) was prepared. Different dilutions of NaDC from its stock (20 mM) were carried out using deionised water then each dilution was used in the preparation of different concentrations of the drug in the corresponding bile salt dilution.

- **Sample preparation**

An excess solid of each drug included in this study (acetaminophen, acetyl salicylic acid, alprenolol, amitriptyline, carbamazepine, cimetidine, diclofenac, diphenhydramine, fenoprofen, fluconazole, flurbiprofen, gemfibrozil, ibuprofen, indomethacin, ketoprofen, lidocaine, mannitol, meloxicam, naproxen, phenylbutazone, piroxicam, propranolol, quinine, and terbutaline) was placed in a microcentrifuge tube to which a 1 mL of each bile salt solution of concentrations over the range (7-20 mM) was added. The samples were equilibrated in a shaking water bath for 2 days at 37 ºC. Samples were centrifuged at 13000 rpm to remove the solid phase. A certain volume of the supernatant was taken, diluted then analysed by ultraviolet spetrophotometry.

Measurement

The absorbance was then determined at the wavelength of maximum absorption of each drug under study in the thermostated cell set at a temperature of 37 ºC using UV-Vis spectrophotometry.

2.2.2. c. Double Reciprocal Method

Standard and sample solution preparation

- **Micellar mobile phase stock solution preparation**

A stock solution of 10 mM NaDC was prepared. From the stock, several dilutions of the bile salt over the concentration range (0.5 - 9.5 mM) were prepared using deionised water.

- **Sample preparation**

A stock solution of 1 mM of each drug was prepared. A fixed volume of this stock was then diluted with a series of freshly prepared bile salt concentrations over the range (0.5 - 9.5 mM) to prepare 0.05 mM of drug in each corresponding bile salt concentration.

Measurement

The prepared samples were incubated in a water bath at 25 ºC in the dark for 12 hours. The absorbance was then determined at the wavelength of maximum absorption of each drug under study in the thermostated cell set at a temperature of 25 ºC by using UV-Vis spectrophotometry.

2.2.3. Permeation tests

Saturated solubility and solutions of drugs under study

An excess amount of each of the drugs under study in this method (acetaminophen, caffeine, carbamazepine, cimetidine, diclofenac, fenoprofen, fluconazole, flurbiprofen, fosinopril, gemfibrozil, haloperidol, ibuprofen, indomethacin, ketoprofen, leflunomide, lidocaine, linezolid, meloxicam, moexipril, naproxen, phenylbutazone, piroxicam, quinine, theophylline and zolmitriptan) was added to 5 mL PBS in 7 mL vials closed with screw cap and stored at 37 ºC. The solutions were then filtered through 0. 45 µm Nylon filters to remove excess solid and then diluted using PBS to assay for the drug under study using UV spectrophotometry at its wavelength of maximum absorption and already established calibration plot of the drug in PBS.

Preparation of bile salt hydrogel with infinite dose of a drug

A NaDC hydrogel (70 mM) was prepared by gradually adding a certain volume of PBS (a mixture of 0.2 M disodium orthophosphate, sodium dihydrogen orthophosphate and sodium chloride at a pH 7.4) and accurately weighed amount of each of the previously mentioned drugs under study (for the formation of drug saturated hydrogel) to an accurately weighed amount of NaDC in a 50 mL beaker. The mixture of NaDC and drug in PBS was then sonicated in an ultrasonic water bath for 2 minutes until the consistency of the mixture solution thickened and the gel began to form. Stiring was then performed after sonication and the gel allowed to stand for 24 hours to ensure homogenous distribution of the drug throughout the gel.

Instrumentation and measurement

Franz diffusion cells

A set up of six 30 mL-Franz cells were used in the study of the permeation of the drugs from the drug saturated hydrogels in the donor chamber to PBS in the receptor chamber. Each Franz cell was formed of two chambers; donor and receptor chambers held together by clamps with a dialysis membrane cut down to cover the diffusion area (3.14 cm^2) mounted between the two chambers as a support for the hydrogel. A 5 mL sample of the drug saturated hydrogel was placed in the donor chamber while the clean, dried receptor chamber was filled with deaerated PBS and allowed to equilibrate at 37 ºC. All openings including donor top and receptor arm were occluded with parafilm to prevent evaporation. The receptor compartment was stirred at 450 rpm using a six stage magnetic stirrer. Using a glass syringe, sample volumes (1 mL) were extracted for UV assay at the wavelength of

maximum absorption (λ_{max}) of each drug and fresh replacement medium of (PBS) of the same volume kept at 37 ºC was reintroduced into the receptor. Sampling was carried out at 45-minute intervals for a total of 6 hours.

Flow through diffusion cells

A set up of 6 flow through cells were used. Each cell consisted of two compartments; the donor and the receptor compartments fixed together by clamps and screws with a dialysis membrane cut down to cover the diffusion area (0.554 cm^2) mounted in between as a support for the hydrogel placed in the donor compartment. 0.8 mL of the drug saturated hydrogel was placed in the donor chamber while PBS was pumped continuously through the six receptor compartments at a flow rate of 0.52 mL/min using a peristaltic pump. All the cells were kept at a temperature of 37 ºC using a heat conducting cell holder using a water circulator adjusted to the same temperature. The receptor compartment did not need to be stirred as PBS flowed continuously through it. The donor compartments were covered by parafilm to avoid drying of the hydrogel. Samples from the six cells were collected in small 7 mL vials every 45 minutes over a duration of 6 hours. The samples were then taken for UV assay at the wavelength of maximum absorption (λ_{max}) of each drug. The cumulative permeated amount was plotted against time and K_p calculated from the slope.

2.2.4. Scanning Electron Microscopy (SEM)

Electron micrographs of hydrogel with no drug as well as hydrogels saturated with each of the following drugs (carbamazepine and meloxicam) were obtained using a scanning electron microscope (Leica Cambridge S360, UK) operating at 15 kV. The hydrogel samples were freeze dried and mounted on a metal stub with double-sided adhesive tape and coated under vacuum with gold in an argon atmosphere prior to observation. Micrographs with different magnifications were taken to facilitate the study of the morphology of the hydrogels.

2.2.5. Fourier transform infrared (FT-IR)

The FT-IR spectra (650-4000 cm^{-1}) of hydrogels saturated with (caffeine, carbamazepine, fluconazole, meloxicam and piroxicam) each of the previously mentioned drugs under study were dried then recorded using ATR with a FT-IR spectrophotometer (PerkinElmer, UK). Spectra with sharp peaks of reasonable intensity were obtained to consider the stability of the hydrogel after the addition of the drugs.

CHAPTER 3

The Use Of Different Bile Salts In MLC

Chapter 3: Micellar Liquid Chromatography

3.1. Introduction

Having the ability to explore the effects of micelles on the behaviour of compounds, the MLC technique has been known, since its development 30 years ago, for providing different analytical information on a wide variety of compounds. A very important physicochemical property indicating lipophilicity, log P_{mw} was obtained using MLC with different types of surfactants as micellar mobile phases and used over the years in modelling of different pharmacokinetics of compounds.

Prior to this study, there have been no previous reports of the use of bile salts as a micellar mobile phase in MLC. In this chapter a number of novel MLC methods were developed. Sections A to D include the study of the effect of the use of different types of bile salts individually (Methods A, B, C and D) or in a mixture resembling that available physiologically (Method E). Section F includes a study of the use of an amino column with NaDC in MLC. Section G includes a study of the effect of the change of temperature using NaDC in MLC. All the log P_{mw} data obtained from sections A to F were then used in statistical modelling of human intestinal absorption and *in vitro* permeation constants of PAMPA and Caco-2 methods. Data from section G was used in calculation of thermodynamic parameters from the obtained polynomial equations which therefore helped explain how complex the nature of bile salt partitioning process is.

CHAPTER 3

Section (A)

The Use Of NaDC In MLC

(As published in Biomedical Chromatography in March 2016)
See Appendix I

Section (A): Use of sodium deoxycholate (NaDC) as a micellar mobile phase in MLC

3.A.1. Results and Discussion

A set of eleven compounds (anionic, cationic and neutral) were used to evaluate the use of NaDC in MLC. Acetaminophen, caffeine, fluconazole and theophylline represented neutral compounds while fenoprofen, gemfibrozil, indomethacin, ibuprofen, phenylbutazone and salicylic acid represented anionic compounds. Lidocaine represented a cationic compound.

Micelle –water partition coefficients were accurately determined by relating the capacity factors, calculated from the recorded retention times of compounds, to the micellar mobile phase composition which makes the obtained P_{mw} independent of the method flow rate. On the other hand, capacity factors are more susceptible to errors if the dead time is not accurately determined. The effect of dead time on the calculated capacity factors was described in literature, where it greatly affected the determination of some physicochemical properties such as solute-micelle association constants [197]

As a result, dead time was accurately determined for all the surfactant concentrations and an average of all of these determinations was taken. The average value of dead time was determined in this work to be 46.83 seconds.

The pH of the micellar mobile phase was measured at both the lowest (0.005 M) and the highest (0.020 M) concentrations of the mobile phase in order to explore the ionisation state of the compounds and therefore be able to explain interactions between the compounds and the micellar mobile phase and the column.

The pH of the mobile phase was determined to be in the range of (6.4-8.0).

Each compound interacted with the stationary phase and the micelles in the mobile phase in which the surfactant was present at a concentration higher than its CMC.

The surfactant monomers adsorbed on the surface of the mobile phase causing changes in the surface properties of the column thus affecting the retention behaviour of compounds. As a result of the surfactant adsorption on the surface of the column and coating its pores, the silanophilic interaction decreased.

Retention behaviour was greatly affected by the type of column used and the surfactant within the mobile phase. This was expected, for example, Lavine *et al.* reported the hydrophobic alkyl group of SDS was found to interact with a C_8 and C_{18} bonded layer with its polar sulphate head group protruding out rendering the stationary phase more negatively charged. On the other hand, an opposite scenario was found with the cyano-bonded column

where the polar group of SDS strongly binds to the cyanopropyl phase electrostatically. Therefore, the negatively charged SDS head group was hidden in the cyano-bonded phase [198]. Usually, less surfactant tends to be adsorbed on the surface of cyanopropyl columns. Therefore, hydrophobic interactions with compounds in the presence of surfactants are predominant in these kinds of columns and antibinding behaviour can be seen.

In this work a cyanopropyl bonded stationary phase was used with NaDC anionic surfactant. The negatively and positively charged compounds were expected to interact electrostatically with charged surfactants where electrostatic repulsion occurs between the negatively charged compounds and negatively charged surfactant while an electrostatic attraction occurs between the positively charged compounds and the negatively charged surfactant.

The obtained log P_{mw} was considered as an apparent value for ionised compounds since they have higher water solubility than the unionised state [199].

Once the retention times were determined, capacity factors (K') and their inverse (1/K') were calculated. Linear plots of (1/K') against (CM) "concentration of micelles in the mobile phase" were obtained as shown in Figures (14-24). CM was calculated by subtraction of CMC of NaDC in water from total surfactant concentration used. CMC of NaDC in water used in this work was 0.005 M [200].

P_{mw} was calculated from the ratio of the slope and the intercept obtained from plotting (1/K') against (CM) [201, 202].

Table 4: Total & micellar surfactant concentrations used as well as the inverse of the capacity factors (1/K') for 0.2 mM phenylbutazone.

Conc. (M)	CM (M)	1/K'
0.007	0.002	1.118
0.009	0.004	0.996
0.013	0.008	0.875
0.015	0.010	0.875

Table 5: Total & micellar surfactant concentrations used as well as the inverse of the capacity factors (1/K') for 0.2 mM fenoprofen.

Conc. (M)	CM (M)	1/K'
0.007	0.002	1.637
0.011	0.006	1.524
0.017	0.012	1.287
0.020	0.015	1.314

Table 6: Total & micellar surfactant concentrations used as well as the inverse of the capacity factors (1/K') for 0.2 mM salicylic acid.

Conc. (M)	CM (M)	1/K'
0.007	0.002	2.364
0.011	0.006	2.333
0.015	0.01	2.327
0.020	0.015	2.162

Table 7: Total & micellar surfactant concentrations used as well as the inverse of the capacity factors (1/K') for 0.2 mM ibuprofen.

Conc. (M)	CM (M)	1/K'
0.011	0.006	0.870
0.013	0.008	0.886
0.017	0.012	1.013
0.020	0.015	1.041

Table 8: Total & micellar surfactant concentrations used as well as the inverse of the capacity factors (1/K') for 0.2 mM gemfibrozil.

Conc. (M)	CM (M)	1/K'
0.007	0.002	0.969
0.013	0.006	1.058
0.015	0.008	1.181
0.020	0.015	1.320

Table 9: Total & micellar surfactant concentrations used as well as the inverse of the capacity factors (1/K') for 0.2 mM indomethacin.

Conc. (M)	CM (M)	1/K'
0.011	0.006	0.477
0.013	0.008	0.511
0.017	0.012	0.622
0.020	0.015	0.642

Table 10: Total & micellar surfactant concentrations used as well as the inverse of the capacity factors (1/K') for 0.2 mM caffeine.

Conc. (M)	CM (M)	1/K'
0.009	0.004	0.265
0.011	0.006	0.279
0.015	0.01	0.306
0.017	0.012	0.318
0.020	0.015	0.340

Table 11: Total & micellar surfactant concentrations used as well as the inverse of the capacity factors (1/K') for 0.2 mM acetaminophen.

Conc. (M)	CM (M)	1/K'
0.011	0.006	0.540
0.013	0.008	0.550
0.015	0.010	0.573
0.020	0.015	0.593

Table 12: Total & micellar surfactant concentrations used as well as the inverse of the capacity factors (1/K') for 0.2 mM fluconazole.

Conc. (M)	CM (M)	1/K'
0.007	0.002	0.244
0.009	0.004	0.262
0.011	0.006	0.276
0.015	0.01	0.297
0.017	0.012	0.312
0.020	0.015	0.332

Table 13: Total & micellar surfactant concentrations used as well as the inverse of the capacity factors (1/K') for 0.2 mM theophylline.

Conc. (M)	CM (M)	1/K'
0.007	0.002	0.627
0.013	0.008	0.647
0.015	0.010	0.676
0.020	0.015	0.729

Table 14: Total & micellar surfactant concentrations used as well as the inverse of the capacity factors (1/K') for 0.2 mM lidocaine.

Conc. (M)	CM (M)	1/K'
0.009	0.004	1.123
0.011	0.006	1.362
0.017	0.012	1.818
0.020	0.015	2.358

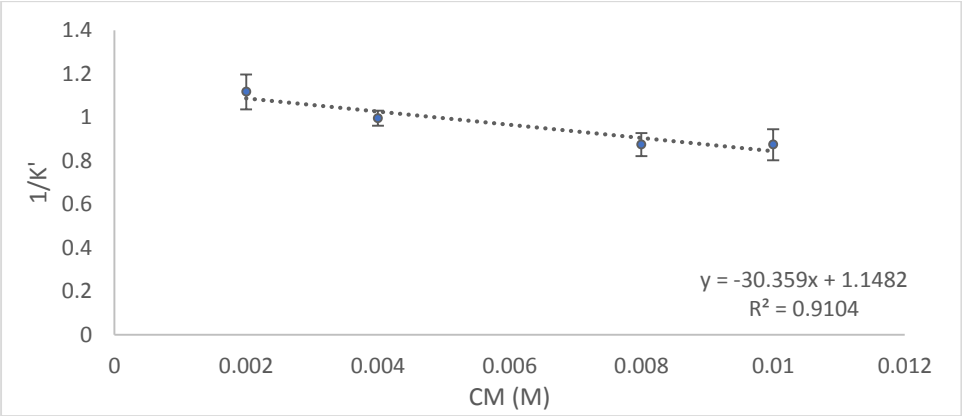

Figure 14: Calibration plot of the inverse of the capacity factor (1/K') versus micellar concentration CM (M) for 0.2 mM phenylbutazone.

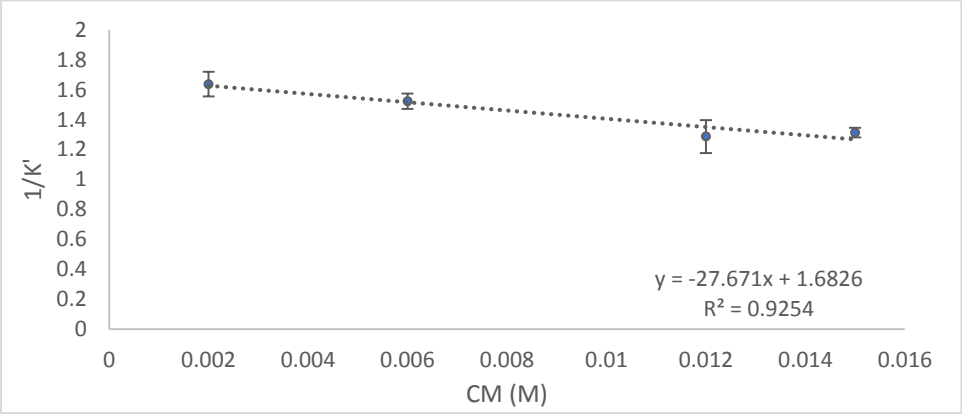

Figure 15: Calibration plot of the inverse of the capacity factor (1/K') versus micellar concentration CM (M) for 0.2 mM fenoprofen.

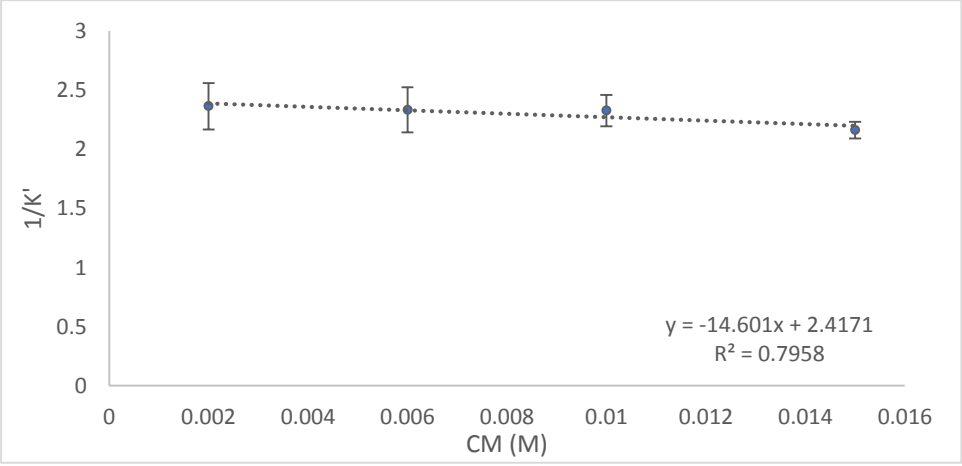

Figure 16: Calibration plot of the inverse of the capacity factor (1/K') versus micellar concentration CM (M) for 0.2 mM salicylic acid.

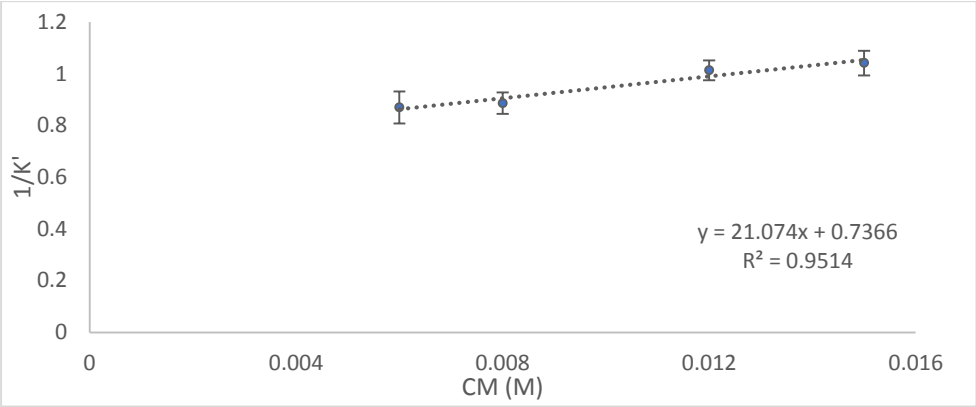

Figure 17: Calibration plot of the inverse of the capacity factor (1/K') versus micellar concentration CM (M) for 0.2 mM ibuprofen.

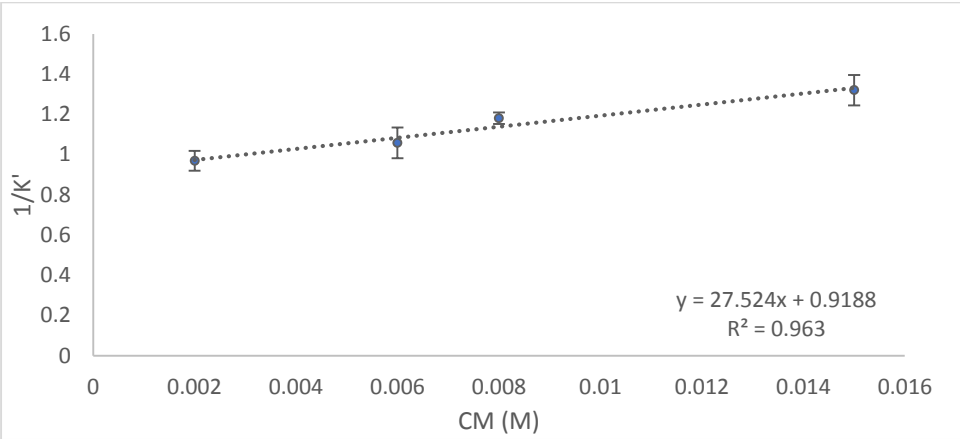

Figure 18: Calibration plot of the inverse of the capacity factor (1/K') versus micellar concentration CM (M) for 0.2 mM gemfibrozil.

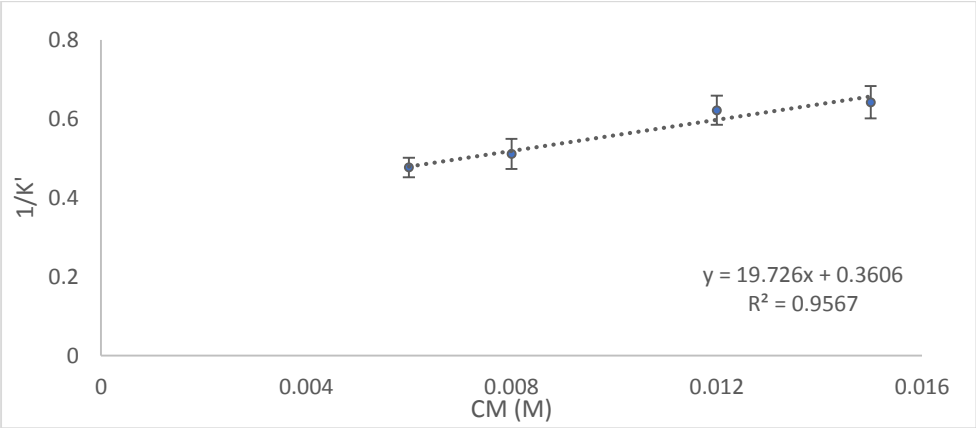

Figure 19: Calibration plot of the inverse of the capacity factor (1/K') versus micellar concentration CM (M) for 0.2 mM indomethacin.

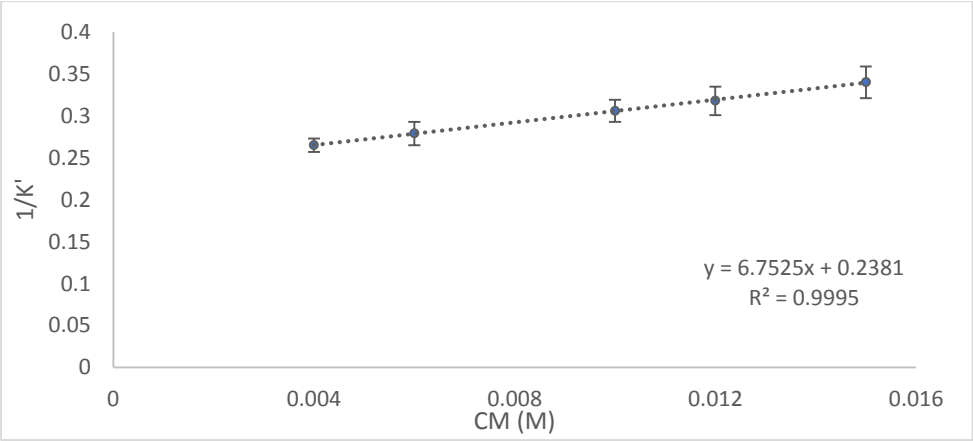

Figure 20: Calibration plot of the inverse of the capacity factor (1/K') versus micellar concentration CM (M) for 0.2 mM caffeine.

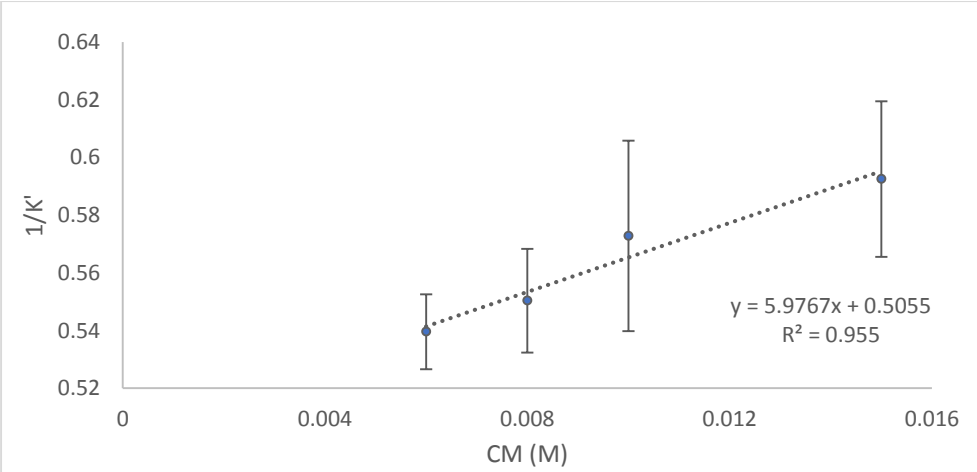

Figure 21: Calibration plot of the inverse of the capacity factor (1/K') versus micellar concentration CM (M) for 0.2 mM acetaminophen.

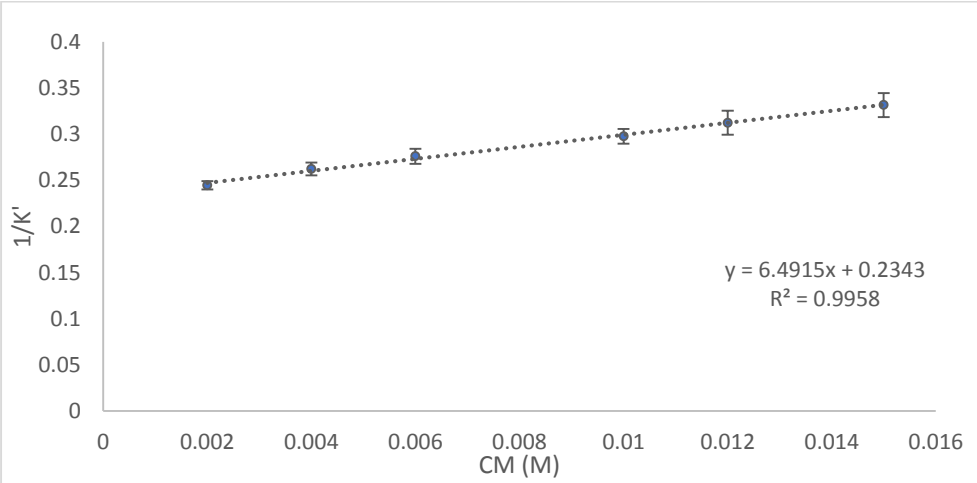

Figure 22: Calibration plot of the inverse of the capacity factor (1/K') versus micellar concentration CM (M) for 0.2 mM fluconazole.

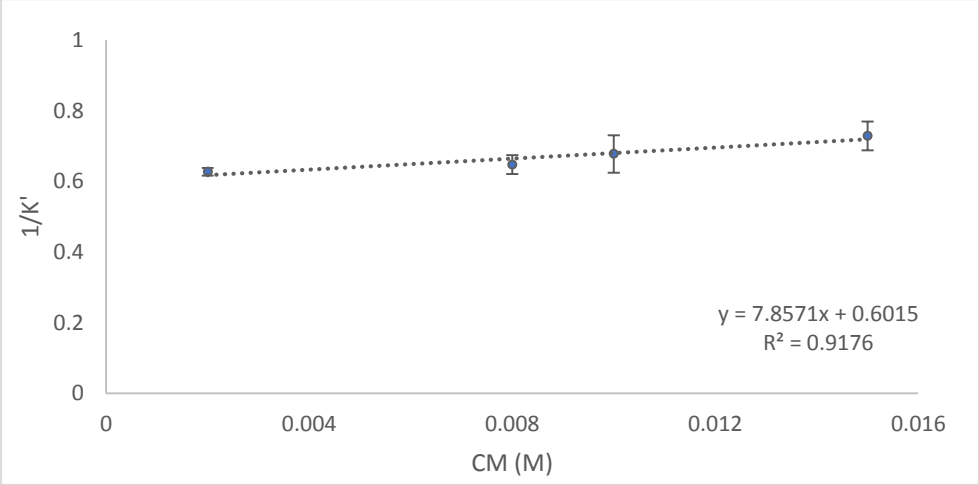

Figure 23: Calibration plot of the inverse of the capacity factor (1/K') versus micellar concentration CM (M) for 0.2 mM theophylline.

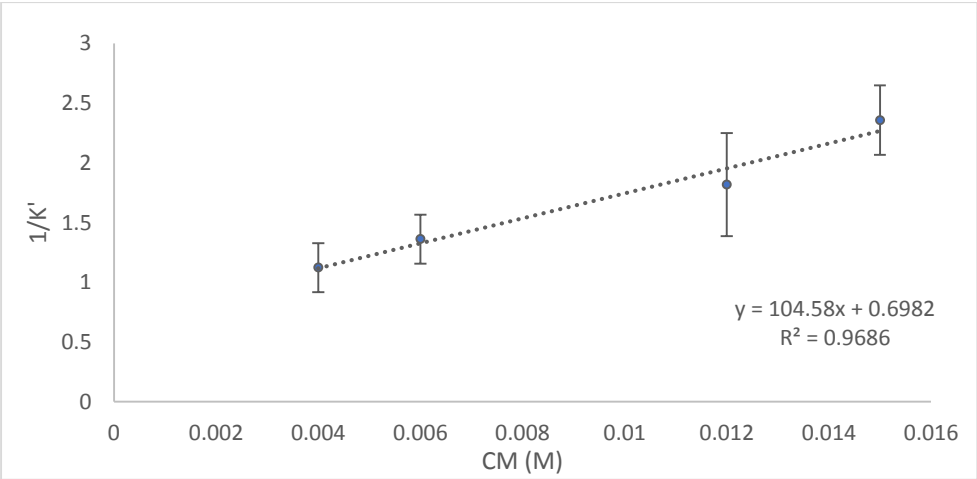

Figure 24: Calibration plot of the inverse of the capacity factor (1/K') versus micellar concentration CM (M) for 0.2 mM lidocaine.

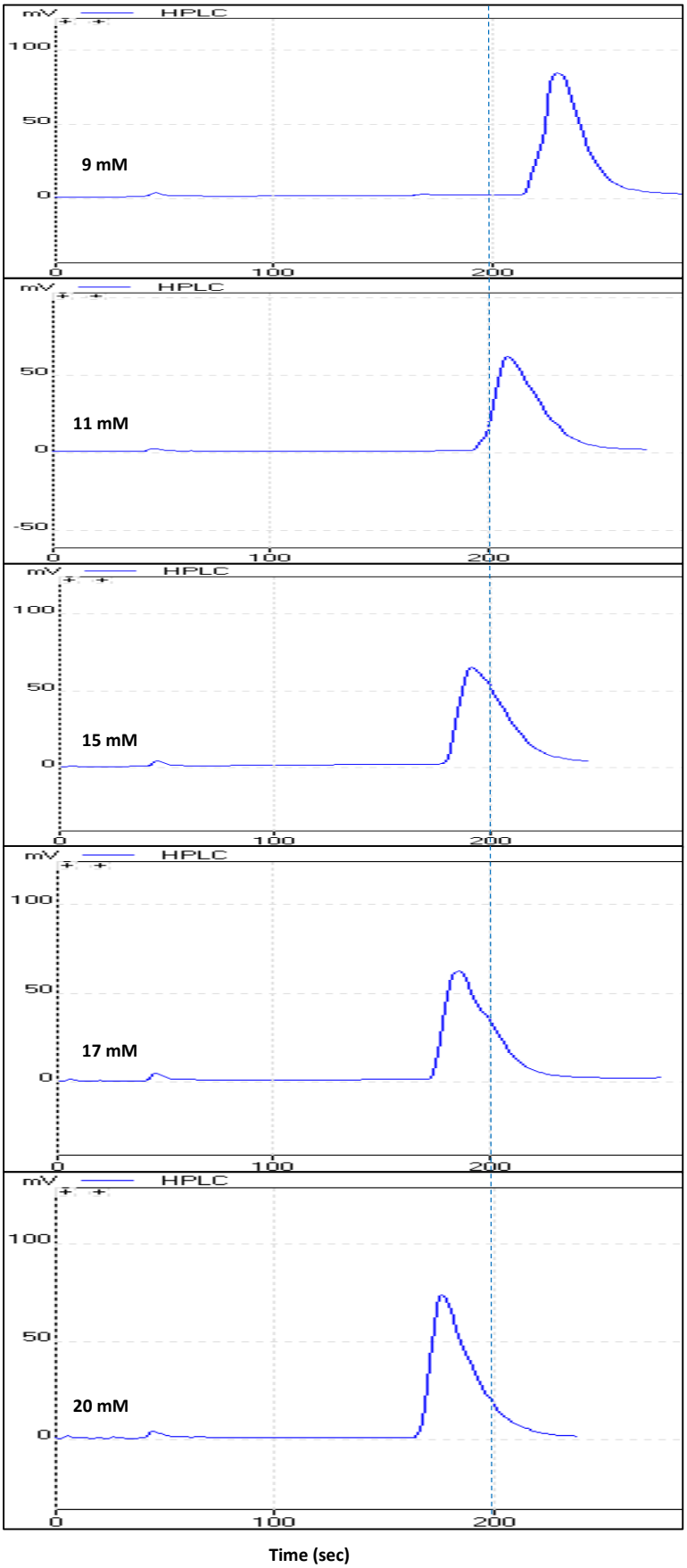

Figure 25: Chromatograms showing binding behaviour of caffeine in different concentrations of NaDC mobile phase. (The dotted line is only used for visual guidance).

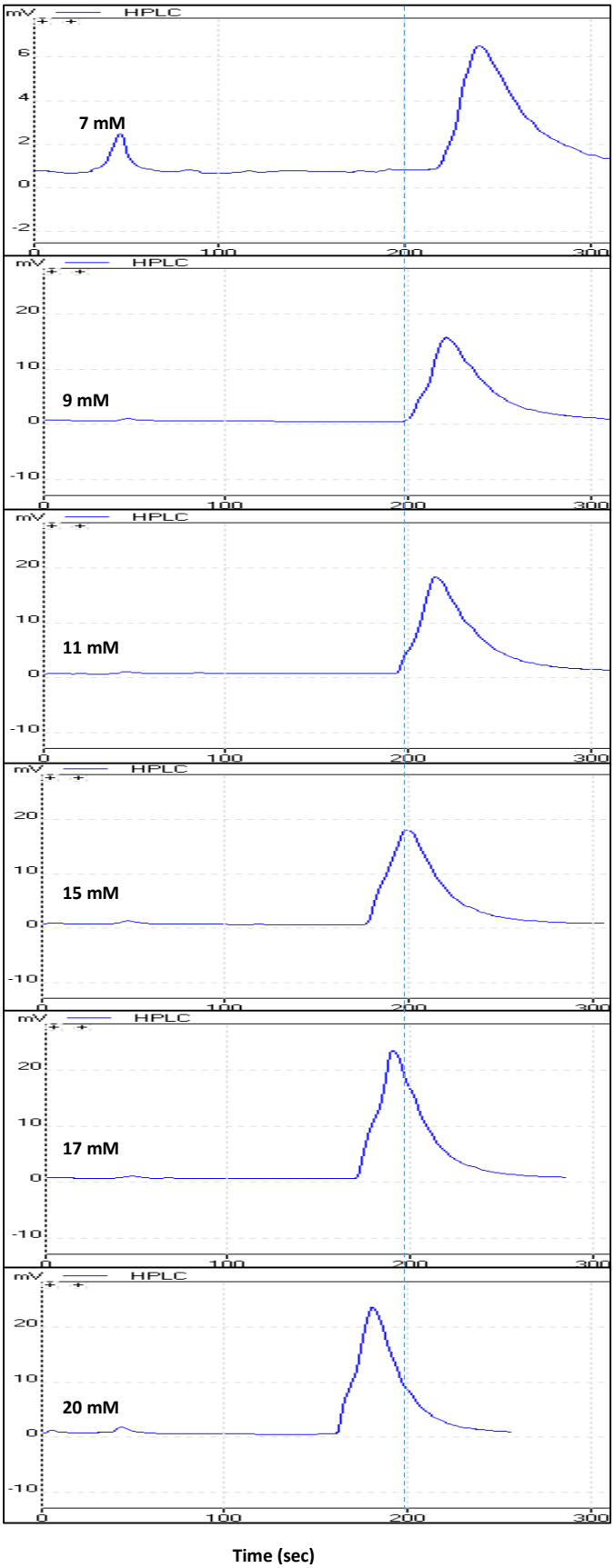

Figure 26: Chromatograms showing binding behaviour of fluconazole in different concentrations of NaDC mobile phase. (The dotted line is only used for visual guidance).

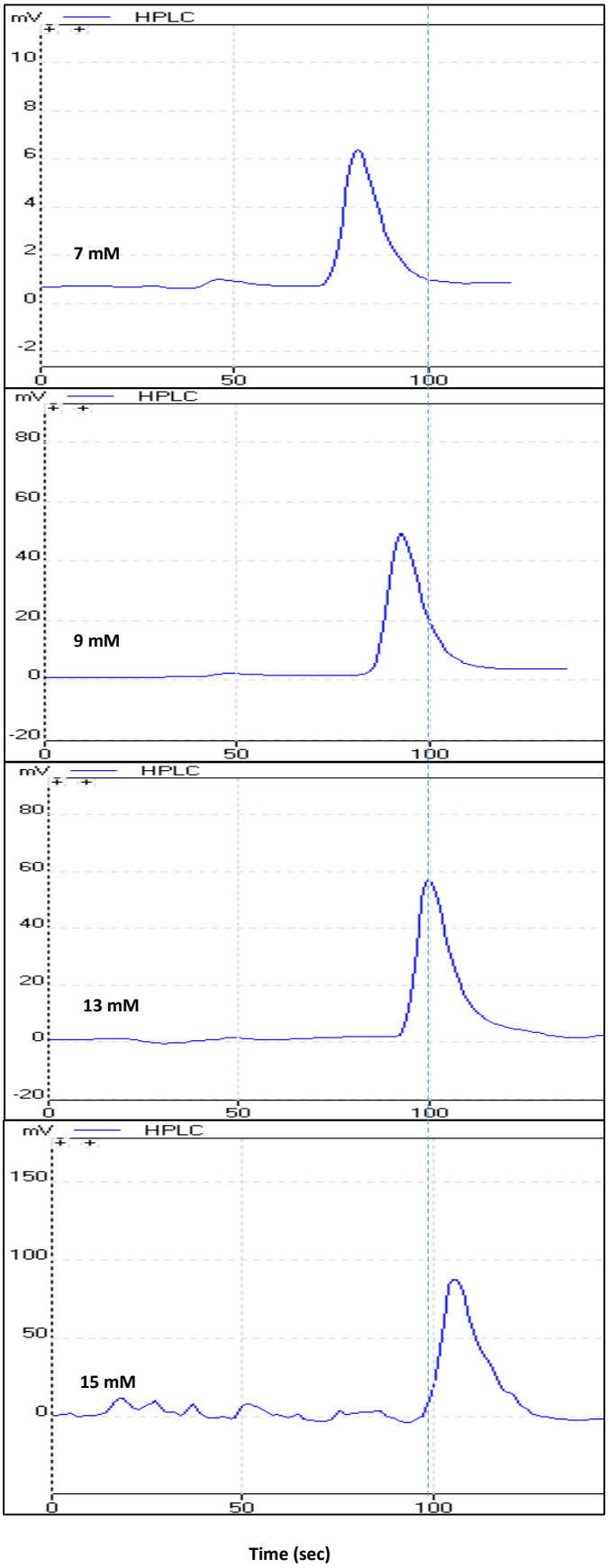

Figure 27: Chromatograms showing antibinding behaviour of phenylbutazone in different concentrations of NaDC mobile phase. (The dotted line is only used for visual guidance).

Table 15: Partition coefficients obtained from the MLC method using NaDC for eleven drugs with their standard deviations against their octanol/water partition coefficients.

Compound	Log P_{mw}	Log $P_{o/w}$ [184]
Acetaminophen	1.26±0.15	0.46
Caffeine	1.45 ± 0.04	-0.07
Fluconazole	1.44±0.07	0.40
Theophylline	1.12±0.27	-0.02
Fenoprofen	1.22±0.7	3.10
Gemfibrozil	1.48±0.04	3.40
Ibuprofen	1.46±0.03	3.97
Indomethacin	1.74±0.02	4.27
Phenylbutazone	1.42±0.003	3.16
Salicylic acid	0.78±0.09	2.26
Lidocaine	2.17±0.16	2.44

In MLC, the increase in the concentration of the micellar mobile phase is expected to result in a decrease in the retention of compounds but this does not apply if the solute-micelle interaction is not strong enough or if the compound undergoes electrostatic repulsion [152]. For compounds which are totally non polar, they reside in the core of the micelle [203].

The location where the compound is incorporated in the micelle is affected to a great extent by the presence of a polar group which represents a small part of the molecule even though the compound is hydrophobic where hydrophobic compounds are mostly expected to be nonpolar.

3.A.1.1. Retention behaviour

A variety of drugs were analysed using the MLC method using NaDC bile salt as a mobile phase to simulate the intestinal environment.

The retention behaviour of selected drugs was observed with an increase in bile salt concentration. Retention times (obtained as an average of 3 replicates for each concentration) were used to calculate the inverse of the capacity factors that were then linearly plotted against each micellar concentration used.

The relevant chromatographic data for eleven selected drugs are represented in Tables 4-14.

Based on these results, two types of behaviour were seen upon increasing the concentration of NaDC; either binding or antibinding behaviour as shown in the selected chromatograms, Figures 25-27.

Anionic drugs such as phenylbutazone, fenoprofen & salicylic acid (pK_a= 4.4, 4.5 & 3 respectively), will be ionised in the mobile phase pH (6.4-7.4). For these drugs the retention time increased with an increase in bile salt concentration (as shown in Tables 4 - 6 and Figures 14 - 16). Antibinding behaviour such as this can be attributed to the repulsion between their negative charge and that of NaDC micelles. Therefore, they are repelled from the hydrophobic core of the micelle and retained on the stationary phase by hydrophobic interactions.

For other anionic drugs (ibuprofen, gemfibrozil and indomethacin) an opposite pattern was observed where the retention times of these drugs decreased with an increase in bile salt concentration (as shown in Tables 7-9 and Figures 17-19). These drugs appear to favour the hydrophobic micellar core more than expected; this might be from possessing more structural apolar properties than the previous drugs. Since water tends to expel apolar solutes this counter-balances the electrostatic repulsion between them and the micelles.

As for neutral drugs, caffeine, acetaminophen, fluconazole and theophylline, they all show decreased retention with an increase in the mobile phase concentration which represents a normal binding phenomenon in MLC thus preference by the compounds for the micelles (as shown in Tables 10-13 and Figures 20-23).

As for the cationic drug, lidocaine, it was expected that it would bind to the micelle through electrostatic interaction and have more chance of residing in the micellar core as a result of hydrophobic interactions. Since this drug is in its ionised form in the mobile phase (pH 6.4-7.4 and pK_a=8.01) it shows normal binding behaviour to the micelle where the retention time decreased with an increase in the concentration of the micellar mobile phase (as shown in Table 14 and Figure 24). In Table 15, the MLC based partition coefficients are listed along with the published octanol-water partition coefficients of the eleven drugs. From this table it was observed that the log P_{mw} of neutral drugs (acetaminophen, caffeine, fluconazole and theophylline) are higher than their log $P_{o/w}$, this increase in the partition coefficient value could be attributed to the preference of these drugs to reside inside the micelle hydrophobic core or at the surface of the micelle. On the other hand, log P_{mw} values were found to be lower than that of log $P_{o/w}$ for the anionic drugs (fenoprofen, phenylbutazone and salicylic

acid) suggesting the preference of these drugs to the aqueous phase promoting greater interactions with the stationary phase than the micelle core. For the anionic drugs (ibuprofen, indomethacin and gemfibrozil) log P_{mw} values were also found to be lower than those of log $P_{o/w}$ suggesting these drugs have a preference for the aqueous phase. However, these drugs displayed binding behaviour suggesting their preference for the micelles. This could be due to these drugs possessing apolar structural properties (as mentioned before) which consequently leads to their partial expelling by water and binding to the micelles' surface through these apolar parts. This gives the drug the chance to associate with the aqueous phase through H-bonding by binding to the micelle at the same time. For the cationic drug lidocaine, the log P_{mw} value was approximately the same as that of log $P_{o/w}$ suggesting its preference for the micelle hydrophobic core leading to its binding behaviour.

3.A.1.2. Method Development

Trials carried out using NaDC in 0.15 M NaCl

During method development a number of trials were carried out using NaDC in 0.15 M NaCl and 0.15 M NaCl with certain ratios of organic modifiers e.g. methanol. Two drugs were analysed (caffeine and acetaminophen) using dilutions of NaDC in 0.15 M NaCl as the micellar mobile phase in an attempt to decrease the electrostatic repulsion between the micelles and therefore decrease the CMC of the bile salt in order to mimic intestinal conditions as 0.15 M NaCl is the physiological concentration of NaCl [176].

Trials of 0.2 mM acetaminophen and caffeine in dilutions of 20 mM of NaDC in 0.15 M NaCl are illustrated in Tables 16-17 and Figures 28-29.

Table 16: Total & micellar concentrations used of NaDC in 0.15M NaCl as well as the inverse of the capacity factors (1/K') for 0.2 mM caffeine.

Conc.(M)	CM (M)	1/k'
0.007	0.004	0.506
0.011	0.008	0.473
0.015	0.012	0.511
0.020	0.017	0.544

Table 17: Total & micellar concentrations used of NaDC in 0.15M NaCl as well as the inverse of the capacity factors (1/K') for 0.2 mM acetaminophen.

Conc. (M)	CM (M)	1/K'
0.007	0.004	1.035
0.011	0.008	1.073
0.015	0.012	1.120
0.020	0.017	1.143

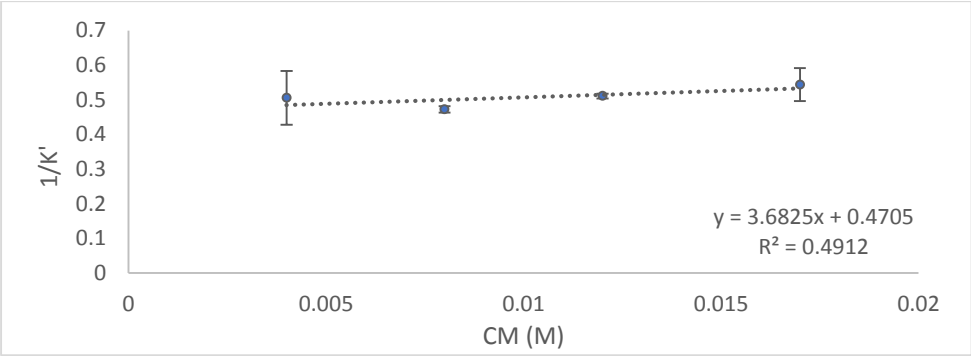

Figure 28: Calibration plot of the inverse of the capacity factor (1/K') versus micellar concentration CM (M) of NaDC in 0.15 M NaCl for 0.2 mM caffeine.
Log P_{mw} = 0.894±0.021

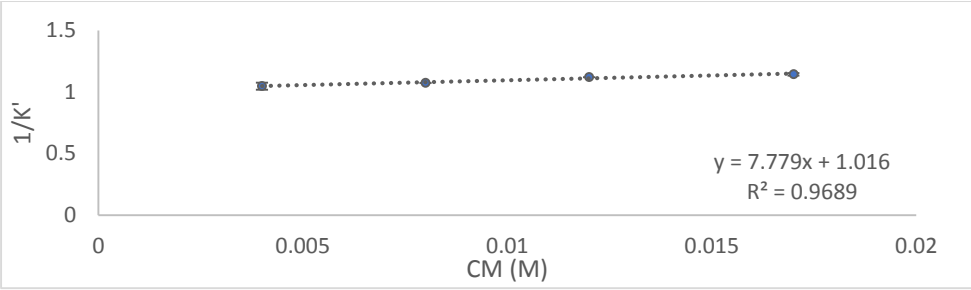

Figure 29: Calibration plot of the inverse of the capacity factor (1/K') versus micellar concentration CM (M) of NaDC in 0.15 M NaCl for 0.2 mM acetaminophen.
Log P_{mw} = 0.884±0.002

Trials of 0.2 mM caffeine in dilutions of 20mM of NaDC in 0.15M NaCl with 10 % methanol are illustrated in Table 18 and Figure 30.

Table 18: Total & micellar concentrations used of NaDC in 0.15M NaCl with 10 % methanol as well as the inverse of the capacity factors (1/K') for 0.2 mM caffeine.

Conc.(M)	CM (M)	1/K'
0.005	0.002	0.906
0.009	0.006	0.870
0.013	0.010	0.838
0.017	0.014	0.790

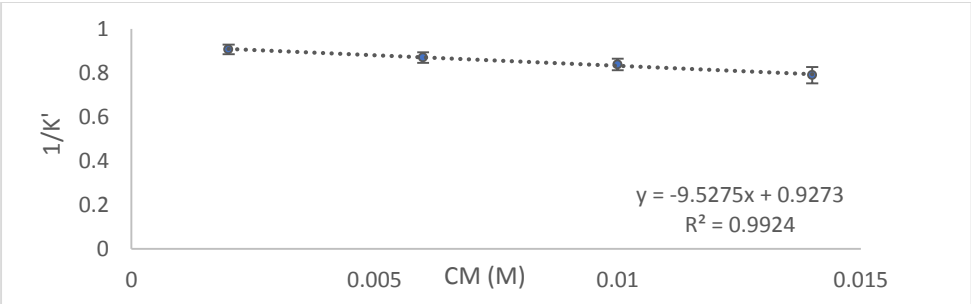

Figure 30: Calibration plot of the inverse of the capacity factor (1/K') versus micellar concentration CM (M) of NaDC in 0.15 M NaCl with 10 % methanol for 0.2 mM Caffeine.
Log P_{mw} =1.012±0.111

It was observed that the viscosity of the mobile phase increased with the increase in concentration of the mobile phase when 0.15 M NaCl was used as a solvent for the preparation of each concentration. As a result,10 % methanol was added to the mobile phase in order to decrease its viscosity and help decrease the back pressure.

In the first trial of caffeine in NaDC in 0.15 M NaCl, a poor correlation between the inverse of the capacity factor (1/K') and micellar concentration (CM) (R^2 = 0.491) was observed. In the second trial the correlation was greatly improved by the addition of 10 % methanol to the mobile phase also an increase in the retention time was observed with the increase in concentration of NaDC. This could be attributed to the ability of methanol to decrease the viscosity of the micellar mobile phase (NaDC in 0.15M NaCl) so caffeine, which has a relatively large molecular weight (194 a.m.u), will move easier in the presence of organic modifier than in its absence. Also the retention behaviour of caffeine changes from binding to antibinding (in trials using NaDC with 0.15 M NaCl and 10 % methanol) where the retention time of caffeine increased with the increase in bile salt concentration which could be due to the drug being sterically hindered by the Na^+ atoms present in the medium that neutralise the charge of the micelles. This prevents its inclusion into, or association with, the micelles in the mobile phase and force it to reside in the stationary phase more than the mobile phase. Correlation between the inverse of the capacity factor (1/K') and micellar concentration (CM) obtained in the case of acetaminophen was better (R^2= 0.992) without the need to add 10 % methanol this could be due it having a lower molecular weight than caffeine. Although the results with NaDC in 0.15 M NaCl and 10 % methanol were relatively good, it was not used as a mobile phase due to the high back pressure also the retention behaviour of caffeine was not typical to what is expected, where it is expected to be binding but it was found to be antibinding. In all of the previous trials the back pressure and background noise were high due to the gelatinous nature of NaDC in 0.15 NaCl. As an attempt to decrease the back pressure by decreasing the viscosity of the gelatinous mobile phase, different ratios of methanol were used with NaDC in 0.15 M NaCl but it was found that a large ratio of methanol had to be added to decrease the background noise and pressure which compromised the stability of the formed micelles in the mobile phase as high amounts of organic solvents destroy micelles.

Also trials included different pH mobile phases, where the mobile phase was prepared at both pH 7.4 and 3.0 using a phosphate buffer mixture. It was observed that the mobile phase turned in to a thick gelatinous matrix at pH 7.4 which cannot be pumped in to the chromatographic system. Precipitation of the mobile phase was observed at pH 3.0 due to

cholic acid precipitating. As a result, NaDC in water was found to be the best mobile phase to be used for this MLC method.

3.A.2. Statistical Modelling

The aim of this part of the work was to expand MLC applications from studying the effect of bile salts on the retention behaviour of drugs to using the data obtained from the retention profile of the diverse set of drugs analysed by the MLC method to calculate their corresponding log P_{mw}. Along with other molecular descriptors (or alone) the obtained log P_{mw} was then used to deduce or develop a model equation correlating the intestinal permeability coefficient obtained experimentally from *in vitro* tests using artificial membranes such as PAMPA or cell cultures (Caco-2 cells) or *in vivo* tests with these descriptors including log P_{mw} by using various statistical methods such as multiple linear regression (MLR). The latter *in vitro* methods are relatively expensive[204], also *in vivo* tests are very rare and their data are limited from the difficulty of carrying out such tests on humans, especially from a moral perspective[67]. Therefore, other cheaper, easier and quick methods are required for assessing such an important pharmacokinetic factor that is intestinal absorption or intestinal permeability.

In the MLC method used in this work biosurfactants were used instead of ordinary synthetic surfactants in order to simulate the intestinal environment to try to get results as close as possible to reality.

3.A.2.1. Statistical Modelling of Human Intestinal absorption (HIA)

After analysis of a group of 20 drugs using NaDC as the mobile phase and then calculation of log P_{mw} (slope/intercept of each calibration plot of (1/K') against CM for each drug), the obtained log P values were used among a number of other molecular descriptors. These included molecular weight (Mwt), polar surface area (PSA), freely rotating bonds (FRB), molar volume (V_M), dissociation constant (pK_a), aqueous solubility (S_w), number of hydrogen bond donors (nHD)and number of hydrogen bond acceptors (nHA). Lipophilicity represented by log P_{mw} experimentally obtained from this work using the MLC method is shown in Table 40. Log $P_{o/w}$ is only included among descriptors just for the purpose of comparison with log P_{mw} to determine the effect of predictability of replacing log P_{mw} in the model equation.

Since Caco-2 and PAMPA methods proved to be successful in prediction of intestinal permeability it was important to try to develop a model equation relating log P_{mw} with each of these methods permeability coefficients obtained from literature and scientific databases as shown in Table 22. Also log P_{mw} was included in a model equation with % HIA experimental values for orally administered drugs (as shown in Table 22) which allows the

prediction of the fraction absorbed of the drug and therefore reflecting the extent of drug absorption in the intestine.

The experimental values for %HIA, PAMPA and Caco-2 were not available for a number of drugs. In addition, some values were removed from each model for being outliers so not all 20 drugs were included in each model construction.

Data analysis was conducted using Minitab 17®. Multiple linear regression analysis was carried out where all the molecular descriptors were included and regressed against the dependant variable [Caco-2 permeability coefficient (log $P_{eff.}$) or PAMPA permeability coefficient (log P_o) or %HIA (%Fa) and backward elimination modelling strategy. Variables with high variance inflation factors (VIF) were removed to take (VIF) to acceptable limits. At the end an optimum model was obtained that provides a good summary of data.

The variables remaining in the optimal model were assessed for significance and relative importance by standardised coefficients and the associated p-values.

The predictive ability of the preferred model was assessed using adjusted-R^2 and R^2 for prediction (R^2_{PRED}) derived from predicted residual error sum of squares (PRESS statistic) which is used to evaluate the predictive ability of the obtained model compared with other candidate models having the same data set. While R^2_{PRED} can indicate the predictive ability of the model itself and consequently reflects the far wider ability to apply the model.

The model obtained for the prediction of %HIA:

$$\text{logit HIA} = -0.410 - 0.482 \log P_{mw} + 0.00852\ \text{Mwt} + 0.04797\ S_w \qquad \text{Eq. (9)}$$

Sixteen drugs were used in the development of the final model. The model's R^2 =86.28 %, $R^2_{adjust.}$= 82.17 % , R^2_{PRED} = 74.97 %, S=0.195

A 95 % confidence interval for log P_{mw} is given by (-0.796, 0.167), t-statistic and standardised coefficient of log P_{mw} are -3.42 ($p<0.05$) and -0.431 respectively suggesting the statistical significance of log P_{mw} as a predictor. Also the F-ratio of the overall model is statistically significant, F=20.97 and P value 0.007 ($p<0.05$). Figure 31 shows no marked relationship between residuals and predicted values through the scattering of points around zero while Figure 32 summarises the model with scatter plots showing a good relationship between the response and the independent variables.

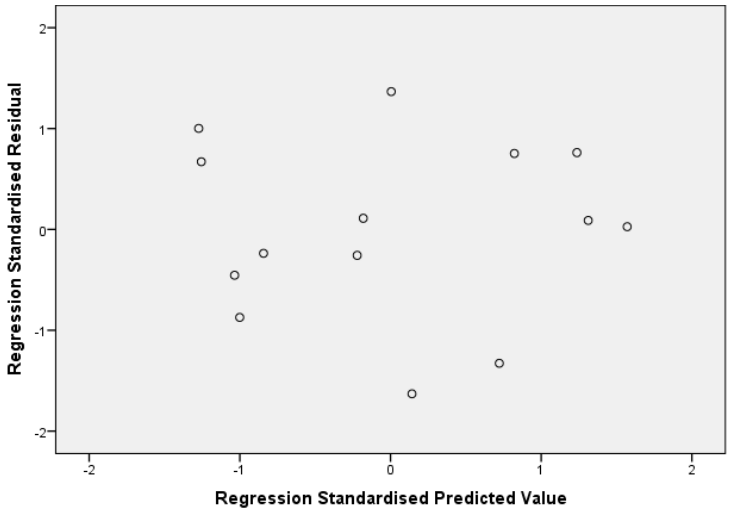

Figure 31: Residual plot for optimal logit HIA regression model.

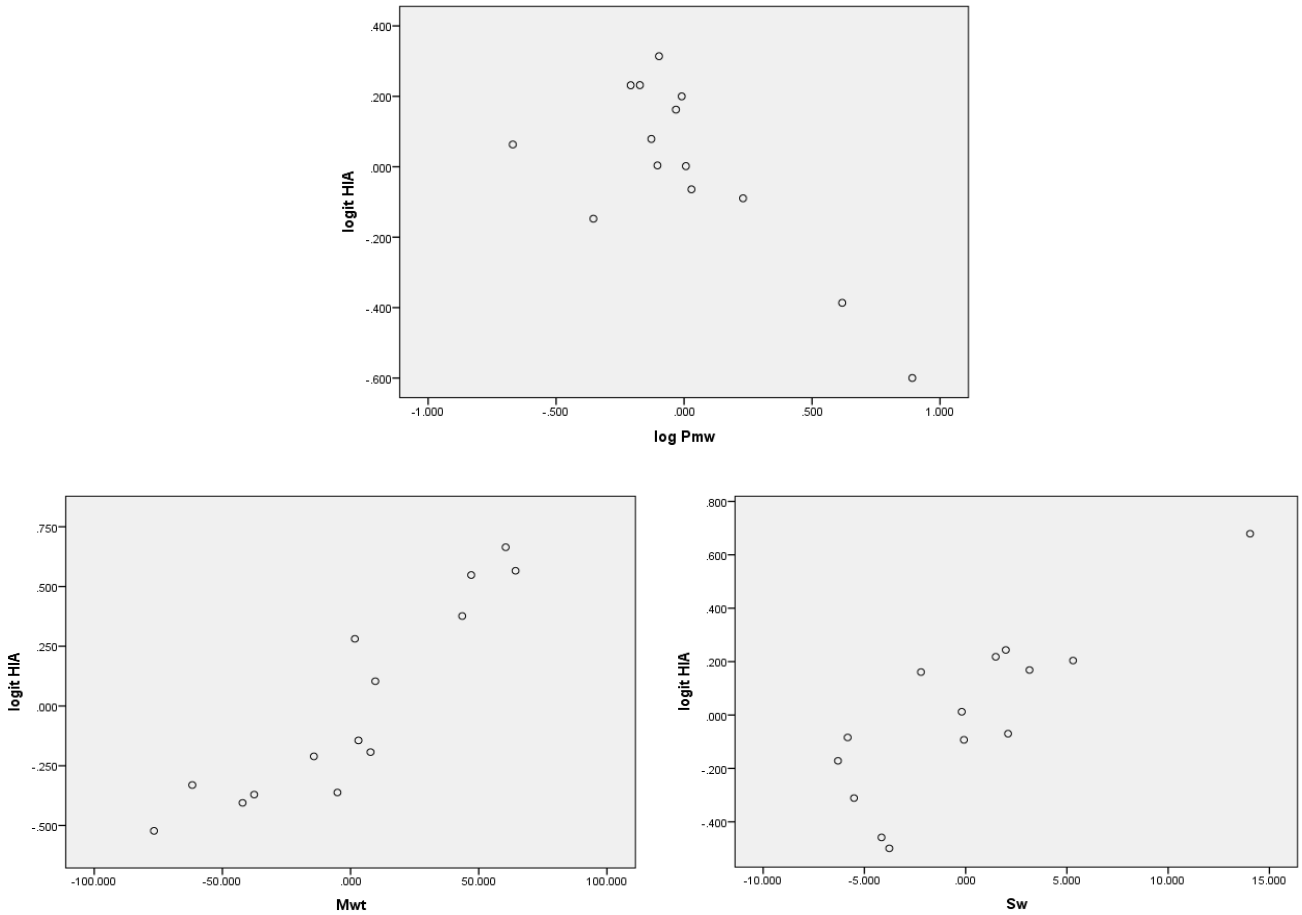

Figure 32: Partial regression plots of experimental logit HIA values against log P_{mw}, Mwt and S_w.

Table 19: Experimentally determined published literature absorption values (Expt. %HIA), calculated and predicted human oral absorption data (Pred. %HIA)

Drug	Expt. %HIA	Pred. %HIA
Acetaminophen	80.00[205]	74.73
Acetylsalicylic acid	82.00[205]	74.40
Diclofenac	97.00[206]	95.85
Diphenhydramine	72.00[205]	79.19
Fenoprofen	85.00[206]	92.18
Fluconazole	97.50[205]	97.40
Gemfibrozil	95.00[207]	91.14
Ibuprofen	80.00[208]	81.65
Indomethacin*	100.00[205]	98.40
Ketoprofen	92.00[205]	95.43
Lidocaine	75.00[209, 210]	78.63
Nicotinic acid	88.00[205]	89.17
Phenylbutazone	98.00[206]	97.21
Piroxicam*	100.00[205]	98.70
Propranolol	90.00[205]	89.54
Theophylline	98.00[33]	97.98

The asterisk (*) indicates the validation compounds.

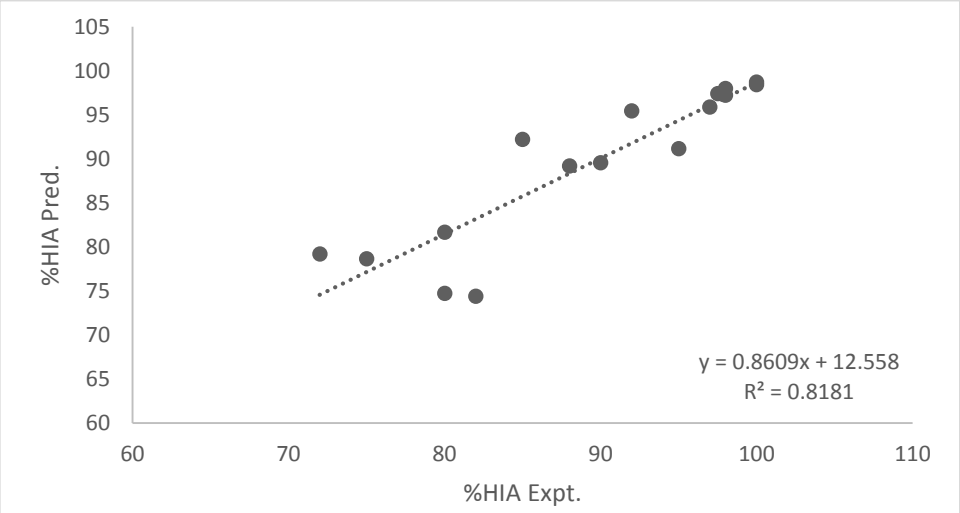

Figure 33: Regression plot of predicted %HIA values against literature %HIA.

In spite of the linear relationship between the published absorption values and experimental log P_{mw} values, logit(Abs) was used to improve this relationship as seen in studies of a similar type [211-213]. The human intestinal absorption values were transformed to logit by substitution in Equation 10, where %HIA = %Human Intestinal Absorption.

$$\text{Logit (\%HIA)} = \log (\text{\%HIA} / (100-\text{\%HIA})) \qquad \text{Eq. (10)}$$

As a result, exclusion of all drugs with absorption percentages of 100 or 0 % from the training set was carried out for simplification. An appropriate equation was developed using multiple linear regression analysis of experimentally determined log P_{mw} alongside a group of molecular descriptors (molecular weight, number of hydrogen bond donors/acceptors, polar surface area, molar volume, freely rotating bonds and solubility). Final model descriptors were assessed for significance and relative importance using standardised coefficients and associated p-values. The standardised coefficients for log P_{mw} (micelle–water partition coefficient), Mwt (molecular weight) and S_w (aqueous solubility) were found to be -0.431, 1.050 and 0.761, respectively, while their p-values at 95 % confidence level were found to be 0.007, 0.000 and 0.001, respectively, proving their statistical significance. Through putting the data together in Tables 19 and 22, a residual plot for optimal regression and partial regression plots of experimental logit(Abs) values against log P_{mw}, Mwt and S_w (Figures 31 and 32) the establishment of an equation using experimental MLC data to predict the percentage of human intestinal absorption *in vivo* was made easier. Overall, as previously stated, the optimal model obtained incorporated 3 descriptors (Equation 9):

$$\text{logit(HIA)} = -0.410 - 0.482 \log P_{mw} + 0.00852\ \text{Mwt} + 0.04799\ S_w \qquad \text{Eq. (9)}$$

where log P_{mw} is the partition coefficient experimentally determined by MLC, Mwt is the molecular weight and S_w is the solubility in water (Table 22). Equation 10 can be used to convert the logit values obtained from Equation 9 into percentage of absorption. R^2=0.86, $R^2_{adj.}$=0.82, $R^2_{Pred.}$=0.75, F = 20.994, Standard error (SE) = 0.195, PRESS=0.7 and Mallows' Cp= 4 where $R^2_{Pred.}$ is defined as the predicted coefficient of determination and it determines the model's predictive power. The predicted residual sum of squares (PRESS) is a statistical term used in the determination of the model's predictive ability when compared with other models of an identical dataset. Mallows's Cp helped in selection of the best model among multiple regression models with a value of 4.0 which is exactly equal to the number of predictors plus the constant showing the model being relatively precise and unbiased in evaluation of the true regression coefficients and predicting future response. The obtained p-values for this model being less than 0.05 indicated statistical significance of the relationship between %HIA and P_{mw} values at the 95 % confidence. An unadjusted R^2 value

of 0.86 obtained from the current data indicated a good fit of the sampled drugs to the model, with about 86 % of the variance in the outcome measure being accounted for by log P_{mw} and other descriptor values included in the final model. A value of 0.75 for $R^2_{Pred.}$ showed suitable fitting of the drugs to the model and verified the potential suitability of MLC using NaDC to predict intestinal drug absorption in the human gastrointestinal tract. Furthermore, log P_{mw} was proved to be a significant predictor in the final model when the experimental log P_{mw} values were replaced with published octanol–water values and there was no predictability of %HIA possible. The 95 % confidence interval for P_{mw}, Mwt and S_w parameter was found to be (-0.796, -0.167), (0.006, 0.011) and (0.026, 0.070) respectively. No marked relationship between residuals and predicted values was found using residual analysis as illustrated. All covariates were statistically significant (t_1 =-3.42, $p< 0.05$ for log P_{mw}; t_1 =-6.93, $p< 0.05$ for molecular weight; t_1=4.84, $p< 0.05$ for aqueous solubility), with the model F-ratio value found to be ($F = 20.99$, $p< 0.05$) suggesting statistical significance of the model. According to studentised residuals or Cook's distance, none of the drugs used in the current dataset for development of the previous model represented by Equation 9 had high residuals or were found to be influential. Also the consistency of the R^2_{adj} and $R^2_{Pred.}$ suggested the absence of any model or data inadequacies in the current model.

In summary, the values presented in Table 19 and plotted in Figure 33 for %HIA predicted with those from literature show remarkably similar trends. For example, differences between the two values are found to be in the range of 0 % (e.g. theophylline) to a maximum of 7.6 % (e.g. acetylsalicylic acid) with the vast majority successfully predicting within 4 % of the literature value. Two extra compounds were investigated, namely indomethacin and piroxicam as a final aspect of investigation to evaluate the success of the model in prediction of %HIA. For indomethacin, with an experimental MLC log P_{mw} value of 1.74 and applying Equation 9, the %HIA was calculated (i.e. predicted) to be 98.4 %. With a literature percentage of human intestinal absorption value of 100 % [205] the model was considered to be a successful method for prediction of *in vivo* behaviour, that is, with <2 % difference between the predicted and literature values. A poorer match was obtained for piroxicam with an experimental MLC log P_{mw} value of 3.37 whereby the published experimental value of %HIA is known to be 100 % [205] and the predicted value was 86.04 %.

3.A.2.2. Statistical Modelling of permeability coefficients obtained from *in vitro* methods (PAMPA and Caco-2).

A key factor for prediction of bioavailability is predicting the extent to which drugs may permeate the intestinal barrier. As previously discussed, several methods are used to predict

intestinal absorption with their data available in published literature allowing comparisons to be made between this MLC-based method and others. Firstly, comparing the MLC method with Caco-2, it can be said that it is comparable in predictive ability but it is simpler, cheaper and faster to carry out. Various values for Caco-2 absorption have been published, such as Stępnik *et al.* work [214], with published data ranging in predictive ability where, in general, the prediction level is similar to the one published in this work. Based on the comparable ability of MLC for prediction along with its various advantages it appears to prove its potential as a method of choice. Secondly, prediction of intestinal absorption has been carried out by artificial membrane based techniques, such as PAMPA. In addition to Caco-2 published data, predictions have been also carried out using PAMPA and their success rates have been generally high as described in the work of Bujard *et al.* (2014) [62]. Again, the MLC method predictive ability shown in this paper is found to be generally comparable with that of an artificial membranes method yet not showing the same limitations as discussed earlier. In addition to their use in the development of a model equation for the prediction of %HIA, experimentally determined log P_{mw} values were used in the prediction of permeability coefficients obtained from PAMPA and Caco-2 which are, as discussed before, two of the most abundant and reliable methods used in the prediction of %HIA using permeability coefficients obtained for a series of model drugs.

3.A.2.2.1. Modelling of permeability coefficients obtained from PAMPA

The model obtained for the prediction of PAMPA log P_o is given by Equation 11:

$$\log P_o = -4.990 + 3.370 \log P_{mw} - 0.4239\, pK_a \qquad \text{Eq. (11)}$$

Fifteen drugs were used in the development of the final model. The model's R^2 =81.80 %, $R^2_{adjust.}$= 78.76 % , R^2_{PRED} = 72.70 %, S=0.831

A 95 % confidence interval for log P_{mw} is given by (2.205, 4.535), t-statistic and standardised coefficient of log P_{mw} are 6.303 ($p<0.05$) and 0.824 respectively suggesting statistical significance of log P_{mw} as a predictor. Also the F-ratio of the overall model is statistically significant, F=26.96 and P value 0.000 ($p<0.05$).

The close agreement of the values of $R^2_{adjust.}$ & R^2_{PRED} indicates that the model does not over-fit the data. The residual analysis did not detect any relationship between residuals and predicted values as shown in Figure 34. The model is shown in Figure 35. The predicted values of PAMPA log P_o were found to be in accordance with the experimental values reported in literature as shown in Table 20 and Figure 36.

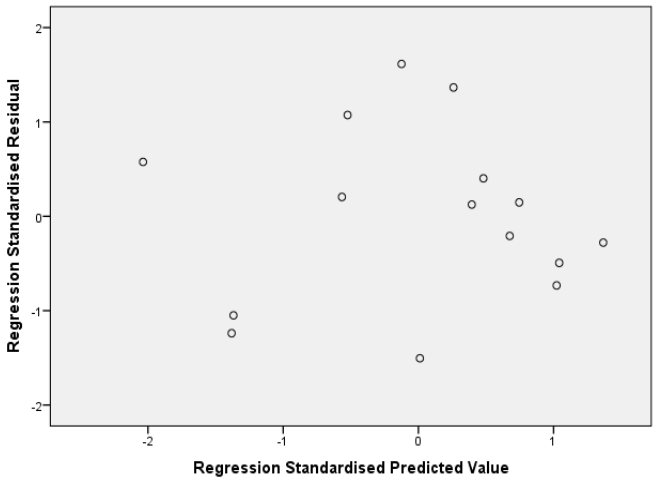

Figure 34: Residual plot for optimal PAMPA regression model.

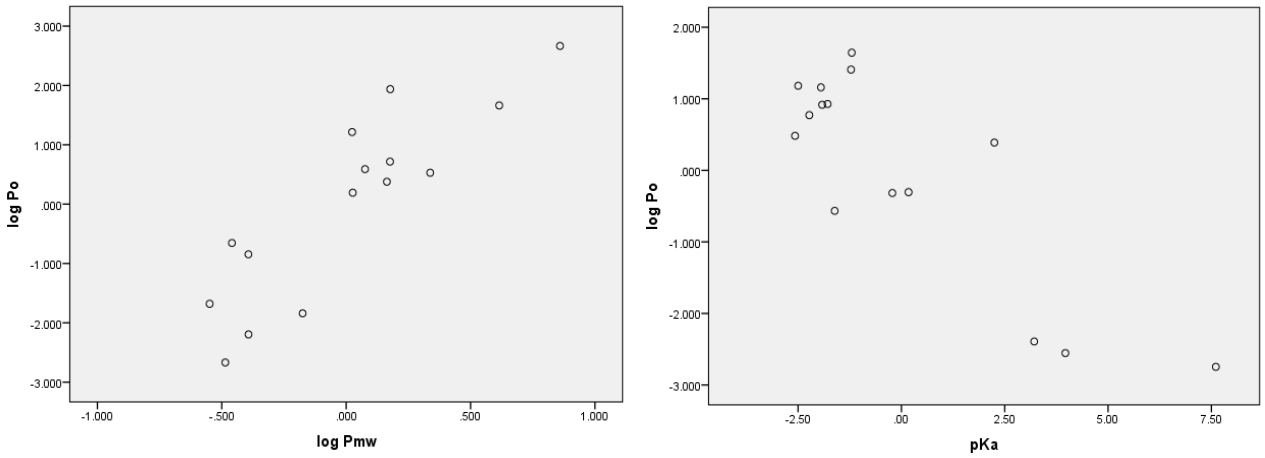

Figure 35: Partial regression plots of experimental log P_o values against log P_{mw} and pK_a.

Table 20: Experimental and predicted values for PAMPA logP_o.

Drug	Expt. PAMPA log P_o [215]	Pred. PAMPA log P_o
Acetaminophen	-5.81	-4.94
Benzoic acid	-3.94	-2.69
Caffeine	-5.55	-6.03
Diclofenac	-1.37	-1.49
Diphenhydramine	-0.71	-0.48
Flurbiprofen	-1.78	-1.61
Gemfibrozil	-1.59	-1.92
Ibuprofen	-1.15[64]	-2.29
Indomethacin	-1.65	-1.04
Ketoprofen	-2.67	-3.56
Lidocaine	-1.42	-1.01
Phenylbutazone	-1.96	-2.06
Propranolol	-1.57[64]	-2.91
Salicylic acid	-3.46[64]	-3.63
Theophylline	-5.99	-4.96

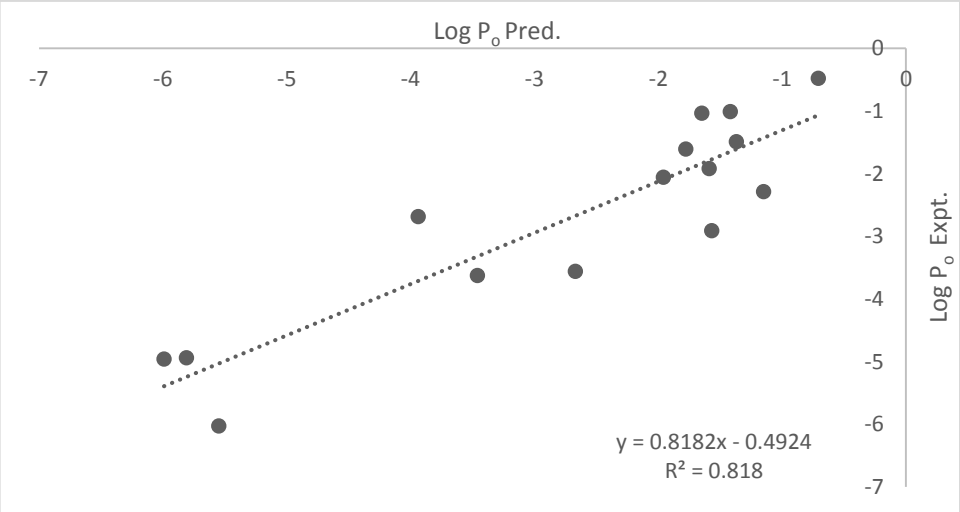

Figure 36: Plot of experimental vs. predicted PAMPA log P_o values.

3.A.2.2.2. Modelling of permeability coefficients obtained from Caco-2 $P_{eff.}$

The model obtained for the prediction of Caco-2 $P_{eff.}$ is shown by Equation 12:

$$\log P_{eff.} = -3.7004 + 0.2138 \log P_{mw} - 0.002953\ Mwt - 0.2510\ nHD + 0.01622\ S_w \quad \text{Eq. (12)}$$

Thirteen drugs were used in the development of the final model. The model's R^2 =98.08 %, $R^2_{adjust.}$= 97.13 % , R^2_{PRED} = 95.14 %, S= 0.035

A 95 % confidence interval for log P_{mw} is given by (0.169, 0.258). t-statistic and standardised coefficient of log P_{mw} are 11.047 ($p<0.05$) and 0.686 respectively suggesting statistical

significance of log P_{mw} as a predictor. Also the F-ratio of the overall model is statistically significant, F= 102.393 and P value 0.000 ($p<0.05$).

Figure 37 shows no marked relationship between residuals and predicted values while Figure 38 summarises the model. A close agreement between both the predicted and experimental log $P_{eff.}$ was found as shown in Table 21 and Figure 39.

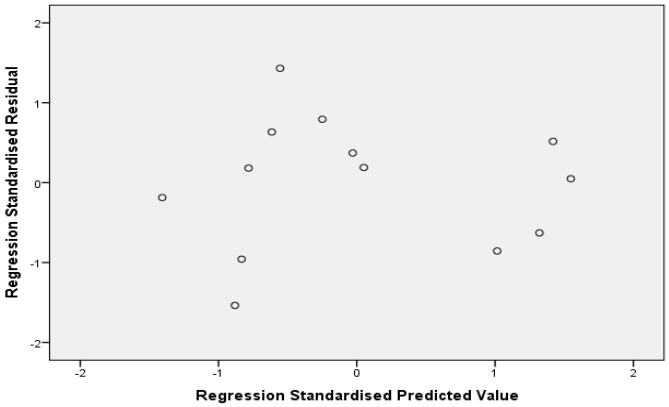

Figure 37: Residual plot for optimal Caco-2 regression model.

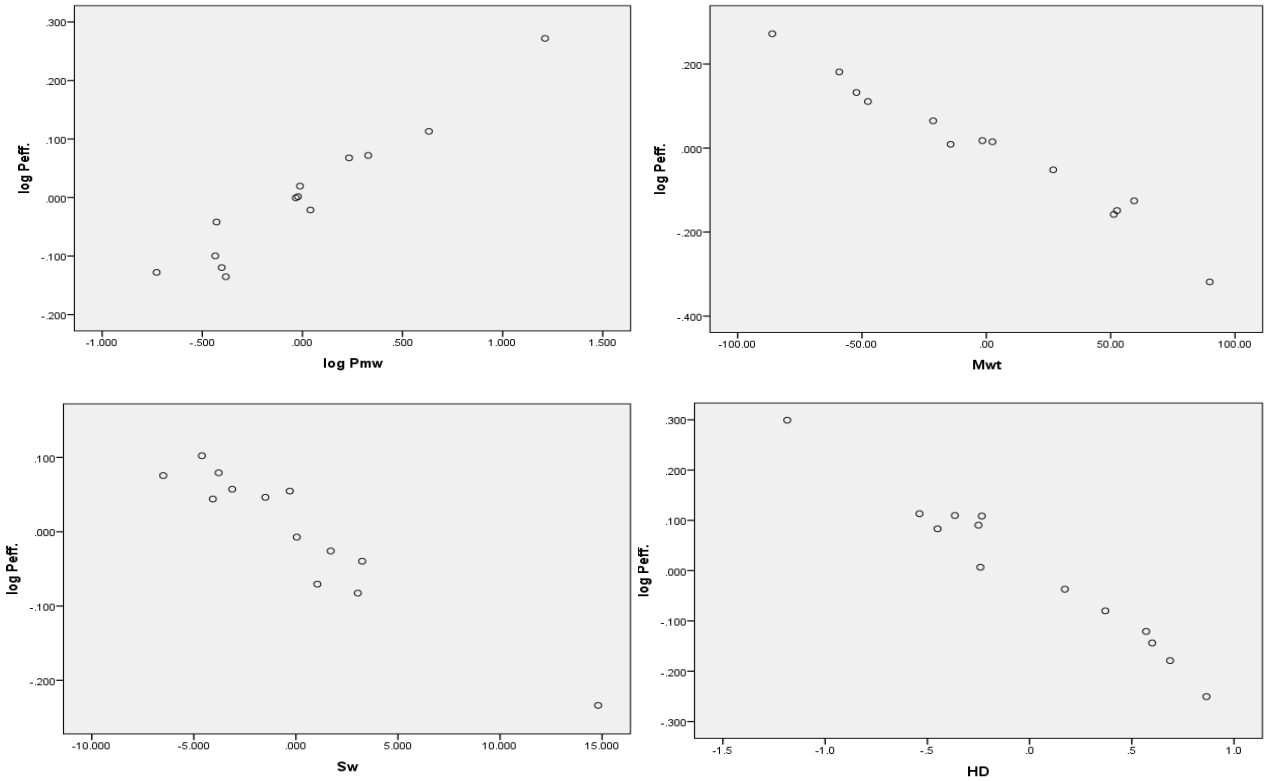

Figure 38: Partial regression plots of experimental Caco-2 log $P_{eff.}$ values against log P_{mw}, Mwt, HD and S_w.

Table 21: Experimental and predicted values for Caco-2 log $P_{eff.}$.

Drug	Expt. Caco-2 log $P_{eff.}$	Pred. Caco-2 log $P_{eff.}$
Acetaminophen	-4.44[56]	-4.45
Benzoic acid	-4.15[56]	-4.17
Caffeine	-4.14[215]	-4.14
Diclofenac	-4.75[56]	-4.74
Fluconazole	-4.52[216]	-4.57
Ibuprofen	-4.28[216]	-4.25
Indomethacin	-4.69[60]	-4.64
Ketoprofen	-4.48[56]	-4.51
Lidocaine	-4.21[217]	-4.19
Piroxicam	-4.45[60]	-4.46
Propranolol	-4.56[60]	-4.58
Salicylic acid	-4.66[60]	-4.63
Theophylline	-4.61[56]	-4.62

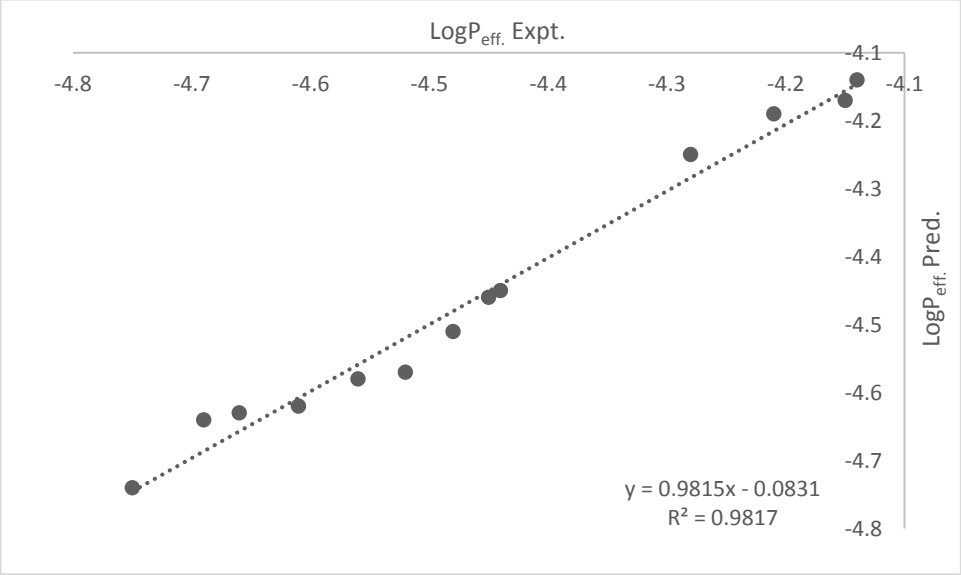

Figure 39: Plot of experimental vs predicted Caco-2 log $P_{eff.}$ values.

Table 22: A summary of molecular descriptors for the selected drugs analysed by MLC using NaDC in water and the reported experimental values of %HIA and permeability coefficients of PAMPA and Caco-2 tests.

Drug	Log P_{mw}	log $P_{o/w}$[184]	Mwt[218]	pK_a[184]	S_w [184]	HD[218]	HA[218]	FRB[218]	PSA[219]	V_M[218]	log P_o[215]	log $P_{eff.}$	%HIA
Acetaminophen	1.26	0.46	151.2	9.90[220]	4.15	2	2[184]	1	49.3	131.1	-5.81	-4.44[56]	80[205]
Acetylsalicylic acid	1.52	1.19	180.16	4.19	1.46	1	4	3	63.6	139.6	NA	NA	82[205]
Benzoic Acid	1.21	1.87	122.12	4.20[221]	7.08	1	2	1	37.0	102.0	-3.94	-4.15[56]	NA
Caffeine	1.45	-0.07	194.19	14.0[222]	11	0	6	0	58.0	133.4	-5.55	-4.14[215]	NI
Diclofenac	1.56	4.51	296.15	4.15	0.00447	2	3	4	49.3	206.8	-1.37	-4.75[56]	97[206]
Diphenhydramine	2.47	3.27	255.35	9.0	0.0752	0	2	6	12.5	249.2	-0.71	NA	72[205]
Fenoprofen	1.22	3.10	242.27	4.5	0.0811	1	3	4	46.5	204.7	NA	NA	85[206]
Fluconazole	1.44	0.40	306.27	12.71	1.39	1	7	5	81.6	205.3	NA	-4.53[216]	97.5[205]
Flurbiprofen	1.56	4.16	244.26	4.42	0.0249	1	2	3	37.0	203.6	-1.78	NA	NI
Gemfibrozil	1.48	3.40	250.33	4.5[219]	0.0278	1	3	6	46.5	239.7	-1.59	NA	95[207]
Ibuprofen	1.46	3.97	206.28	5.2[223]	0.0684	1	2	4	37.3	200.3	-1.15[64]	-4.28[216]	80[208]
Indomethacin	1.74	4.27	357.79	4.5	0.0024	1	4[184]	4	68.5	269.6	-1.65	-4.69[60]	100[205]
Ketoprofen	0.91	3.12	254.28	3.88	0.0213	1	3	4	54.4	212.2	-2.67	-4.48[56]	92[205]
Lidocaine	2.18	2.44	234.34	7.9[224]	0.593	1	2[184]	5	32.3	238.8	-1.42	-4.21[217]	75[209, 210]
Nicotinic acid	1.22	0.36	123.11	4.75	18	1	3	1	50.2	95.2	NA	NA	88[205]
Phenylbutazone	1.42	3.16	308.37	4.4[225]	0.144	0	2[184]	5	40.6	262.8	-1.96	NA	98[206]
Piroxicam	3.37	3.06	331.35	6.3	0.023/0.14	2	6[219]	2	108.0	222.8	NI	-4.45[60]	100[205]
Propranolol	1.81	3.48	259.34	9.5[226]	0.0794	2	3	6	41.5	237.2	-1.57[64]	-4.56[60]	90[205]
Salicylic acid	0.78	2.26	138.12	3.0[227]	11.3	2	3	1	58.0	100.4	-3.46[64]	-4.66[60]	NI
Theophylline	1.12	-0.02	180.16	8.8[228]	22.9	1	3[184]	0	69.3	122.9	-5.99	-4.61[56]	98[33]

NA: no available data, NI: value not included in training set.

3.A.3. Conclusion

Prior to this work MLC has been considered in a limited manner with the use of simpler and conventional surfactant systems, such as sodium dodecyl sulfate and Brij 35. The advantage of using bile salt surfactants can be clearly seen in the enhanced predictive ability due to the increased similarity to the *in vivo* environment.

A good prediction of intestinal absorption using MLC is considered to be an exciting advance in analysis for many reasons, not only for the replacement of using animal models but also to enhance the development of new drugs therefore, saving time and money. Based on analysis for the model compounds it has been found that NaDC can be used for prediction of human intestinal absorption as well as for prediction of the PAMPA and Caco-2 permeability coefficients which are also used in prediction of HIA.

CHAPTER 3

Section (B)

The Use Of NaTDC In MLC

Section (B): Use of sodium taurodeoxycholate (NaTDC) as a micellar mobile phase in MLC

3.B.1. Introduction

In this section a set of ten compounds (anionic, cationic and neutral) were used to evaluate the use of NaTDC in MLC. Acetaminophen, caffeine, fluconazole and theophylline represented neutral compounds while fenoprofen, gemfibrozil, ibuprofen, phenylbutazone and salicylic acid represented anionic compounds. The cationic compound used was lidocaine.

Micelle-water partition coefficients were accurately determined in the same way explained in Section (3A) by relating the capacity factors, calculated from the recorded retention times of compounds, to the micellar mobile phase composition.

Dead time was accurately determined for all the surfactant concentrations and an average of all of these determinations was taken. The average value of dead time was determined in this work to be 44.82 seconds which is close to that of NaDC.

The pH of the micellar mobile phase was measured at both the lowest (0.006 M) and the highest (0.020 M) concentrations of the mobile phase in order to have an idea about the ionisation state of the used compounds and therefore be able to explain the expected kind of interactions between the used compounds and the micellar mobile phase and the column. The pH of the mobile phase was determined to be in the range of 5.2-6.1.

3.B.2. Results & Discussion

3.B.2.1. Retention behaviour

The injected test compounds are said to interact with: the stationary phase, the micelles in the micellar mobile phase and the water in between. The stationary phase was represented by the cyanopropyl column (CN-RP) used in this work while the micellar mobile phase used was NaTDC. As mentioned before in Section (3A) a small amount of the used surfactant in the mobile phase (NaTDC in this section) is adsorbed on the surface of the used CN-RP column. The CMC of NaTDC in water used in this work was 0.006 M [229].

P_{mw} was calculated from the ratio of the slope and the intercept obtained from linear plots of (1/K') against (CM) represented by Tables 23-32 and Figures 40-49.

Table 23: Total & micellar concentrations used of NaTDC in water as well as the inverse of the capacity factors (1/K') for 0.2 mM phenylbutazone.

Conc. (M)	CM (M)	1/K'
0.008	0.002	0.196
0.010	0.004	0.168
0.012	0.006	0.154
0.016	0.010	0.120

Table 24: Total & micellar concentrations used of NaTDC in water as well as the inverse of the capacity factors (1/K') for 0.2 mM fenoprofen.

Conc. (M)	CM (M)	1/K'
0.008	0.002	0.466
0.010	0.004	0.442
0.014	0.008	0.396
0.016	0.01	0.367

Table 25: Total & micellar concentrations used of NaTDC in water as well as the inverse of the capacity factors (1/K') for 0.2 mM salicylic acid.

Conc. (M)	CM (M)	1/K'
0.008	0.002	0.894
0.010	0.004	0.833
0.012	0.006	0.784
0.014	0.008	0.742
0.020	0.014	0.594

Table 26: Total & micellar concentrations used of NaTDC in water as well as the inverse of the capacity factors (1/K') for 0.2 mM ibuprofen.

Conc. (M)	CM (M)	1/K'
0.010	0.004	0.285
0.012	0.006	0.289
0.014	0.008	0.308
0.020	0.014	0.360

Table 27: Total & micellar concentrations used of NaTDC in water as well as the inverse of the capacity factors (1/K') for 0.2 mM gemfibrozil.

Conc. (M)	CM (M)	1/K'
0.007	0.001	0.575
0.008	0.002	0.580
0.010	0.004	0.585
0.012	0.006	0.599

Table 28: Total & micellar concentrations used of NaTDC in water as well as the inverse of the capacity factors (1/K') for 0.2 mM caffeine.

Conc. (M)	CM (M)	1/K'
0.007	0.001	0.262
0.012	0.006	0.290
0.014	0.008	0.301
0.016	0.010	0.303

Table 29: Total & micellar concentrations used of NaTDC in water as well as the inverse of the capacity factors (1/K') for 0.2 mM acetaminophen.

Conc. (M)	CM (M)	1/K'
0.008	0.002	0.567
0.010	0.004	0.585
0.014	0.008	0.606
0.016	0.010	0.608

Table 30: Total & micellar concentrations used of NaTDC in water as well as the inverse of the capacity factors (1/K') for 0.2 mM fluconazole.

Conc. (M)	CM (M)	1/K'
0.007	0.001	0.433
0.010	0.004	0.451
0.016	0.010	0.493
0.020	0.014	0.528

Table 31: Total & micellar concentrations used of NaTDC in water as well as the inverse of the capacity factors (1/K') for 0.2 mM theophylline.

Conc. (M)	CM (M)	1/K'
0.008	0.002	0.435
0.012	0.006	0.457
0.016	0.010	0.466
0.020	0.014	0.499

Table 32: Total & micellar concentrations used of NaTDC in water as well as the inverse of the capacity factors (1/K') for 0.2 mM lidocaine.

Conc. (M)	CM (M)	1/K'
0.007	0.001	1.038
0.008	0.002	1.063
0.012	0.006	1.353
0.016	0.010	1.563

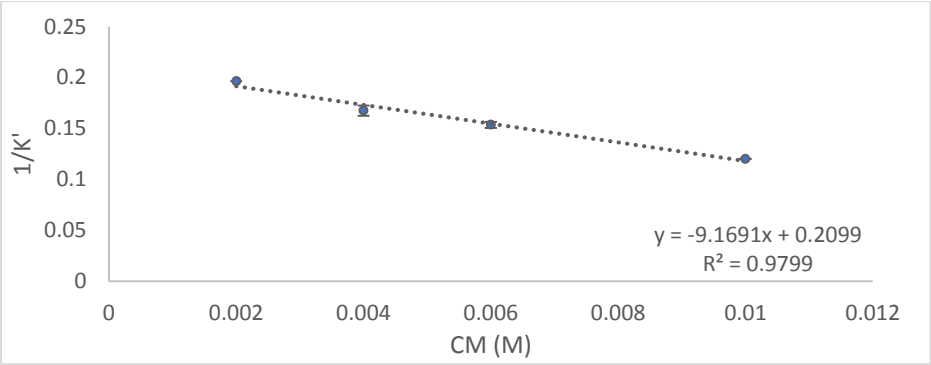

Figure 40: Calibration plot of the inverse of the capacity factor (1/K') versus micellar concentration CM (M) of NaTDC in water for 0.2 mM phenylbutazone.

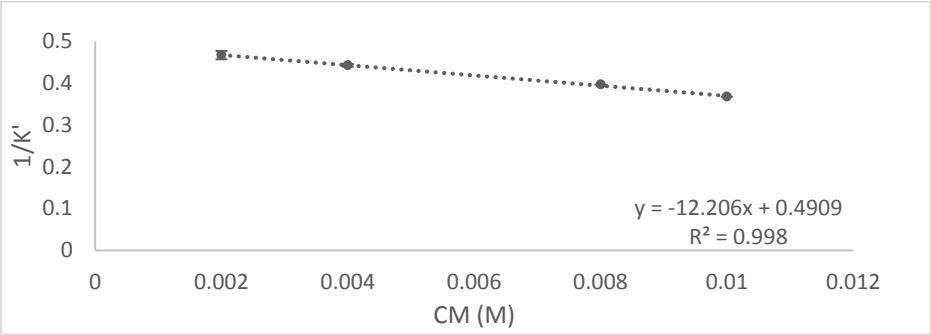

Figure 41: Calibration plot of the inverse of the capacity factor (1/K') versus micellar concentration CM (M) of NaTDC in water for 0.2 mM fenoprofen.

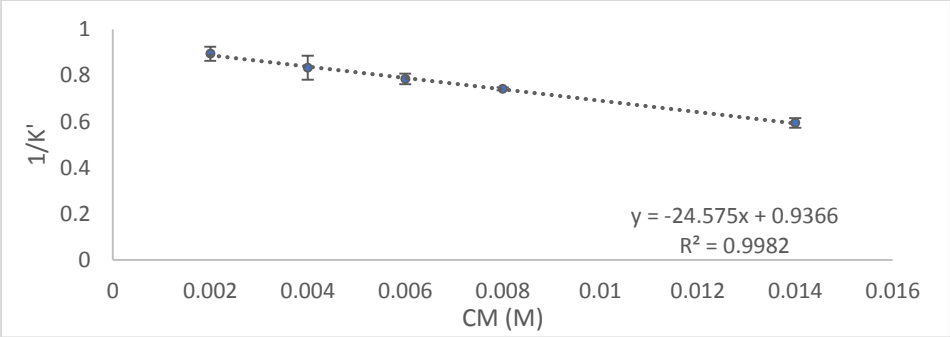

Figure 42: Calibration plot of the inverse of the capacity factor (1/K') versus micellar concentration CM (M) of NaTDC in water for 0.2 mM salicylic acid.

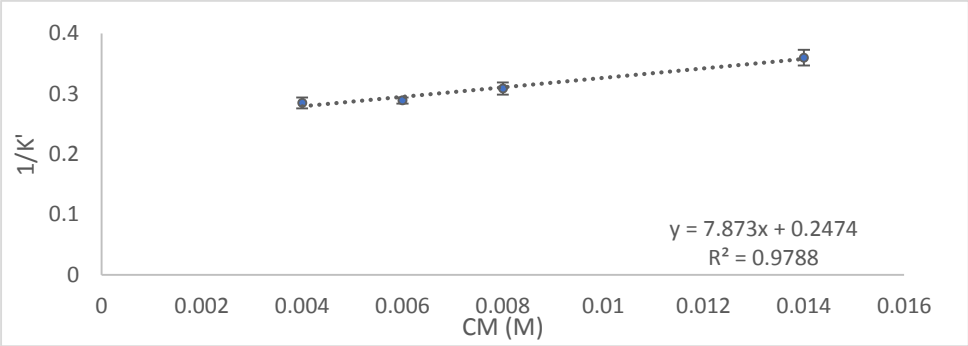

Figure 43: Calibration plot of the inverse of the capacity factor (1/K') versus micellar concentration CM (M) of NaTDC in water for 0.2 mM ibuprofen.

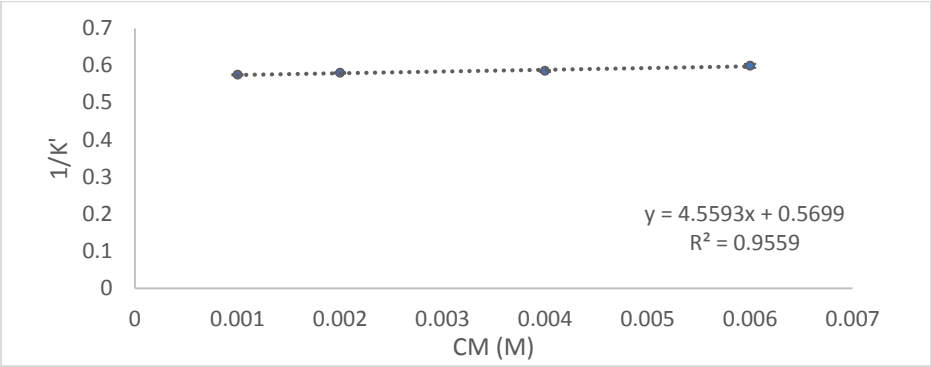

Figure 44: Calibration plot of the inverse of the capacity factor (1/K') versus micellar concentration CM (M) of NaTDC in water for 0.2 mM gemfibrozil.

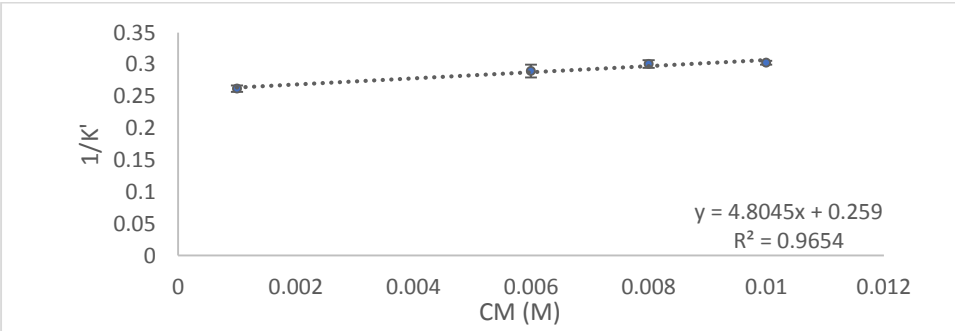

Figure 45: Calibration plot of the inverse of the capacity factor (1/K') versus micellar concentration CM (M) of NaTDC in water for 0.2 mM caffeine.

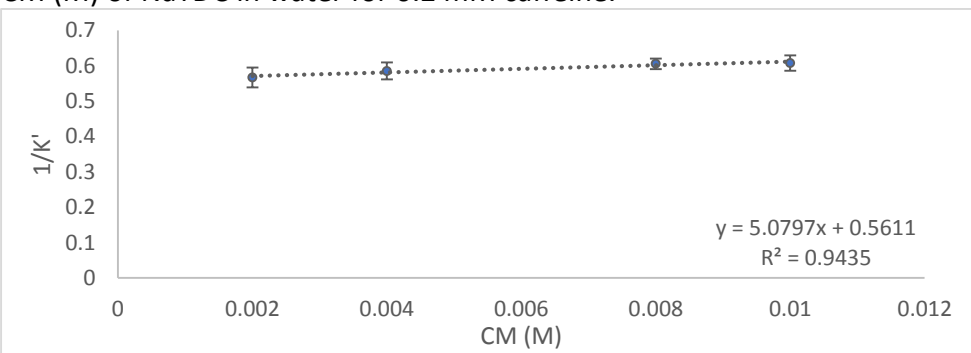

Figure 46: Calibration plot of the inverse of the capacity factor (1/K') versus micellar concentration CM (M) of NaTDC in water for0.2 mM acetaminophen.

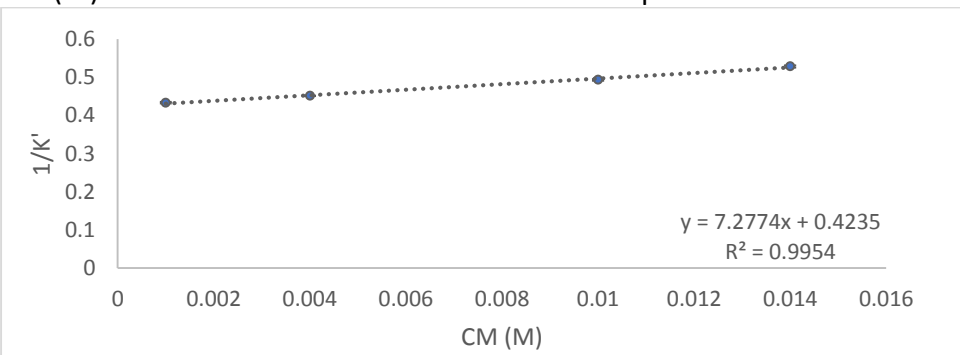

Figure 47: Calibration plot of the inverse of the capacity factor (1/K') versus micellar concentration CM (M) of NaTDC in water for 0.2 mM fluconazole.

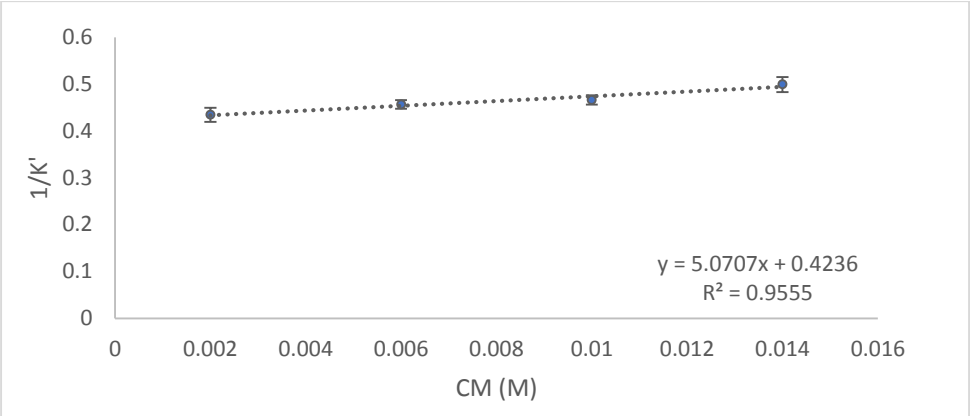

Figure 48: Calibration plot of the inverse of the capacity factor (1/K') versus micellar concentration CM (M) of NaTDC in water for 0.2 mM theophylline.

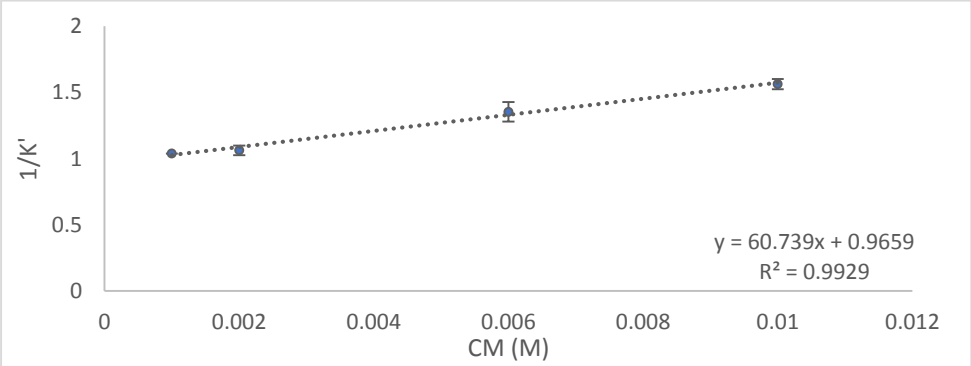

Figure 49: Calibration plot of the inverse of the capacity factor (1/K') versus micellar concentration CM (M) of NaTDC in water for 0.2 mM lidocaine.

Table 33: Partition coefficients obtained from MLC using NaTDC for ten drugs with their standard deviations against their octanol/water partition coefficients.

Compound	Log P_{mw}	Log $P_{o/w}$ [184]
Acetaminophen	0.96±0.15	0.46
Caffeine	1.27±0.01	-0.07
Fluconazole	1.24±0.01	0.40
Theophylline	1.08±0.03	-0.02
Fenoprofen	1.40±0.04	3.10
Gemfibrozil	0.90±0.04	3.40
Ibuprofen	1.50±0.08	3.97
Phenylbutazone	1.64±0.002	3.16
Salicylic acid	1.42±0.02	2.26
Lidocaine	1.80±0.02	2.44

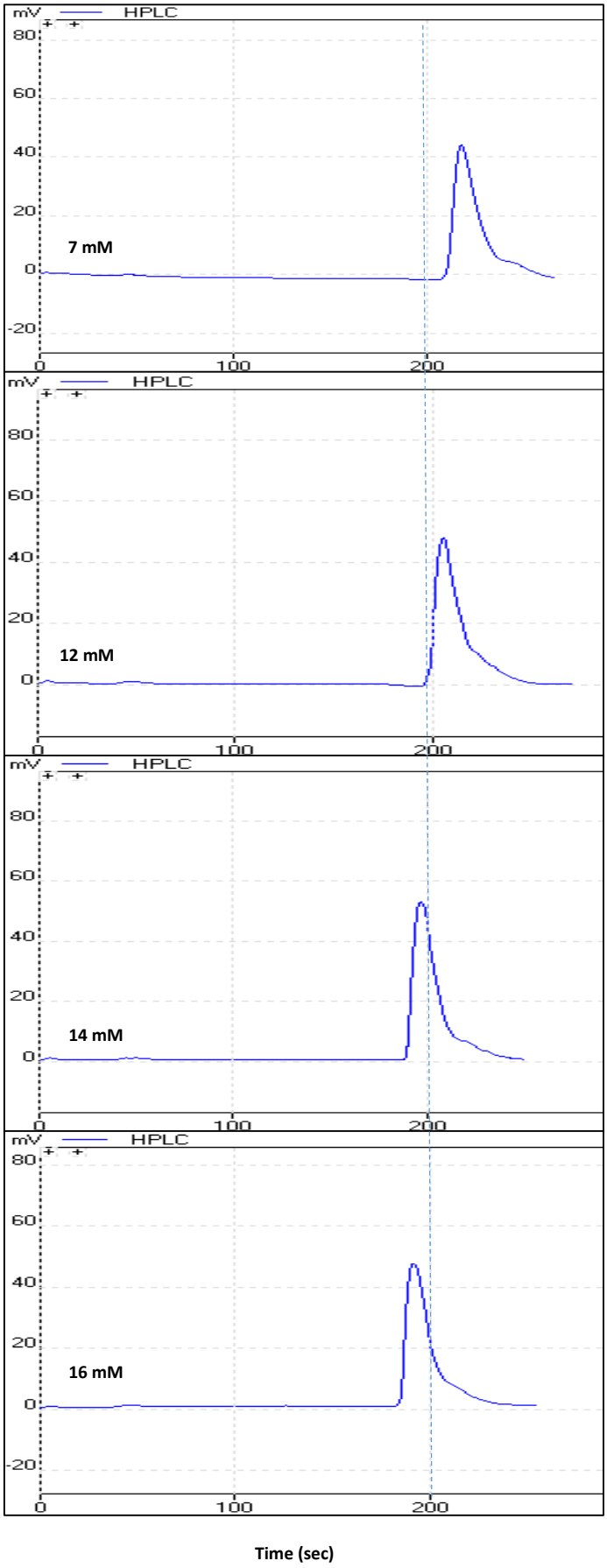

Figure 50: Chromatograms showing binding behaviour of caffeine in different concentrations of NaTDC mobile phase. (The dotted line is only used for visual guidance).

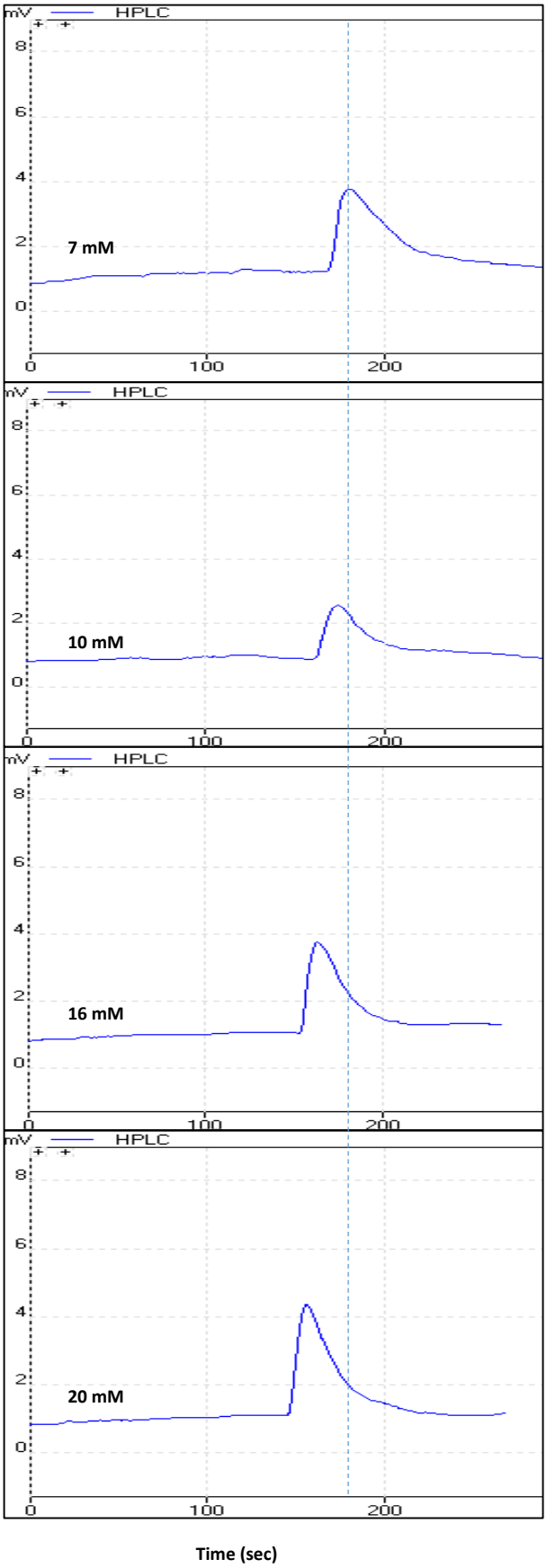

Figure 51: Chromatograms showing binding behaviour of fluconazole in different concentrations of NaTDC mobile phase. (The dotted line is only used for visual guidance).

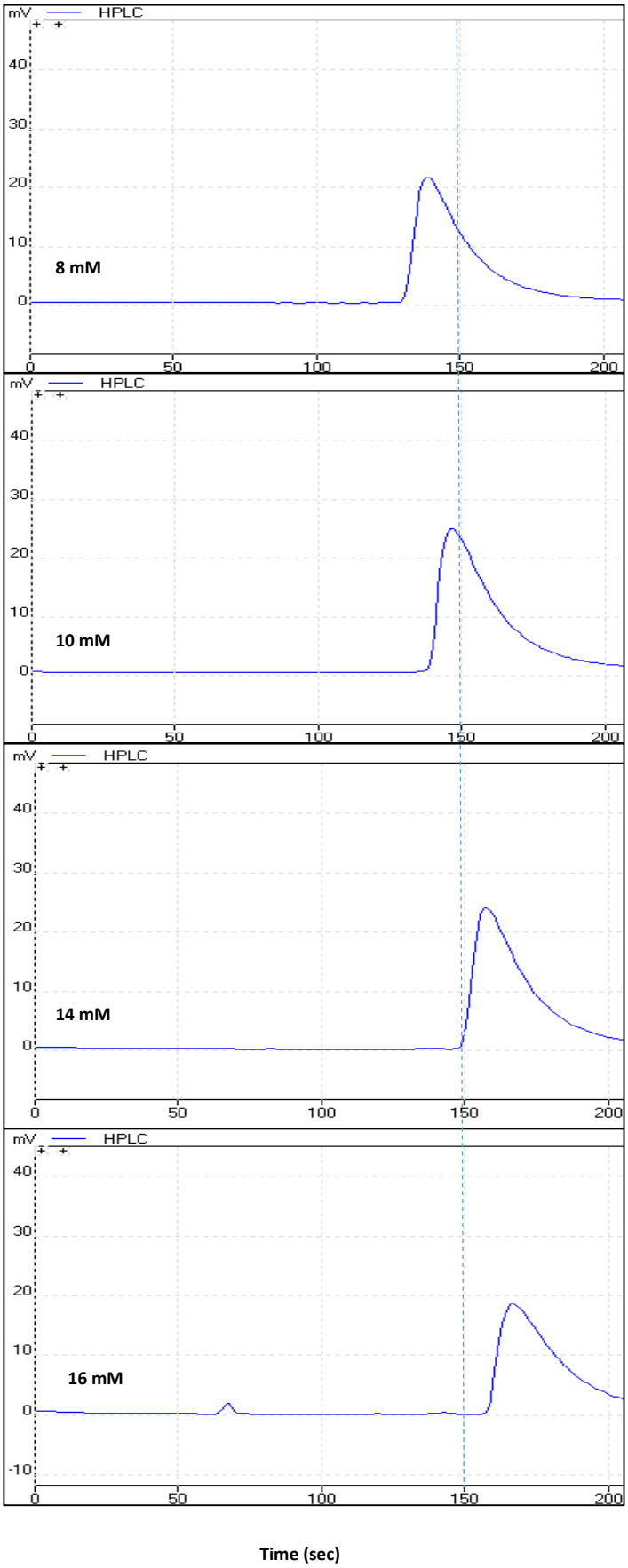

Figure 52: Chromatograms showing binding behaviour of fenoprofen in different concentrations of NaTDC mobile phase. (The dotted line is only used for visual guidance).

Anionic, neutral and cationic drugs used in this work followed the same retention behaviour as seen with NaDC. Phenylbutazone, fenoprofen, salicylic acid, ibuprofen and gemfibrozil were the anionic drugs used in this work. Except for ibuprofen and gemfibrozil all of the previously mentioned drugs exhibited antibinding behaviour with their retention times increasing with an increase in the mobile phase concentration (Tables 23-25 and Figures 40-42). Ibuprofen and gemfibrozil displayed the same behaviour they showed when using NaDC, as explained in Section (3A), (Tables 26-27 and Figures 43-44).

Caffeine, acetaminophen, fluconazole and theophylline were the neutral drugs used. Since their retention times decreased with an increase in mobile phase concentration it can be concluded that these solutes interacted with the bile salt micelles as binding solutes (Tables 28-31 and Figures 45-48).

As shown from the data in Table 32 and Figure 49, the cationic drug lidocaine followed the same pattern of interaction with NaTDC as with NaDC, where it was ionised in the pH of the mobile phase medium, and consequently attached strongly to the micelles. This decreased retention time with the increase in the micelle concentration in the mobile phase, i.e. typical of what is expected with a cationic compound.

The chromatograms for some selected drugs showing their binding or antibinding behaviour can be seen in Figures 50-52.

In Table 33, it can be seen that log P_{mw} values for neutral drugs (acetaminophen, caffeine, theophylline and fluconazole) were higher than those of the published log $P_{o/w}$ values while log P_{mw} values for anionic drugs (fenoprofen, ibuprofen, gemfibrozil, phenylbutazone and salicylic acid) and the cationic drug lidocaine were lower than those of log $P_{o/w}$, as discussed in Section (3A). It was also observed that the salicylic acid log P_{mw} value obtained with NaTDC was higher than that obtained with NaDC suggesting more solubilisation of salicylic acid in NaTDC than NaDC because of the preference of salicylic acid to NaTDC micelles. On the other hand, the gemfibrozil log P_{mw} value obtained with NaTDC was found to be lower than that obtained with NaDC suggesting less preference of gemfibrozil to NaTDC micelles than NaDC micelles. This preference for the aqueous phase is in spite of it being a binding solute, as discussed in Section (3A).

3.B.3. Statistical Modelling

3.B.3.1. Statistical Modelling of Human Intestinal absorption (HIA)

Statistical modelling of %HIA, PAMPA & Caco-2 log P was carried out as discussed in Section (3A). Analysis of 15 drugs using NaTDC facilitated calculation of log P_{mw} and data

analysis of log P_{mw} with a number of molecular descriptors (listed in Table 37) to establish a model equation for the prediction of each of %HIA, PAMPA & Caco-2 log P using multiple linear regression. Significance of the included model descriptors was given by P and t values while statistical significance of the model itself was given by F-ratio.

The predictive ability of the preferred model was assessed using adjusted-R^2 and R^2 for prediction (R^2_{PRED}) which can indicate the predictive ability of the model itself.

A summary of the experimental values for each of (%HIA) and PAMPA & Caco-2 log P along with the molecular descriptors and the dependant variables is shown in Table 37.

The model obtained for the prediction of % HIA is given by Equation 13:

$$\text{Logit HIA} = -0.998 - 0.747 \log P_{mw} - 0.3675\,HD + 0.05782\,PSA + 0.0082\,HA + 0.0686\,pK_a \quad \text{Eq. (13)}$$

Fourteen drugs were used to develop the final model.

The model's R^2 =97.70 %, $R^2_{adjust.}$= 95.73 % , R^2_{PRED} = 91.21 %, S=0.107

A 95 % confidence interval for log P_{mw} is given by (-1.044, -0.451), t-statistic and standardised coefficient of log P_{mw} are -5.958 ($p<0.05$) and -0.443 respectively suggesting statistical significance of log P_{mw} as a predictor. Also the F-ratio of the overall model is statistically significant, F=49.579 and P value 0.000 ($p<0.05$). The close agreement of the values of $R^2_{adjust.}$ & R^2_{PRED} indicates that the model does not over-fit the data.

The residual analysis did not detect any relationship between residuals and predicted values as shown in Figure 53. The model is shown in Figure 54. The predicted % HIA values were found to be in close agreement with experimental values obtained from literature as shown in Figure 55 and listed in Table 34.

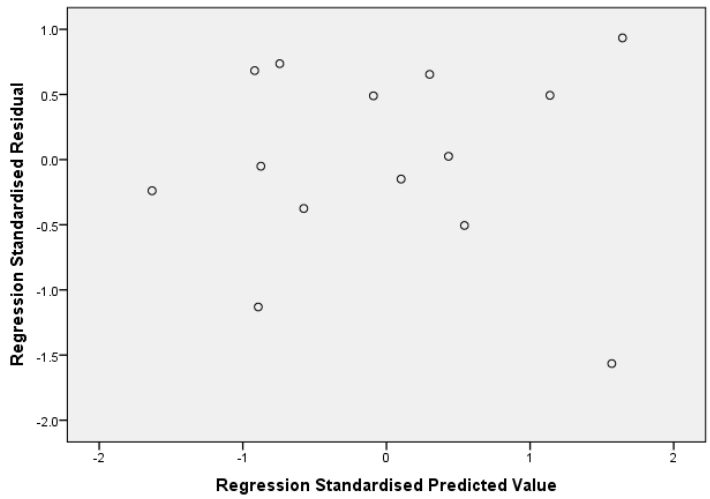

Figure 53: Residual plot for optimal logit HIA regression model.

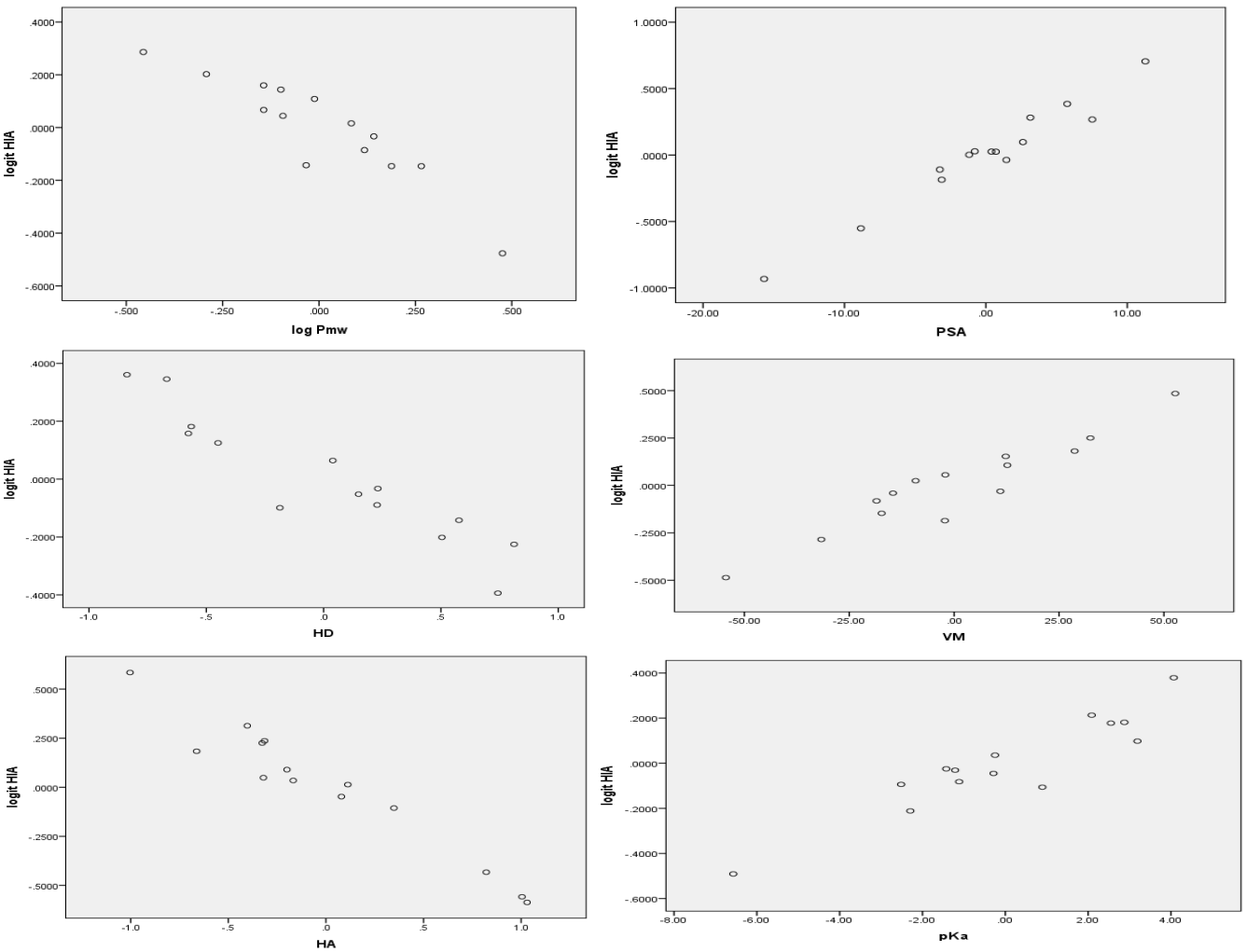

Figure 54: Partial regression plots of experimental logit HIA values against log P_{mw}, HD, HA, PSA and V_M, pKa.

Table 34: Experimental and predicted values for %HIA.

Drug	Expt. %HIA	Pred. %HIA
Acetaminophen	95.00[205]	94.18
Acetylsalicylic acid	84.00[213]	85.19
Caffeine	99.00[230]	98.75
Diclofenac	82.00[63, 207]	79.36
Diphenhydramine	61.00[207] [209]	62.40
Fenoprofen	85.00[206]	82.55
Fluconazole	95.00[205]	94.97
Gemfibrozil	95.00[207]	95.56
Ibuprofen	80.00[208]	80.18
Ketoprofen	92.00[205]	91.06
Lidocaine	75.00[127, 132]	79.85
Phenylbutazone	98.00[206]	97.75
Propranolol	92.50[231]	92.75
Theophylline	98.00[33]	98.60

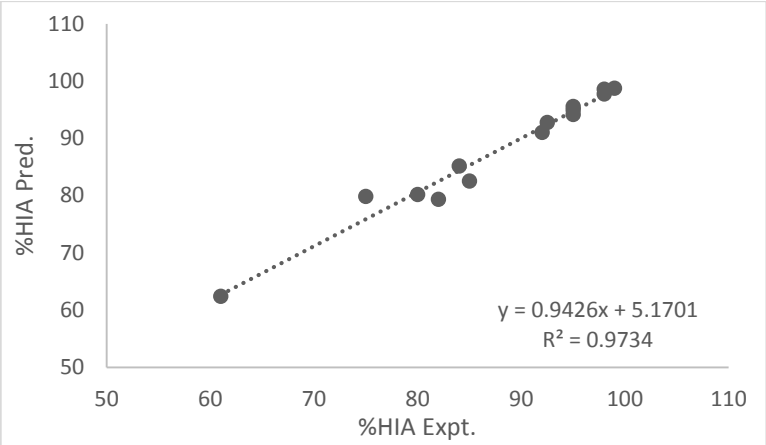

Figure 55: Plot of experimental vs. predicted %HIA.

3.B.3.2. Modelling of permeability coefficients obtained from PAMPA

The model obtained for the prediction of PAMPA log P_o is given by Equation 14:

$$\log P_o = -7.051 + 1.313 \log P_{mw} + 0.7266\ FRB \qquad \text{Eq. (14)}$$

Twelve drugs were used to develop the final model.

The model's R^2 = 91.66 %, $R^2_{adjust.}$= 89.81 % , R^2_{PRED} = 87.14 %, S= 0.608

A 95 % confidence interval for log P_{mw} is given by (0.046, 2.58), t-statistic and standardised coefficient of log P_{mw} are 2.344 ($p<0.05$) and 0.228 respectively suggesting statistical significance of log P_{mw} as a predictor. Also the F-ratio of the overall model is statistically significant, F= 49.46 and P value 0.000 ($p<0.05$). The close agreement of the values of $R^2_{adjust.}$ & R^2_{PRED} indicates that the model does not over-fit the data. The residual analysis did not detect any relationship between residuals and predicted values as shown in Figure 56. The model is shown in Figure 57. Plotting of the experimental values obtained from literature against predicted values calculated from the obtained model (Figure 58) showed a close agreement between both values listed in Table 35.

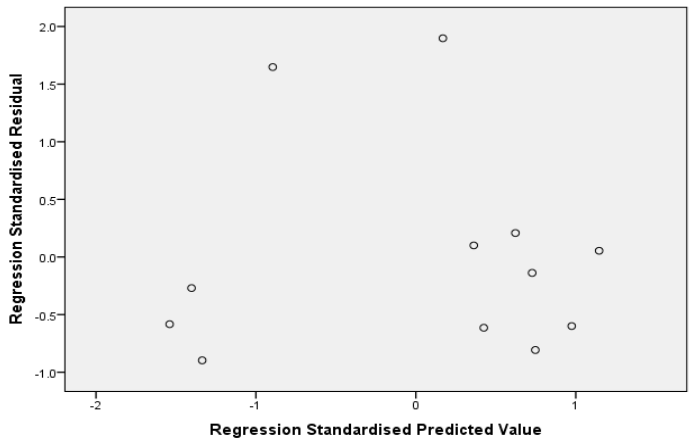

Figure 56: Residual plot for optimal PAMPA regression model.

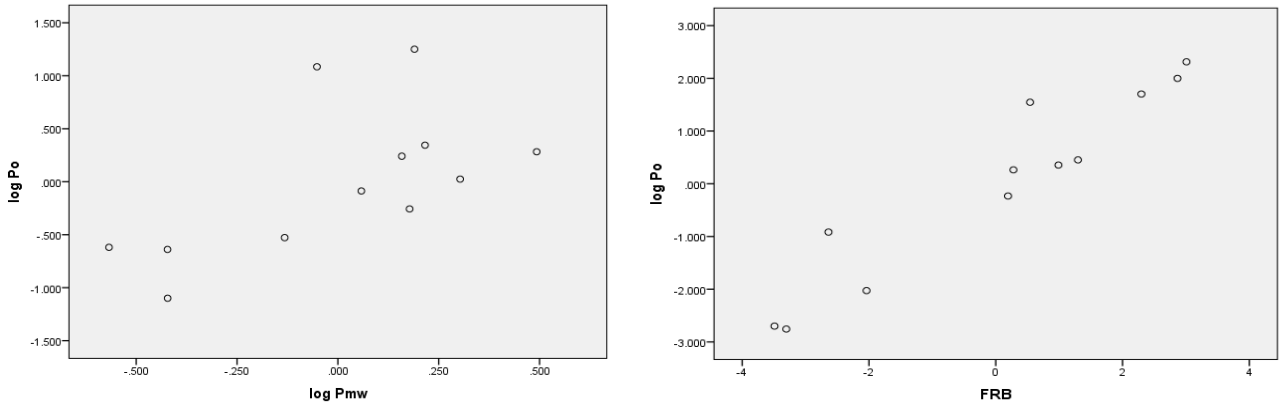

Figure 57: Partial regression plots of experimental PAMPA log P_o values against log P_{mw} and FRB.

Table 35: Experimental and predicted values for PAMPA log P_o.

Drug	Expt. PAMPA log P_0[215]	Pred. PAMPA log P_0
Acetaminophen	-5.81	-5.26
Caffeine	-5.55	-5.39
Diclofenac	-1.37	-2.52
Diphenhydramine	-0.71	-0.74
Gemfibrozil	-1.59	-1.51
Ibuprofen	-2.11	-2.17
Ketoprofen	-2.43[64]	-2.06
Lidocaine	-1.42	-1.06
Phenylbutazone	-1.96	-1.47
propranolol	-1.57[64]	-1.7
Salicylic acid	-3.46	-4.46
Theophylline	-5.99	-5.64

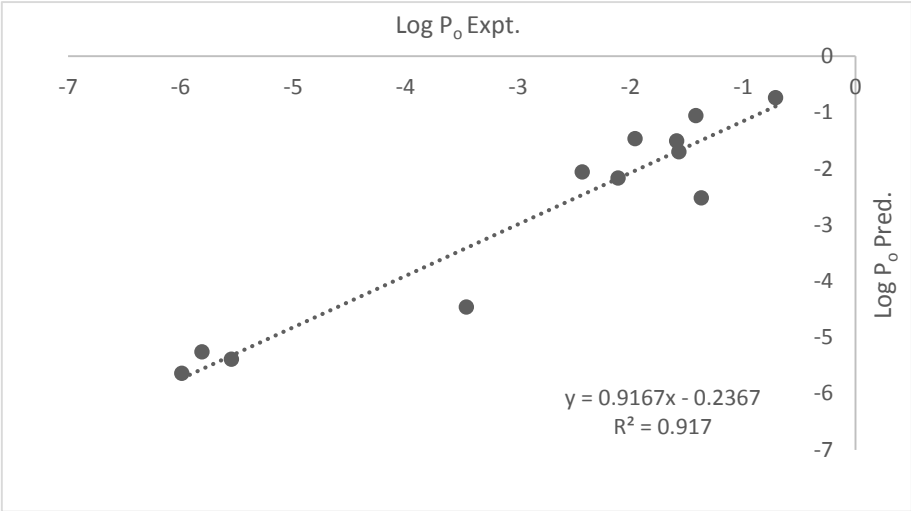

Figure 58: Plot of experimental vs. predicted log P_o.

3.B.3.3. Modelling of permeability coefficients obtained from Caco-2 $P_{eff.}$

The model obtained for the prediction of Caco-2 log $P_{eff.}$ is given by Equation 15:

$$\log P_{eff.} = -4.929 + 0.940 \log P_{mw} + 0.432\ HA - 0.04982\ PSA \qquad \text{Eq. (15)}$$

Twelve drugs were used to develop the final model.

The model's R^2 =84.49 %, $R^2_{adjust.}$= 78.67 % , R^2_{PRED} = 63.32 %, S=0.337

A 95 % confidence interval for log P_{mw} is given by (0.139, 1.742), t-statistic and standardised coefficient of log P_{mw} are 2.706 ($p<0.05$) and 0.399 respectively suggesting statistical significance of log P_{mw} as a predictor. Also the F-ratio of the overall model is statistically significant, F=14.526 and P value 0.001 ($p<0.05$). The close agreement of the values of $R^2_{adjust.}$ & R^2_{PRED} indicates that the model does not over-fit the data. The residual analysis did not detect any relationship between residuals and predicted values as shown in Figure 59. The model is shown in Figure 60. The values presented in Table 36 and plotted in Figure 61 for %HIA predicted vs those from the literature show remarkably similar trends.

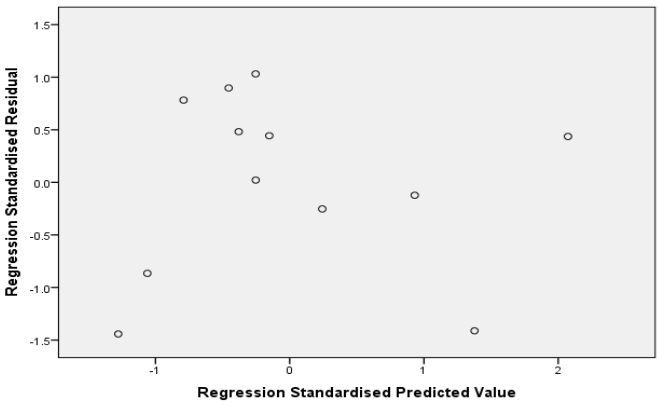

Figure 59: Residual plot for optimal Caco-2 regression model.

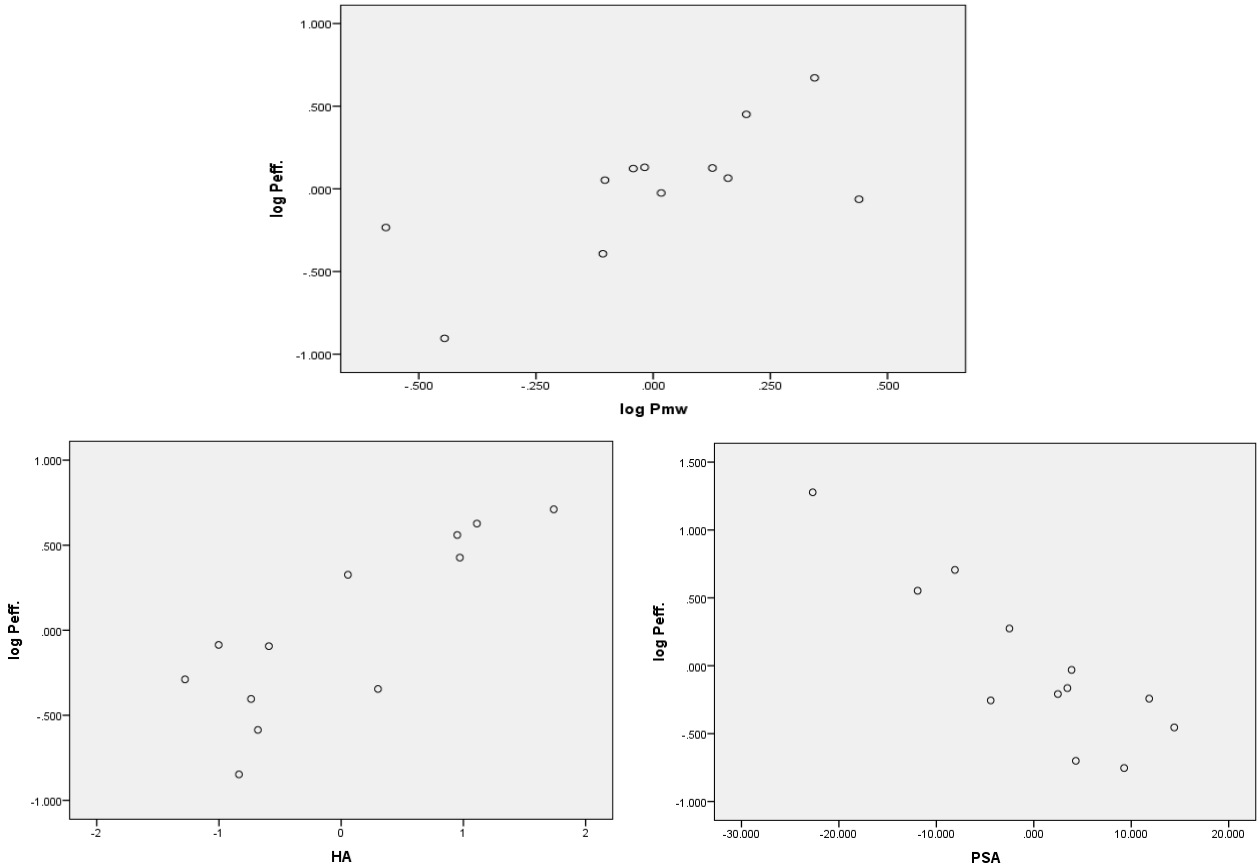

Figure 60: Partial regression plots of experimental log $P_{eff.}$ values against log P_{mw}, HA & PSA.

Table 36: Experimental and predicted values for Caco-2 log $P_{eff.}$

Drug	Expt. Caco-2 log $P_{eff.}$	Pred. Caco-2 log $P_{eff.}$
Acetaminophen	-6.00[216]	-5.51
Acetylsalicylic acid	-5.66[217]	-5.37
Caffeine	-4.07[216]	-4.03
Diclofenac	-4.75[56]	-4.91
Diphenhydramine	-3.12[215]	-3.27
fluconazole	-4.82[56]	-4.83
Ibuprofen	-4.58[56]	-4.49
Ketoprofen	-4.48[56]	-4.83
Lidocaine	-4.21[217]	-3.73
Propranolol	-4.66[60]	-4.96
Salicylic acid	-4.92[217]	-5.19
Theophylline	-4.61[56]	-4.76

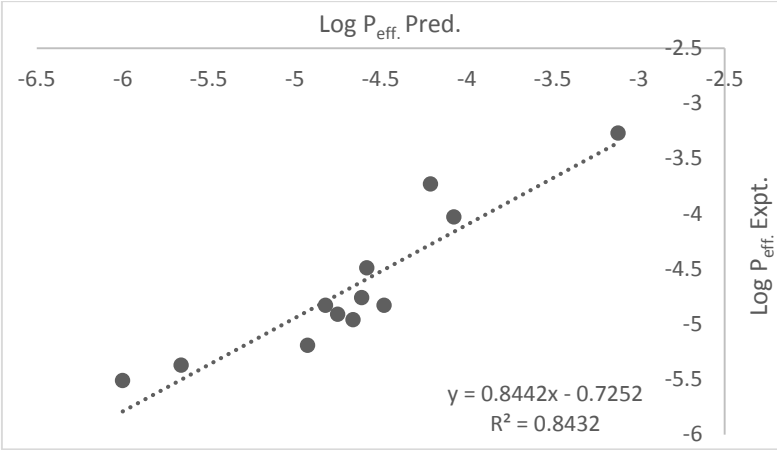

Figure 61: Plot of experimental vs. predicted log $P_{eff.}$

The use of log P_{mw} derived from NaTDC appears to give model equations with better predictive power (higher adjusted-R^2 & R^2_{PRED}) than that derived from NaDC but it has to be taken into consideration that different variables and numbers of variables were used to establish these final models. The inclusion of Caco-2 log $P_{eff.}$ in an equation with log P_{mw} gave the best model with the best predictability in the case of NaDC related data followed by %HIA then PAMPA log P_o. While in case of NaTDC, the obtained models were able to predict %HIA better than PAMPA log P_o and Caco-2 log $P_{eff.}$.

Table 37: A summary of molecular descriptors for the selected drugs analysed by MLC using NaTDC in water and the experimental values of PAMPA log P_o, Caco-2 log $P_{eff.}$ and %HIA.

Drug	Log P_{mw}	log $P_{o/w}$[184]	Mwt[218]	pK_a[184]	S_w[184]	HD[218]	HA[218]	FRB[218	PSA[219]	V_M[218]	Log P_o [215]	Log $P_{eff.}$	%HIA
Acetaminophen	0.81	0.46	151.2	9.9	4.15	2	2[184]	1	49.3	131.1	-5.81	-6.00[216]	95[205]
Acetyl salicylic acid	1.09	1.19	180.16	3.41	1.46	1	4	3	63.6	139.6	NA	-5.66[217]	84[213]
Caffeine	1.27	-0.07	194.19	14	11	0	3[184]	0	58.4	133.4	-5.55	-4.07[216]	99[230]
Diclofenac	1.24	4.51	296.15	4.15	0.0044	2	3	4	49.3	206.8	-1.37	-4.75[56]	82[63, 207]
Diphenhydramine	1.48	3.27	255.35	9	0.0752	0	2	6	12.5	249.2	-0.71	-3.12[215]	61[207] [209]
Fenoprofen	1.22	3.1	242.27	4.5	0.0811	1	3	4	46.5	204.7	NA	NA	85[206]
Fluconazole	1.24	0.4	306.27	12.71	1.39	1	7	5	81.6	205.3	NA	-4.82[56]	95[205]
Gemfibrozil	1.48	3.4	250.33	4.5	0.0278	1	3	6	46.5	239.7	-1.59	NA	95[207]
Ibuprofen	1.40	3.97	206.28	5.2	0.0684	1	2	4	37.3	200.3	-2.11	-4.58[56]	80[208]
Ketoprofen	1.50	3.12	254.28	3.88	0.0213	1	3	4	54.4	212.2	-2.43[64]	-4.48[56]	92[205]
Lidocaine	1.59	2.44	234.34	7.9	0.593	1	2[184]	5	32.3	238.8	-1.42	-4.21[217]	75[209, 210]
Phenylbutazone	1.80	3.16	308.37	4.4	0.144	0	2[184]	5	40.6	262.8	-1.96	NA	98[206]
propranolol	0.76	3.48	259.34	9.5[226]	0.0794	2	3	6	41.5	237.2	-1.57[64]	-4.66[60]	92.5[231]
Salicylic acid	1.48	2.26	138.12	2.97	11.3	2	3	1	58	100.4	-3.46	-4.92[217]	NI
Theophylline	1.08	-0.02	180.16	8.8[228]	22.9	1	3[184]	0	69.3	122.9	-5.99	-4.61[56]	98[33]

NA: no available data, NI: value not included in training set.

3.B.4. Conclusion

Overall, log P obtained from NaDC was more predictive of the *in vitro* Caco-2 permeability coefficient rather than the *in vivo* %HIA data. In contrast, log P obtained from NaTDC was more predictive of the *in vivo* %HIA data rather than the *in vitro* permeability coefficients. In summary, by combining the findings of Sections 3A and 3B it can be concluded that NaTDC is a more suitable MLC surfactant for simulating the intestinal environment for the prediction of %HIA.

CHAPTER 3

Section (C)

The Use Of NaC In MLC

Section (C): Use of sodium cholate (NaC) as a micellar mobile phase in MLC

3.C.1. Introduction

A set of eleven compounds (anionic, cationic and neutral) were used to evaluate the use of NaC in MLC. Acetaminophen, caffeine, fluconazole and theophylline represented the neutral compounds while fenoprofen, gemfibrozil, indomethacin, ibuprofen, phenylbutazone and salicylic acid represented the anionic compounds. Lidocaine represented a cationic compound.

In the same manner as in the previous two sections (A&B), micelle-water partition coefficients were determined from the relation between the inverse of capacity factors (1/K') and micellar concentration (CM). Dead time was accurately determined for all the surfactant concentrations and an average of all of these determinations was taken. The average value of dead time was determined in this work to be 47.41 seconds.

The pH of the micellar mobile phase was measured at both the lowest (0.017 M) and the highest (0.035 M) concentrations of the mobile phase to determine the ionisation state. The pH of the mobile phase was determined to be in the range of (7.1-9.6). All MLC runs were carried out at 37 ºC in order to simulate intestinal conditions. Linear plots of (1/K') against (CM) were obtained as shown in Figures (64-74). Micellar concentration in the mobile phase was calculated by subtraction of CMC of NaC in water from the total surfactant concentration used. CMC of NaC in water was determined at 37 ºC by means of spectrophotometry using dichlorofluorescein dye and it was found to be 0.017 M.

3.C.2. Results and Discussion

3.C.2.1. Determination of CMC of NaC at 37 ºC

Theory

The dye micellisation method was applied for the determination of CMC of NaC at 37 ºC using dichlorofluorescein dye where the dye attaches to the hydrophobic part of the micelle causing a change in the absorbance of the micellised dye at a fixed wavelength (503 nm) as a function of surfactant concentration [232].

The effect of the anionic surfactant NaC on the absorption spectrum of dichlorofluorescein dye was studied and the visible spectra of aqueous dichlorofluorescein solution in several NaC concentrations ranging from (0.003 M to 0.035 M) for a fixed dye concentration of 10^{-5} M (Figure 62). The dye exhibits a maximum absorption band at 503 nm.

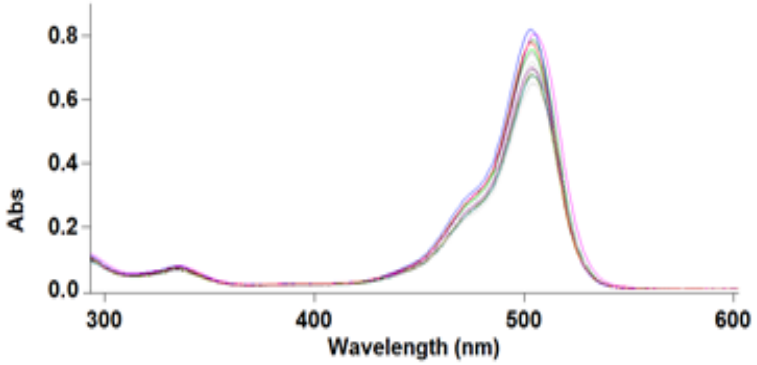

Figure 62: Spectra of 10^{-5} M Dye in increasing concentrations of NaC at 37 ºC .

It was found that, below the CMC, as the NaC concentration gradually increased, the dye absorbance at 503 nm decreased. The decrease in the absorbance indicates the formation of a molecular complex between the dye and the surfactant molecules due to the interaction between the dye and the surfactant molecules. Above the CMC, the absorbance at 503 nm increased significantly. The increase in absorbance values with the increase in surfactant concentration above CMC was attributed to the incorporation of dye molecules with micelles.

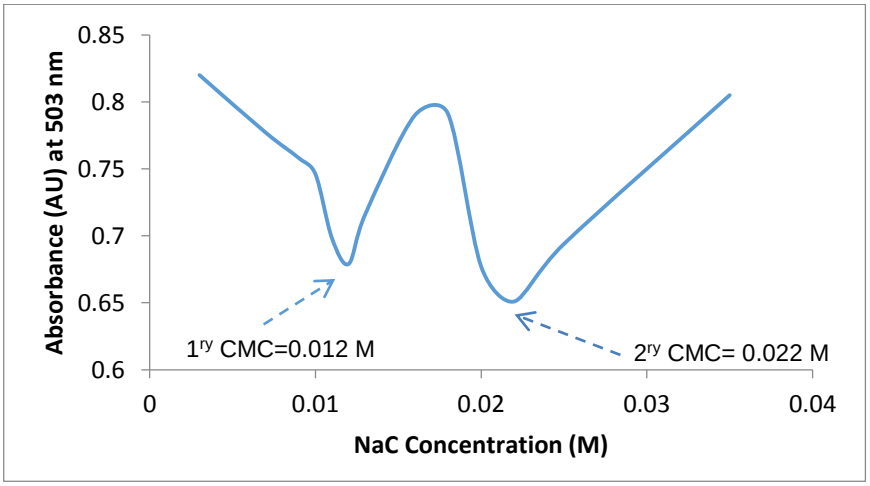

Figure 63: A plot of NaC concentration versus absorbance of the micellised dye showing the 1ry and 2ry CMC of NaC at 37 ºC .

Two critical micellar concentrations were detected as shown in Figure 63. The values of the primary CMC and the secondary CMC were found to be 0.012 M and 0.022 M respectively. The value of CMC was taken as an average of the two CMC values ($CMC_{AV.}$=0.017 M) which is consistent with the value in literature [233]. According to literature the CMC value of NaC is 0.014 M at 25 ºC [190] or (0.009-0.015 M) at 20-25 ºC according to the manufacturer specification sheet, this shows that as the temperature increased to 37 ºC, the CMC value

increased. This increase in the CMC value with the increase in temperature was because of its negative effect on micellisation where it decreases the surfactant hydration of the hydrophilic groups and also disrupts the structural water around the hydrophobic groups hence the CMC increases [234].

3.C.2.1. Retention behaviour

In this section, a cyanopropyl column was used as the stationary phase where the anionic surfactant NaC adsorbed on its surface. The binding and antibinding behaviour of some selected drugs are shown in Figures 75-77.

Chromatographic data for anionic drugs: phenylbutazone, fenoprofen, salicylic acid, ibuprofen, gemfibrozil and indomethacin are shown in Tables 38-43 and Figures 64-69. Using NaC with the MLC system, it was observed that phenylbutazone changed from an antibinding solute to a binding solute which could be as a result of the presence of the extra hydroxyl group in the NaC structure which leads to a decrease in the repulsion between the negatively charged group of the drug and that of the micelle [109] or because of the higher pH of sodium cholate bile salt used than the previous two bile salts. Another assumption is that NaC forms a type of “inverse micelles”. The inner core of this micelle is negatively charged while its surface is uncharged and hydrophobic; such a structure gives more opportunity for hydrophobic interaction [235]. As a result, phenylbutazone binds to the hydrophobic surface of the inverse cholate micelles.

Similar to the previous two sections (A & B) the neutral drugs (acetaminophen, caffeine, fluconazole and theophylline) and the cationic drug (lidocaine) displayed binding behaviour where their retention decreased with the increase in NaC concentration as shown in Tables 44-48 and Figures 70-74.

Table 38: Total & micellar concentrations used of NaC in water as well as the inverse of the capacity factors (1/K’) for 0.2 mM phenylbutazone.

Conc. (M)	CM (M)	1/K'
0.017	0	0.796
0.019	0.002	0.868
0.021	0.004	0.937
0.025	0.008	1.088
0.027	0.010	1.113
0.030	0.013	1.168
0.035	0.018	1.261

Table 39: Total & micellar concentrations used of NaC in water as well as the inverse of the capacity factors (1/K') for 0.2 mM fenoprofen.

Conc. (M)	CM (M)	1/K'
0.017	0	1.640
0.019	0.002	1.602
0.021	0.004	1.585
0.025	0.008	1.550
0.027	0.010	1.371
0.030	0.013	1.296
0.035	0.018	1.176

Table 40: Total & micellar concentrations used of NaC in water as well as the inverse of the capacity factors (1/K') for 0.2 mM salicylic acid.

Conc. (M)	CM (M)	1/K'
0.017	0	2.303
0.019	0.002	2.303
0.021	0.004	2.303
0.025	0.008	2.196
0.027	0.010	2.099
0.030	0.013	2.010
0.035	0.018	1.928

Table 41: Total & micellar concentrations used of NaC in water as well as the inverse of the capacity factors (1/K') for 0.2 mM ibuprofen.

Conc. (M)	CM (M)	1/K'
0.017	0	1.501
0.019	0.002	1.658
0.021	0.004	1.718
0.025	0.008	1.783
0.027	0.010	1.853
0.030	0.013	1.928
0.035	0.018	2.001

Table 42: Total & micellar concentrations used of NaC in water as well as the inverse of the capacity factors (1/K') for 0.2 mM gemfibrozil.

Conc. (M)	CM (M)	1/K'
0.017	0	1.122
0.019	0.002	1.250
0.021	0.004	1.276
0.025	0.008	1.426
0.027	0.010	1.501
0.030	0.013	1.603
0.035	0.018	1.829

Table 43: Total & micellar concentrations used of NaC in water as well as the inverse of the capacity factors (1/K') for 0.2 mM indomethacin.

Conc. (M)	CM (M)	1/K'
0.017	0	0.919
0.019	0.002	0.997
0.021	0.004	1.029
0.025	0.008	1.206
0.027	0.010	1.320
0.030	0.013	1.489
0.035	0.018	1.658

Table 44: Total & micellar concentrations used of NaC in water as well as the inverse of the capacity factors (1/K') for 0.2 mM caffeine.

Conc. (M)	CM (M)	1/K'
0.017	0	0.389
0.019	0.002	0.420
0.021	0.004	0.413
0.025	0.008	0.435
0.027	0.010	0.453
0.030	0.013	0.481
0.035	0.018	0.504

Table 45: Total & micellar concentrations used of NaC in water as well as the inverse of the capacity factors (1/K') for 0.2 mM acetaminophen.

Conc. (M)	CM (M)	1/K'
0.017	0	0.723
0.019	0.002	0.734
0.021	0.004	0.746
0.025	0.008	0.770
0.027	0.010	0.853
0.030	0.013	0.868
0.035	0.018	0.976

Table 46: Total & micellar concentrations used of NaC in water as well as the inverse of the capacity factors (1/K') for 0.2 mM fluconazole.

Conc. (M)	CM (M)	1/K'
0.017	0	0.356
0.019	0.002	0.399
0.021	0.004	0.407
0.025	0.008	0.429
0.027	0.010	0.433
0.030	0.013	0.446
0.035	0.018	0.496

Table 47: Total & micellar concentrations used of NaC in water as well as the inverse of the capacity factors (1/K') for 0.2 mM theophylline.

Conc. (M)	CM (M)	1/K'
0.017	0	0.853
0.019	0.002	0.885
0.021	0.004	0.902
0.025	0.008	0.919
0.027	0.010	0.956
0.030	0.013	0.976
0.035	0.018	0.996

Table 48: Total & micellar concentrations used of NaC in water as well as the inverse of the capacity factors (1/K') for 0.2 mM lidocaine.

Conc. (M)	CM (M)	1/K'
0.017	0	1.371
0.019	0.002	1.485
0.021	0.004	1.829
0.025	0.008	2.420
0.027	0.010	2.550
0.030	0.013	2.658
0.035	0.018	3.781

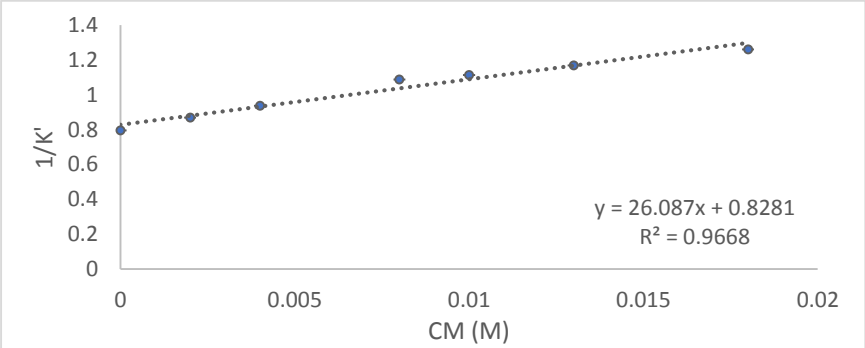

Figure 64: Calibration plot of the inverse of the capacity factor (1/K') versus micellar concentration CM (M) of NaC in water for 0.2 mM phenylbutazone.

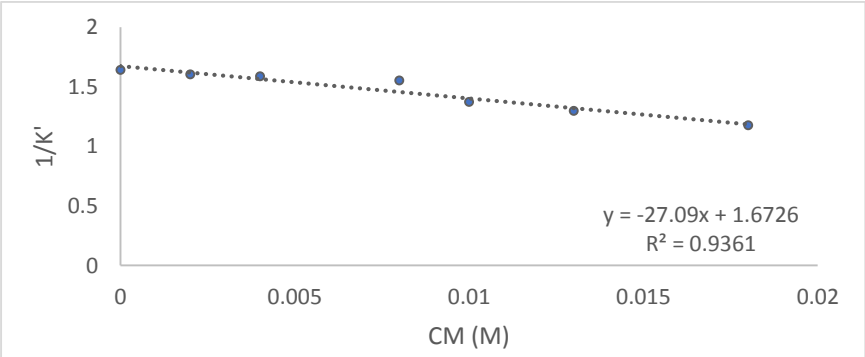

Figure 65: Calibration plot of the inverse of the capacity factor (1/K') versus micellar concentration CM (M) of NaC in water for 0.2 mM fenoprofen.

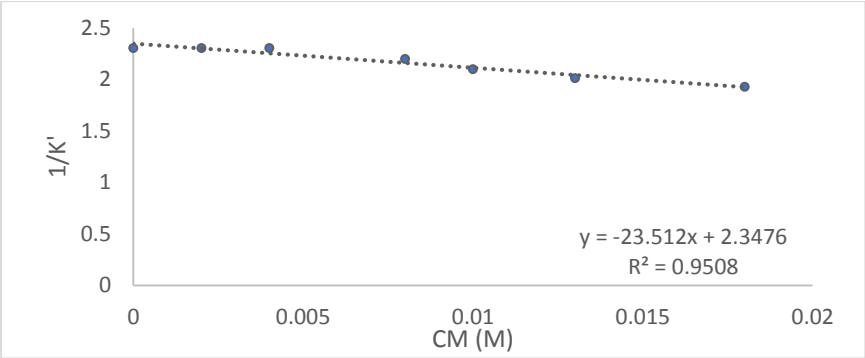

Figure 66: Calibration plot of the inverse of the capacity factor (1/K') versus micellar concentration CM (M) of NaC in water for 0.2 mM salicylic acid.

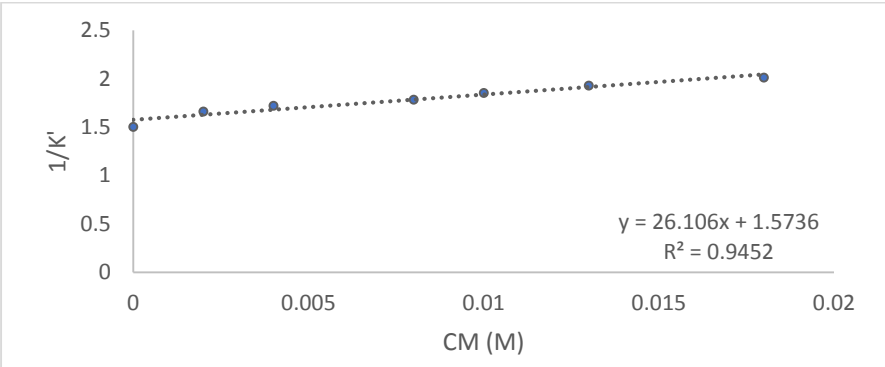

Figure 67: Calibration plot of the inverse of the capacity factor (1/K') versus micellar concentration CM (M) of NaC in water for 0.2 mM ibuprofen.

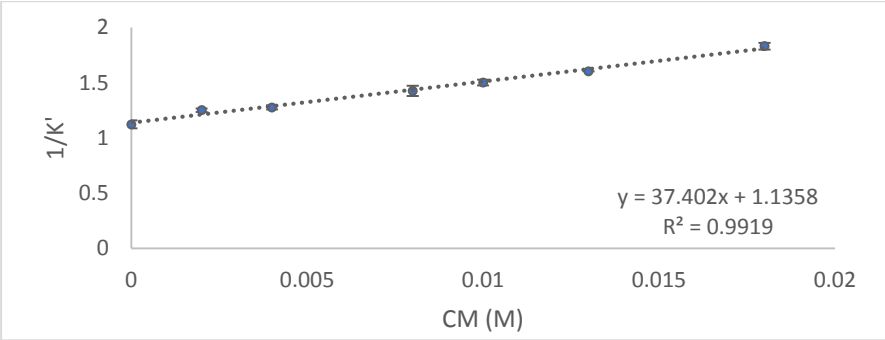

Figure 68: Calibration plot of the inverse of the capacity factor (1/K') versus micellar concentration CM (M) of NaC in water for 0.2 mM gemfibrozil.

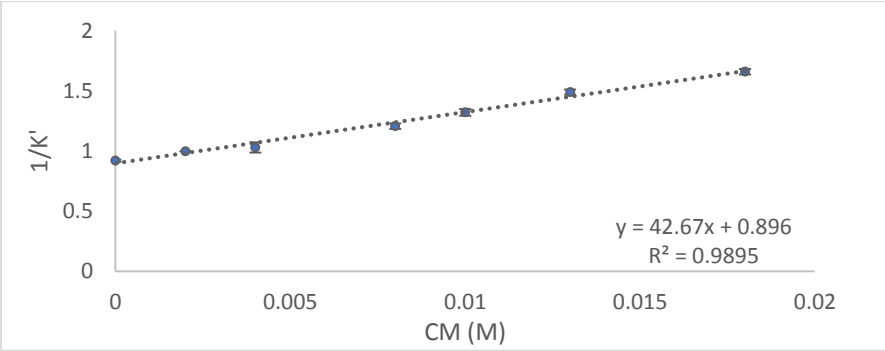

Figure 69: Calibration plot of the inverse of the capacity factor (1/K') versus micellar concentration CM (M) of NaC in water for 0.2 mM indomethacin.

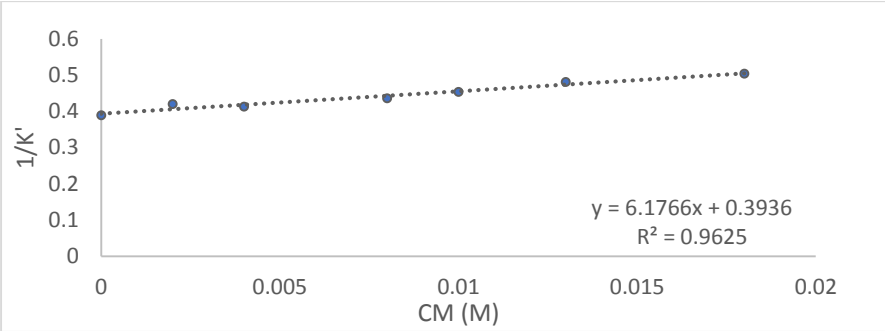

Figure 70: Calibration plot of the inverse of the capacity factor (1/K') versus micellar concentration CM (M) of NaC in water for 0.2 mM caffeine.

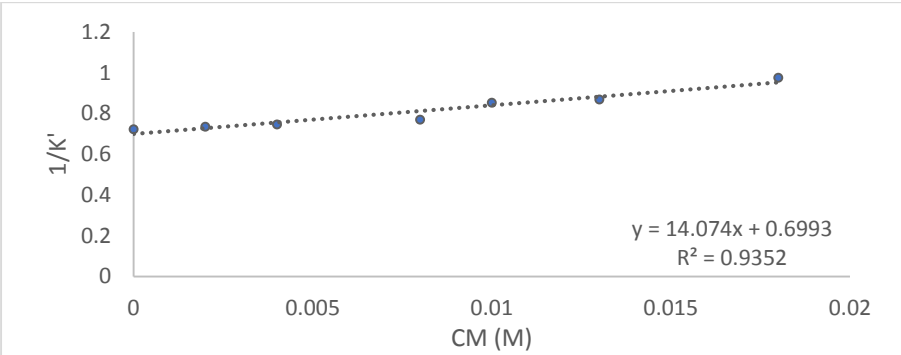

Figure 71: Calibration plot of the inverse of the capacity factor (1/K') versus micellar concentration CM (M) of NaC in water for 0.2 mM acetaminophen.

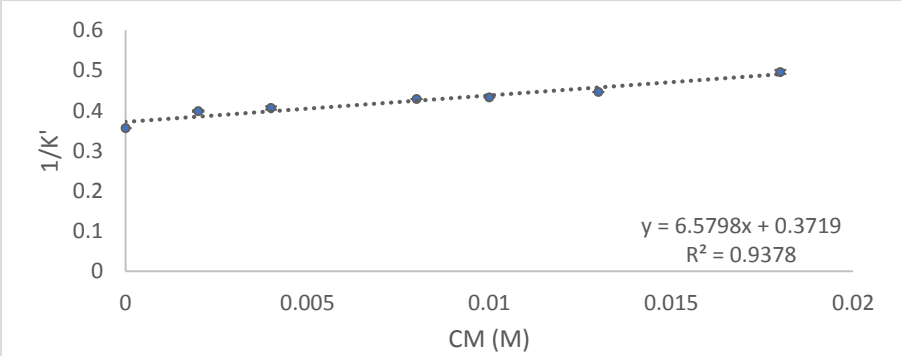

Figure 72: Calibration plot of the inverse of the capacity factor (1/K') versus micellar concentration CM (M) of NaC in water for 0.2 mM fluconazole.

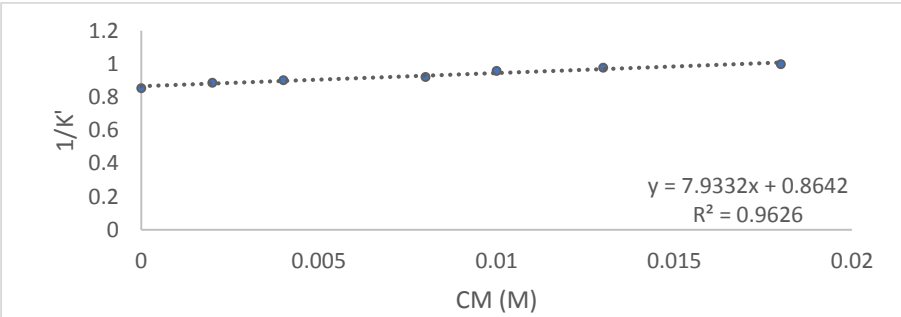

Figure 73: Calibration plot of the inverse of the capacity factor (1/K') versus micellar concentration CM (M) of NaC in water for 0.2 mM theophylline.

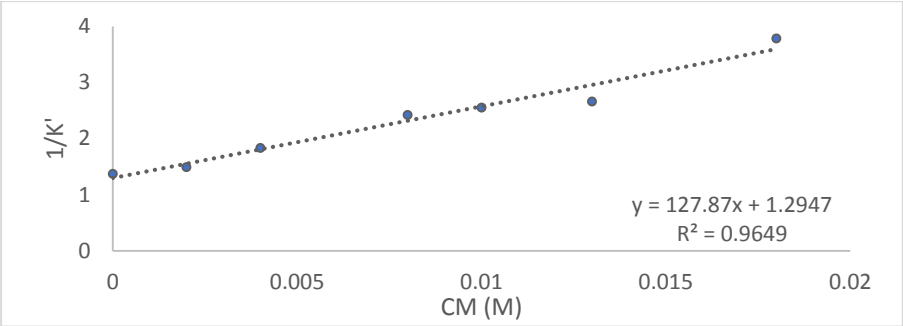

Figure 74: Calibration plot of the inverse of the capacity factor (1/K') versus micellar concentration CM (M) of NaC in water for 0.2 mM lidocaine.

Table 49: Partition coefficients obtained from MLC using NaC for eleven drugs with their standard deviations against their octanol/water partition coefficients.

Compound	Log P_{mw}	Log $P_{o/w}$[184]
Acetaminophen	1.30±0.00	0.46
Caffeine	1.20±0.01	-0.07
Fluconazole	1.25±0.01	0.40
Theophylline	0.96±0.00	-0.02
Fenoprofen	1.21±0.08	3.10
Gemfibrozil	1.52±0.01	3.40
Ibuprofen	1.21±0.00	3.97
Indomethacin	1.68±0.03	4.27
Phenylbutazone	1.50±0.00	3.16
Salicylic acid	1.00±0.00	2.26
Lidocaine	2.00±0.09	2.44

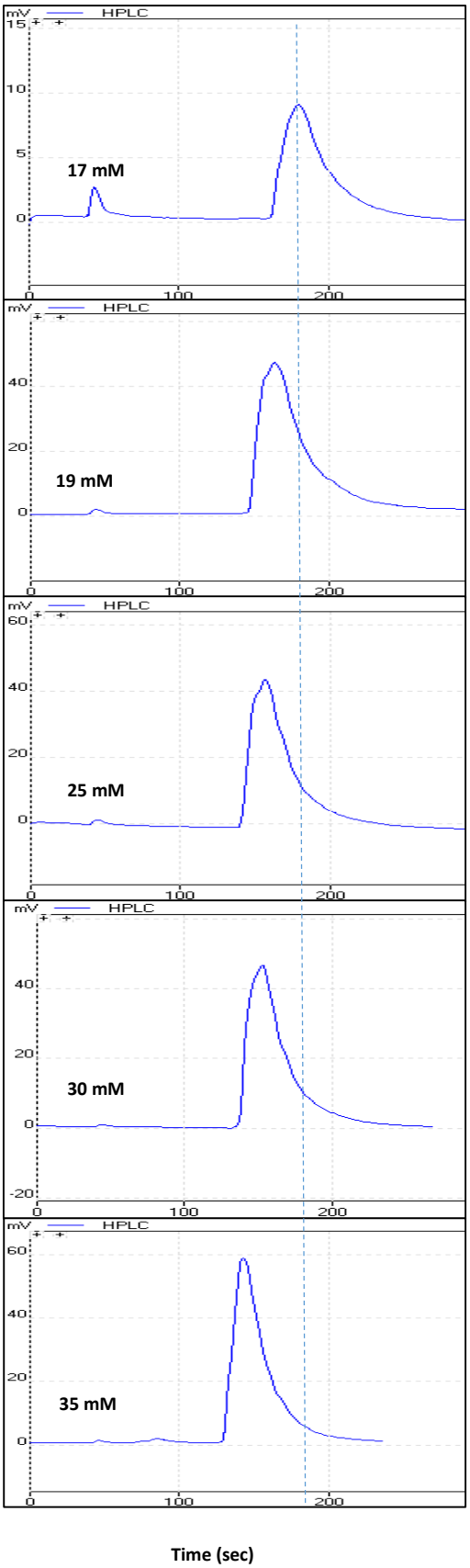

Figure 75: Chromatograms showing binding behaviour of fluconazole in selected concentrations of NaC mobile phase. (The dotted line is only used for visual guidance).

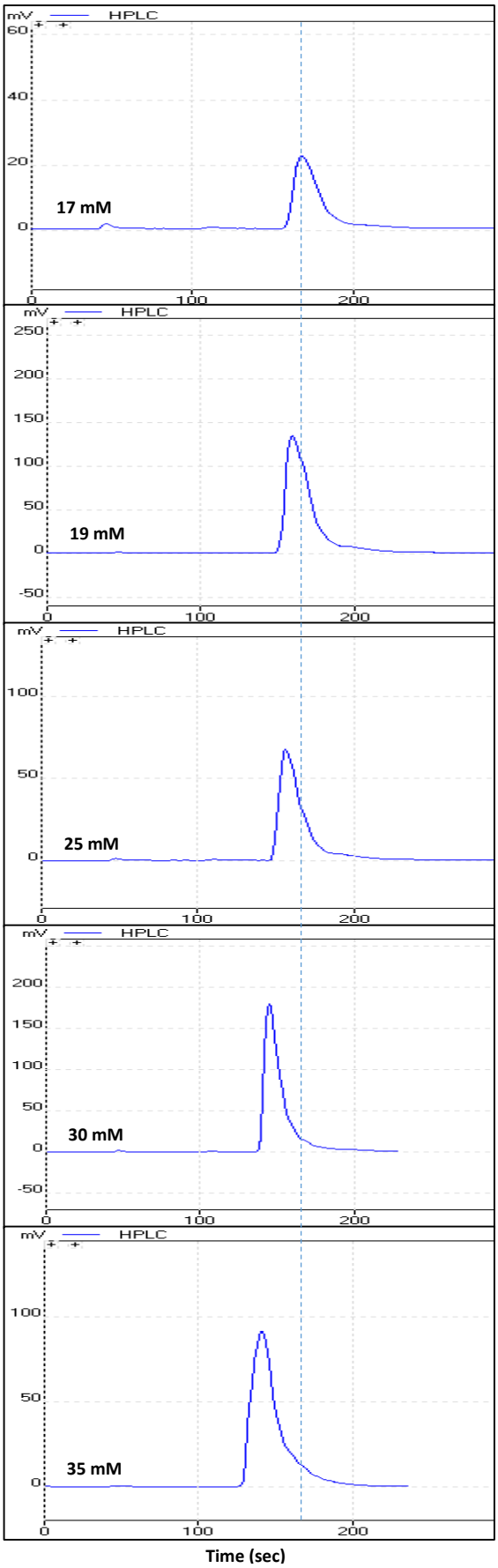

Figure 76: Chromatograms showing binding behaviour of caffeine in selected concentrations of NaC mobile phase. (The dotted line is only used for visual guidance).

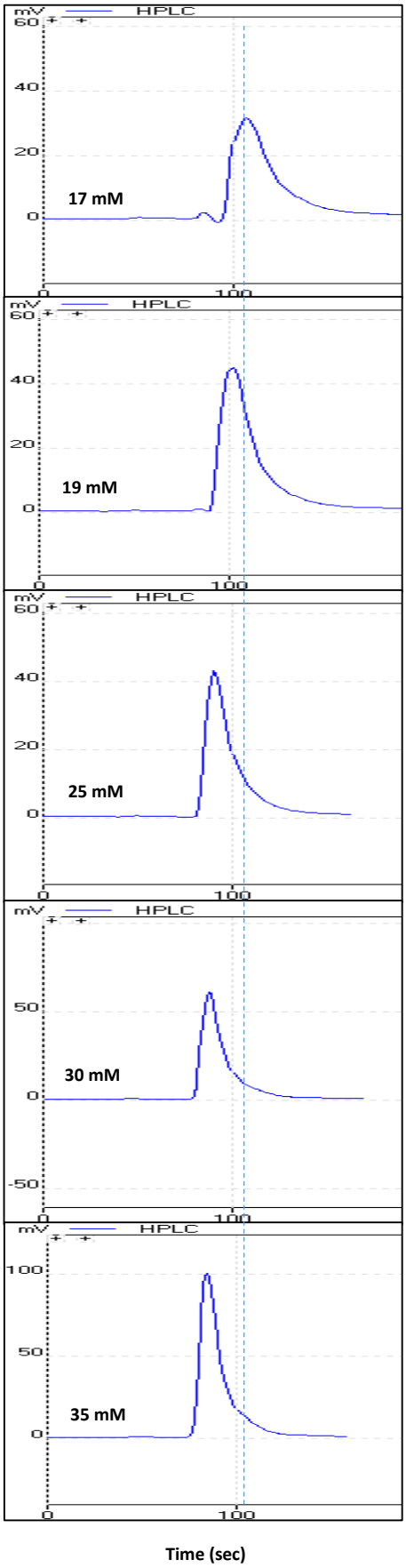

Figure 77: Chromatograms showing binding behaviour of phenybutazone in selected concentrations of NaC mobile phase. (The dotted line is only used for visual guidance).

In agreement with Sections (3A & 3B), Table 49 log P_{mw} values were less than those of log $P_{o/w}$ for the anionic drugs (fenoprofen, ibuprofen, gemfibrozil, phenylbutazone and salicylic acid) and cationic drug lidocaine. Furthermore, the log P_{mw} values were more than those of log $P_{o/w}$ for neutral drugs acetaminophen, caffeine, theophylline and fluconazole as previously discussed in Section (3A).

3.C.3. Statistical Modelling

3.C.3.1. Statistical Modelling of Human Intestinal absorption (HIA)

The model obtained for the prediction of %HIA is given by Equation 16:

$$\%HIA = 79.88 + 24.18 \log P_{mw} + 0.1254\ Mwt - 0.2377\ V_M \qquad \text{Eq. (16)}$$

Fourteen drugs were used in the development of the final model. The model's R^2 = 66.94 %, $R^2_{adjust.}$= 57.02 % , R^2_{PRED} = 43.33 %, S= 3.5

A 95 % confidence interval for log P_{mw} is given by (10.617, 37.736), t-statistic and standardised coefficient of log P_{mw} are 3.973 ($p<0.05$) and 1.267 respectively suggesting statistical significance of log P_{mw} as a predictor. Also the F-ratio of the overall model is statistically significant, F= 6.749 and P value 0.009 ($p<0.05$). The residual analysis did not detect any relationship between residuals and predicted values as shown in Figure 78 but the model had poor predictive power 43.33 %, Figure 79. The literature and predicted values of %HIA are listed in Table 50 and plotted against each other in Figure 80.

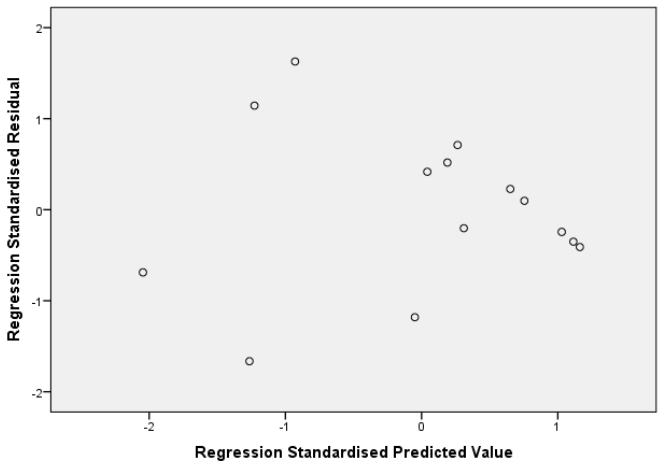

Figure 78: Residual plot for optimal %HIA regression model.

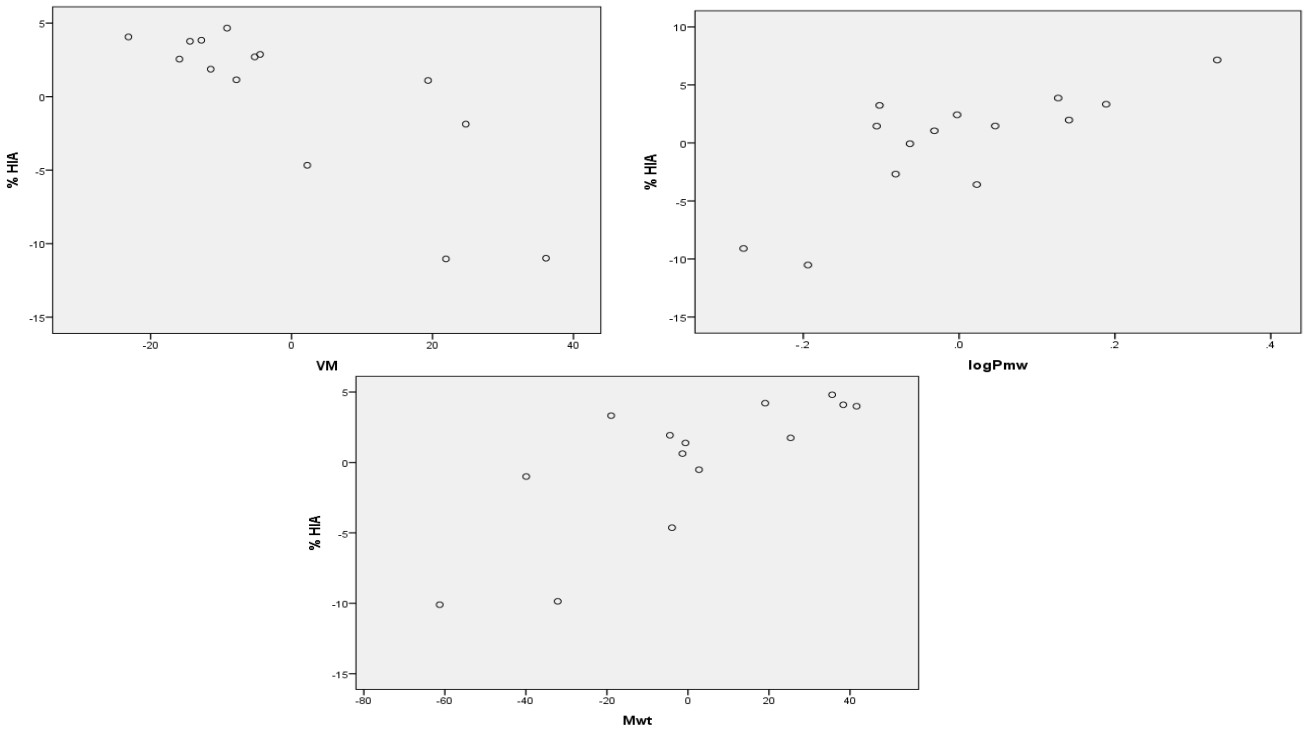

Figure 79: Partial regression plots of experimental %HIA values against log P_{mw} , Mwt and V_M.

Table 50: Experimental and predicted values for %HIA.

Drug	Expt. %HIA	Pred. %HIA
Acetaminophen	100.00[205]	99.20
Caffeine	100.00[205]	101.44
Diclofenac	99.00[208]	97.18
Fenoprofen	85.00[206]	90.83
Fluconazole	100.00[205]	99.66
Gemfibrozil	95.00[207]	90.99
Ibuprofen	85.00[207]	87.41
Indomethacin	100.00[205]	101.23
Ketoprofen	92.00[205]	96.14
Lidocaine	100.00[236]	100.86
meloxicam	97.00[207]	97.71
Phenylbutazone	98.00[206]	92.30
Salicylic acid	100.00[205]	97.51
Theophylline	98.00[33]	96.54

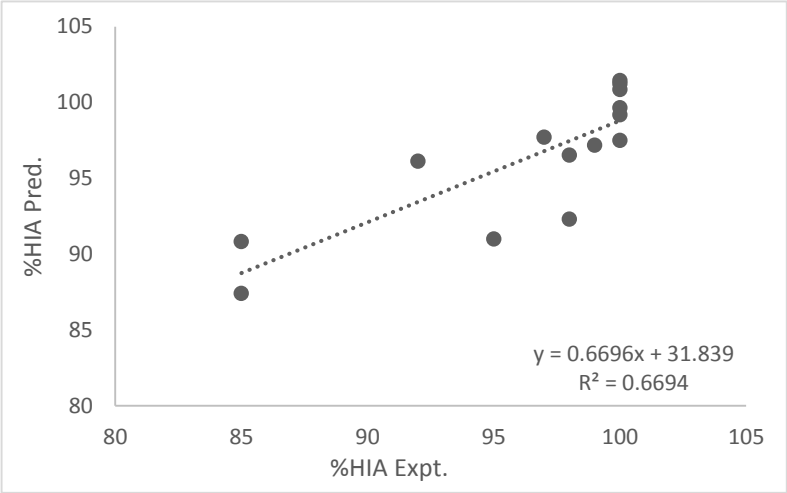

Figure 80: Plot of experimental vs. predicted %HIA.

3.C.3.2. Modelling of permeability coefficients obtained from PAMPA

The model obtained for the prediction of PAMPA log P_o is given by Equation 17:

$$\log P_o = -4.55 + 3.441 \log P_{mw} - 0.528\, pK_a \qquad \text{Eq. (17)}$$

Eleven drugs were used in the development of the final model. The model's R^2 =83.81 %, $R^2_{adjust.}$= 79.76 % , R^2_{PRED} = 71.04 %, S=0.749

A 95 % confidence interval for log P_{mw} is given by (1.68, 5.202), t-statistic and standardised coefficient of log P_{mw} are 4.505 ($p<0.05$) and 0.645 respectively suggesting statistical significance of log P_{mw} as a predictor. Also the F-ratio of the overall model is statistically significant, F=20.707 and P value 0.001 ($p<0.05$). The close agreement of the values of $R^2_{adjust.}$ & R^2_{PRED} indicates that the model does not over-fit the data. The residual analysis did not detect any relationship between residuals and predicted values as shown in Figure 81. The model is shown in Figure 82. The literature and predicted values for log P_o were listed in Table 51 and plotted in Figure 83 showing good predictability of the model.

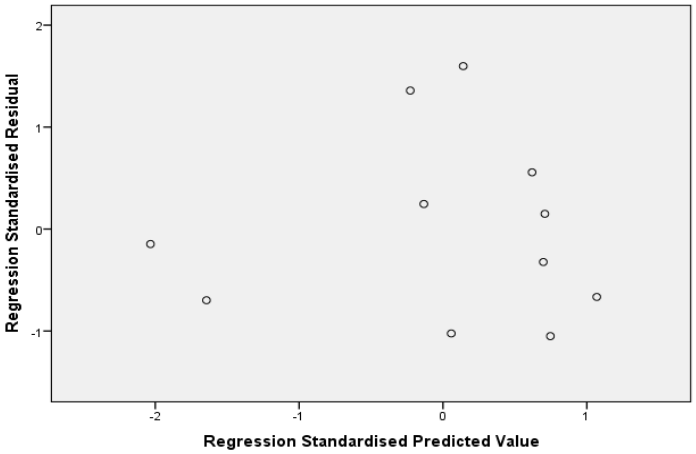

Figure 81: Residual plot for optimal PAMPA regression model.

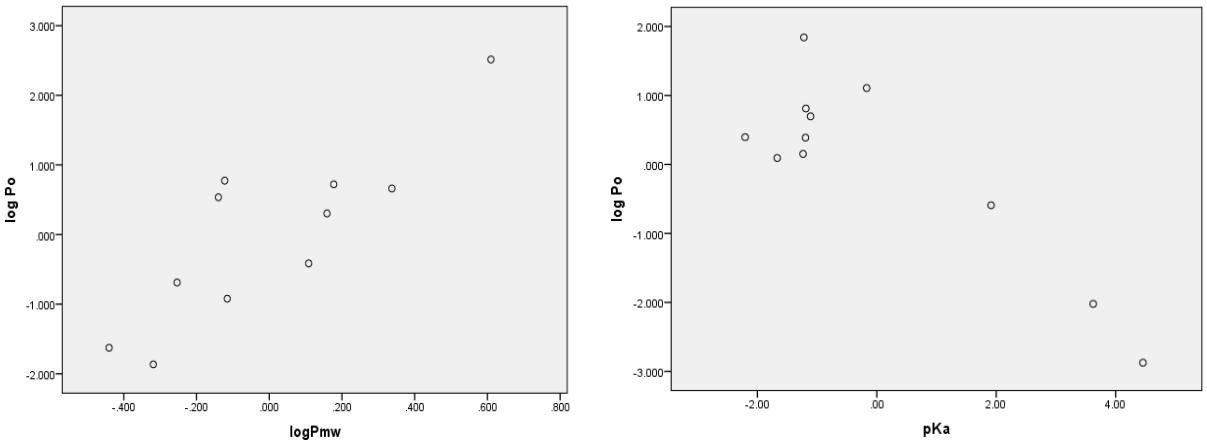

Figure 82: Partial regression plots of experimental log P_o values against log P_{mw} and pKa.

Table 51: Experimental and predicted values for PAMPA log P_o.

Drug	Expt. PAMPA log P_o[215]	Pred. PAMPA log P_o
Acetaminophen	-5.81	-5.29
Diclofenac	-1.37	-2.57
Gemfibrozil	-1.59	-1.7
Ibuprofen	-2.11	-3.13
Indomethacin	-1.65	-1.15
Ketoprofen	-2.43[64]	-1.64
Lidocaine	-1.42	-1.84
meloxicam	-2.8	-2.98
Phenylbutazone	-1.96	-1.72
Salicylic acid	-3.46[64]	-2.69
Theophylline	-5.99	-5.88

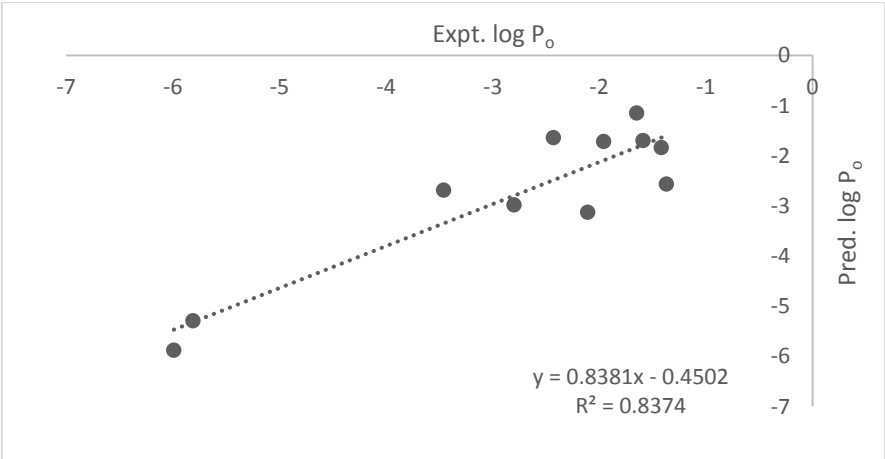

Figure 83: Plot of experimental vs. predicted log P_o.

3.C.3.3. Modelling of permeability coefficients obtained from Caco-2 $P_{eff.}$

The model obtained for the prediction of Caco-2 log $P_{eff.}$ is given by Equation 18:

$$\log P_{eff.} = -4.837 + 0.2494 \log P_{mw} - 0.000856\ Mwt + 0.02327\ pK_a \qquad \text{Eq. (18)}$$

Eleven drugs were used in the development of the final model. The model's R^2 =81.15 %, $R^2_{adjust.}$= 73.07 % , R^2_{PRED} = 58.31 %, S=0.077

A 95 % confidence interval for log P_{mw} is given by (0.053, 0.446), t-statistic and standardised coefficient of log P_{mw} are 3.006 ($p<0.05$) and 0.516 respectively suggesting statistical significance of log P_{mw} as a predictor. Also the F-ratio of the overall model is statistically significant, F=10.042 and P value 0.006 ($p<0.05$). The residual analysis did not detect any relationship between residuals and predicted values as shown in Figure 84. The model is shown in Figure 85. The predictive power of this model (58.31 %) was not as high as that of the model used for prediction of log P_o (71.04 %) as shown in Table 52 and Figure 86.

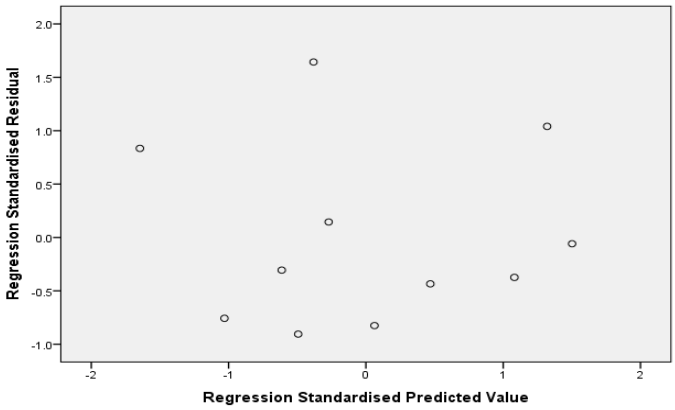

Figure 84: Residual plot for optimal log $P_{eff.}$ regression model.

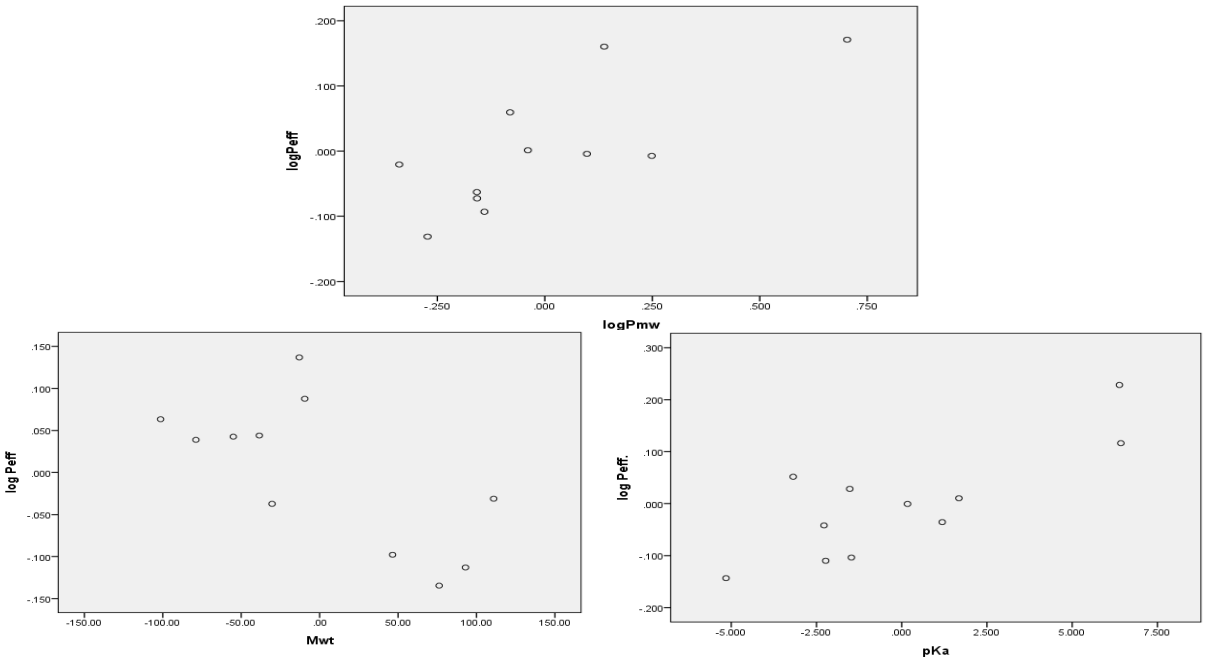

Figure 85: Partial regression plots of experimental log $P_{eff.}$ values against log P_{mw} , Mwt and pK_a.

Table 52: Experimental and predicted values for log $P_{eff.}$.

Drug	Expt. log $P_{eff.}$ [56]	Pred. log $P_{eff.}$
Acetaminophen	-4.44	-4.41
Caffeine	-4.30[60]	-4.38
Diclofenac	-4.75	-4.69
Fluconazole	-4.53[216]	-4.49
Ibuprofen	-4.58	-4.59
Indomethacin	-4.69[60]	-4.62
Ketoprofen	-4.48	-4.61
Lidocaine	-4.36	-4.36
meloxicam	-4.71	-4.77
Salicylic acid	-4.66[60]	-4.64
Theophylline	-4.61	-4.55

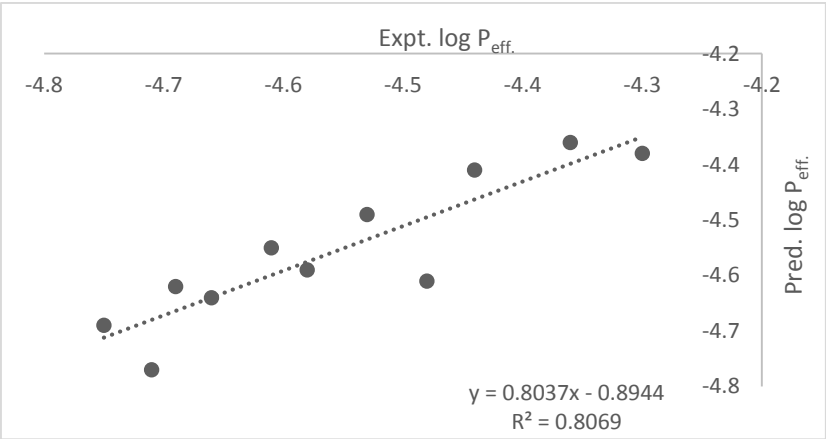

Figure 86: Plot of experimental vs. predicted log $P_{eff.}$.

Table 53: A summary of molecular descriptors for the selected drugs analysed by MLC using NaC in water and the experimental values of PAMPA log P_o, Caco-2 log $P_{eff.}$ and %HIA.

Drug	Log P_{mw}	Log $P_{O/W}$[184]	Mwt[218]	pK_a[184]	S_w[184]	HD[218]	HA[218]	FRB[218]	PSA[219]	V_M[218]	Log P_o [215]	Log $P_{eff.}$	%HIA
Acetaminophen	1.30	0.46	151.2	9.38	4.15	2	3	1	49.3	120.9	-5.81	-4.44[56]	100.00[205]
Caffeine	1.20	-0.07	194.2	10.4	11.00	0	6	0	58.4	133.4	-5.55	-4.30[60]	100.00[205]
Diclofenac	1.21	4.51	296.20	4.15	0.00447	2	3	4	49.3	206.8	-1.37	-4.75[56]	99.00[208]
Fenoprofen	1.21	3.10	522.6	4.5	0.0811	1	3	4	46.5	204.7	NA	NI	85.00[206]
Fluconazole	1.25	0.4	306.27	1.76[237]	1.39	1	7	5	81.6	205.3	NA	-4.526[216]	100.00[205]
Gemfibrozil	1.52	3.40	250.33	4.50	0.0278	1	3	6	46.5	239.7	-1.59	NA	95.00[207]
Ibuprofen	1.21	3.97	206.3	4.91	0.0684	1	2	4	37.3	200.3	-2.11	-4.58[56]	85.00[207]
Indomethacin	1.68	4.27	357.80	4.50	0.0024	1	5	4	68.5	269.6	-1.65	-4.69[60]	100.00[205]
Ketoprofen	1.44	3.12	254.3	4.45	0.0213	1	3	4	54.4	212.2	-2.43[64]	-4.48[56]	92.00[205]
Lidocaine	2.00	2.44	234.4	8.01	0.593	1	3	5	32.3	228.3	-1.42	-4.36[56]	100.00[236]
Meloxicam	1.08	3.43	351.40	4.08	0.154	2	7	2	136	220.3	-2.80	-4.71[56]	97.00[207]
Phenylbutazone	1.50	3.16	308.4	4.5	0.144	0	4	5	40.6	262.8	-1.96	NA	98.00[206]
Salicylic acid	1.00	2.26	138.1	2.97	11.3	2	3	1	57.5	100.4	-3.46[64]	-4.66[60]	100.00[205]
Theophylline	0.97	-0.02	180.17	8.80[228]	22.9	1	6	0	69.3	122.9	-5.99	-4.61[56]	98.00[33]

NA: no available data, NI: value not included in training set.

3.C.4. Conclusion

Generally, it can be concluded that the predictive ability of NaC when used as a micellar mobile phase in MLC was poor and not as promising as the other two bile salts considered (NaDC and NaTDC) since NaC is a less hydrophobic trihydroxy bile salt. Therefore, using NaC alone as a MLC mobile phase is not recommended for prediction of either human intestinal absorption or *in vitro* Caco-2 permeability constants yet its use in a mixture with other bile salts could potentially still be beneficial for prediction of human intestinal absorption (HIA).

CHAPTER 3

Section (D)

The Use Of NaTC In MLC

Section (D): Use of sodium taurocholate (NaTC) as a micellar mobile phase in MLC

3.D.1. Results and Discussion

In this section results of trials using trihydroxy bile salt sodium taurocholate (NaTC) as a micellar mobile phase in MLC are reported.

Trials of NaTC in water

An evaluation of MLC using NaTC in water was carried out through the analysis of a set of drugs with aqueous dilutions of NaTC. The drugs used in these trials were ketoprofen, caffeine, diphenhydramine and lidocaine. Unfortunately, retention times obtained with ketoprofen and caffeine using different concentrations of NaTC in water were inconsistent and the obtained plots of the inverse of the capacity factors against NaTC micellar concentration were not linear so determination of log P_{mw} was not possible. The use of NaTC in the analysis of the cationic drugs (diphenhydramine and lidocaine) was very difficult because of the great tailing these drugs exhibited. This could be attributed to the fact that NaTC is a trihydroxy bile salt where these types of bile salts are known for having high CMCs compared with dihydroxy bile salts so as a result, high concentrations of the surfactant were used [238] which might have led to more surfactant adsorbed on the column surface. This assumption was supported by the fact that the dead time of NaTC in water was found to be higher than that obtained with the previous bile salts used, (93.64 seconds). This led to a magnification of the tailing problem of the basic drugs with NaTC and therefore failure to facilitate analysis.

Trials of NaTC in 0.15 M NaCl

A second trial where 0.15 M NaCl was used as a solvent for NaTC was used in an attempt to decrease the repulsion between NaTC micelles therefore, reaching the CMC at a lower concentration.

Analysis of acetaminophen, caffeine, ketoprofen, lidocaine and diphenhydramine using dilutions of 20 mM NaTC in 0.15 M NaCl was used to evaluate the system. Data calculated and plotted from the retention profiles obtained are shown in Tables 54-56 and Figures 87-89.

Dead time was accurately determined for all the surfactant concentrations and an average of all of these determinations was taken. The average value of dead time for NaTC in 0.15 NaCl was determined to be 35.23 seconds which indicates less interaction and adsorption

of NaTC with the stationary phase (CN-RP column) in the presence of 0.15 M NaCl. CMC of NaTC in 0.15 M NaCl was taken to be 0.004 M [239].

3.D.1.1. Retention behaviour

Table 54: Total & micellar concentrations used of NaTC in 0.15 M NaCl as well as the inverse of the capacity factors (1/K') for 0.2 mM caffeine.

Conc. (M)	CM (M)	1/K'
0.006	0.002	0.160
0.008	0.004	0.169
0.013	0.009	0.184
0.018	0.014	0.192

Table 55: Total & micellar concentrations used of NaTC in 0.15 M NaCl as well as the inverse of the capacity factors (1/K') for 0.2 mM acetaminophen.

Conc. (M)	CM (M)	1/K'
0.005	0.001	0.362
0.008	0.004	0.388
0.009	0.005	0.391
0.013	0.009	0.428
0.016	0.012	0.450

Table 56: Total & micellar concentrations used of NaTC in 0.15 M NaCl as well as the inverse of the capacity factors (1/K') for 0.2 mM ketoprofen.

Conc. (M)	CM (M)	1/K'
0.005	0.001	0.781
0.006	0.002	0.715
0.010	0.006	1.196
0.013	0.009	1.238

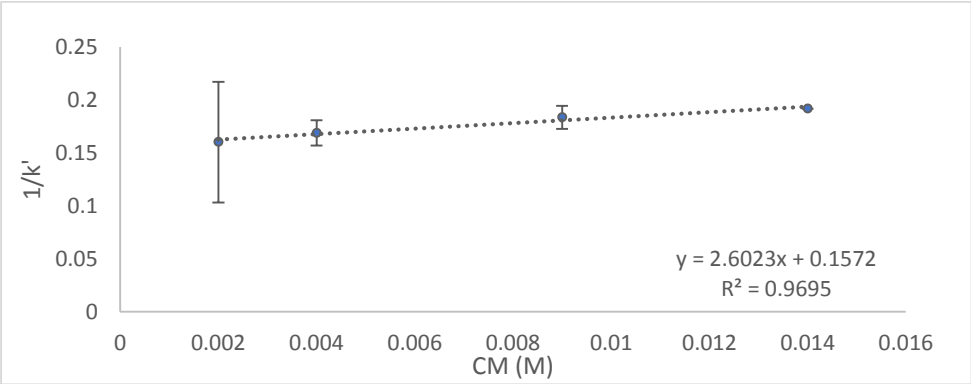

Figure 87: Calibration plot of the inverse of the capacity factor (1/K') versus micellar concentration CM (M) of NaTC in 0.15 M NaCl for 0.2 mM caffeine.
Log P_{mw}= 1.219±0.554

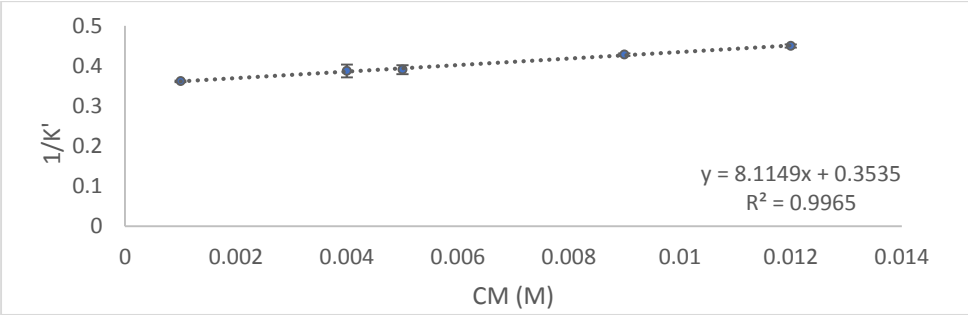

Figure 88: Calibration plot of the inverse of the capacity factor (1/K') versus micellar concentration CM (M) of NaTC in 0.15 M NaCl for 0.2 mM acetaminophen.
Log P_{mw}= 1.361±0.046

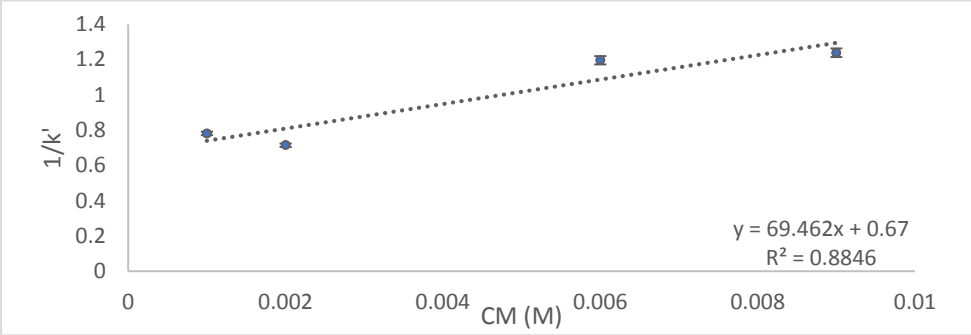

Figure 89: Calibration plot of the inverse of the capacity factor (1/K') versus micellar concentration CM (M) of NaTC in 0.15 M NaCl for 0.2 mM ketoprofen.
Log P_{mw}= 2.016±0.012

Acetaminophen, caffeine and ketoptofen showed more binding to the micelles of the NaTC surfactant as their concentration increased which can be seen in the shorter retention times of the previously mentioned drugs with the increase in the surfactant micellar concentration. The unexpected behaviour of ketoprofen as a binding solute could be attributed to the use of 0.15 M NaCl as a solvent as it neutralises the charge on the micelles therefore cancelling or decreasing the effect of repulsion forces in the medium.

As an attempt to solve the cationic drugs tailing problem with NaTC, as well as to mimic the conditions inside the intestine more closely, trials using simulated intestinal fluid (adjusted to pH 6.8) were used instead of 0.15 M NaCl.

Using NaTC in Simulated Intestinal Fluid (SIFsp)

Table 57: Total & micellar concentrations used of NaTC in (SIFsp) as well as the inverse of the capacity factors (1/K') for 0.2 mM caffeine.

Conc. (M)	CM (M)	1/K'
0.009	0.032	0.580
0.013	0.027	0.600
0.017	0.042	0.630
0.02	0.018	0.650

Table 58: Total & micellar concentrations used of (SIFsp) as well as the inverse of the capacity factors (1/K') for 0.2 mM theophylline.

Conc. (M)	CM (M)	1/K'
0.009	0.005	1.673
0.013	0.009	1.600
0.018	0.014	1.433
0.02	0.016	1.442

Table 59: Total & micellar concentrations used of NaTC in (SIFsp) as well as the inverse of the capacity factors (1/K') for 0.2 mM ibuprofen.

Conc. (M)	CM (M)	1/K'
0.005	0.001	1.231
0.008	0.004	1.341
0.01	0.006	1.475
0.018	0.014	1.741

Table 60: Total & micellar concentrations used of (SIFsp) as well as the inverse of the capacity factors (1/K') for 0.2 mM ketoprofen.

Conc. (M)	CM (M)	1/K'
0.008	0.004	1.110
0.01	0.006	1.055
0.013	0.009	0.967
0.016	0.012	0.692

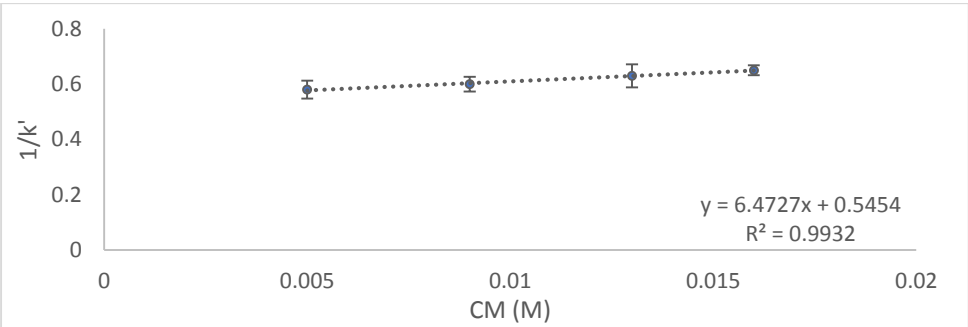

Figure 90: Calibration plot of the inverse of the capacity factor (1/K') versus micellar concentration CM (M) of NaTC in (SIFsp) for 0.2 mM caffeine.
Log P_{mw}= 1.07±0.13

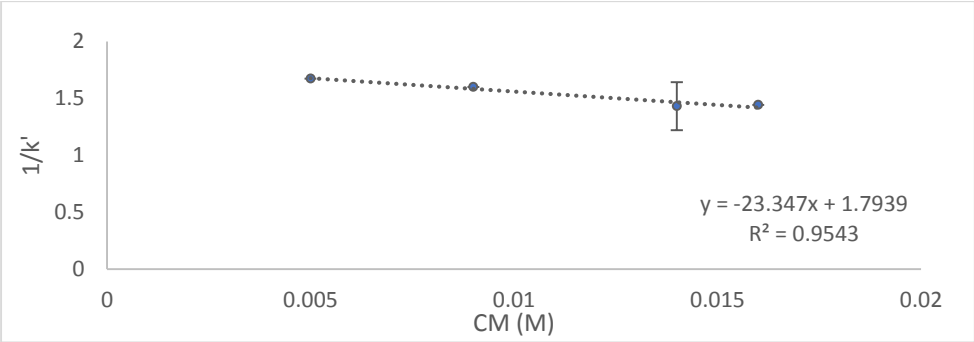

Figure 91: Calibration plot of the inverse of the capacity factor (1/K') versus micellar concentration CM (M) of (SIFsp) for 0.2 mM theophylline.
Log P_{mw}= 1.11±0.24

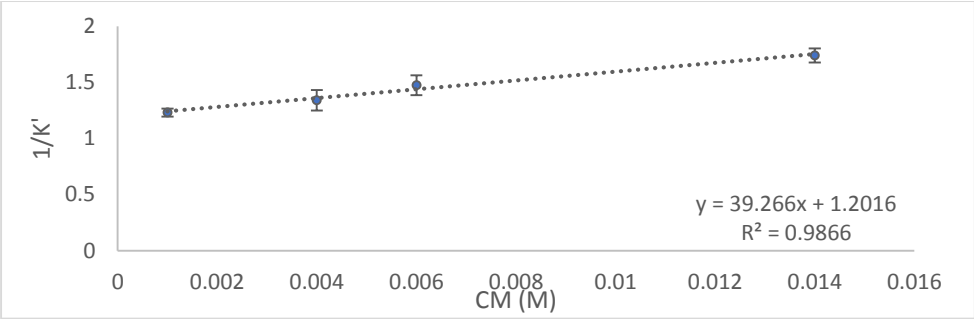

Figure 92: Calibration plot of the inverse of the capacity factor (1/K') versus micellar concentration CM (M) of NaTC in (SIFsp) for 0.2 mM ibuprofen.
Log P_{mw}= 1.51±0.03

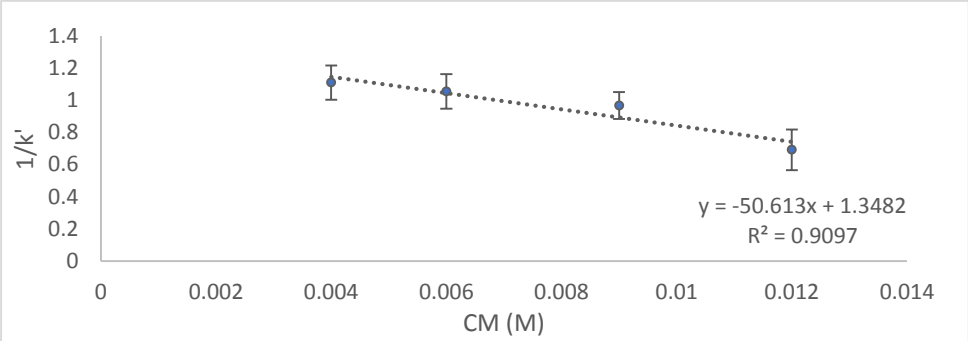

Figure 93: Calibration plot of the inverse of the capacity factor (1/K') versus micellar concentration CM (M) of (SIFsp) for 0.2 mM ketoprofen.
Log P_{mw}= 1.58± 0.08

Caffeine and theophylline differ in the way they interact with the mobile phase and stationary phase as shown in Tables 57-58 and Figures 90-97. As expected caffeine interacts as a binding solute while theophylline unexpectedly interacts as an antibinding solute. This is assumed to be as a result of the high hydrophilicity of theophylline which makes it favour the aqueous phase rather than the micelle core so it becomes more available to associate with the surfactant monomers adsorbed in a relatively high amount on the surface of the

column (indicated by a dead time value of 73.23 seconds) via hydrogen bonding with the extra hydroxyl group of trihydroxy NaTC.

The anionic drugs ketoprofen and ibuprofen also show opposite types of interaction in Tables 59-60 and Figures 92-93, where ketoprofen as expected acts as an antibinding solute while ibuprofen, as in previous sections, acts as a binding solute.

The retention times for cationic drugs diphenhydramine and lidocaine could not be determined because of a tailing problem with NaTC, as discussed before.

3.D.2. Conclusion

Based on the previous trials carried out for developing an MLC method with NaTC in water, 0.15 M NaCl or in simulated intestinal fluid it can be concluded that aqueous solutions of NaTC cannot be used as a micellar mobile phase in MLC for determination of a reliable retention profile for the analysed drugs. Furthermore, NaTC in 0.15 M NaCl or in (SIFsp) could not be used for analysis of cationic drugs because of the tailing phenomenon. Therefore if a method was developed with NaTC in 0.15 M NaCl or (SIFsp), the dataset obtained would be restricted to a narrow range of compounds and so it would not be a good general method for prediction of %HIA.

CHAPTER 3

Section (E)

The Use Of A Physiologically Relevant Mixed Micellar System Of Bile Salts In MLC

Section (E): Use of physiological mixture of bile salts as a micellar mobile phase in MLC

3.E.1. Results and Discussion

In this section an attempt to use a combination of bile salts in molar ratios similar to that present physiologically rather than using individual bile salts was carried out to investigate its effect on the retention behaviour of the analysed compounds and whether this developed method provides a better method than the previous methods for prediction of human intestinal absorption.

Since bile salts and lecithin (phosphatidylcholine) are considered to be two of the most common biosurfactants present in bile and involved in the digestion process, it was important to study the effect of using a mixed micellar system consisting of six bile salts and lecithin phospholipid as a mobile phase in MLC with the cyanopropyl column as a stationary phase.

The mixed micellar system used in this method consisted of a mixture of six bile salts (NaDC, NaC, NaTDC, NaTC, NaGC and NaGDC) which included dihydroxy, trihydroxy, conjugated and unconjugated bile salts with lecithin phospholipid in 0.15 M NaCl with the pH controlled by HEPES buffer at 6.5. The CMC of the mixed micellar system was 0.00458 M which is an average value of all the CMCs of the bile salts included in the mixture in 0.15 M NaCl (NaTC CMC =0.004 M [239], NaDC CMC =0.0024 M [239], NaTDC CMC =0.0024 M [239], NaC CMC =0.0075 M [192], NaGC CMC =0.009 M [239] and NaGDC CMC =0.0022 M [239]). A 0.002 M dilution mixed micellar solution with the same bile salts-lecithin molar ratios as that of the mixed micellar stock was used for preparation of different concentrations of this stock. The size of the micelles was constant, while concentration changed, by keeping the bile salt monomer concentration, represented by the dilution mixture, constant in each solution. The bile salt-lecithin mixed micellar solution was used over a concentration range of (0.005-0.017 M). Also its dead time was measured to be 106.4 seconds.

The mixed micellar system was prepared in molar ratios similar to that present physiologically [240]. Having both a positively charged choline head group and a negatively charged phosphate group, lecithin is considered to be a zwitterionic compound that tends to self-assemble in water forming characteristic bilayer membrane like structures [241]. Bile salts are distinguishable from conventional amphiphiles by their facial structure as they are amphiphiles with polar and nonpolar faces. Such unique structures is what leads to the unusual micelle structures formed upon bile salts' self-assembly in water which further

separates them from conventional head and tail surfactants. Various models have been proposed for bile salt micelle formation and several hypotheses have been made regarding their aggregates' structures formed through hydrophobic interactions between the steroid nuclei of bile salts (nonpolar face) and the hydrogen bonding between the bile salts hydroxyl groups (polar face) [242]. It was reported in previous studies that short rod like micelles were formed upon combining both bile salts and lecithin in a mixture [241]. The lecithin-bile salt complex is considered as a balanced system where the lecithin on its own in water forms unstable bilayer structures of low aqueous solubility because of its bulky hydrophobic tails inhibiting its solubility in water that is compensated and balanced by the presence of the bile salts of much greater water solubility. These can, in small amounts, stabilise the lecithin self-assembled structures by intercalating into these structures and thus promoting their water solubility which is one of the main physiological applications of bile salts.

Initially, it was suggested by Mazer, Benedek and Carey that the aqueous lecithin/bile salt micelles were disc-like in shape but later on, different techniques provided evidence that these micelles are cylindrical in shape that can further grow into long flexible cylindrical micellar chains termed "worms" which are similar to polymer chains where they entangle in a transient network rendering the solution highly viscous. This transformation of short cylinders to worms depends on the molar ratio of the two species and the ionic strength where molar ratio of bile salt: lecithin near equimolar with high background counterion concentration would induce the growth of the cylindrical micelles to worms [241]. As a result, caution was taken to avoid the previous conditions that lead to the formation of a highly viscous solution since the prepared micellar mixture was intended to be pumped in to the MLC chromatographic system. Additionally, the bile salt-lecithin mixed micellar system was prepared in a molar ratio of bile salt to lecithin much higher than one while using an optimum counterion concentration (0.15 M NaCl).

Lecithin prefers to be present in the form of low curvature cylindrical shaped bodies owing to its molecule possessing two tails. It is expected for the bile salts to form and stabilise the hemispherical end caps of these cylinders as bile salts are generally present in water as highly curved small micelles. Since stable end caps prevent the formed cylindrical micelles from further growing into long chains, adding more bile salts will result in more end caps being formed and therefore shorter cylinders. Figure 94 summarises the mechanism of micellisation in the bile salt-lecithin mixed micellar system where lecithin prefers to form bilayers when alone in water (left side of the figure). On the other hand, when bile salts are added to the solution they bind to lecithin head groups with themselves binding back-to-back

to each other resulting in expansion of the head group area (right side of the figure). As a result, bilayers turn into cylinders where the net geometry changes from a cylinder to truncated cone. In the case of low ionic strength, the negatively charged groups of bile salts suffer from high repulsion forces therefore bile salts get packed at the curved hemispherical end caps of the cylinders. The presence of a counterion (NaCl) of an optimum concentration is important because it decreases or neutralises the surface charge on the micelle thereby diminishing electrostatic repulsion and encouraging interaction between micelle forming species and hydrophobic association of bile salts and lecithin to give mixed micelles. It has to be taken into consideration that upon increasing the concentration of counterion, the electrostatic repulsion between the bile salts decreases, therefore the aggregation number of bile salt micelles increase and bile salts become less likely to form the highly curved end caps of the cylindrical mixed micelles inducing the growth of cylinders in to long chains which increase the viscosity of solution. So in the current method the concentration of the counterion should not be too high to avoid the formation of the long chains that render the solution viscous.

Eight drugs were used in the evaluation of the MLC method in this study. Acetaminophen, caffeine and fluconazole represented neutral drugs while ibuprofen, ketoprofen and phenylbutazone represented anionic drugs. Terbutaline and zolmitriptan represented cationic drugs.

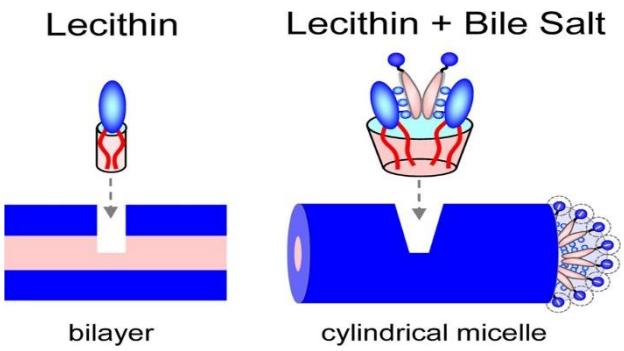

Figure 94: Schematic of the self-assembled structures formed by lecithin with and without bile salt in water (reference [241]).

3.E.1.1. Retention behaviour

Micelle-water partition coefficients were calculated as before. Data calculated and plotted from the retention profile obtained for the eight drugs are shown in Tables 61-68 and from Figures 95-102.

All the analysed drugs showed a binding interaction with the bile salt-lecithin mixed micelles as they showed a decrease in the retention time with the increase in the concentration of the mixed micellar system (Figures 103-104).

Table 61: Total & micellar concentrations used of physiologically simulating bile salt micellar mixture as well as the inverse of the capacity factors (1/K') for 0.2 mM acetaminophen.

Conc. (M)	CM (M)	1/K'
0.007	0.00242	2.189
0.010	0.00542	2.189
0.014	0.00942	2.404
0.017	0.01242	2.589

Table 62: Total & micellar concentrations used of physiologically simulating bile salt micellar mixture as well as the inverse of the capacity factors (1/K') for 0.2 mM caffeine.

Conc. (M)	CM (M)	1/K'
0.005	0.00042	0.821
0.007	0.00242	0.868
0.010	0.00542	0.860
0.014	0.00942	0.902
0.017	0.01242	0.915

Table 63: Total & micellar concentrations used of physiologically simulating bile salt micellar mixture as well as the inverse of the capacity factors (1/K') for 0.2 mM fluconazole.

Conc. (M)	CM (M)	1/K'
0.005	0.00042	0.878
0.007	0.00242	0.893
0.01	0.00542	0.935
0.014	0.00942	1.121
0.017	0.01242	1.090

Table 64: Total & micellar concentrations used of physiologically simulating bile salt micellar mixture as well as the inverse of the capacity factors (1/K') for 0.2 mM ibuprofen.

Conc. (M)	CM (M)	1/K'
0.005	0.00042	0.404
0.007	0.00242	0.415
0.010	0.00542	0.469
0.014	0.00942	0.514

Table 65: Total & micellar concentrations used of physiologically simulating bile salt micellar mixture as well as the inverse of the capacity factors (1/K') for 0.2 mM ketoprofen.

Conc. (M)	CM (M)	1/K'
0.005	0.00042	0.752
0.007	0.00242	0.783
0.010	0.00542	0.800
0.014	0.00942	1.001
0.017	0.01242	1.058

Table 66: Total & micellar concentrations used of physiologically simulating bile salt micellar mixture as well as the inverse of the capacity factors (1/K') for 0.2 mM phenylbutazone.

Conc. (M)	CM (M)	1/K'
0.005	0.00042	0.467
0.007	0.00242	0.498
0.010	0.00542	0.684
0.014	0.00942	1.076
0.017	0.01242	1.061

Table 67: Total & micellar concentrations used of physiologically simulating bile salt micellar mixture as well as the inverse of the capacity factors (1/K') for 0.2 mM terbutaline.

Conc. (M)	CM (M)	1/K'
0.007	0.00242	0.370
0.010	0.00542	0.373
0.014	0.00942	0.989
0.017	0.01242	1.081

Table 68: Total & micellar concentrations used of physiologically simulating bile salt micellar mixture as well as the inverse of the capacity factors (1/K') for 0.2 mM zolmitriptan.

Conc. (M)	CM (M)	1/K'
0.005	0.00042	0.154
0.007	0.00242	0.272
0.01	0.00542	0.420
0.014	0.00942	0.518
0.017	0.01242	0.587

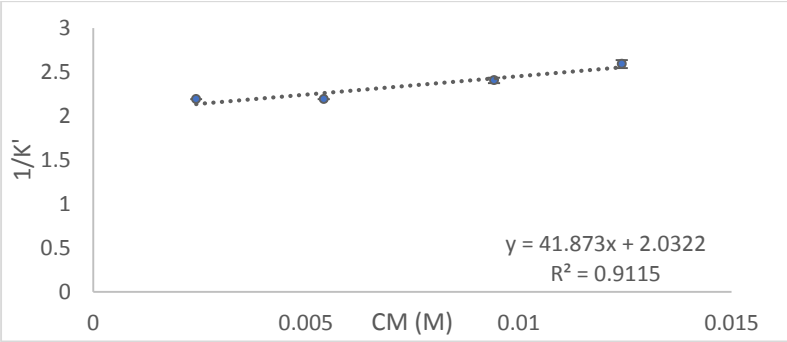

Figure 95: Calibration plot of the inverse of the capacity factor (1/K') versus micellar concentration CM (M) of physiologically simulating bile salt micellar mixture for 0.2 mM acetaminophen.

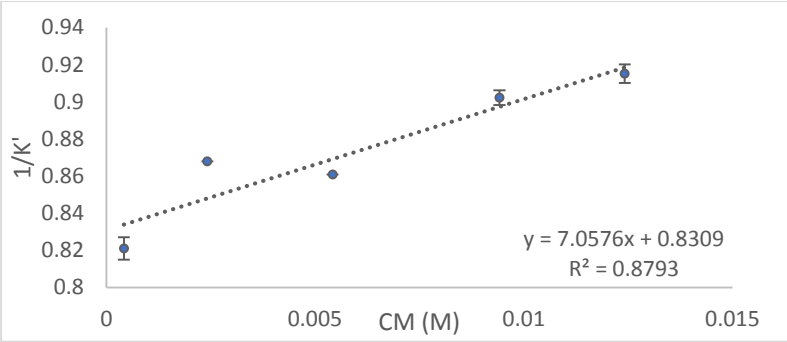

Figure 96: Calibration plot of the inverse of the capacity factor (1/K') versus micellar concentration CM (M) of physiologically simulating bile salt micellar mixture for 0.2 mM caffeine.

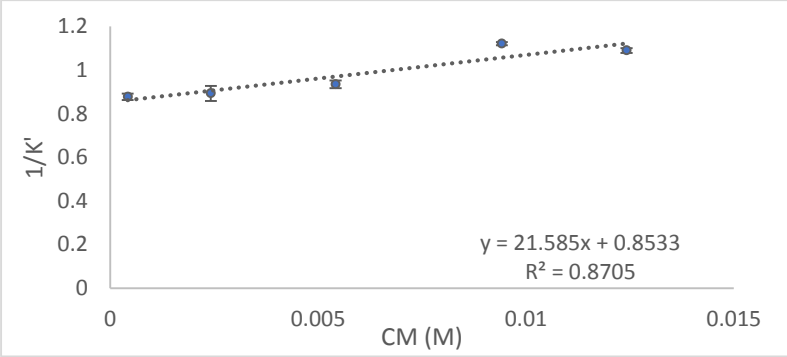

Figure 97: Calibration plot of the inverse of the capacity factor (1/K') versus micellar concentration CM (M) of physiologically simulating bile salt micellar mixture for 0.2 mM fluconazole.

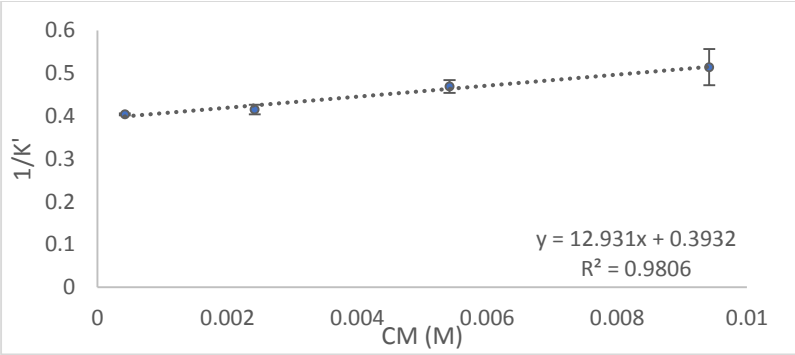

Figure 98: Calibration plot of the inverse of the capacity factor (1/K') versus micellar concentration CM (M) of physiologically simulating bile salt micellar mixture for 0.2 mM ibuprofen.

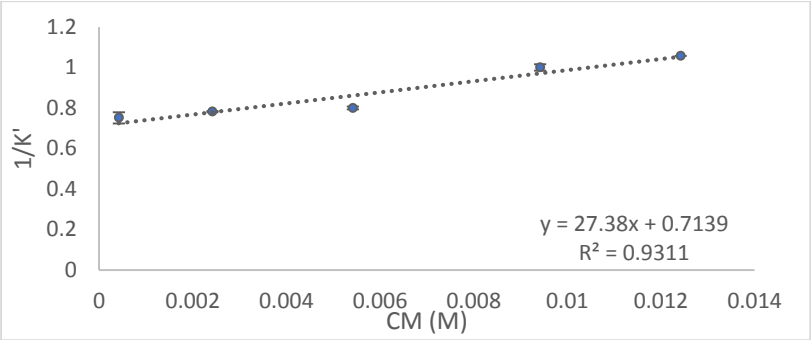

Figure 99: Calibration plot of the inverse of the capacity factor (1/K') versus micellar concentration CM (M) of physiologically simulating bile salt micellar mixture for 0.2 mM ketoprofen.

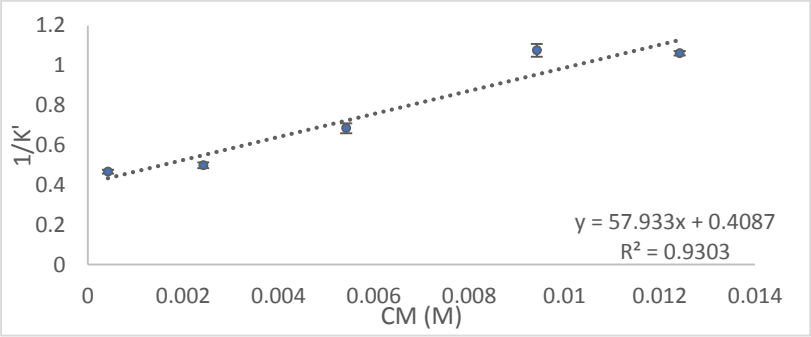

Figure 100: Calibration plot of the inverse of the capacity factor (1/K') versus micellar concentration CM (M) of physiologically simulating bile salt micellar mixture for 0.2 mM phenylbutazone.

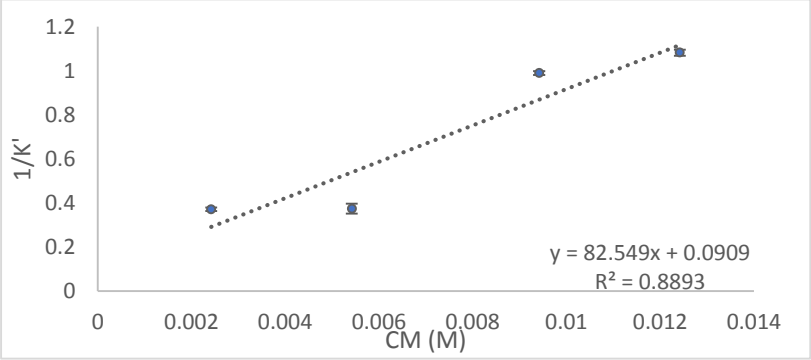

Figure 101: Calibration plot of the inverse of the capacity factor (1/K') versus micellar concentration CM (M) of physiologically simulating bile salt micellar mixture for 0.2 mM terbutaline.

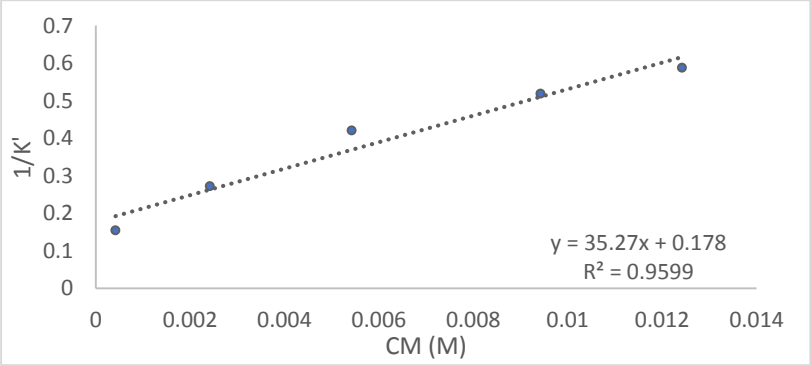

Figure 102: Calibration plot of the inverse of the capacity factor (1/K') versus micellar concentration CM (M) of physiologically simulating bile salt micellar mixture for 0.2 mM zolmitriptan.

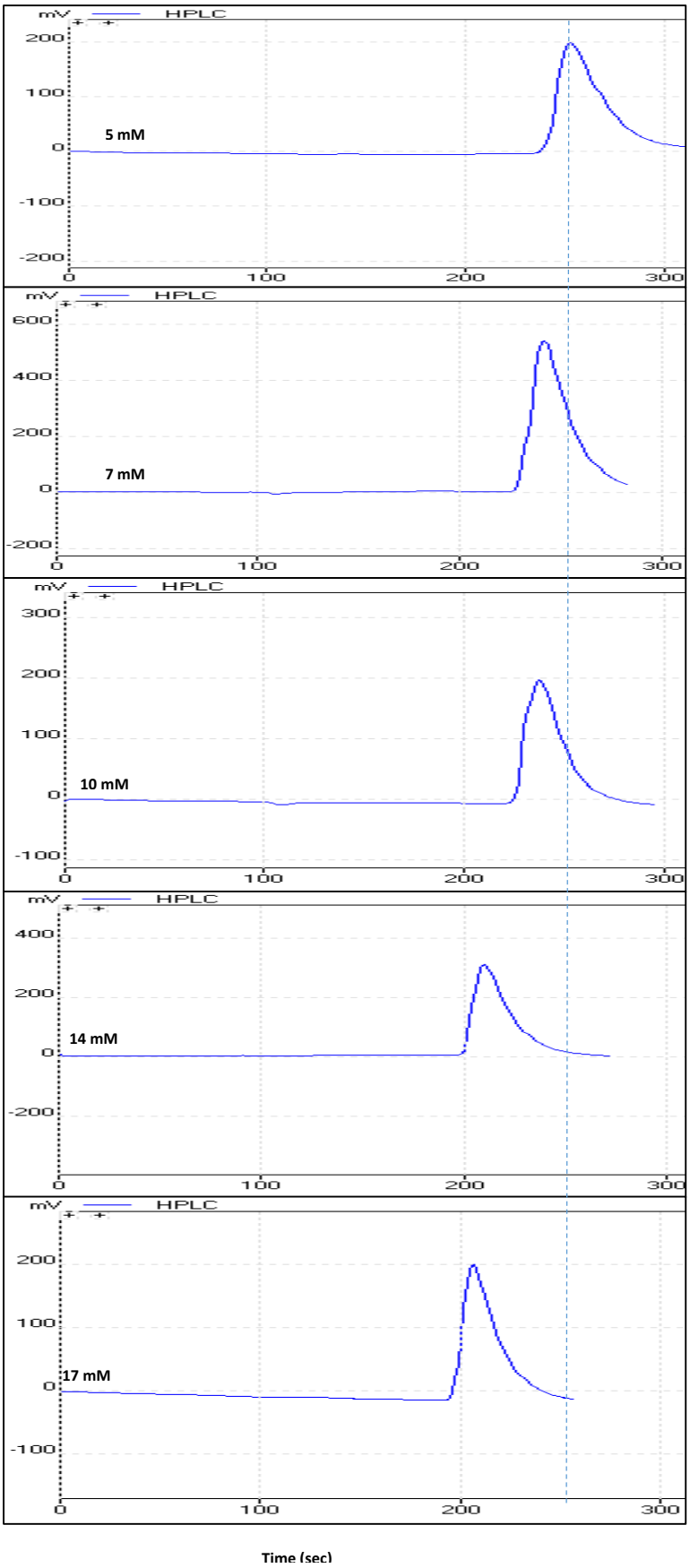

Figure 103: Chromatograms showing binding behaviour of ketoprofen in increasing concentrations of physiological micellar bile salts mixture as a mobile phase. (The dotted line is only used for visual guidance).

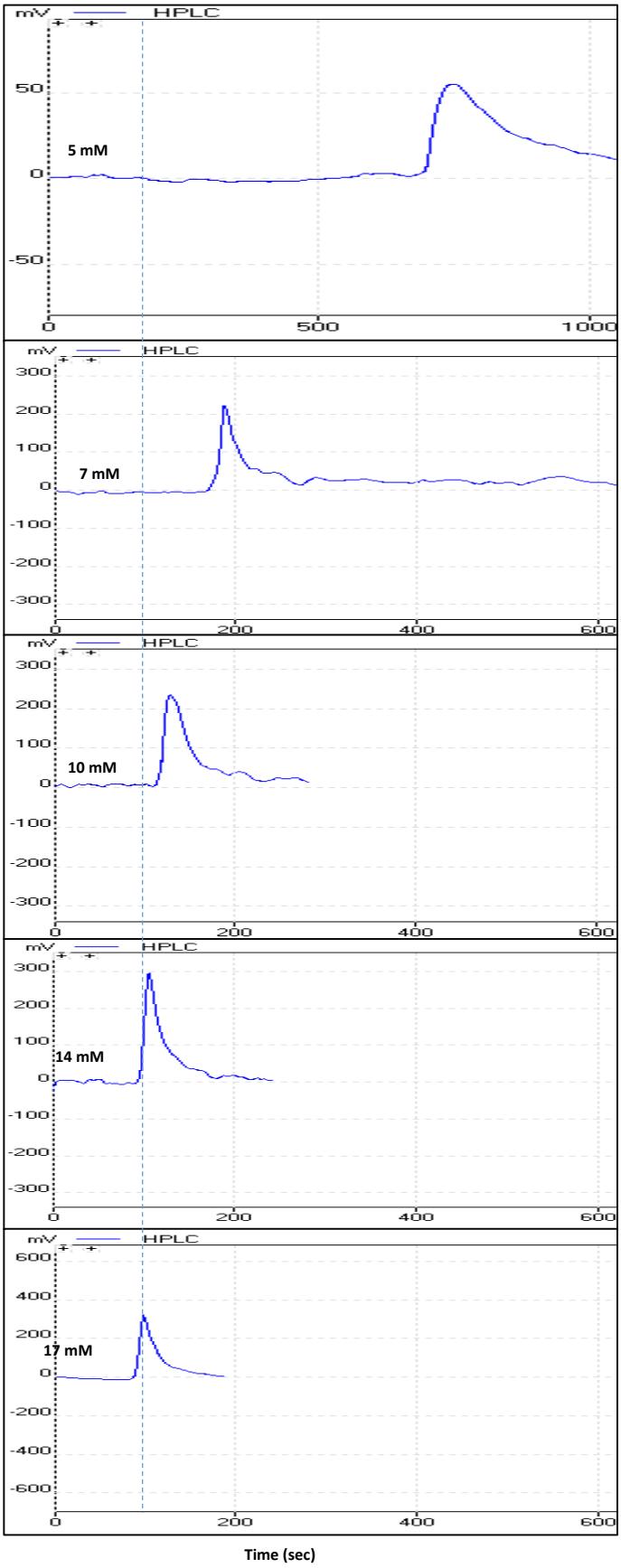

Figure 104: Chromatograms showing binding behaviour of zolmitriptan in increasing concentrations of physiological micellar bile salts mixture as a mobile phase. (The dotted line is only used for visual guidance).

The neutral drugs (acetaminophen, caffeine and fluconazole) showed a binding interaction with the bile salt-lecithin mixed micelles. The neutral analysed drugs are solubilised inside the hydrophobic core of the cylindrical mixed micelles.

Also the anionic drugs (ibuprofen, ketoprofen and phenylbutazone) showed atypical retention behaviour where they acted as binding solutes rather than acting as antibinding solutes. This could be attributed to the diminished repulsion forces between micelles resulting from charge neutralisation brought about by counterion (NaCl) binding. As a result, these anionic drugs could overcome any remaining weak repulsion forces and were not repelled away from the micelles thus they became solubilised inside the hydrophobic core of the mixed micelles.

The cationic drugs (terbutaline and zolmitriptan), behaved as binding solutes as expected. Binding of these drugs to the mixed micelles takes place through electrostatic attraction between the positively charged drug and the remaining non-neutralised negatively charged groups within the mixed micelles in addition to binding to the hydrophobic core of the mixed micelle thereby resulting in the solubilisation of these drugs in both cases.

As shown in Table 69, it can be seen that for all the analysed drugs the obtained log P_{mw} values were greater than those of log $P_{o/w}$ which reflects the preference of the analysed drugs to the bile salt-lecithin mixed micelles due to their stability, bigger hydrophobic core diameter and core fluidity [110].

Table 69: Partition coefficients obtained from MLC using a physiological bile salt micellar mixture for eight drugs with their standard deviations against their octanol/water partition coefficients.

Compound	Log P_{mw}	Log $P_{o/w}$[184]
Acetaminophen	1.31±0.06	0.46
Caffeine	0.93±0.001	-0.07
Fluconazole	1.40±0.05	0.40
Ibuprofen	1.52±0.21	3.97
Ketoprofen	1.58±0.04	3.12
Phenylbutazone	2.15±0.02	3.16
Terbutaline	2.96±0.08	0.90
Zolmitriptan	2.30±0.11	1.60

3.E.2. Statistical Modelling

After the analysis of a group of 18 drugs using a physiologically simulating bile salt-lecithin mixed micellar solution, followed by calculation of log P_{mw} from the calibration plots of (1/K') against (CM), the obtained log P with a number of other molecular descriptors such as molecular weight (Mwt), polar surface area (PSA), freely rotating bonds (FRB), molar volume (V_M), dissociation constant (pK_a), aqueous solubility (S_w), number of hydrogen bond donors (nHD) and number of hydrogen bond acceptors (nHA) were used for developing models for prediction of %HIA and Caco-2 and PAMPA permeability coefficients. Experimentally obtained log P_{mw} using this MLC method with the other molecular descriptors used in developing the three models are shown in Table 73.

3.E.2.1. Statistical Modelling of Human Intestinal absorption (HIA)

Log P_{mw} was included in a model equation with %HIA experimental values for orally administered drugs (as shown in Table 70) which allowed the prediction of human intestinal absorption (%HIA). The model obtained for the prediction of %HIA is given by Equation 19:

$$\text{logit HIA} = 4.103 - 0.939 \log P_{mw} - 0.02218\ \text{PSA} \quad \text{Eq. (19)}$$

Fifteen drugs were used in the development of the final model. The model's R^2 = 86.40 %, $R^2_{adjust.}$= 84.13 % , R^2_{PRED} = 80.73 %, S= 0.247

A 95 % confidence interval for log P_{mw} is given by (-1.18, -0.699), t-statistic and standardised coefficient of log P_{mw} are -8.51 ($p<0.05$) and -0.964 respectively suggesting statistical significance of log P_{mw} as a predictor. Also the F-ratio of the overall model is statistically significant, F=38.12 and P value 0.007 ($p<0.05$). Figure 105 shows no marked relationship between residuals and predicted values while Figure 106 summarises the model. The literature and predicted values of %HIA are shown in Table 70 and Figure 107. Three drugs (acetaminophen, ibuprofen and salicylic acid) were used to test the obtained model. The model was able to predict the %HIA for these compounds within a minimum of 0.61 % and a maximum of 4.43 % difference between predicted and published data for %HIA.

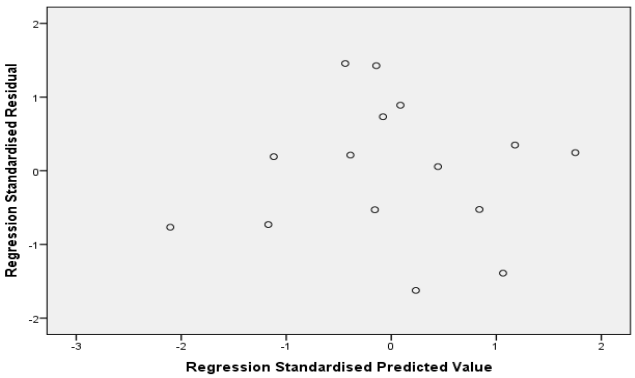

Figure 105: Residual plot for optimal logit HIA regression model.

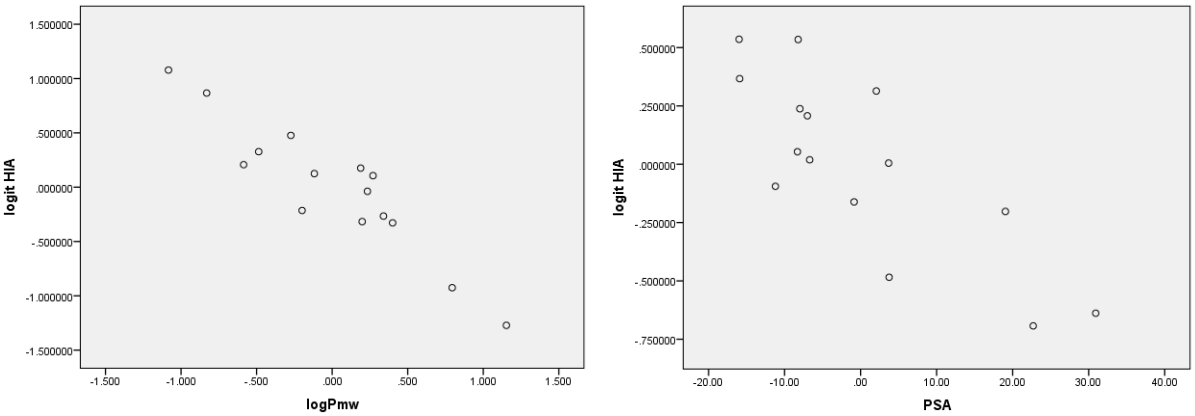

Figure 106: Partial regression plots of experimental logit HIA values against log P_{mw} and PSA**.**

Table 70: Experimental and predicted values for % HIA.

Drug	Expt. %HIA	Pred. %HIA
Acetaminophen*	100.00[205]	98.35
Acetylsalicylic acid	82.00[205]	91.98
Caffeine	99.00[230]	98.85
Carbamazepine	83.50[209, 243]	87.24
Cimetidine	68.00[205, 244]	65.58
Diclofenac	54.00[245]	64.00
Fenoprofen	85.00[206]	83.39
Fluconazole	94.00[246]	90.42
Flurbiprofen	92.00[247]	88.34
Ibuprofen*	98.00[246]	98.61
Ketoprofen	95.00[246]	96.24
Naproxen	94.00[205]	87.44
Nicotinic acid	94.00[246]	97.19
Phenylbutazone	94.00[206, 245]	93.82
Salicylic acid*	99.00[247]	94.57
Terbutaline	25.00[248]	34.01
Theophylline	98.00[33]	97.57
Zolmitriptan	91.50[246]	82.46

The asterisk (*) indicates the validation compounds.

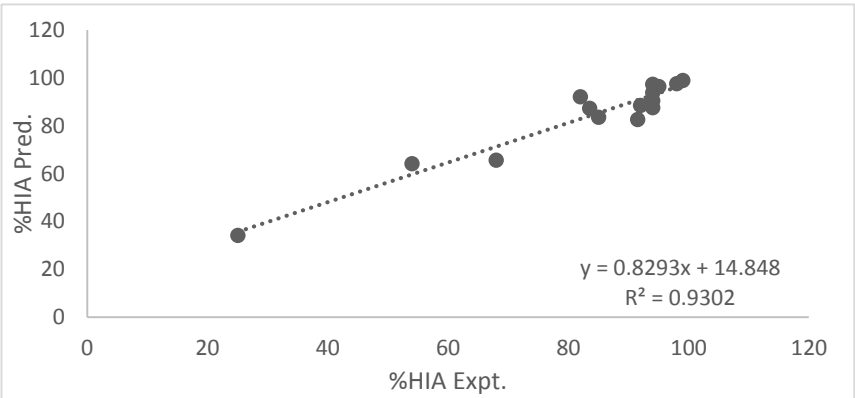

Figure 107: Regression plot of predicted %HIA values against Literature %HIA.

3.E.2.2. Modelling of permeability coefficients obtained from PAMPA

The model obtained for the prediction of PAMPA log P_o is given by Equation 20:

$$\log P_o = -7.180 + 2.104 \log P_{mw} \qquad \text{Eq. (20)}$$

Thirteen drugs were used in the development of the final model. The model's R^2 = 59.24 %, $R^2_{adjust.}$= 55.54 % , R^2_{PRED} = 46.33 %, S= 1.122

A 95 % confidence interval for log P_{mw} is given by (0.946, 3.262). t-statistic and standardised coefficient of log P_{mw} are 4 ($p<0.05$) and 0.77 respectively suggesting that its statistical significance of log P_{mw} as a predictor. Also the F-ratio of the overall model is statistically significant, F=15.99 and P value 0.002 ($p<0.05$).

The close agreement of the values of $R^2_{adjust.}$ & R^2_{PRED} indicates that the model does not over-fit the data. The residual analysis did not detect any relationship between residuals and predicted values as shown in Figure 108. The model had poor prediction power for log P_o (46.33 %) as shown in Table 71 and Figure 109.

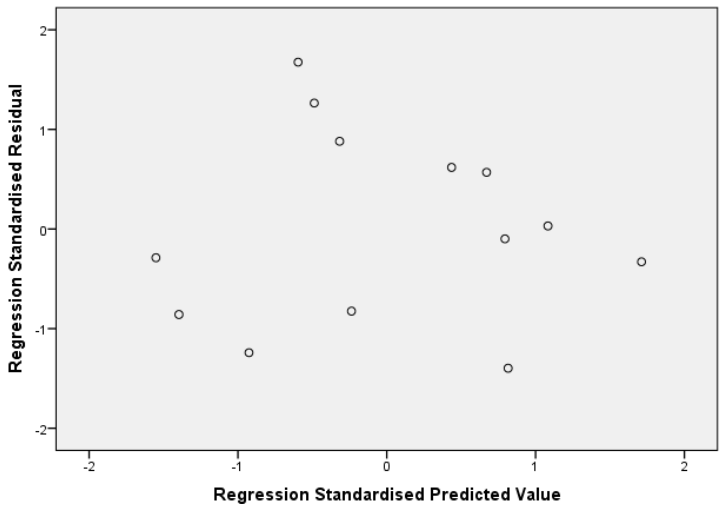

Figure 108: Residual plot for optimal PAMPA regression model.

Table 71: Experimental and predicted values for PAMPA logP_o.

Drug	Expt. PAMPA log P_o[215]	Pred. PAMPA log P_o
Acetaminophen	-5.81	-4.42
Aspirin	-4.45	-3.53
Caffeine	-5.55	-5.23
carbamazepine	-3.73	-2.16
Diclofenac	-1.37	-1.00
Flurbiprofen	-1.78	-1.82
Ibuprofen	-2.11	-3.99
Ketoprofen	-2.43[64]	-3.85
Naproxen	-2.30	-2.19
Phenylbutazone	-1.96	-2.65
Salicylic acid	-2.64	-3.63
Theophylline	-5.99	-5.03
Zolmitriptan	-1.71	-2.35

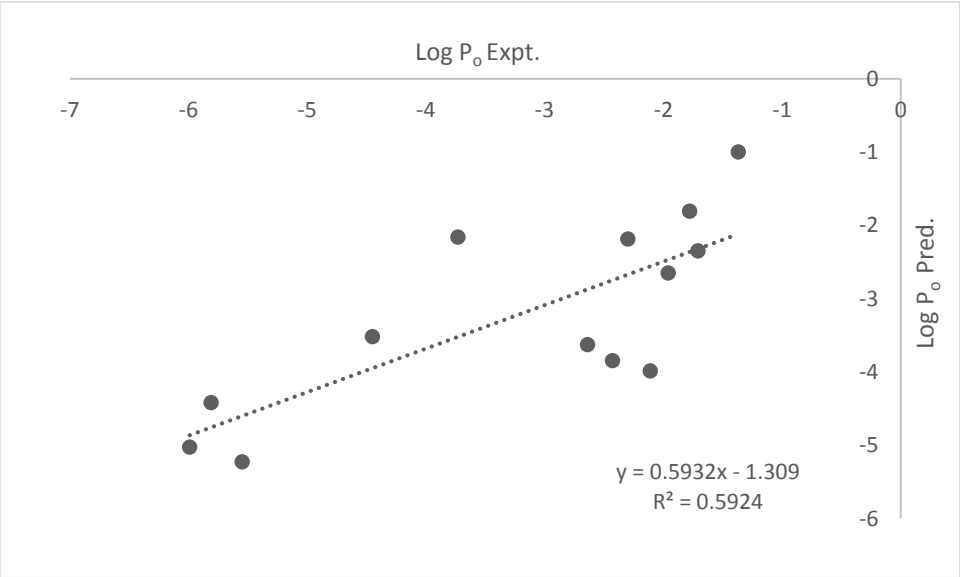

Figure 109: Plot of experimental vs. predicted log P_o values.

3.E.2.3. Modelling of permeability coefficients obtained from Caco-2 $P_{eff.}$

The model obtained for the prediction of Caco-2 $P_{eff.}$ is given by Eq. (21):

$$\log P_{eff.} = -3.697 - 0.3913 \log P_{mw} + 0.288\ nHD - 0.1672\ nHA \qquad \text{Eq. (21)}$$

Fourteen drugs were used in the development of the final model. The model's R^2 = 79.97 %, $R^2_{adjust.}$= 73.96 % , R^2_{PRED} = 65.77%, S= 0.147

A 95 % confidence interval for log P_{mw} is given by (-0.554, -0.228), t-statistic and standardised coefficient of log P_{mw} are -5.35 ($p<0.05$) and -0.854 respectively suggesting statistical significance of log P_{mw} as a predictor. Also the F-ratio of the overall model is statistically significant, F=13.31 and P value 0.001 ($p<0.05$).

Figure 110 shows no marked relationship between residuals and predicted values while Figure 111 summarises the model. The log $P_{eff.}$ values obtained from literature were plotted against that predicted by the model (Figure 112) showing its good prediction power. The literature and predicted log $P_{eff.}$ values are listed in Table 72.

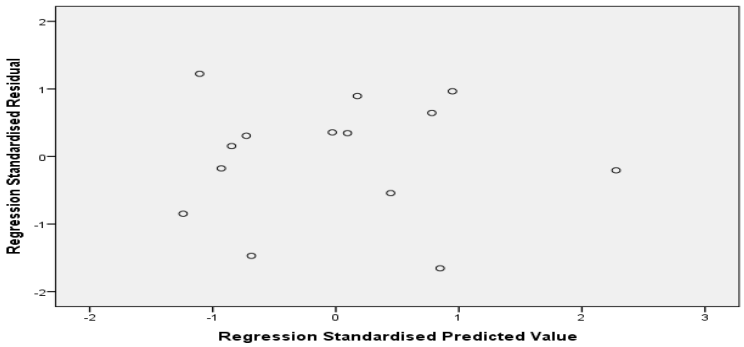

Figure 110: Residual plot for optimal Caco-2 regression model.

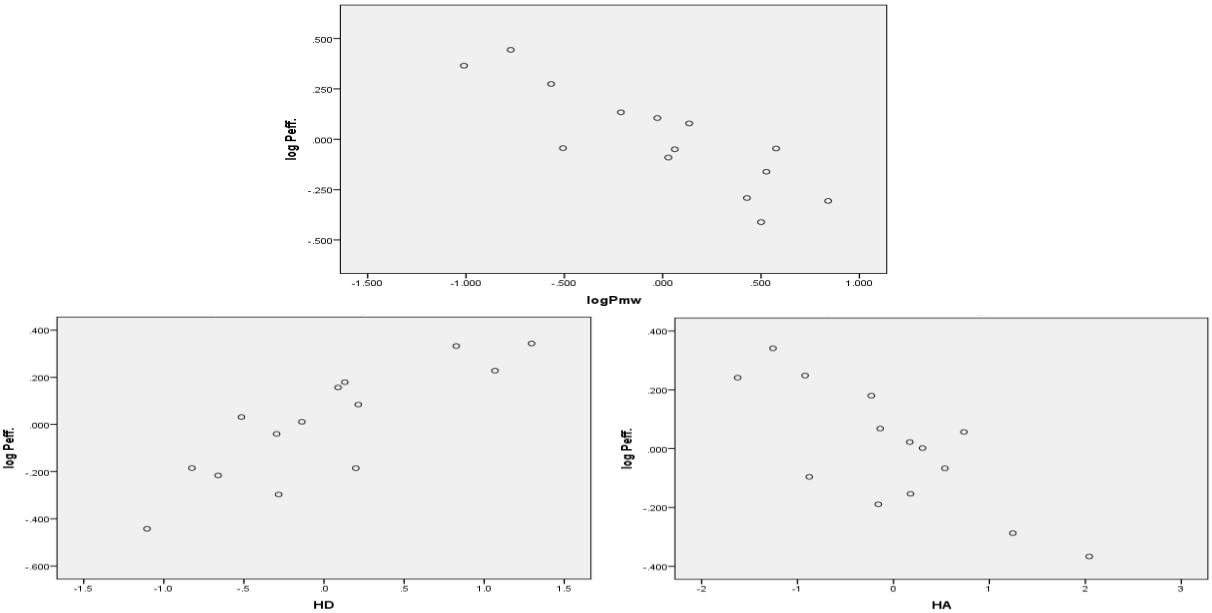

Figure 111: Partial regression plots of experimental Caco-2 log $P_{eff.}$ values against log P_{mw}, HD and HA.

Table 72: Experimental and predicted values for Caco-2 log $P_{eff.}$.

Drug	Expt. Caco-2 log $P_{eff.}$	Pred. Caco-2 log $P_{eff.}$
Acetaminophen	-4.00	-3.97
Caffeine	-4.51[63]	-4.56
carbamazepine	-4.38[56]	-4.51
cimetidine	-4.52[249]	-4.44
Diclofenac	-4.75[56]	-4.77
Fenoprofen	-4.95[230]	-4.73
Fluconazole	-4.82[56]	-4.79
Flurbiprofen	-4.70[230]	-4.74
Ibuprofen	-4.58[56]	-4.34
Ketoprofen	-4.48[56]	-4.53
Naproxen	-4.66[56]	-4.84
Phenylbutazone	-5.00[250]	-4.87
Theophylline	-4.17[215]	-4.31
Zolmitriptan	-4.26[215]	-4.35

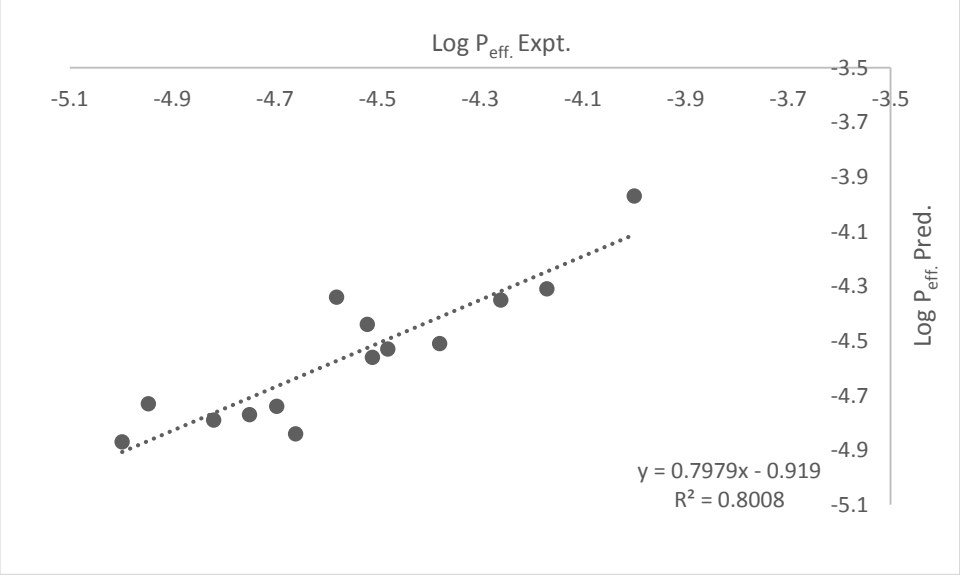

Figure 112: Plot of experimental vs predicted Caco-2 log $P_{eff.}$ values.

Table 73: A summary of molecular descriptors for the selected drugs analysed by MLC using physiologically resembling bile salt-lecithin mixed micellar system and experimental human intestinal absorption (%HIA), permeability coefficients of PAMPA and Caco-2 tests.

Drug	Log P_{mw}	Log $P_{o/w}$[184]	Mwt[218]	pK_a[184]	S_w[184]	HD[218]	HA[218]	FRB[218]	PSA[219]	V_M[218]	Log P_o[215]	Log $P_{eff.}$	%HIA
Acetaminophen	1.31	0.46	151.20	9.9	14	2	2	1	49.3	131.1	-5.81	-4.00	100[205]
Acetylsalicylic acid	1.74	1.19	180.15	3.41	10[219]	1	4	3	63.6	139.6	-4.45	NA	82[205]
Caffeine	0.93	-0.07	194.20	14	21.6	0	3	0	58.4	133.4	-5.55	-4.51[63]	99[230]
Carbamazepine	2.39	2.45	236.36	13.9	0.21	1	1	0	46.3	186.6	-3.73	-4.38[56]	83.5[205, 243]
Cimetidine	1.97	0.4	252.34	6.8	9.38	3	5	8	88.89	198.2	NI	-4.52[249]	68[205, 244]
Diclofenac	2.94	4.51	296.20	4.15	0.00237	2	3	4	49.3	206.8	-1.37	-4.75[56]	54[245]
Fenoprofen	2.52	3.1	242.27	4.5	0.033	1	2	4	46.5	204.7	NA	-4.95[230]	85[206]
Fluconazole	1.40	0.4	306.27	12.71	9	1	5	5	81.6	205.3	NA	-4.82[56]	94[246]
Flurbiprofen	2.55	4.16	244.26	4.42	0.008	1	2	3	37.3	203.6	-1.78	-4.7[230]	92[247]
Ibuprofen	1.52	3.97	206.30	5.2	0.0684	1	2	4	37.3	200.3	-2.11	-4.58[56]	98[246]
Ketoprofen	1.58	3.12	254.30	3.88	0.051	1	3	4	54.4	212.2	-2.43[64]	-4.48[56]	95[246]
Naproxen	2.37	3.18	230.26	4.15	0.0159	1	3	3	46.5	192.3	-2.3	-4.66[56]	94[205]
Nicotinic acid	1.55	0.36	123.11	4.75	83.1	1	3	1	50.2	95.2	NA	NA	94[230]
Phenylbutazone	2.15	3.16	308.37	4.4	0.7	0	2	5	40.6	262.8	-1.96	-5[250]	94[206, 245]
Salicylic acid	1.69	2.26	138.12	3	11.3	2	3	1	57.5	100.4	NI	NI	99[247]
Terbutaline	2.96	0.9	225.28	9.76	213	4	4	4	72.7	192.3	NI	NI	25[248]
Theophylline	1.02	-0.02	180.16	8.8[228]	22.9	1	3	1	69.3	122.9	-5.99	-4.17[215]	98[33]
Zolmitriptan	2.30	1.6	287.36	9.52	0.19	2	2	5	57.4	236.1	-1.71	-4.26[215]	91.5[246]

NA: no available data, NI: value not included in training set.

3.E.3. Conclusion

Developing an MLC method that used a physiologically resembling bile salt-lecithin mixed micellar system was successful. Such a method had a significant impact on the elution of compounds and the type of interaction they experienced upon being injected into used MLC system. The bile salt/phospholipid combination had a higher solubilising capacity for compounds than that of the individual bile salt systems used in the previous sections which is confirmed by the switch of all compounds into binding solutes favouring the formed micelles. This developed MLC method appears to be a closer approach for prediction of HIA than for prediction of *in vitro* methods which is reflected in the model obtained for prediction of %HIA having higher predictive power (R^2_{PRED}= 81 %) compared with *in vitro* permeability (R^2_{PRED}= 46 % for PAMPA and R^2_{PRED}= 66 % for Caco-2). Overall, it can be concluded that there is a close resemblance between the physiologically occurring and the synthetic bile salt/phospholipid micellar mixture used in this MLC method which helped the compounds to act in a way closer to how they permeate through the human intestine therefore simulating the human intestinal absorption process to some extent.

CHAPTER 3

Section (F)

The Effect Of Change Of Column Type In MLC

"The Use Of An Amino Column In MLC"

Section (F): Effect of using amino column with sodium deoxycholate (NaDC) as a micellar mobile phase in MLC

3.F.1. Results and Discussion

This section reports results arising from changing the type of stationary phase, represented by the column used, on the partitioning of analysed compounds in MLC. The change in the type of the column used in an MLC method has a great impact on the retention pattern of the analysed compounds and consequently on the obtained log P_{mw} which is a reflection of the partitioning process of the compounds under study. In the previous sections the effect of the change in the mobile phase type used was considered. In this section the column type used was changed from cyanopropyl to aminopropyl in order to investigate the effect of the change in the stationary phase on the way the analysed drugs interact with both the stationary phase and micellar mobile phase.

NaDC was used as the micellar mobile phase with the same conditions and concentration range (0.005-0.020 M) as used in Section (3A) in this chapter. As before, the pH was measured at both the lowest and the highest concentrations of the mobile phase and found to be in the range of (6.4-8.0).

The dead time average value was determined to be 79.40 seconds reflecting more interaction of the micellar mobile phase NaDC with the amino column rather than the cyanopropyl column, which suggests a higher amount of NaDC adsorbed on the column surface.

A set of fourteen compounds (anionic, cationic and neutral) were used to evaluate the amino column with NaDC in MLC. Acetaminophen, caffeine, fluconazole and theophylline represented neutral compounds while fenoprofen, gemfibrozil, ibuprofen, lornoxicam, meloxicam, phenylbutazone, piroxicam and salicylic acid represented anionic compounds. Lidocaine and terbutaline represented cationic compounds.

Micelle-water partition coefficients were determined and calculated in the same way as in the previous sections. The CMC value of NaDC was taken to be 0.005 M [200].

3.F.1.1. Retention behaviour

Data calculated and plotted from the retention profile obtained for the previously mentioned fourteen drugs, used for evaluation of the current MLC system, using

dilutions of 20 mM NaDC in water as a mobile phase and aminopropyl (APS) column as a stationary phase are shown in Tables 74-86 and Figures 113-126.

A significant change in the retention behaviour of the analysed drugs was observed upon the use of the amino column as a stationary phase in this MLC method. Opposite to what was expected, neutral drugs showed antibinding behaviour while cationic and anionic drugs showed both binding and antibinding behaviour according to their molecular weight. Salt bridge formation is assumed to be the theory behind the change in the way drugs interacted with the stationary phase (aminopropyl column) that leads to unconventional patterns of elution taking place. This assumption is supported by the work of Takeuchi *et al.* who showed the possibility of using bile acids as stationary phases in liquid chromatography through their immobilisation on aminopropyl silica through electrostatic interactions [179]. Salt bridge is a combination of two noncovalent interactions which are hydrogen bonding and electrostatic interaction. Although such bridges are abundant in protein folded conformations giving them stability they are also found in supramolecular chemistry. Since the pH of the medium was found to be in the range of (6.4-8) the amino group ($-NH_2$) is thought to undergo protonation converting to the ammonium ion ($-NH_3^+$) and in this case rendering the column positively charged. As a result, a salt bridge is assumed to be formed through electrostatic attraction between the negatively charged carboxylic group ($–COO^-$) of NaDC bile salt and the positively charged ammonium group ($-NH_3^+$) of the column also through hydrogen bonding between the hydrogen atom of the ammonium group ($-NH_3^+$) and the oxygen atom of the carboxylic group ($–COO^-$) which adds up to the overall stability of the formed network as it acts as a small stabilising interaction [251]. The charge on both the column and the bile salt adsorbed on its surface are masked by their electrostatic attraction. Salt bridges form between the bile salt monomers and the column creating a stable network. Also, H-bonds form in between the bile salts hydroxyl groups as well as the nonpolar binding of the hydrophobic moiety of NaDC molecules, creating a network with the free monomers from the mobile phase leading to the formation of what looks like bilayers of bile salt.

Table 74: Total & micellar concentrations used of NaDC in water as well as the inverse of the capacity factors (1/K') for 0.2 mM acetaminophen obtained with amino column.

Conc. (M)	CM (M)	1/K'
0.007	0.002	2.867
0.009	0.004	2.745
0.011	0.006	2.437
0.013	0.008	2.381
0.015	0.010	2.210
0.017	0.012	2.112
0.020	0.015	2.075

Table 75: Total & micellar concentrations used of NaDC in water as well as the inverse of the capacity factors (1/K') for 0.2 mM caffeine obtained with amino column.

Conc. (M)	CM (M)	1/K'
0.007	0.002	3.854
0.009	0.004	3.567
0.011	0.006	3.144
0.013	0.008	2.985
0.015	0.010	2.714
0.017	0.012	2.595
0.020	0.015	2.461

Table 76: Total & micellar concentrations used of NaDC in water as well as the inverse of the capacity factors (1/K') for 0.2 mM fluconazole obtained with amino column.

Conc. (M)	CM (M)	1/K'
0.007	0.002	2.877
0.009	0.004	2.776
0.011	0.006	2.540
0.013	0.008	2.487
0.015	0.010	2.273
0.017	0.012	2.190
0.020	0.015	2.022

Table 77: Total & micellar concentrations used of NaDC in water as well as the inverse of the capacity factors (1/K') for 0.2 mM theophylline obtained with amino column.

Conc. (M)	CM (M)	1/K'
0.005	0.000	3.513
0.007	0.002	3.319
0.009	0.004	3.063
0.011	0.006	2.776
0.013	0.008	2.682

Table 78: Total & micellar concentrations used of NaDC in water as well as the inverse of the capacity factors (1/K') for 0.2 mM fenoprofen obtained with amino column.

Conc. (M)	CM (M)	1/K'
0.009	0.004	4.783
0.011	0.006	4.511
0.013	0.008	4.269
0.015	0.010	3.985
0.017	0.012	3.985

Table 79: Total & micellar concentrations used of NaDC in water as well as the inverse of the capacity factors (1/K') for 0.2 mM gemfibrozil obtained with amino column.

Conc. (M)	CM (M)	1/K'
0.007	0.002	2.542
0.009	0.004	2.411
0.011	0.006	2.210
0.013	0.008	1.989
0.015	0.010	1.741

Table 80: Total & micellar concentrations used of NaDC in water as well as the inverse of the capacity factors (1/K') for 0.2 mM ibuprofen obtained with amino column.

Conc. (M)	CM (M)	1/K'
0.009	0.004	6.302
0.011	0.006	5.322
0.013	0.008	4.519
0.015	0.010	3.838
0.017	0.012	3.513
0.020	0.015	2.985

Table 81: Total & micellar concentrations used of NaDC in water as well as the inverse of the capacity factors (1/K') for 0.2 mM phenylbutazone obtained with amino column.

Conc. (M)	CM (M)	1/K'
0.009	0.004	4.693
0.011	0.006	4.430
0.013	0.008	3.985
0.015	0.010	3.676
0.017	0.012	3.027
0.020	0.015	2.985

Table 82: Total & micellar concentrations used of NaDC in water as well as the inverse of the capacity factors (1/K') for 0.2 mM lornoxicam obtained with amino column.

Conc. (M)	CM (M)	1/K'
0.011	0.006	4.383
0.013	0.008	8.263
0.015	0.010	17.261
0.017	0.012	30.538
0.020	0.015	49.625

Table 83: Total & micellar concentrations used of NaDC in water as well as the inverse of the capacity factors (1/K') for 0.2 mM meloxicam obtained with amino column.

Conc. (M)	CM (M)	1/K'
0.013	0.008	1.741
0.015	0.010	1.921
0.017	0.012	2.150
0.020	0.015	2.340

Table 84: Total & micellar concentrations used of NaDC in water as well as the inverse of the capacity factors (1/K') for 0.2 mM piroxicam obtained with amino column.

Conc. (M)	CM (M)	1/K'
0.007	0.002	2.057
0.009	0.004	2.295
0.011	0.006	2.461
0.013	0.008	3.063
0.015	0.010	3.567
0.017	0.012	3.854
0.020	0.015	4.051

Table 85: Total & micellar concentrations used of NaDC in water as well as the inverse of the capacity factors (1/K') for 0.2 mM lidocaine obtained with amino column.

Conc. (M)	CM (M)	1/K'
0.009	0.004	0.186
0.011	0.006	0.151
0.013	0.008	0.125
0.015	0.010	0.109
0.017	0.012	0.093
0.020	0.015	0.084

Table 86: Total & micellar concentrations used of NaDC in water as well as the inverse of the capacity factors (1/K') for 0.2 mM terbutaline obtained with amino column.

Conc. (M)	CM (M)	1/K'
0.011	0.006	0.277
0.013	0.008	0.283
0.015	0.010	0.303
0.017	0.012	0.450
0.020	0.015	0.565

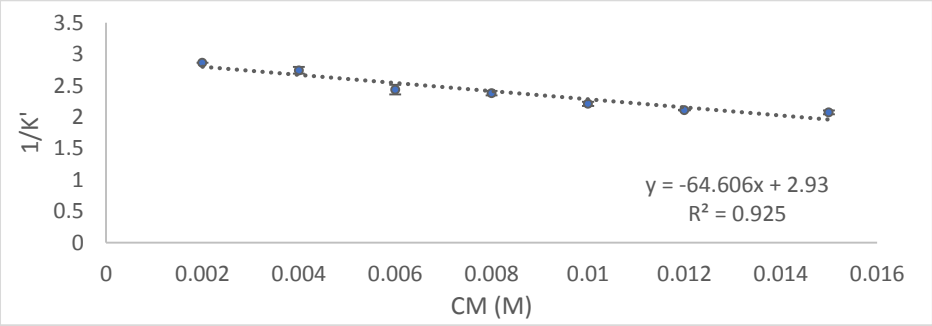

Figure 113: Calibration plot of the inverse of the capacity factor (1/K') versus micellar concentration CM (M) of NaDC in water with amino column for 0.2 mM acetaminophen.

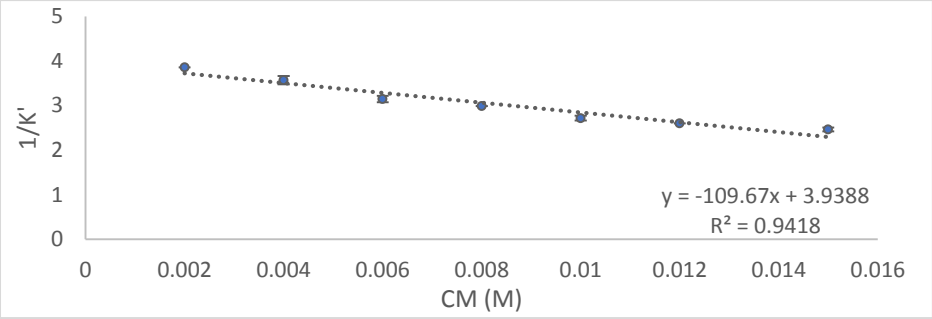

Figure 114: Calibration plot of the inverse of the capacity factor (1/K') versus micellar concentration CM (M) of NaDC in water with amino column for 0.2 mM caffeine.

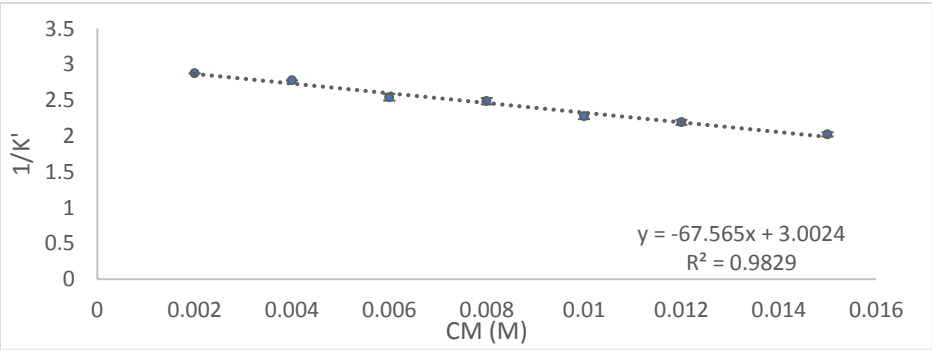

Figure 115: Calibration plot of the inverse of the capacity factor (1/K') versus micellar concentration CM (M) of NaDC in water with amino column for 0.2 mM fluconazole.

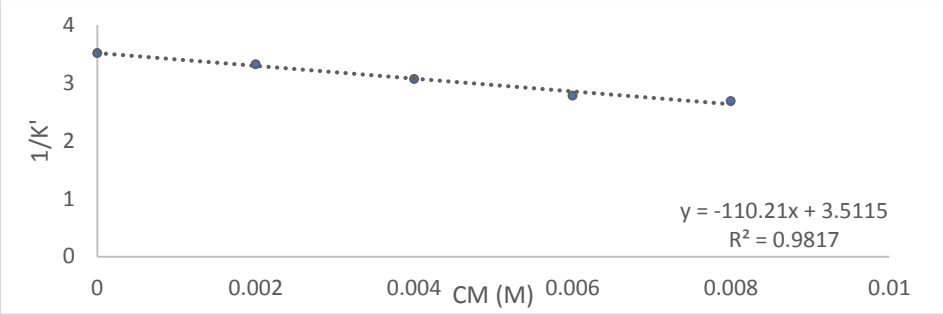

Figure 116: Calibration plot of the inverse of the capacity factor (1/K') versus micellar concentration CM (M) of NaDC in water with amino column for 0.2 mM theophylline.

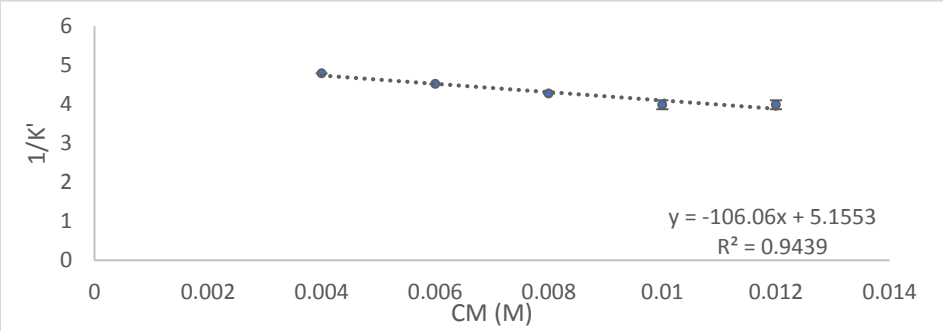

Figure 117: Calibration plot of the inverse of the capacity factor (1/K') versus micellar concentration CM (M) of NaDC in water with amino column for 0.2 mM fenoprofen.

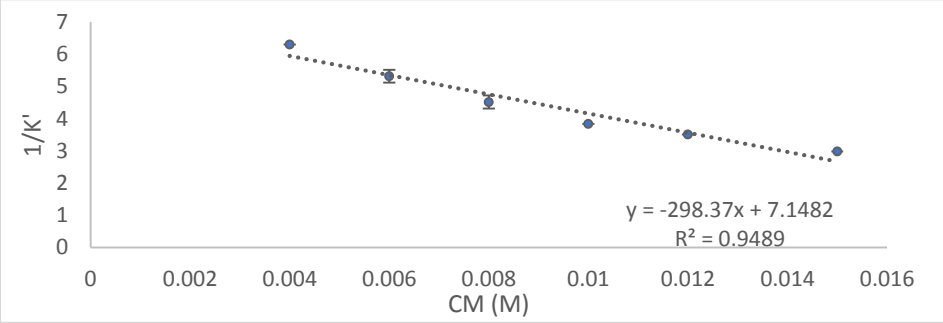

Figure 118: Calibration plot of the inverse of the capacity factor (1/K') versus micellar concentration CM (M) of NaDC in water with amino column for 0.2 mM ibuprofen.

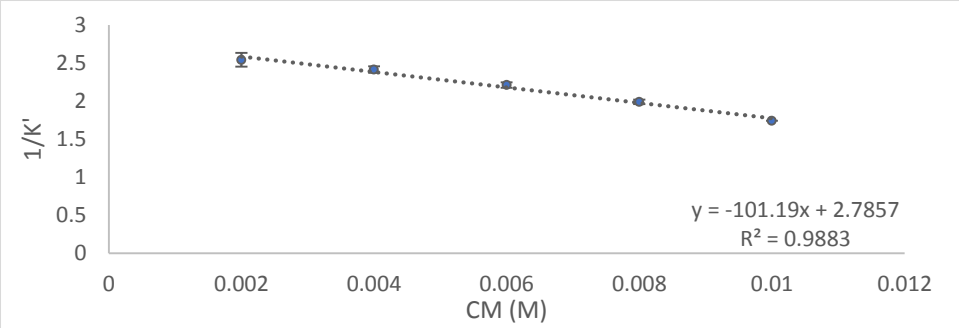

Figure 119: Calibration plot of the inverse of the capacity factor (1/K') versus micellar concentration CM (M) of NaDC in water with amino column for 0.2 mM gemfibrozil.

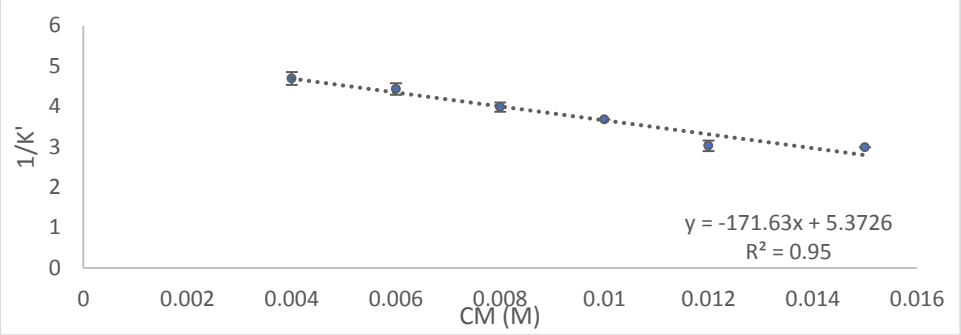

Figure 120: Calibration plot of the inverse of the capacity factor (1/K') versus micellar concentration CM (M) of NaDC in water with amino column for 0.2 mM phenylbutazone.

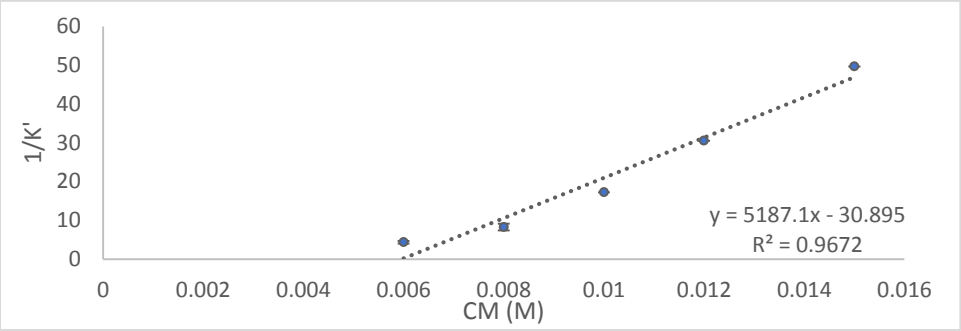

Figure 121: Calibration plot of the inverse of the capacity factor (1/K') versus micellar concentration CM (M) of NaDC in water with amino column for 0.2 mM lornoxicam.

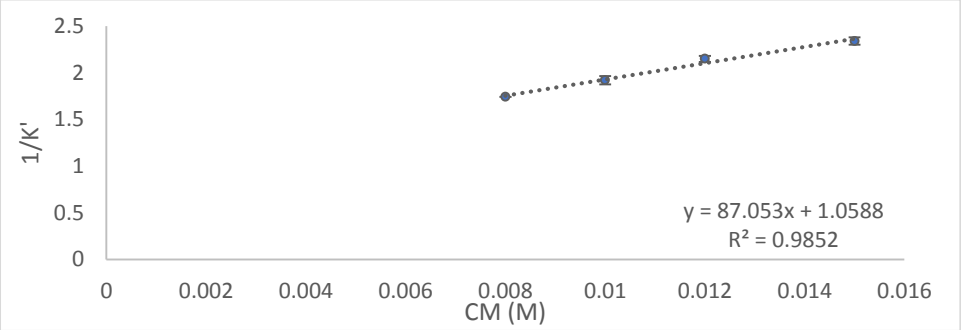

Figure 122: Calibration plot of the inverse of the capacity factor (1/K') versus micellar concentration CM (M) of NaDC in water with amino column for 0.2 mM meloxicam.

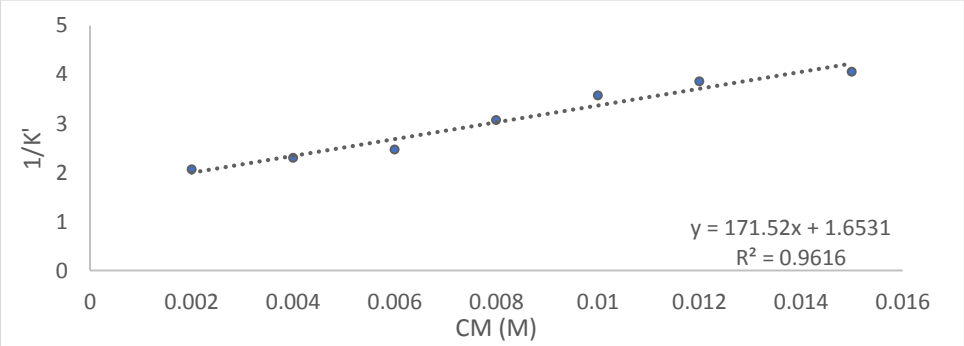

Figure 123: Calibration plot of the inverse of the capacity factor (1/K') versus micellar concentration CM (M) of NaDC in water with amino column for 0.2 mM piroxicam.

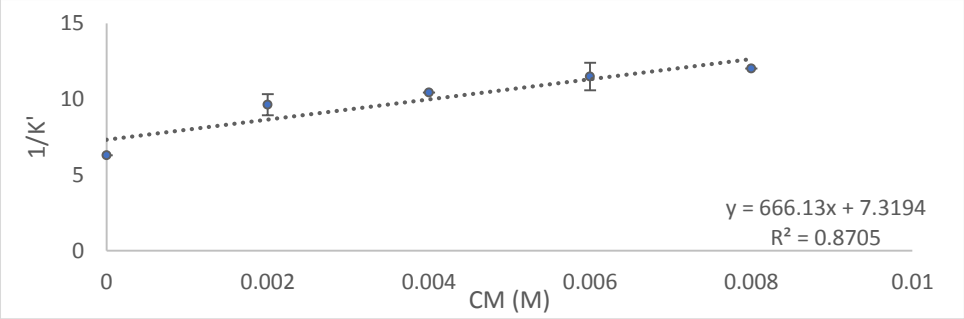

Figure 124: Calibration plot of the inverse of the capacity factor (1/K') versus micellar concentration CM (M) of NaDC in water with amino column for 0.2 mM salicylic acid.

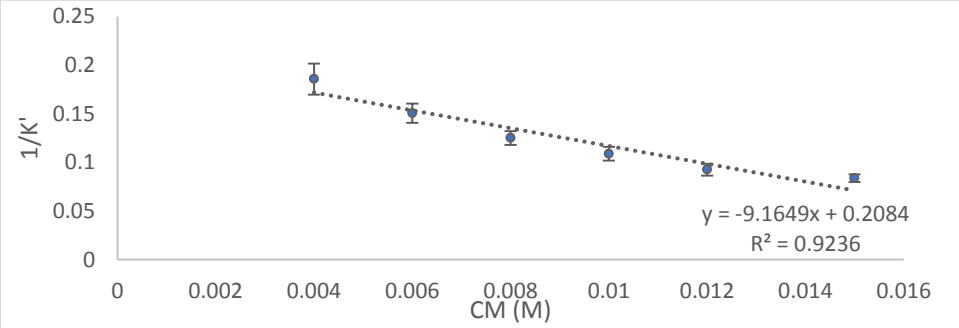

Figure 125: Calibration plot of the inverse of the capacity factor (1/K') versus micellar concentration CM (M) of NaDC in water with amino column for 0.2 mM lidocaine.

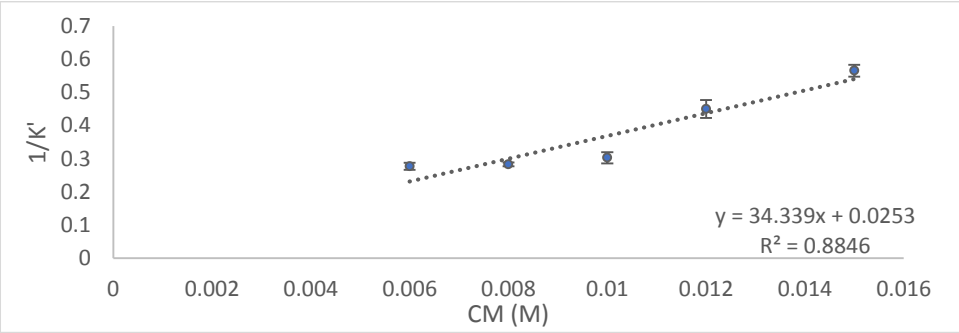

Figure 126: Calibration plot of the inverse of the capacity factor (1/K') versus micellar concentration CM (M) of NaDC in water with amino column for 0.2 mM terbutaline.

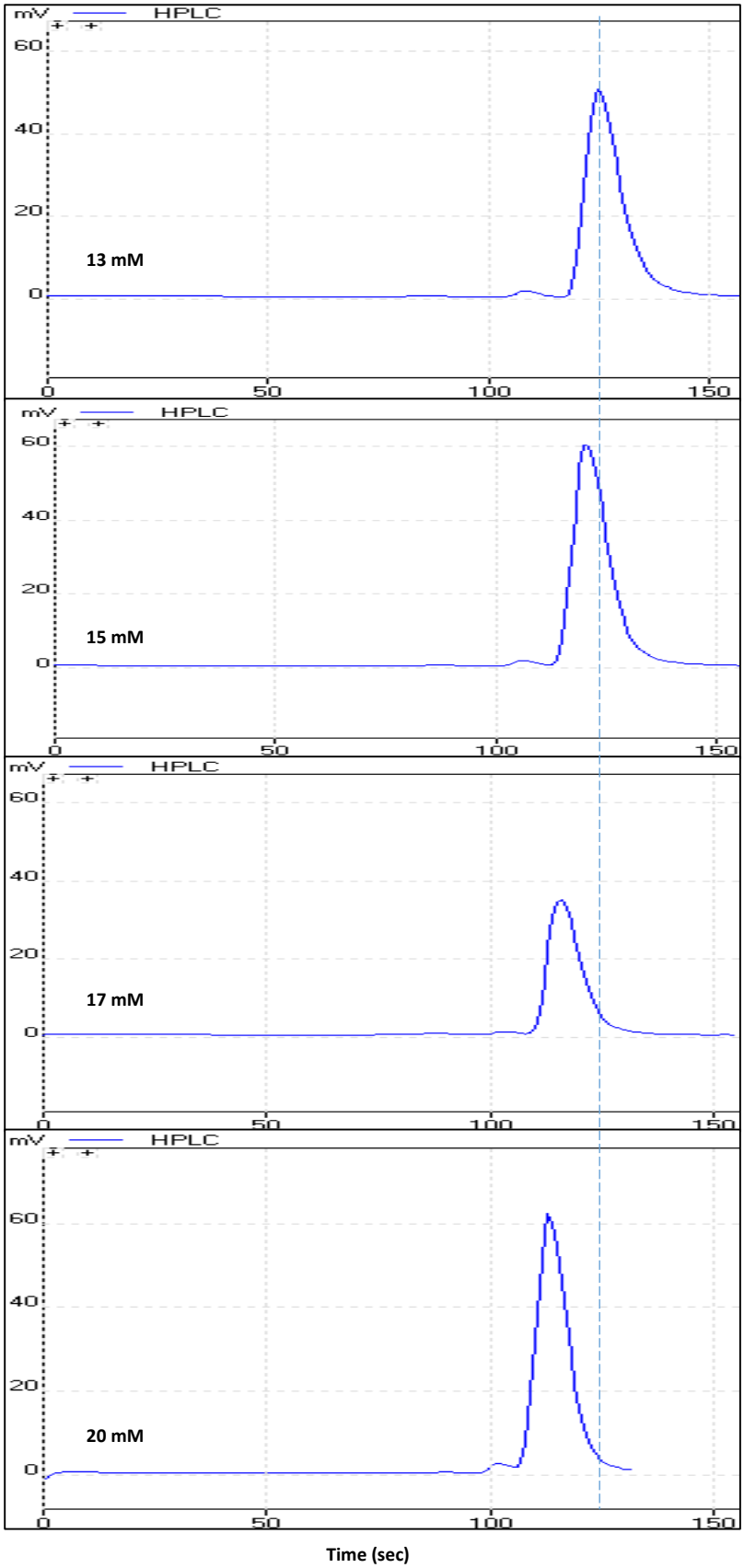

Figure 127: Chromatograms showing binding behaviour of meloxicam in different concentrations of NaDC mobile phase using amino column as a stationary phase. (The dotted line is only used for visual guidance).

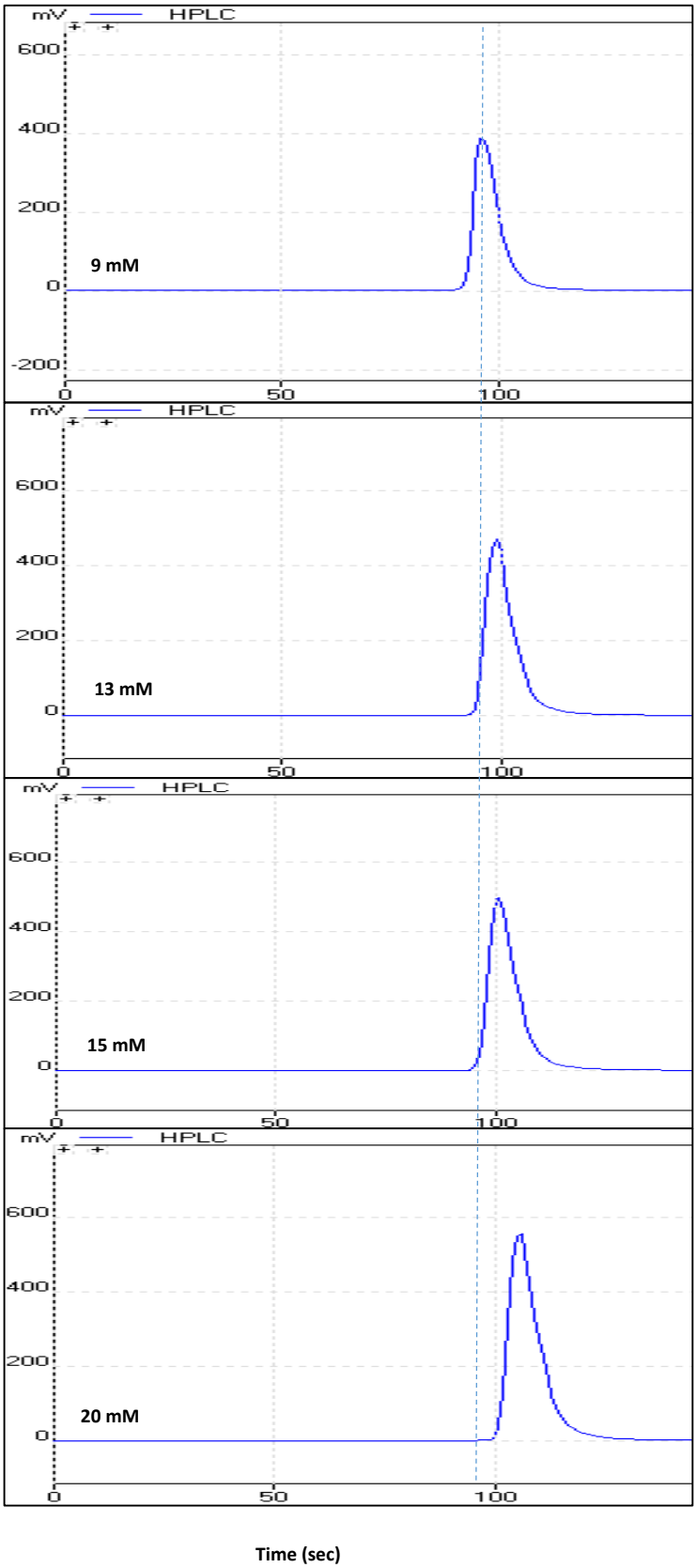

Figure 128: Chromatograms showing binding behaviour of phenylbutazone in different concentrations of NaDC mobile phase using amino column as a stationary phase. (The dotted line is only used for visual guidance).

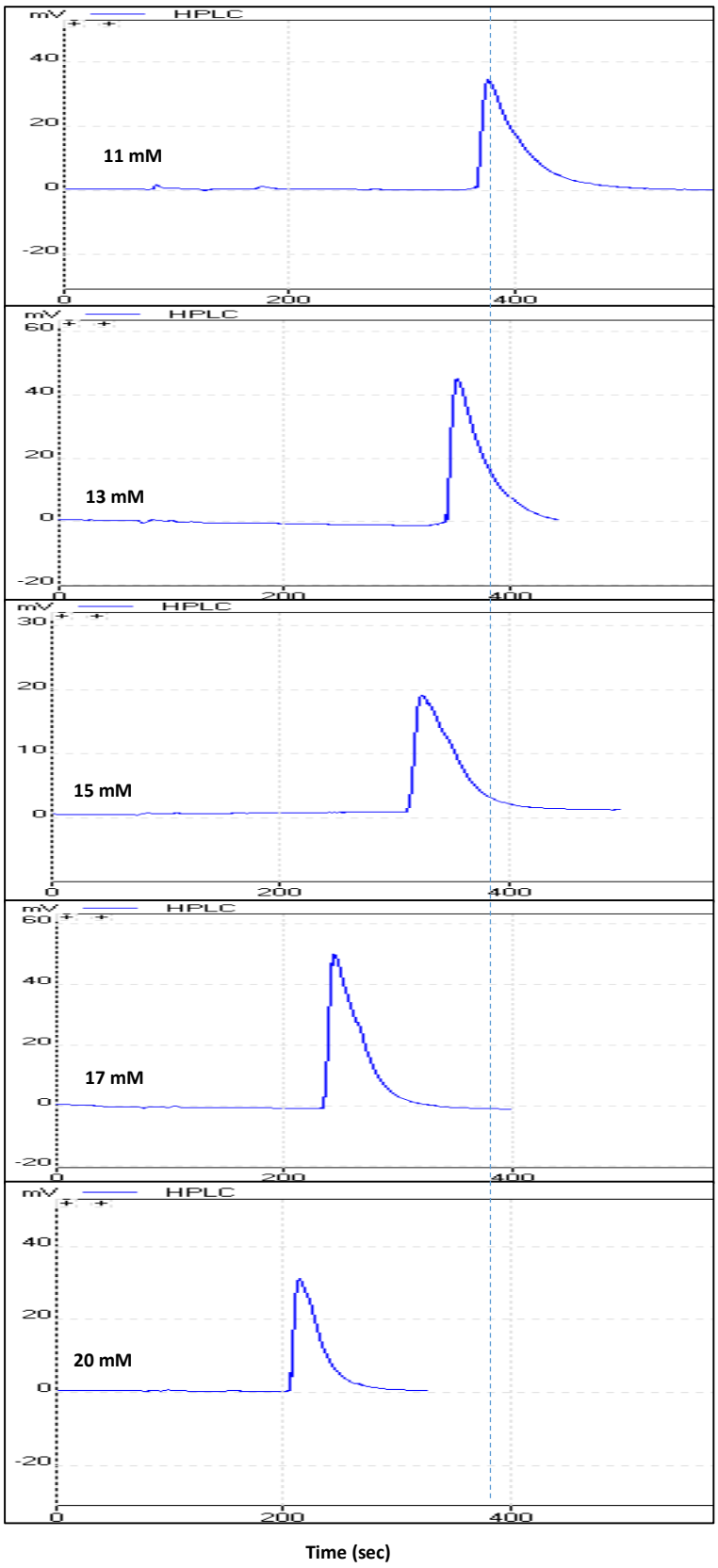

Figure 129: Chromatograms showing binding behaviour of terbutaline in different concentrations of NaDC mobile phase using amino column as a stationary phase. (The dotted line is only used for visual guidance).

Table 87: Partition coefficients obtained from MLC using NaDC with amino propyl column as a stationary phase for fourteen drugs with their standard deviations against their octanol/water partition coefficients.

Compound	Log P_{mw}	Log $P_{o/w}$[184]
Acetaminophen	1.34±0.001	0.46
Caffeine	1.45±0.001	-0.07
Fluconazole	1.35±0.02	0.40
Theophylline	1.50±0.01	-0.02
Fenoprofen	1.31±0.07	3.10
Gemfibrozil	1.56±0.03	3.40
Ibuprofen	1.62±0.01	3.97
Phenylbutazone	1.50±0.02	3.16
Lornoxicam	2.23±0.03	2.62
Meloxicam	1.92±0.03	3.43
Piroxicam	2.02±0.01	3.06
Lidocaine	1.64±0.01	2.44
Terbutaline	3.13±0.07	0.90

Anionic drugs showed an antibinding behaviour which is typical for conventional retention however a number of anionic drugs showed the opposite behaviour i.e. a binding interaction with NaDC. Both cases can be explained according to the previously mentioned theory for bile salt (micellar mobile phase) interaction with the amino column used in this method as follows:

The anionic drugs fenoprofen, ibuprofen, gemfibrozil and phenylbutazone showed a retention behaviour typical to what is expected for anionic drugs with anionic surfactant where they undergo antibinding interaction with the NaDC micelles. The retention time of these drugs increased with the increase in the concentration of the micelles in the mobile phase.

Other anionic drugs, namely lornoxicam, meloxicam and piroxicam showed an opposite pattern of interaction as they acted as binding solutes where the retention time of these drugs decreased with the increased concentration of micelles in the mobile phase. This is unusual for anionic drugs when analysed with anionic surfactants in MLC. The typical antibinding behaviour of anionic surfactants can be attributed to the electrostatic repulsion taking place between the negatively charged

drugs and the negatively charged surfactant. As a result of this repulsion the drug binds to the column showing an increase in retention on the column with the increase in the surfactant concentration. In this case the drug also has to have a low molecular weight in order to be entrapped inside the layers of the bile salt network structure formed with the amino column by means of electrostatic attraction and H-bonding. As a result, fenoprofen, ibuprofen, gemfibrozil and phenylbutazone, having relatively low molecular weight values of 242.3, 206.3, 250.3 and 308.4 g/mol respectively, were entrapped inside the bile salt network structure showing antibinding interaction. On the other hand, lornoxicam, meloxicam and piroxicam, having relatively higher molecular weight values of 371.8, 351.4 and 331.4 g/mol respectively, could not be entrapped inside the bile salt network structure. Instead, they were entrapped inside the micellar core as they overcame the repulsion forces with the micelles as they have high molecular weights.

Neutral drugs (acetaminophen, caffeine, fluconazole and theophylline) exhibited an antibinding retention behaviour which is again, against convention, where neutral drugs are supposed to undergo a binding interaction. This can be attributed to the preference of these drugs to bind to the more stable hydrophobic core of the bile salt network structure rather than that of the bile salt micelles in the mobile phase. Also these drugs have significantly lower molecular weights of 151.2, 194.2, 306.27, 180.2 g/mol respectively so they could easily get entrapped inside the hydrophobic core of the bile salt network structure within the column therefore showing antibinding retention behaviour.

The cationic drug terbutaline showed a binding behaviour which is consistent with what was expected to take place for cationic drugs analysed with anionic surfactants in MLC. On the other hand lidocaine, which is also a cationic drug, acted as an antibinding solute. It is assumed that terbutaline acts as a binding solute not only because of the electrostatic attraction between the positively charged drug and the negatively charged surfactant but also because terbutaline has a higher water solubility so it is more exposed and available in the aqueous medium so it binds easily to the micelles. As for the unusual antibinding behaviour that was observed with lidocaine, it is thought that lidocaine being a more lipophilic drug (log $P_{o/w}$ =2.44) than terbutaline (log $P_{o/w}$=0.9) preferred to bind to the more hydrophobic core of the bile salt network structure within the column and also its relatively low molecular weight (234.4 g/mol) made it easier for it to get entrapped inside this network structure.

In Table 86, it can be seen that the log P_{mw} values for the analysed drugs were found to be higher than their log $P_{o/w}$ reflecting their preference to the bile salt surfactant. Also a significant difference can be seen between the binding and the antibinding solutes in their log P_{mw} values. This can, to some extent, allow comparison of the type of retention phenomenon for the analysed drug when compared with other drugs analysed using the same method where log P_{mw} was found to be in the range of (1.31-1.64) for antibinding solutes and in the range of (1.92-3.33) for binding solutes. For the previously used micellar systems with a cyanopropyl column the obtained log P_{mw} values were only a reflection of the drug's preference to the surfactant in general whether it is in the aqueous phase as micelles (binding phenomenon) or adsorbed on the surface of the column (antibinding phenomenon).

3.F.2. Statistical Modelling

After analysis of a group of 23 drugs using NaDC with an aminopropyl (APS) column and calculation of log P_{mw}, a number of molecular descriptors such as molecular weight, polar surface area, freely rotating bonds, molar volume, dissociation constant (pK_a), aqueous solubility (S_w), number of hydrogen bond donors and number of hydrogen bond acceptors were used along with the obtained log P_{mw} to develop models for prediction of %HIA and PAMPA & Caco-2 permeability coefficients using multiple linear regression. Lipophilicity represented by log P_{mw} experimentally obtained using this MLC method is shown in Table 90.

3.F.2.1. Statistical Modelling of Human Intestinal absorption (HIA)

Log P_{mw} was successfully included with 2 other molecular descriptors in the final model equation with %HIA experimental values for orally administered drugs (shown in Table 88) which successfully predicts %HIA with 72 % predictability. The final model was validated using a set of seven compounds.

The model obtained for the prediction of %HIA is given by Equation 22:

$$\text{logit HIA} = -0.758 - 0.369 \log P_{mw} + 0.01157\, V_M + 0.0714\, S_w \qquad \text{Eq. (22)}$$

Sixteen drugs were used in the development of the final model. The model's $R^2 = 84.62$ %, $R^2_{adjust.} = 80.77$ % , $R^2_{PRED} = 71.51$ %, S= 0.203

A 95 % confidence interval for log P_{mw} is given by (-0.726, -0.011), t-statistic and standardised coefficient of log P_{mw} are –2.25 ($p<0.05$) and -0.294 respectively suggesting statistical significance of log P_{mw} as a predictor. Also the F-ratio of the overall model is statistically significant, F= 22 and P value 0.000 ($p<0.05$). Figure 130

shows no marked relationship between residuals and predicted values while Figure 131 summarises the model.

Seven drugs (cimetidine, fenoprofen, lornoxicam, nicotinic acid, piroxicam, salicylic acid and terbutaline) were used to test the model predictability. The model was able to predict the %HIA for these drugs within a minimum of 0.1 % and a maximum of 8.07 % difference between the predicted %HIA and the published %HIA. The model appears to have underestimated %HIA for both lornoxicam and salicylic acid with a 12 % and 24 % difference between the two predicted and published values. The MLC method used here was able to develop a model for prediction of HIA with a reliable predictability. It is thought that if trials were carried out using the amino column with other bile salts that had good predictability with a CN-RP column, models with an even higher predictive ability could have been developed.

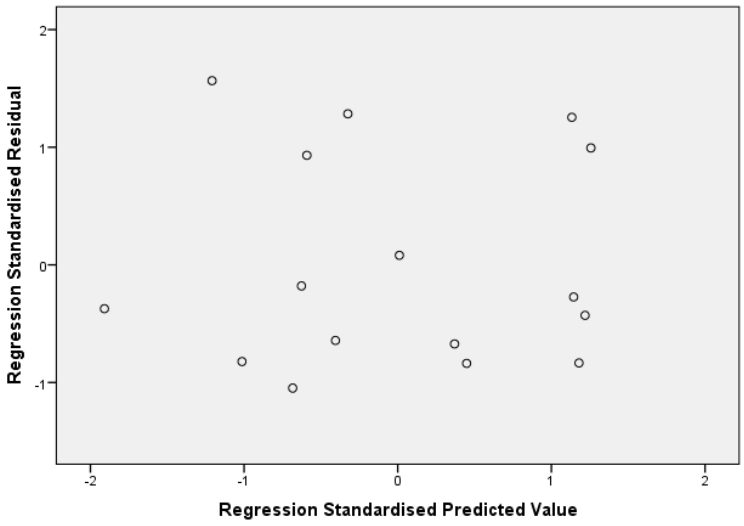

Figure 130: Residual plot for optimal logit HIA regression model.

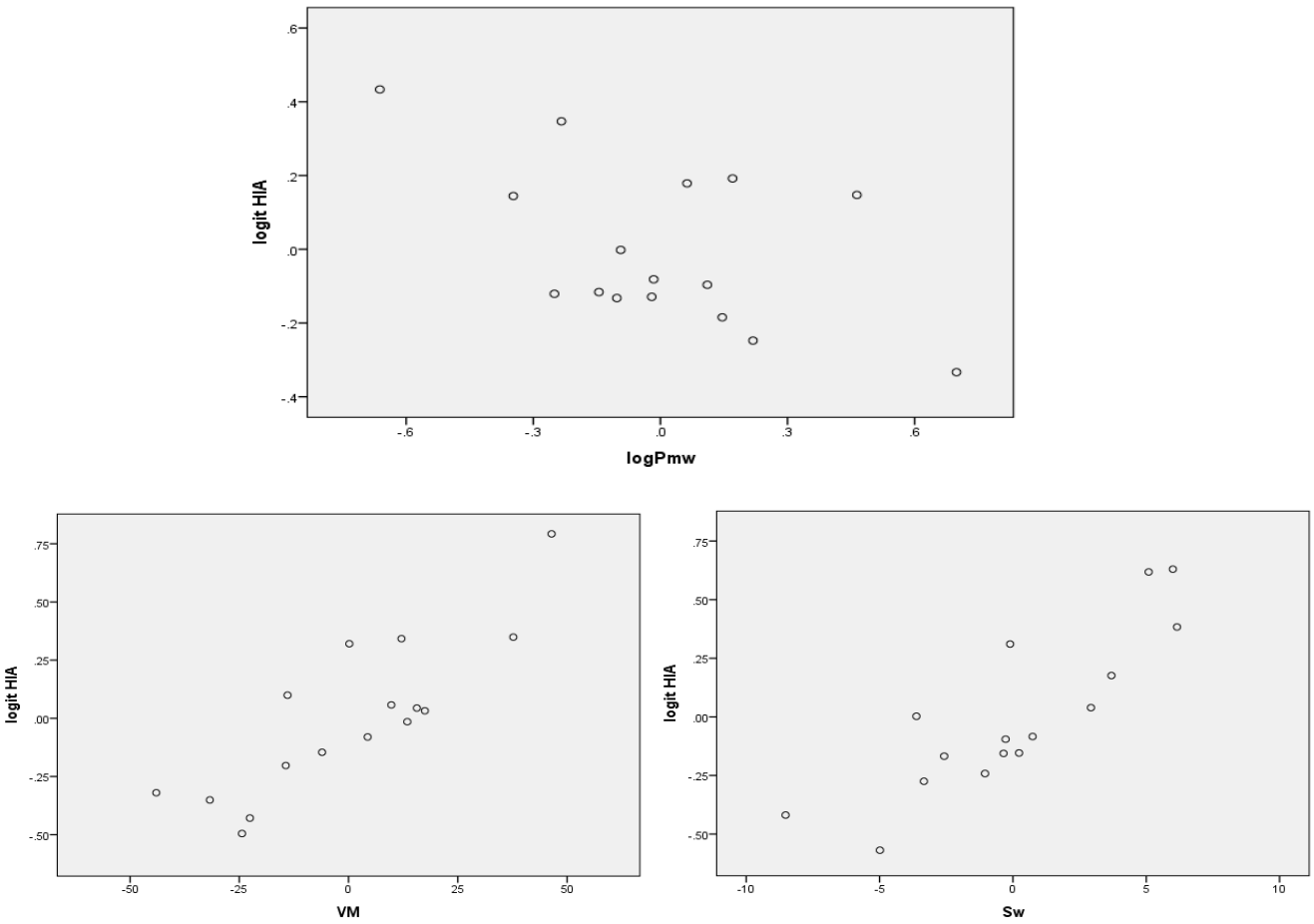

Figure 131: Partial regression plots of experimental logit HIA. values against log P_{mw}, V_M and S_w .

Table 88: Experimental and predicted values for %HIA.

Drug	Expt. %HIA	Pred. %HIA
Acetaminophen	95.00[205]	94.82
Acetylsalicylic acid	82.00[205]	87.00
Caffeine	99.00[230]	98.42
Carbamazepine	70.00[209]	73.53
Cimetidine*	73.50[230, 245]	73.60
Diclofenac	90.00[210]	90.73
Fenoprofen*	85.00[206]	93.07
Fluconazole	97.50[205]	98.29
Flurbiprofen	92.00[247]	84.68
Gemfibrozil	95.00[207]	96.57
Ibuprofen	85.00[207]	90.25
Indomethacin	99.00[252]	98.22
Ketoprofen	96.00[205]	92.94
Lidocaine	95.00[210, 252]	96.30
Lornoxicam*	100.00[246]	88.67
Meloxicam	90.00[205]	92.40
Naproxen	94.00[205]	91.02
Nicotinic acid*	94.00[230]	100.00
Phenylbutazone	98.00[206]	98.36
Piroxicam*	99.00[252]	92.28
Salicylic acid*	99.00[247]	75.44
Theophylline	98.00[33]	98.24
Terbutaline*	80.00[248]	84.25

The asterisk (*) indicates the validation compounds.

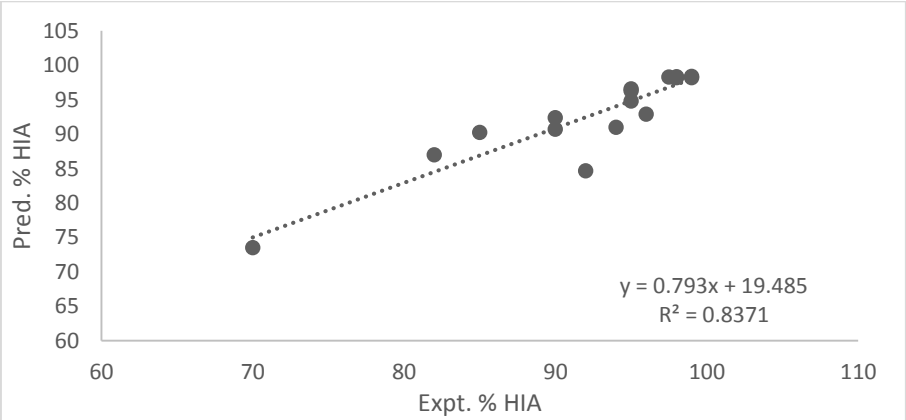

Figure 132: Plot of experimental vs. predicted %HIA.

3.F.2.2. Modelling of permeability coefficients obtained from PAMPA

The model obtained for the prediction of PAMPA log P_o is given by Equation 23:

$$\log P_o = 0.897 - 1.504 \log P_{mw} - 0.771\ HD - 0.1894\ S_w \qquad \text{Eq. (23)}$$

Sixteen drugs were used in the development of the final model. The model's R^2 =84.96 %, $R^2_{adjust.}$= 81.20 % , R^2_{PRED} = 76.53 %, S= 0.742

A 95 % confidence interval for log P_{mw} is given by (-2.525, -0.484), t-statistic and standardised coefficient of log P_{mw} are -3.21 ($p<0.05$) and -0.439 respectively suggesting statistical significance of log P_{mw} as a predictor. The statistical significance of the overall model was tested by F-ratio and P-value which were found to be; F= 22.6 and P value 0.000 ($p<0.05$) confirming the model's significance.

The close agreement of the values of $R^2_{adjust.}$ & R^2_{PRED} indicates that the model does not over-fit the data.

The residual analysis did not detect any relationship between residuals and predicted values as shown in Figure 133. The model is shown in Figure 134.

The MLC method used in this section showed a resemblance to the PAMPA method. This could be attributed to the possibility of the presence of similarity between the membrane used in PAMPA and the formed bile salt network structure adsorbed on the surface of the amino column, i.e. creating a system with which the analysed drugs interact in a similar manner to how they interact with the lipid membrane in PAMPA.

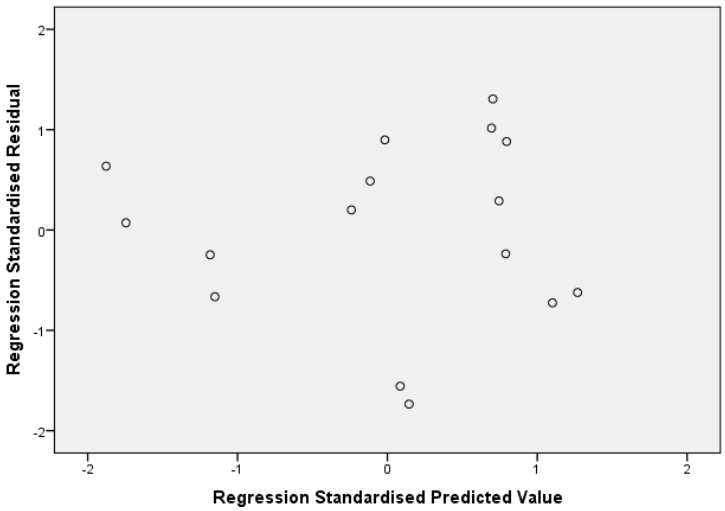

Figure 133: Residual plot for optimal PAMPA regression model.

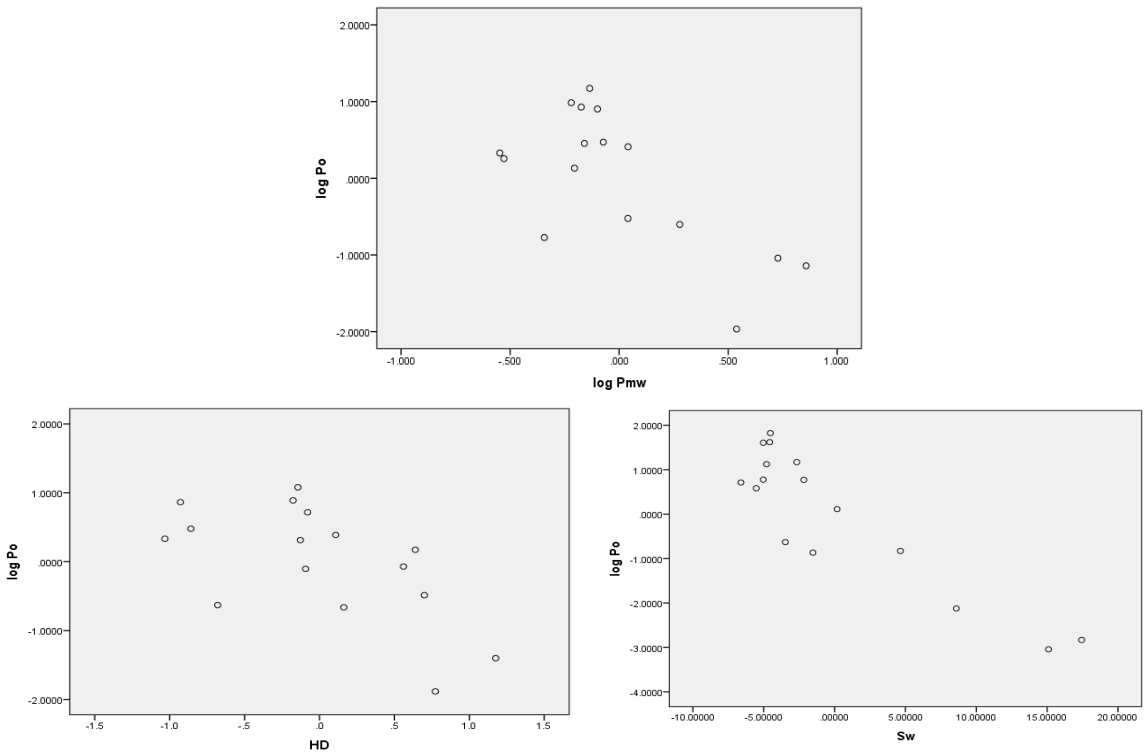

Figure 134: Partial regression plots of experimental PAMPA log P_o values against log P_{mw}, HD and S_w.

Table 89: Experimental and predicted values for PAMPA.

Drug	Expt. PAMPA $logP_0$ [215]	Pred. PAMPA $logP_0$
Acetaminophen	-5.81	-5.32
Caffeine	-5.55	-5.37
Carbamazepine	-3.73	-3.88
Cimetidine	-6.20	-6.25
Diclofenac	-1.37	-3.27
Flurbiprofen	-1.78	-3.37
Gemfibrozil	-1.59	-2.25
Ibuprofen	-2.11	-2.33
Indomethacin	-1.65	-2.40
Ketoprofen	-2.43[64]	-2.25
Lidocaine	-1.42	-2.39
Meloxicam	-2.86	-3.53
Naproxen	-2.30	-1.76
Phenylbutazone	-1.96	-1.50
Piroxicam	-3.32	-3.68
Theophylline	-5.99	-6.46

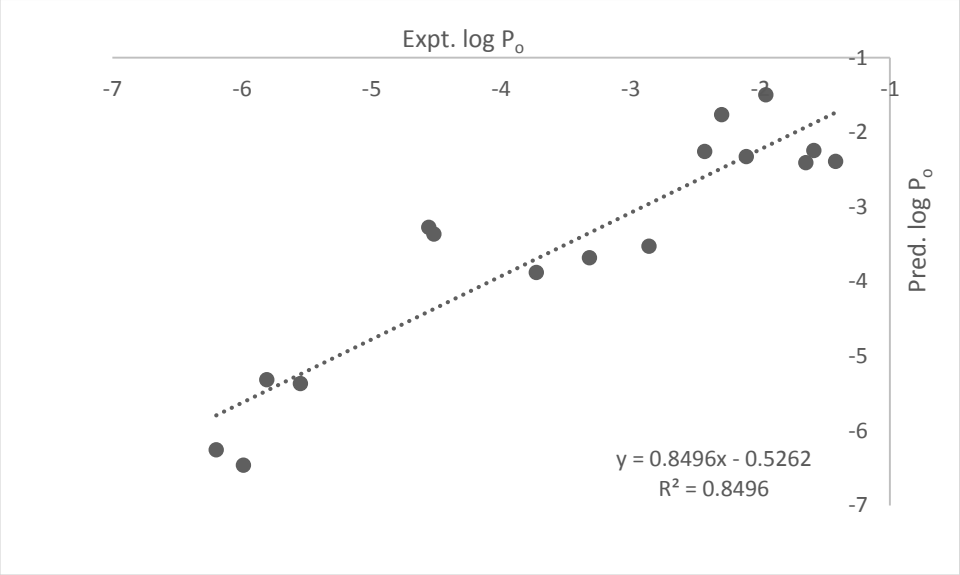

Figure 135: Plot of experimental vs. predicted log P_o.

3.F.2.3. Modelling of permeability coefficients obtained from Caco-2

Log P_{mw} obtained in the current study, alongside all the other published molecular descriptors listed in Table 90, were considered for their inclusion in a model for prediction of Caco-2 permeability coefficient using multiple linear regression. No model equation could be obtained having log P_{mw} (either alone or with other descriptors) included with the published experimentally determined Caco-2 log $P_{eff.}$ where the obtained P values for log P_{mw} were always greater than 0.05 at 95 % confidence interval, i.e. suggesting statistical nonsignificance as a descriptor. Also the obtained R^2_{PRED} value was always zero. As a result, this MLC system was not successful in the prediction of the *in vitro* Caco-2 permeability coefficient as there was no correlation found between the MLC based log P_{mw} data and Caco-2 log P.

Table 90: A summary of molecular descriptors for the selected drugs analysed by MLC using NaDC in water with amino column and the experimental values of PAMPA log P_o and %HIA.

Drug	Log P_{mw}	Log $P_{o/w}$[184]	Mwt[218]	pK_a[184]	S_w[184]	HD[218]	HA[218]	FRB[218]	PSA[219]	V_M[218]	log P_o[215]	%HIA
Acetaminophen	1.34	0.46	151.20	9.9	14	2	2[184]	1	49.3	131.1	-5.81	95.00[205]
Acetylsalicylic acid	2.02	1.19	180.15	3.41	10[219]	1	4	3	63.6	139.6	NA	82.00[205]
Caffeine	1.45	-0.07	194.20	14	21.6	0	3[184]	0	58.4	133.4	-5.55	99.00[230]
Carbamazepine	2.64	2.45	236.36	13.9	0.21	1[184]	3	0	46.3	186.6	-3.73	70.00[209]
Cimetidine	3.11	0.4	252.34	6.8	0.816	3	6	8	114	198.2	-6.20	73.50[230, 245]
Diclofenac	1.75	4.51	296.20	4.15	0.00237	2	3	4	49.3	206.8	-4.56[62]	90.00[210]
Fenoprofen	1.31	3.1	242.27	4.5	0.033	1	3	4	46.5	204.7	NA	85.00[206]
Fluconazole	1.35	0.4	306.27	12.71	9	1	7	5	81.6	205.3	NA	97.50[205]
Flurbiprofen	2.32	4.16	244.26	4.42	0.008	1	2	3	37.3	203.6	-4.52[62]	92.00[247]
Gemfibrozil	1.56	3.4	250.33	4.5	0.13	1	3	6	46.5	239.7	-1.59	95.00[207]
Ibuprofen	1.62	3.97	206.30	5.2	0.0684	1	2	4	37.3	200.3	-2.11	85.00[207]
Indomethacin	1.68	4.27	357.79	4.5	0.000937	1	5	4	68.5	269.6	-1.65	99.00[252]
Ketoprofen	1.58	3.12	254.30	3.88	0.051	1	3	4	54.4	212.2	-2.43[64]	96.00[205]
Lidocaine	1.64	2.44	234.40	7.9	0.2337	1	2[184]	5	32.3	238.8	-1.42	95.00[210, 252]
Lornoxicam	2.23	2.62	371.81	6.8	0.0437	2	7	2	136	213.4	NA	100.00[246]
Meloxicam	1.92	3.43	351.40	4.08	0.00715	2	7	2	136	220.3	-2.86	90.00[205]
Naproxen	1.25	3.18	230.26	4.15	0.0159	1	3	3	46.5	192.3	-2.30	94.00[205]
Nicotinic acid	1.45	0.36	123.11	4.75	83.1	1	3	1	50.2	95.2	NA	94.00[230]
Phenylbutazone	1.50	3.16	308.37	4.4	0.7	0	2[184]	5	40.6	262.8	-1.96	98.00[206]
Piroxicam	2.02	3.06	331.35	6.3	0.023	2	7	2	108	222.8	-3.32	99.00[252]
Salicylic acid	1.96	2.26	138.12	3[227]	11.3	2	3	1	57.5	100.4	NI	99.00[247]
Terbutaline	3.13	0.9	225.28	9.76	213	4	4	4	72.7	192.3	NA	80.00[248]
Theophylline	1.50	-0.02	180.16	8.8[228]	22.9	1	3	0	69.3	122.9	-5.99	98.00[33]

NA: no available data, NI: value not included in training set.

3.F.3. Conclusion

The change in the type of the stationary phase used in the MLC method from cyanopropyl to aminopropyl (APS) had a significant impact on the interaction of the analysed drugs with both the micellar mobile phase and the stationary phase used and consequently on their elution therefore affecting its predictive ability. This method was able to predict %HIA using a reliable model also it provided another model for prediction of PAMPA permeability coefficient with better predictability showing more resemblance to the PAMPA *in vitro* method. On the other hand, the log P_{mw} obtained using this method had no correlation with Caco-2 permeability coefficients therefore the method was unable to provide a model for its prediction.

CHAPTER 3

Section (G)

The Effect Of Change Of Temperature In MLC

Section (G): Investigating the effect of temperature on partitioning of drugs in MLC using sodium deoxycholate (NaDC)

3.G.1. Results & Discussion

3.G.1.1. Determination of CMC of NaDC in water over the temperature range (30-45 ^{o}C)

In this section the effect of temperature on the elution of selected drugs was investigated by carrying out the chromatographic runs using MLC with the column set at different temperatures in the range of (30-45 ^{o}C). The mobile phase used in this method consisted of the biosurfactant NaDC in water whose CMC is known to change with temperature. Therefore, the CMC of NaDC in water was measured spectroscopically at all temperatures (30, 35, 40 and 45 ^{o}C) considered for the MLC study.

As in Section (3C), the dye micellisation method was applied for the determination of CMC of NaDC at (30, 35, 40 and 45 ^{o}C) using dichlorofluorescein dye where the dye attaches to the hydrophobic part of the micelle causing a change in the absorbance of the micellised dye at a fixed wavelength (503 nm) as a function of surfactant concentration [232].

The effect of anionic surfactant on the absorption spectrum of dichlorofluorescein dye was studied and the visible spectra of aqueous dichlorofluorescein solution in several NaDC concentrations ranging from (0.0005 M to 0.02 M) for a fixed dye concentration of 10^{-5} M are represented in Figure 136. The dye exhibits a maximum absorption at 503 nm.

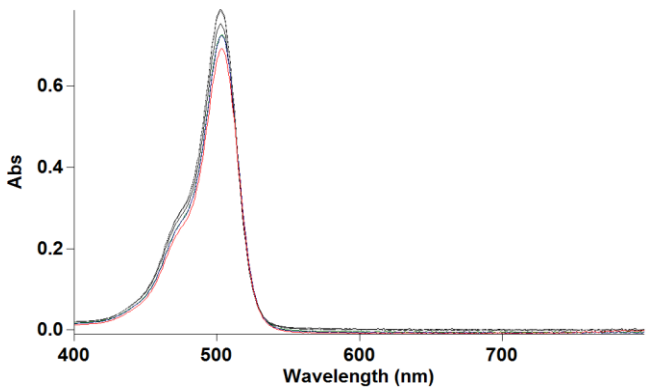

Figure 136: Spectra of 10^{-5} M dye in increasing concentrations of NaDC at 30 ^{0}C .

Below the CMC, as the NaDC concentration gradually increased, the dye absorbance at 503 nm decreased. The decrease in the absorbance indicates the molecular complex formation between the dye and the surfactant molecules due to the interaction between the dye and the surfactant. Above the CMC, absorbance at 503 nm increased significantly. The increase in absorbance values with the increase in surfactant concentrations above the CMC is attributed to the incorporation of dye molecules into the micelles.

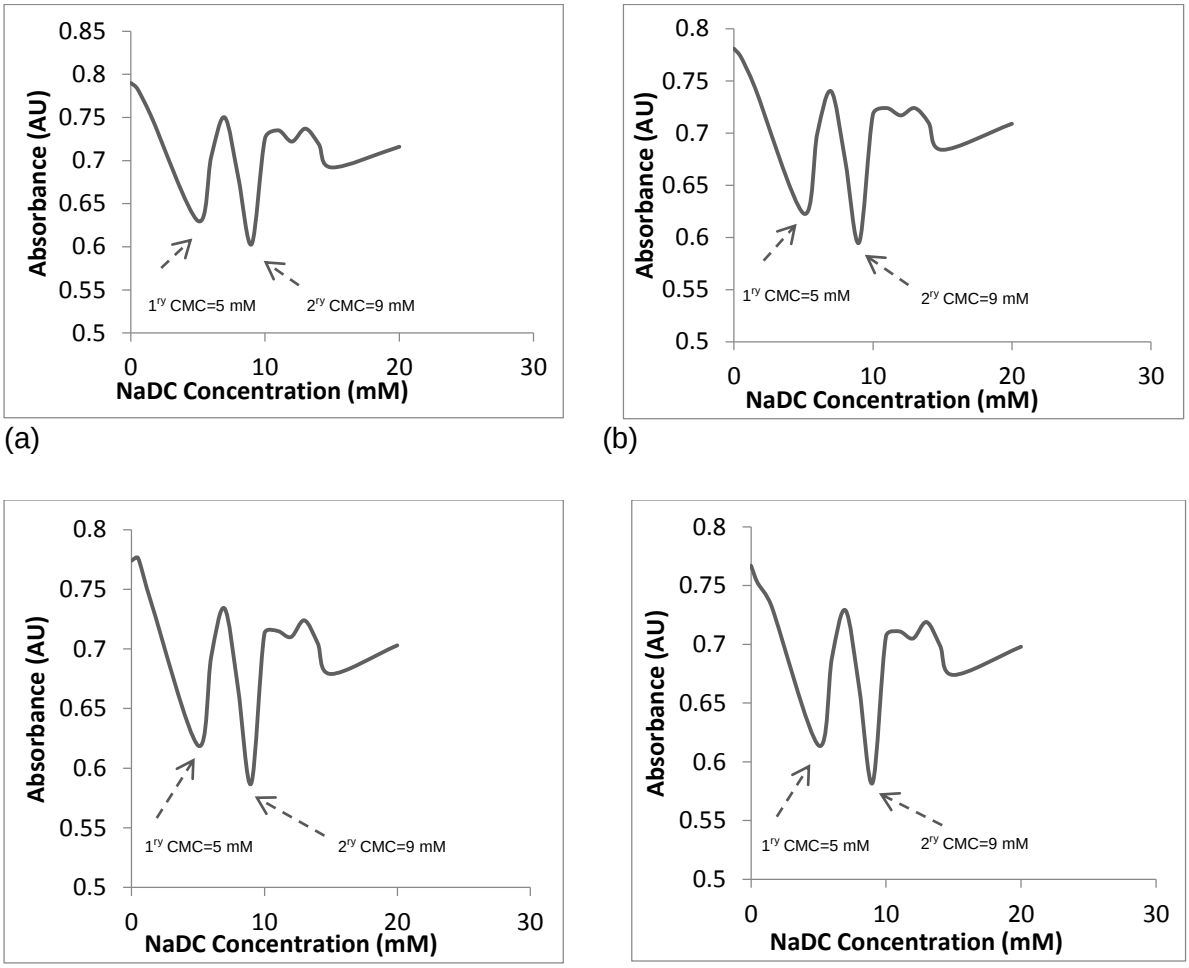

Figure 137: Plots of NaDC concentration versus absorbance of the micellised dye showing the 1ry and 2ry CMC of NaDC at (a) 30 ºC, (b) 35 ºC, (c) 40 ºC and (d) 45 ºC .

The CMC was found to be in the range of (0.005-0.009 M) (Figure 137) where the primary CMC was found to be 0.005 M while the secondary CMC was found to be 0.009 M. Values of the CMC of NaDC at 25 ºC have been reported in literature to be 0.005 M [190] and within the range of (0.002-0.006 M) according to the manufacturer specification sheet, thus confirming the values reported here. This shows that when the temperature increased an increase in the surfactant CMC value followed which is

an expected behaviour. The CMC value for NaDC over the temperature range (30-45 ºC) was taken to be 0.009 M which is the higher end of the experimentally obtained CMC range. This value was used in calculation of micelle-water partition coefficients for the MLC analysed drugs at the selected temperature range so that the whole range of CMC values that NaDC could have throughout the experiments be taken into consideration which could have an impact on the calculated thermodynamic parameters.

3.G.1.2. Effect of temperature change on the partitioning of analysed compounds in MLC

Many papers in literature described the use of thermodynamics in studying solute retention in various chromatographic methods such as reversed phase liquid chromatography, liposome electrokinetic chromatography (LEKC), gas chromatography (GC) and others [170, 253, 254]. van't Hoff analysis is the most commonly used method for providing thermodynamic information for studying retention in chromatography. One of the earliest applications of van't Hoff studies was the characterisation of a stationary phase developed by DuPont by means of calculating heats of transfer for selected solutes by Knox and Vasvari [255]. For many decades van't Hoff studies have been used for studying the thermodynamics of solute transfer from the mobile phase to the stationary phase which has helped in studying retention mechanisms and understanding the whole process [170, 256]. In chromatography the calculation of enthalpies and entropies of transfer is feasible using the classical representation of the van't Hoff equation (Equation 24) as in Melander *et al.*'s work [257].

$$\ln K' = -\frac{\Delta H}{RT} + \frac{\Delta S}{R} + \ln\varphi \quad \text{(Eq. 24)}$$

where K' is the capacity factor, R is the gas constant and equals 8.314 J K^{-1} mol^{-1}, T is the temperature in Kelvin, ΔH and ΔS are the enthalpy and entropy of transfer of the solute from mobile phase to the stationary phase, and φ is the volume phase ratio that is the ratio of volume of stationary phase to the volume of the mobile phase.

MLC is considered as a form of reversed phase liquid chromatography but a limited number of publications for describing MLC using thermodynamic parameters have been published. A direct application of the previously mentioned equation was carried out in the work of Dorsey *et al.* for detecting the effect of temperature change on the thermodynamics of compounds partitioning in MLC [170]. More recently,

thermodynamic information including enthalpy, entropy and Gibbs free energy, were calculated based on the relation between the partitioning data obtained from MLC and the change in the temperature at which the MLC experiments were carried out for studying the partitioning of three dialkyl phthalate esters in MLC [258].

Two equations are used to describe Gibbs free energy which can be expressed as

$$\Delta G^{o} = -RT\ln K \qquad \text{(Eq. 25)}$$

$$\Delta G^{o} = \Delta H^{o} - T\Delta S^{o} \qquad \text{(Eq. 26)}$$

where ΔG^{o} is Gibbs free energy, R is the gas constant, T is the temperature in Kelvin and K is the thermodynamic distribution constant.

In a study by Waters *et al.* [258], K' was replaced with P_{mw} where P_{mw} is the micelle-water partition coefficient of the solute in MLC. Therefore, a description of the dependence of partition coefficient P_{mw} between the micellar pseudo-phase and the stationary phase is given by a linear function of the van't Hoff equation as follows:

$$\ln P_{mw} = -\frac{\Delta H}{RT} + \frac{\Delta S}{R} \qquad \text{(Eq. 27)}$$

where P_{mw}, R, ΔH and ΔS were defined previously. Furthermore, φ is the volume phase ratio and considered constant and can be neglected from the equation as the adsorbed surfactant on the bonded phase is stated to be constant with micellar mobile phases [259].

It is reported that the linear relationship between partition coefficient (P_{mw}) and (1/T) is an indication that the changes in enthalpy and entropy are independent of temperature change. Where enthalpy is considered a reflection of bonds being formed, broken or distorted (H-bonds) also it is related to van der Waals interactions while entropy is related to the hydrophobic effect [253] which results from the transfer of non-polar molecules to water from a less polar environment or even transfer of polar molecules from water to a non-polar environment. Accordingly, the thermodynamic parameters, ΔH and ΔS, can be calculated respectively from the slope and the intercept of van't Hoff plots as described in (Eq. 28 and Eq. 29).

$$\text{Slope} = -\frac{\Delta H}{RT} \qquad \text{(Eq. 28)}$$

$$\text{Intercept} = \frac{\Delta S}{R} \qquad \text{(Eq. 29)}$$

According to Fisher and co-workers such a linear relationship is believed to be evidence of the maintenance of the micellar structure integrity throughout the studied temperature range [170]. On the other hand, nonlinearity of van't Hoff plots have been

reported several times in literature presenting different assumptions for this anomaly. Cole and Dorsey reported that a phase transition was the reason for the non-linear van't Hoff plots they obtained when the bonding density was above a certain limit [260]. Also the parabolic van't Hoff plot obtained with benzene was attributed to the hydrophobic effect rather than a change in phase ratio by Cole and co-workers [261]. Liu and co-workers observed an unusual van't Hoff plot of two linear regions disjoined at a certain temperature and they attributed such anomalous behaviour to a stationary phase conformation above this temperature. They also observed that the plot might have been linear if the studied temperature range was smaller [262]. Furthermore, Bidlingmeyer and Henderson investigated the concept of a change in phase ratio where they observed the retention mechanism of selected compounds on bare silica at different temperatures. Non-linear van't Hoff plots resulted, therefore ruling out phase ratio as being the reason for such nonlinearity, which led them to the conclusion that changes in the adsorptive or electrostatic forces or change in the amount of the adsorbed mobile phase on the silica surface with the change in temperature could be the reason for the unusual plots [263]. Also non-linear van't Hoff plots were obtained with partitioning of selected compounds into lipid bilayers in LEKC [253]. In total, obtaining nonlinear van't Hoff plots is not considered an anomaly but justification can be complex.

Non-linear van't Hoff plots can be considered beneficial as they facilitate studying the thermodynamics of a system where ΔH and ΔS can still be obtained at each temperature by fitting the obtained data to a polynomial eqaution of an order that gives the best fit. In literature, Horvath and co-workers described the dependence of the retention factor in hydrophobic interaction chromatography on temperature using a quadratic equation [264]. Also Hearn and co-workers described the dependence of the natural logarithm of partition coefficient on temperature for the interaction of polypeptides with ligands using a third order polynomial equation [265, 266].

In summary, the aim of this section was to study the thermodynamic changes that take place in the micellar microenvironment that arise due to changes in the interaction and the retention mechanism of the eluted drugs or changes in the micellisation process. Since the surfactant used in this work is a bile salt whose micelles look and behave differently compared with conventional surfactants, it was expected that the changes

in this system upon the change in temperature would be more complicated than the changes seen with conventional surfactants.

3.G.1.3. A thermodynamic study of partitioning in MLC

In this section the influence of temperature on the partitioning and consequently the retention of selected compounds was studied where the chromatographic retention of these compounds was determined at different column temperatures in the range of (303 K – 318 K) using different micellar concentrations of NaDC bile salt in water. Log P_{mw} was calculated from the slope and the intercept of the linear plots of (1/K') versus CM at 303, 308, 313 and 318 K as shown in Figures 138-142.

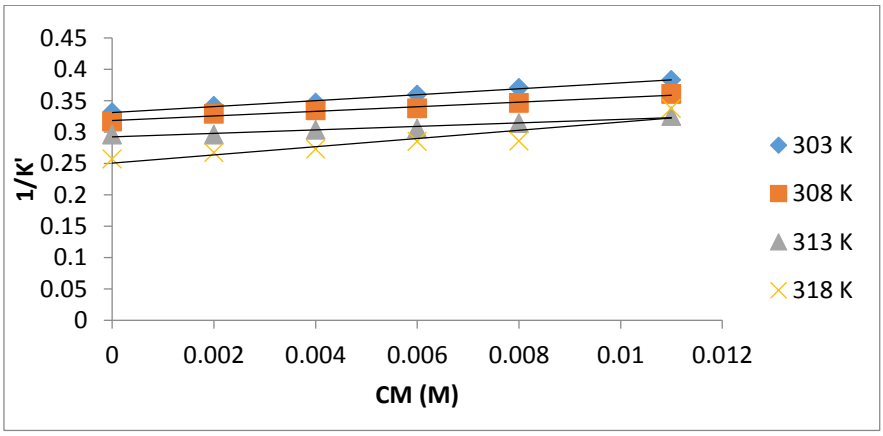

Figure 138: A plot of inverse of the capacity factors versus micellar concentration for caffeine at various temperatures.

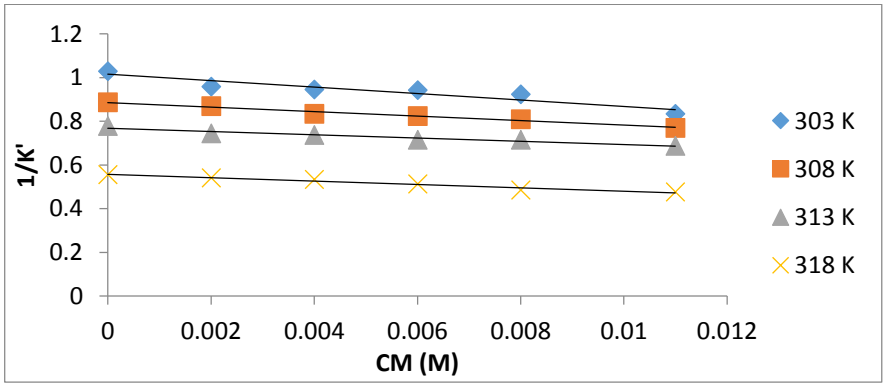

Figure 139: A plot of inverse of the capacity factors versus micellar concentration for ibuprofen at various temperatures.

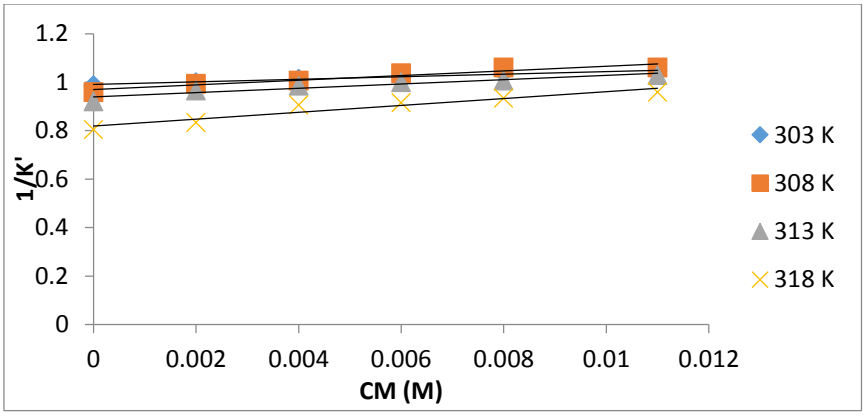

Figure 140: A plot of inverse of the capacity factors versus micellar concentration for ketoprofen at various temperatures.

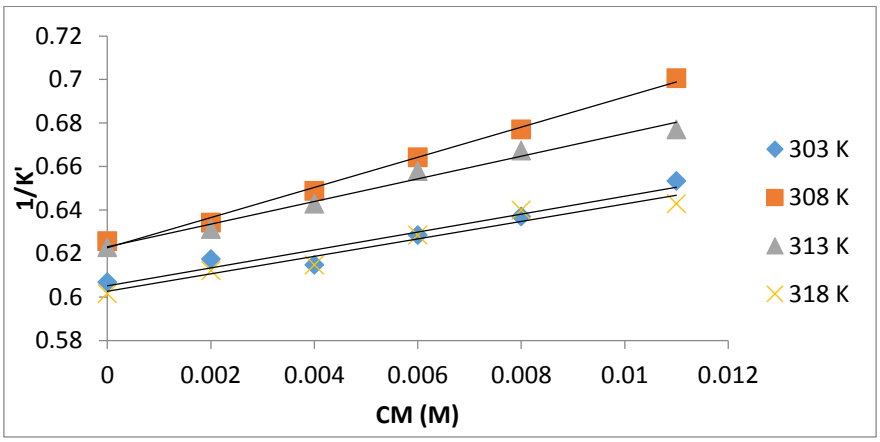

Figure 141: A plot of inverse of the capacity factors versus micellar concentration for acetaminophen at various temperatures.

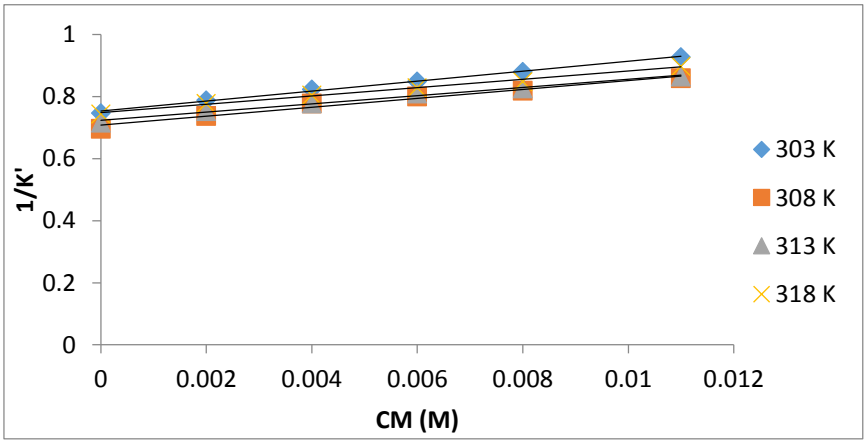

Figure 142: A plot of inverse of the capacity factors versus micellar concentration for theophylline at various temperatures.

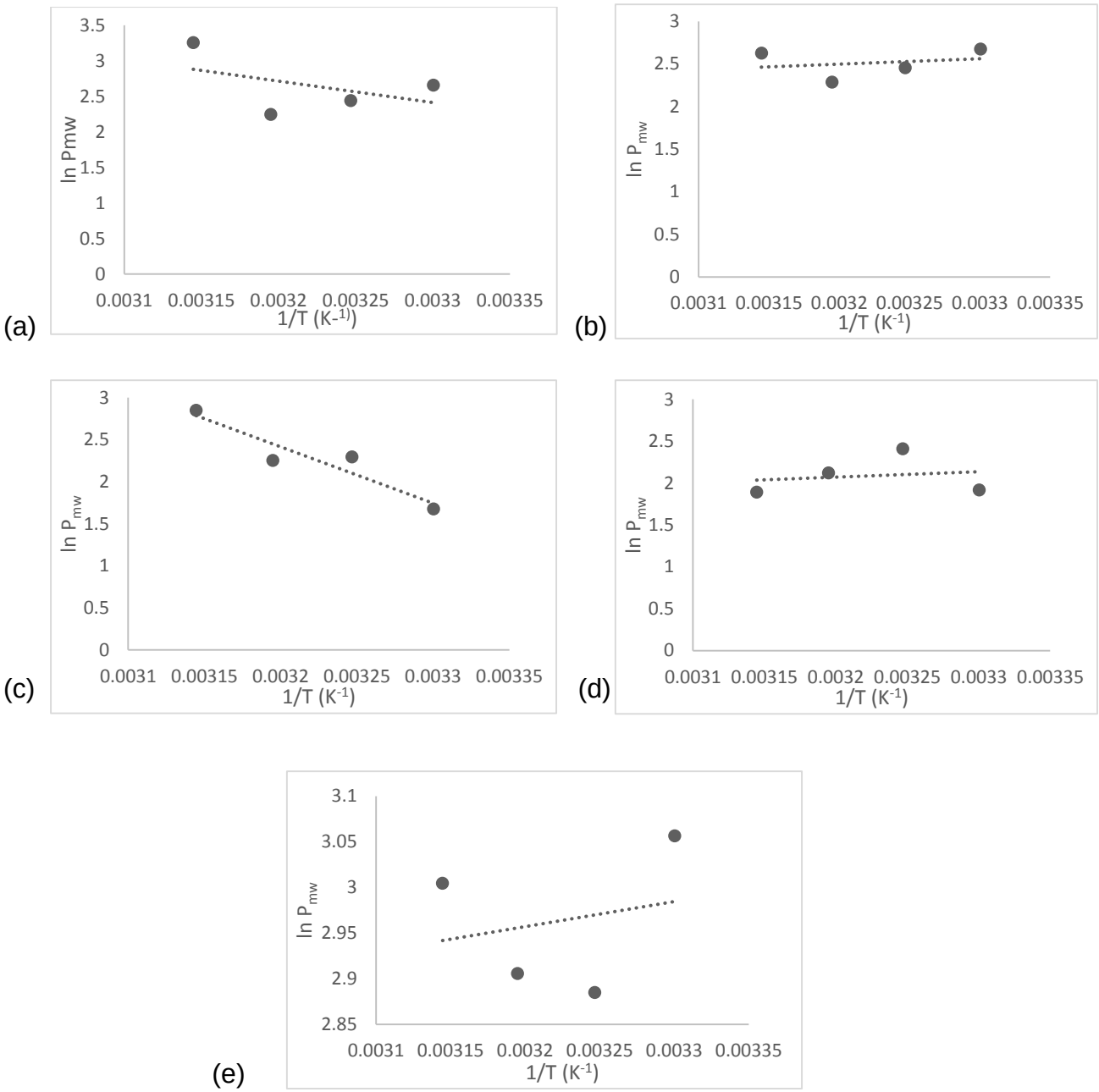

Figure 143: van't Hoff plots for (a) caffeine, (b) ibuprofen, (c) ketoprofen, (d) acetaminophen, (e) Theophylline at 303, 308, 313 and 318 K.

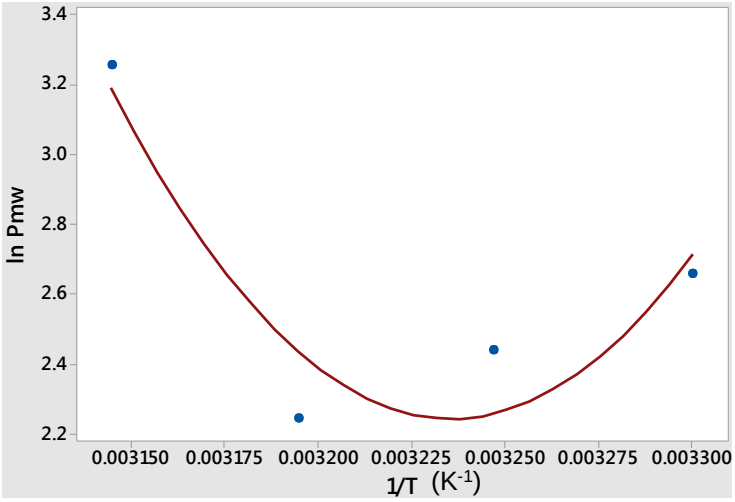

Figure 144: Second order polynomial van't Hoff plots for caffeine at 303, 308, 313 and 318 K.

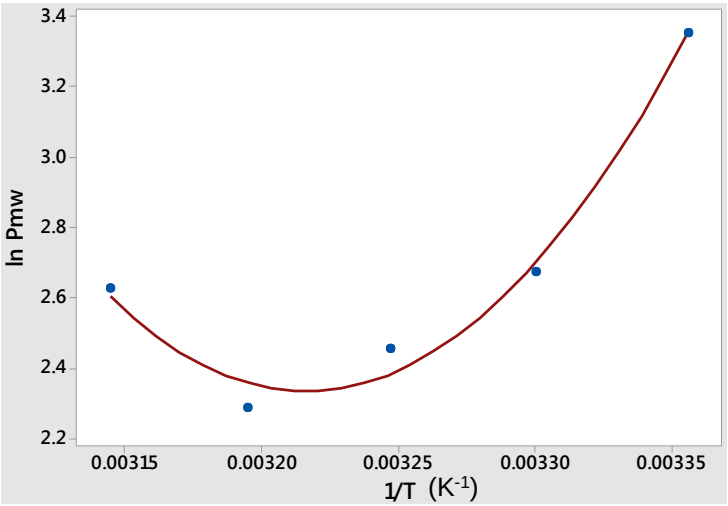

Figure 145: Second order polynomial van't Hoff plots for ibuprofen at 303, 308, 313 and 318 K.

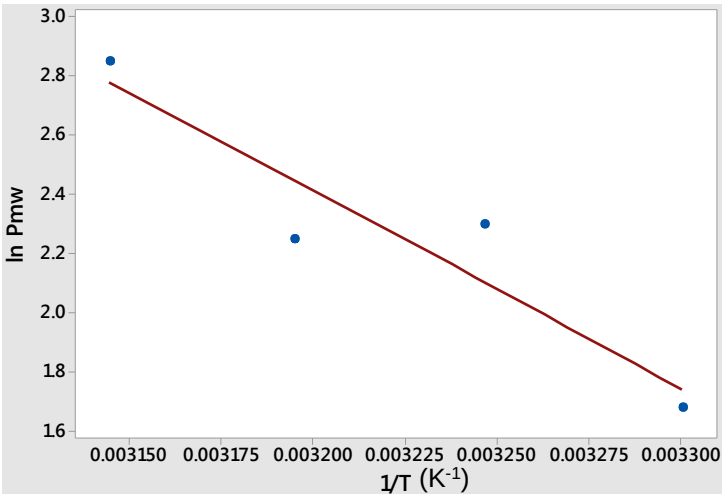

Figure 146: Second order polynomial van't Hoff plots for ketoprofen at 303, 308, 313 and 318 K.

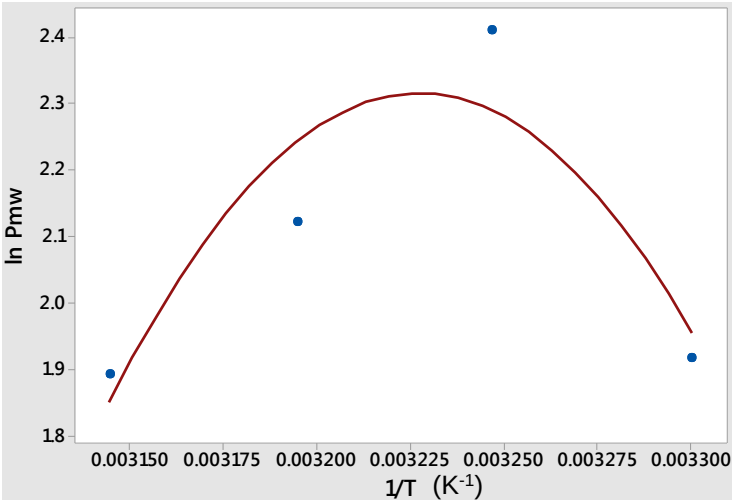

Figure 147: Second order polynomial van't Hoff plots for acetaminophen at 303, 308, 313 and 318 K.

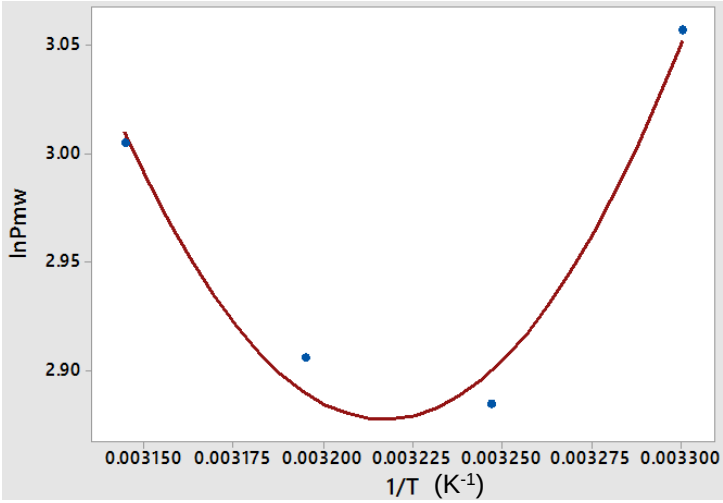

Figure 148: Second order polynomial van't Hoff plots for theophylline at 303, 308, 313 and 318 K.

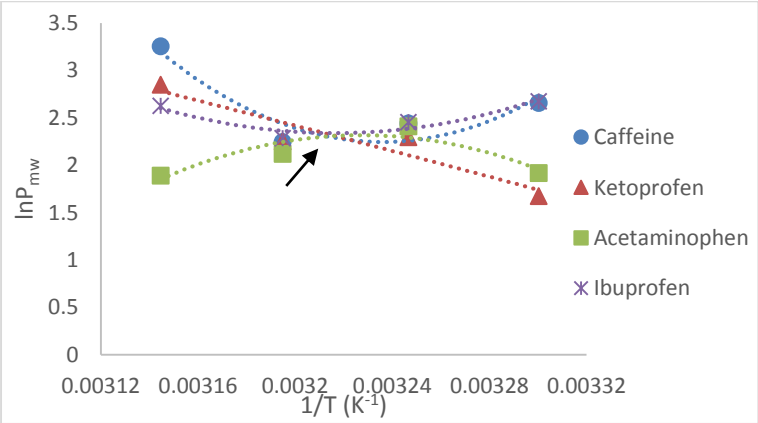

Figure 149: Second polynomial van't Hoff plots of caffeine, ketoprofen, acetaminophen and ibuprofen intersecting at one point.

Table 91: Partition coefficient and thermodynamic parameters from nonlinear van't Hoff plots at different column temperatures.

Drugs	Temp. K	P_{mw}	Ln P_{mw}	ΔH Kcal.mol^{-1}	ΔS Kcal.mol^{-1}.K^{-1}	ΔG Kcal.mol^{-1}	ΔC_p Kcal.mol^{-1}
Acetaminophen	303	6.801	1.917	19.607	0.069	-1.189	-2.93
	308	11.134	2.410	5.195	0.021	-1.414	-2.836
	313	8.344	2.122	-8.756	-0.024	-1.4078	-2.746
	318	6.640	1.893	-22.268	-0.066	-1.182	-2.660
Caffeine	303	14.271	2.658	-33.019	-0.096	-3.797	4.917
	308	11.497	2.442	-8.832	-0.017	-3.514	4.759
	313	9.461	2.247	14.582	0.058	-3.618	4.608
	318	25.971	3.257	37.259	0.130	-4.09	4.464
Ibuprofen	303	14.501	2.674	-17.345	-0.052	-1.661	2.251
	308	11.669	2.457	-6.273	-0.016	-1.494	2.179
	313	9.855	2.288	4.446	0.019	-1.503	2.11
	318	13.837	2.627	14.828	0.052	-1.681	2.044
Ketoprofen	303	5.348	1.677	13.502	0.048	-1.061	-0.042
	308	9.938	2.296	13.296	0.047	-1.3	-0.041
	313	9.530	2.255	13.097	0.047	-1.535	-0.039
	318	17.282	2.85	12.904	0.046	-1.767	-0.038
Theophylline	303	21.253	3.057	-8.270	-0.021	-1.845	1.083
	308	17.904	2.885	-2.943	-0.004	-1.783	1.048
	313	18.282	2.906	2.215	0.013	-1.806	1.015
	318	20.181	3.005	7.210	0.029	-1.910	0.983

Table 92: Second order polynomial forms of van't Hoff equations with their coefficient values.

Drugs	van't Hoff quadratic Equations	a	b	c
Acetaminophen	$lnP_{mw} = -705.2 + \frac{438455}{T} - \frac{67926153}{T^2}$	-67926153	438455	-705.2
Caffeine	$lnP_{mw} = 1193 - \frac{735799}{T} + \frac{1.14*10^8}{T^2}$	$1.14*10^8$	-735799	1193
Ibuprofen	$lnP_{mw} = 542.3 - \frac{335716}{T} + \frac{52188135}{T^2}$	52188135	-335716	542.3
Ketoprofen	$lnP_{mw} = 13.7 - \frac{411}{T} - \frac{970849}{T^2}$	-970849	-411	13.7
Theophylline	$lnP_{mw} = 262.8 - \frac{161570}{T} + \frac{25110653}{T^2}$	25110653	-161570	262.8

Van't Hoff plots were constructed for the five compounds analysed using MLC by plotting the natural logarithm of their micelle-water partition coefficients ln P_{mw} against the inverse of temperature 1/T as shown in Figure (143). The obtained van't Hoff plots were nonlinear showing that the change in heat capacity (ΔC_p) is nonzero and the dependence of the thermodynamic parameters on temperature. This nonlinear behaviour also suggests that the partitioning process is more complex, similar to partitioning through lipid bilayers which also follows the same nonlinear pattern suggesting the presence of a mixed retention mechanism.

For calculation of the thermodynamic parameter values (enthalpy (ΔH) entropy (ΔS) free energy (ΔG) and heat capacity (ΔC_p)) the data were fitted to second order polynomial equations generally expressed as [253]:

$$\ln P_{mw} = \frac{a}{T^2} + \frac{b}{T} + c \qquad \text{(Eq. 30)}$$

Enthalpy was derived as [267]:

$$\Delta H = -R\left[\frac{2a}{T} + b\right] \qquad \text{(Eq. 31)}$$

And entropy was given by [267]:

$$\Delta S = R\left[c - \frac{a}{T^2}\right] \qquad \text{(Eq. 32)}$$

While heat capacity was calculated from [267]:

$$\Delta C_p = R\left[\frac{2a}{T^2}\right] \qquad \text{(Eq. 33)}$$

The values of a, b and c of the second order polynomial equations obtained by fitting the data to second order polynomial using Minitab 17® are listed in Table 92. Using parameters listed in Table 91.

As shown in Table 91, ΔG values for all compounds were negative confirming that partitioning from the aqueous to the micellar phase was thermodynamically favoured. Also when comparing ΔH values to ΔS it was observed that ΔH values were greater than that of ΔS which suggest that the partitioning process was enthalpically driven.

It was observed that in some cases a pattern in the change of micelle-water partition coefficient with temperature was apparent. Acetaminophen displayed an initial increase followed by a decrease while, other drugs showed an initial decrease

followed by an increase (caffeine, ibuprofen and theophylline) giving the characteristic dome-shaped and inverted dome-shaped van't Hoff plots (Figures 144-148). Similar plots have been reported for unfolding of proteins in bulk solutions and in solid/liquid interfaces as well as protein-ligand interactions [267]. It was interesting to consider if there was a common temperature between these drugs before and after which the P_{mw} pattern changed. It was found that by overlaying all the second order polynomial plots of ln P_{mw} against 1/T, the four compounds intersected at the same point corresponding to a temperature of approximately 311 K (38 ^{o}C) as shown in Figure (149). This temperature could be an indication of a critical point after which the pattern of partitioning changes or a change in the micelle structure.

A negative ΔC_p is an indication of the transfer of nonpolar solute from water to the nonpolar phase while a large positive heat capacity is an indication of a hydrophobic effect of a nonpolar solute in water [253]. For ΔS a positive value is commonly interpreted as a hydrophobic interaction where the molecules' hydrophobic moieties come in contact with each other forming aggregates rejecting water molecules from the surrounding contact surface therefore increasing the system entropy by the disordered state of the rejected water molecules. According to a recent theory the positive ΔS could be attributed to the cavity reduction at the interface resulting from reconstruction of water molecules leading to solvent volume expansion. Therefore, it would be assumed that no intermolecular short bonds formed only hydrophobic association (not hydrophobic bonding), as molecular surfactant self-assemblies [268]. A negative value could be a result of the loss of entropy of a solute upon partitioning in to the micellar pseudophase being greater than the gain of entropy resulting from the H-bond vanishing within the water network surrounding the solute in the aqueous phase [253].

A positive enthalpy (ΔH) is said to be an indication of the partitioning of solute in to the micellar pseudophase [253, 269] while a negative enthalpy indicates the occurrence of hydrogen bond breaking or formation between solutes and micelles showing an interaction between the solute and the micelles. It could also be an indication of solutes being transferred to micelles by a van der Waals interaction between them [253].

The process of partitioning of solute in to micelles is said to be mainly enthalpically driven with a small contribution of entropy as reported by Terabe. However, Woodrow and Dorsey reported the opposite as per their results i.e. the partitioning process was entropically driven [253, 270].

From Table (91), it can be concluded that for acetaminophen, the partitioning process is enthalpically driven with a small contribution of hydrophobic interaction (positive ΔS) where the drug appears to be deeply incorporated into the core of micelles (negative ΔC_p and positive ΔH) within the temperature range (303-308 K). Within the range (313-318 K) a decreased drug preference to the micelles is noted which is reflected by negative values of ΔS and ΔH within this range, which is consistent with the initial increase followed by the decrease in the P_{mw} values. As for the three drugs (caffeine, ibuprofen and theophylline) the partitioning process appears to be enthalpically driven with decreased binding to the micelles reflected by negative values of ΔH and ΔS within the temperature range (303-308 K). Within the range (313-318 K) an increased drug preference to the micelles is noted which is reflected by a switch of the negative ΔS and ΔH values to positive within this range, which is consistent with the initial decrease followed by the increase in the P_{mw} values. For ketoprofen, it appears to be deeply incorporated in the micellar pseudophase with the partitioning process being enthalpically driven which is reflected by the positive values of ΔH and ΔS and negative ΔC_p confirming the transfer of the drug to the micellar core within the temperature range (303-318 K) which is consistent with the increase in the P_{mw} of ketoprofen over the temperature range (303-318 K).

3.G.2. Conclusion

The partitioning process of solutes into micelles of naturally occurring biosurfactant, such as NaDC, appears to be more complex than that of conventional synthetic surfactants which is evident from the nonlinear van’t Hoff plots. Bui reported that nonlinear van’t Hoff plots described the more complex partitioning process of solutes through lipid bilayers as in LEKC [253]. Additionally, Waters *et al.* found that the process of micelle formation compared well with properties of the complexes formed by substrates with proteins [268]. Accordingly, it can be concluded that there are many common findings between the micelle formation process and many physiological processes. Since one of the main advantages of MLC over alternative methods is the formation of a hydrophobic micellar interior mimicking the bilayer, this thermodynamic study could be confirmation that this MLC method fulfils this advantage to a great extent. In summary, MLC can be considered a successful approach to achieve the main aim of this work, i.e. to develop a method simulating drug absorption through the human intestinal membrane.

CHAPTER 4

Predicting Human Intestinal Absorption Using Spectrophotometry

Chapter 4: Predicting Human Intestinal Absorption Using Spectrophotometry

4. Introduction

Cholanology is the science of bile acids and plays a very important role in biotechnology and the pharmaceutical industry. Such a role is attributed to the uniqueness of the bile salt structure having hydrophilic and hydrophobic binding sites that enables them to deliver both hydrophilic and hydrophobic drug entities. Among the various advantages of bile salts inside the human body is their capacity to solubilise and dissolve both soluble substances and nonpolar/lipidic substances such as cholesterol, phospholipids and monoglycerides by the formation of bile salt simple and mixed micelles with different structures and characteristics [242]. Based on these valuable characteristics, many investigations have been made regarding the effect of bile salt micelles on the dissolution and solubilisation of poorly water soluble drug molecules and thereby their effect on the oral administration of these drugs. Furthermore, other studies have utilised the solubilising capacity of bile salt micelles in the calculation of a micelle/aqueous partition coefficient of selected compounds through measurement of the extent of solubilisation of these drugs spectrophotometrically from the changes in drug absorbance [240, 271].

The study of the absorption of poorly soluble drug molecules with bile salt micelles is thought to be advantageous for further investigation of bile salt-drug interactions yet is a field that has not been extensively investigated.

Such studies could be helpful in overcoming drug induced liver injury (DILI) which is considered a major unresolved scientific problem [242]. Peterson *et al.* recently reported studies that have involved measuring the extent of drug dissolution or solubilisation in media (containing bile salt micellar systems) which closely resemble the reported physiological bile salts composition in the human intestine. The results of these studies suggest that the bile salt micellar system is a promising method for predicting *in vivo* drug solubilisation [272, 273].

CHAPTER 4
Section (A)

Predicting Human Intestinal Absorption Using solubilisation method

(As published in Journal of Pharmaceutical Sciences in October 2016)

See Appendix I

Section (A): Predicting human intestinal absorption through measurement of solubilisation

In this section, the solubilising capacity of an increasing concentration of NaDC micelles in water for a selected number of drugs was used for the calculation of partition coefficients.

4.A.1. Results and Discussion

4.A.1.1. Solubilisation Measurement Method

The micelle solubilisation of drugs can be expressed by what is called the solubilisation ratio (SR), which is calculated from the slope of the linear portion of the plot of the total drug concentration in solution at saturation against the total bile salt concentration above its CMC. For micelle solubilisation, the two-state model was assumed in Equation 34 as follows[240]:

$$SR = N_D / N_{BS} \qquad \text{Eq. (34)}$$

Where N_D is defined as the number of moles of drug in solution while N_{BS} is defined as the number of moles of the bile salt in solution.

Mole fraction solubilised (X_m) was calculated from (SR) which was obtained from the slope of the linear portion of the graph of total drug concentration versus the total NaDC concentration used in this work as shown in Equation 35.

$$X_m = SR/(1 + SR) \qquad \text{Eq. (35)}$$

Micelle-water partition coefficient (log $K_{xm/a}$) was calculated from the mole fraction of drug solubilised in the bile salt micelle (X_m) and the mole fraction aqueous solubility (X_a) (Eq. (36). For calculation of the mole fraction aqueous solubility (X_a), drug aqueous solubility data was extracted from literature.

$$K_{xm/a} = X_m / X_a \qquad \text{Eq. (36)}$$

The solubilising effect of different concentrations of NaDC in water within the concentration range of (0.007-0.02 M) was investigated upon its addition to an excess amount of each of the drugs within the studied data set. Additionally, this solubilising effect was quantified and expressed as a solubilisation ratio by means of UV-spectrophotometric determination of the amount of drug solubilised within the NaDC micelles and using the calibration plots previously constructed for each drug in each of the used NaDC concentrations (0.007, 0.009, 0.011, 0.013, 0.017 and 0.020 M).

The total concentration of solubilised drug by NaDC (mM) with the total NaDC concentration used for a selected number of drugs under investigation are shown in Figures 150-155 with their data listed in Tables 93-98.

Figures 150-155 and Tables 93-98 show an increase in the amount of solubilised drug as the concentration of the bile salt used increased.

Table 93: NaDC concentration (mM) against solubilised amitriptyline (mM).

NaDC (mM)	Solubilised Drug (mM)
9	0.577
11	0.865
13	1.442
17	2.596
20	2.740

Table 94: NaDC concentration (mM) against solubilised acetylsalicylic acid (mM).

NaDC (mM)	Solubilised Drug (mM)
9	8.876
11	10.624
13	12.933
17	15.392
20	18.917

Table 95: NaDC concentration (mM) against solubilised propranolol (mM).

NaDC (mM)	Solubilised Drug (mM)
9	0.887
11	1.272
13	1.388
17	2.005
20	2.159

Table 96: NaDC concentration in (mM) against solubilised flurbiprofen (mM).

NaDC (mM)	Solubilised Drug (mM)
7	2.804
9	3.296
11	3.553
13	3.570
17	4.078
20	4.233

Table 97: NaDC concentration (mM) against solubilised alprenolol (mM).

NaDC (mM)	Solubilised Drug (mM)
7	0.630
9	0.794
11	0.818
13	1.007
17	1.400

Table 98: NaDC concentration (mM) against solubilised terbutaline (mM).

NaDC (mM)	Solubilised Drug (mM)
9	291.011
13	322.633
17	331.293
20	359.972

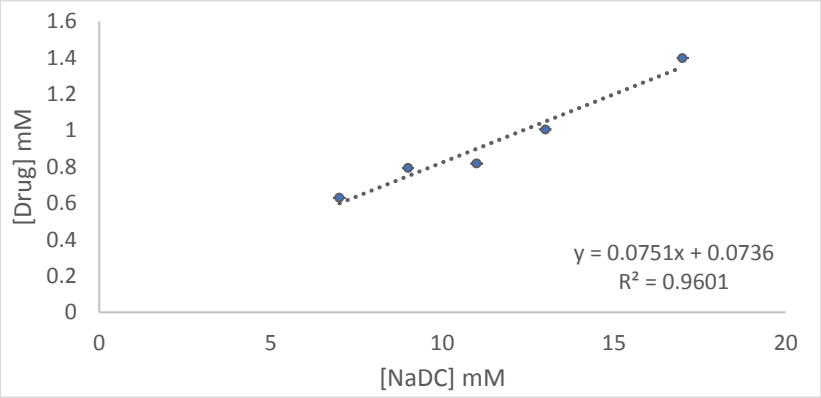

Figure 150: NaDC Concentration (mM) with solubilised alprenolol (mM).

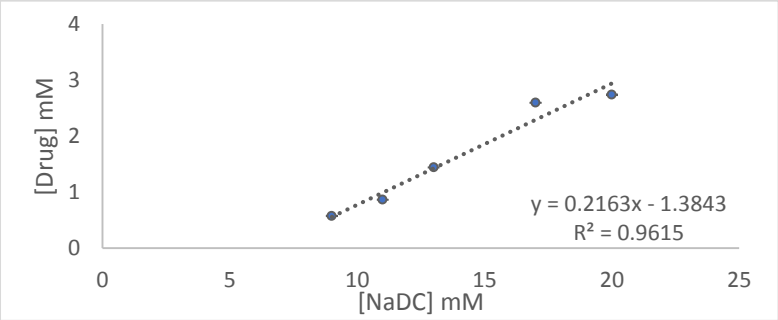

Figure 151: NaDC Concentration (mM) with solubilised amitriptyline (mM).

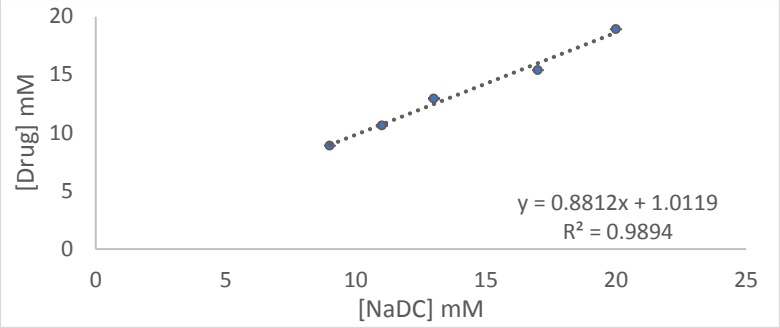

Figure 152: NaDC Concentration (mM) with solubilised acetylsalicylic acid (mM).

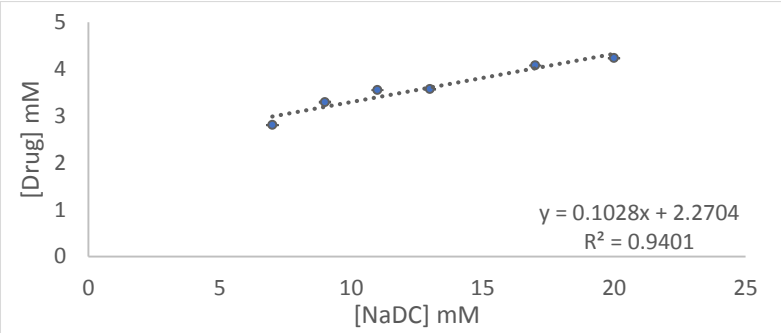

Figure 153: NaDC Concentration in (mM) with solubilised flurbiprofen (mM).

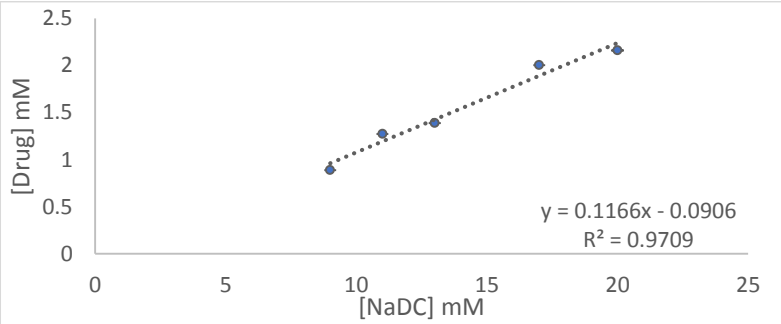

Figure 154: NaDC Concentration in (mM) with solubilised propranolol (mM).

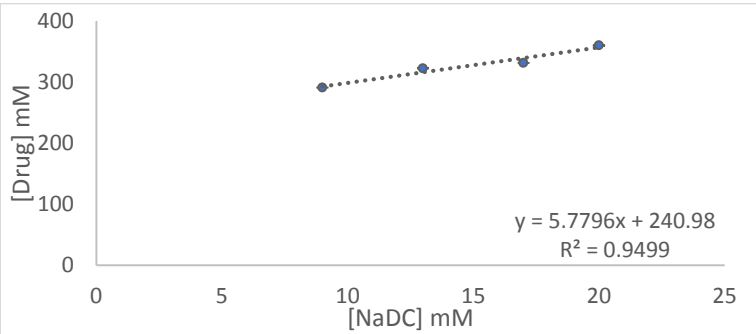

Figure 155: NaDC Concentration (mM) against solubilised terbutaline (mM).

Table 99: Calculated solubilisation ratio (*SR*), mole fraction solubilised (X_m), mole fraction aqueous solubility (X_a) and micelle/water partition coefficient ($K_{xm/a}$) for the 26 compounds

Drug	*SR*	X_m	X_a	*Log* $K_{xm/a}$	log $P_{o/w}$[184]
Acetaminophen	2.569	0.720	4.94E-04	3.16	0.46
Acetylsalicylic acid	0.881	0.468	9.98E-04	2.67	1.19
Alprenolol	0.075	0.070	1.36E-05	3.71	3.10
Amitriptyline	0.216	0.178	6.30E-07	5.45	4.92
Caffeine	5.174	0.838	10.18 E-04	2.92	-0.07
Carbamazepine	0.055	0.052	1.35E-06	4.59	2.45
Cimetidine	1.240	0.554	6.69E-4	2.92	0.40
Diclofenac	0.079	0.073	1.34E-07	5.74	4.51
Diphenhydramine	5.867	1.206	2.16E-04	3.75	3.27
Fenoprofen	0.075	0.070	2.79 E-06	4.40	3.10
Fluconazole	0.040	0.039	5.88E-08	5.82	0.50
Flurbiprofen	0.103	0.093	5.89E-07	5.20	4.16
Gemfibrozil	0.056	0.053	2.00E-06	4.42	3.40
Ibuprofen	0.129	0.114	5.97E-06	4.28	3.97
Indomethacin	0.030	0.029	4.71 E-08	5.79	4.27
Ketoprofen	0.141	0.123	3.61E-06	4.53	3.12
Lidocaine	0.539	0.350	3.15E-04	3.05	2.44
Mannitol	3.179	0.761	2.09E-02	1.56	-3.1
Meloxicam	0.031	0.030	3.66E-07	4.92	3.43
Naproxen	0.115	0.103	1.24E-06	4.92	3.18
Nicotinic acid	3.520	0.779	1.2 E-02	1.81	0.36
Phenylbutazone	0.090	0.083	8.40E-06	3.99	3.16
Piroxicam	0.013	0.012	1.25 E-06	4.00	3.06
Propranolol	0.117	0.104	4.28E-06	4.39	3.48
Quinine	2.047	0.672	2.77E-05	4.38	3.44
Terbutaline	5.780	0.853	1.67E-02	1.71	0.90

A group of twenty-six drugs were analysed using this method for calculation of their micelle-water partition coefficient (log $K_{xm/a}$). A linear relationship can be seen between the total solubilised drug concentration and the total NaDC concentration used over the range (7-20 mM) for the majority of the drugs under investigation notwithstanding that some drugs showed nonlinear relationships at low or high concentrations of NaDC. This could be attributed to drug-drug interactions rather than drug-NaDC interactions if the drugs are known to self-associate [274].

In a study involving an investigation of the solubilisation of steroids by taurocholate bile salt, it was observed that for all of the studied compounds the solubilising capacity of the bile salt was on the same order of magnitude while the solubilising capacity of

water for the same compounds varied widely. This proves that the hydrophobicity of these compounds is the driving force determining their solubilisation by the bile salt rather than their affinity for the bile salt micelles [271]. Additionally, it was noted by several authors that an increase in a compound's lipophilicity increases its tendency for solubilisation by a surfactant where linear relationships were reported between lipophilicity, that can be represented by $P_{o/w}$, and its micelle water partition coefficient. As a result, predictions of the increase in solubility can be made on the basis of aqueous solubility and partition coefficient [271].

Looking at the results obtained with this method it was observed that lipophilic compounds with a high log $P_{o/w}$ (representing the majority of the compounds in the dataset) showed high micelle-water partition coefficient (log $K_{xm/a}$) values while hydrophilic compounds with a low log $P_{o/w}$ (such as mannitol, nicotinic acid and terbutaline) had lower (log $K_{xm/a}$) values. However, some hydrophilic drugs with very small log $P_{o/w}$ values had a high log $K_{xm/a}$ such as acetaminophen, cimetidine and fluconazole, this could be attributed to their low aqueous solubility compared with other hydrophilic compounds.

Generally, for all compounds the concentration of the solubilised drug increased with the increase in the total NaDC concentration used which could be attributed to the full or partial incorporation of the drug molecule in the NaDC micellar hydrophobic core via strong hydrophobic interactions with the NaDC hydrophobic steroid nucleus (mainly for neutral compounds) and/or polar/electrostatic interactions for charged compounds. Compared with conventional surfactants, bile salts especially dihydroxy-based structures have a more solubilising capacity because of the presence of hydroxyl groups in the surface of the micelles which contributes to reducing the net surface charge on the micelles. This subsequently reduces the electrostatic repulsion between the negatively charged drug molecules and the micelles [109].

4.A.2. Statistical Modelling

Calculating log $K_{xm/a}$ from the solubilisation ratio (*SR*), other molecular descriptors such as molecular weight (Mwt), polar surface area (PSA), freely rotating bonds (FRB), molar volume (V_M), dissociation constant (pK_a), aqueous solubility (S_w), number of hydrogen bond donors (nHD) and number of hydrogen bond acceptors (nHA) were collected from literature to be used alongside the experimentally determined log $K_{xm/a}$ for the statistical modelling of human intestinal absorption (HIA) and permeability

coefficients obtained by (PAMPA and Caco-2) in *vitro* methods. Lipophilicity represented by log $K_{xm/a}$ experimentally obtained from this work using the solubility method was combined with data in the following sections and included as a part of the summary data as shown in Table 103.

4.A.2.1. Statistical Modelling of Human Intestinal absorption (HIA)

Analysing the experimentally obtained log $K_{xm/a}$ values alongside other molecular descriptors against the reported %HIA values enabled the application of simple linear regression and therefore the successful inclusion of log $K_{xm/a}$ in a model equation with %HIA experimental values for orally administered drugs (as shown in Table 100). The generated model allows the prediction of the %HIA of any compound when its solubility is experimentally determined in a NaDC simple micellar system in water with a prediction ability of 82 %. The model obtained for the prediction of %HIA is shown by Equation 37 as follows:

$$\text{logit HIA} = -0.919 + 0.4618 \log K_{xm/a} \qquad \text{Eq. (37)}$$

Twenty drugs were used in the development of the final model. The model's $R^2 = 84.92$ %, $R^2_{adjust.} = 84.09$ % , $R^2_{PRED} = 82.32$ %, S= 0.236

A 95 % confidence interval for log $K_{xm/a}$ is given by (0.365, 0.558), t-statistic and standardised coefficient of log $K_{xm/a}$ are 10.069 ($p<0.05$) and 0.922 respectively suggesting statistical significance of log $K_{xm/a}$ as a predictor. Also the F-ratio of the overall model is statistically significant, F= 101.388 and P value 0.000 ($p<0.05$). Absence of autocorrelation in the current regression model was proved by a Durbin-Watson statistic value of 2.309. Figure 156 shows no marked relationship between residuals and predicted values. A plot of literature values of %HIA against their corresponding predicted values can be seen in Figure 157. Four compounds (acetylsalicylic acid, fenoprofen, indomethacin and piroxicam) were used in testing the validation of the generated model. The model was able to successfully predict the %HIA for the compounds in the test set within a minimum of 0.63 % and a maximum of 9.6 % difference between the predicted %HIA and the published %HIA.

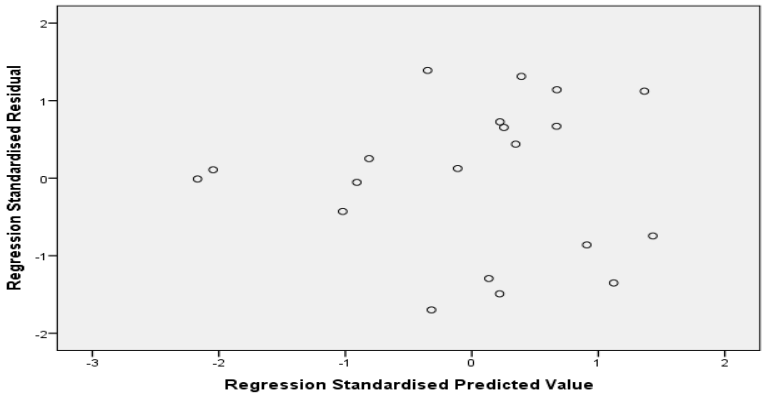

Figure 156: Residual plot for optimal logit HIA regression model.

Table 100: Experimental micelle/water partition coefficient (log $K_{xm/a}$), predicted %HIA (%$HIA_{pred.}$) and experimentally determined published literature %HIA (% $HIA_{Expt.}$) values for the compounds analysed including four validation compounds (*).

Drug	% $HIA_{Expt.}$	% $HIA_{Pred.}$
Acetaminophen	80.00[205]	77.71
Acetylsalicylic acid*	68.00[245]	67.37
Alprenolol	93.00[205]	86.18
Amitriptyline	95.00[209]	97.54
Carbamazepine	97.00[243]	94.06
Cimetidine	68.00[244]	72.86
Diclofenac	99.00[208]	98.17
Diphenhydramine	72.00[207]	86.63
Fenoprofen*	85.00[206]	92.83
Fluconazole	97.50[205]	98.32
Flurbiprofen	95.00[210]	96.81
Gemfibrozil	95.00[207]	93.01
Ibuprofen	85.00[208, 275]	91.97
Indomethacin*	100.00[205]	98.26
Ketoprofen	95.00[205, 210]	93.74
Lidocaine	75.00[206, 207, 230]	75.54
Mannitol	38.67[276]	38.81
Meloxicam	97.00[207]	95.74
Naproxen	97.67[205]	95.75
Phenylbutazone	90.00[245]	89.37
Piroxicam*	99.00 [205]	89.40
Propranolol	95.00[205]	92.75
Quinine	85.00[246]	92.73
Terbutaline	44.00[216, 275]	42.55

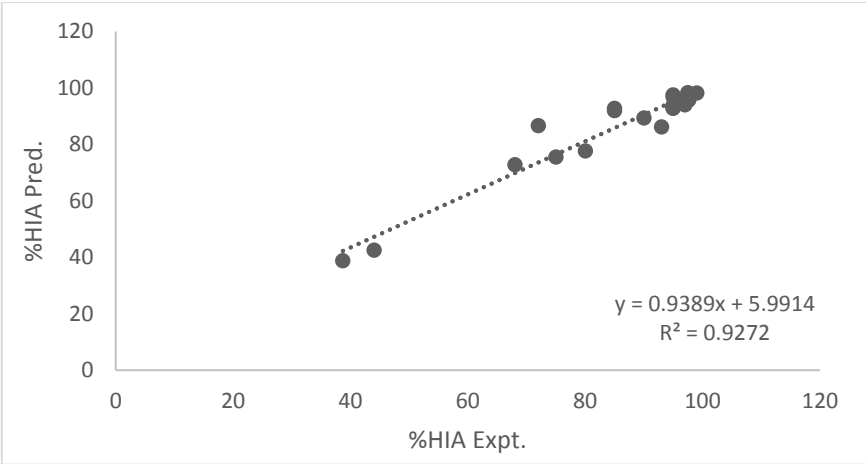

Figure 157: Regression plot of Literature %HIA against predicted %HIA values.

4.A.2.2. Modelling of permeability coefficients obtained from PAMPA

The model obtained for the prediction of PAMPA log P_o is shown in Equation (38):

$$\log P_o = -8.910 + 1.414 \log K_{xm/a} \qquad \text{Eq. (38)}$$

Seventeen drugs were used in the development of the final model. The model's R^2 =58.70 %, $R^2_{adjust.}$= 55.95 % , R^2_{PRED} = 48.22 %, S= 1.101

A 95 % confidence interval for log $K_{xm/a}$ is given by (0.761, 2.067), t-statistic and standardised coefficient of log $K_{xm/a}$ are 4.617 ($p<0.05$) and 0.766 respectively suggesting statistical significance of log $K_{xm/a}$ as a predictor. Also the F-ratio of the overall model is statistically significant, F= 21.318 and P value 0.000 ($p<0.05$).

The close agreement of the values of $R^2_{adjust.}$ & R^2_{PRED} indicates that the model does not over-fit the data. The residual analysis did not detect any relationship between residuals and predicted values as shown in Figure 158. The literature and predicted values of PAMPA permeability coefficients are listed in Table 101 and plotted in Figure 159.

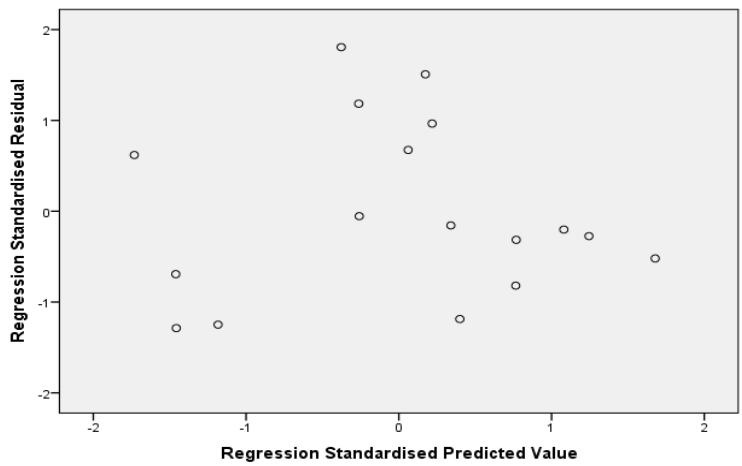

Figure 158: Residual plot for optimal PAMPA regression model.

Table 101: Experimental and predicted values for PAMPA logP_o.

Drug	Expt. PAMPA log P_o[215]	Pred. PAMPA log P_o
Acetaminophen	-5.81	-4.44
Acetylsalicylic acid	-4.45	-5.13
Caffeine	-5.55	-4.79
Carbamazepine	-3.73	-2.42
Cimetidine	-6.20	-4.78
Diclofenac	-1.37	-0.80
Flurbiprofen	-1.78	-1.56
Gemfibrozil	-1.59	-2.65
Ibuprofen	-2.11	-2.85
Indomethacin	-1.65	-1.35
Ketoprofen	-2.67	-2.50
Lidocaine	-1.42	-3.41
Meloxicam	-2.86	-1.96
Naproxen	-2.30	-1.95
Phenylbutazone	-1.96	-3.26
Piroxicam	-3.32	-3.26
Quinine	-1.05	-2.71

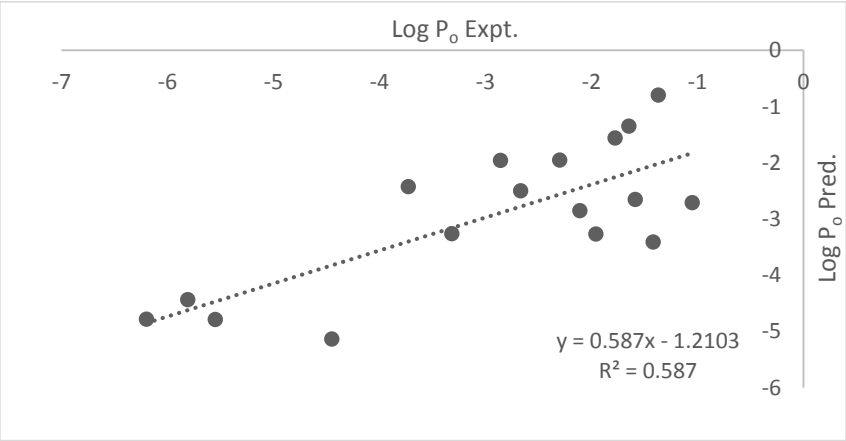

Figure 159: Plot of experimental vs. predicted log P_o values.

4.A.2.3. Modelling of permeability coefficients obtained from Caco-2 $P_{eff.}$

The model obtained for the prediction of Caco-2 $P_{eff.}$ is shown in Equation (39):

$$\log P_{eff.} = -3.7871 - 0.1643 \log K_{xm/a} \qquad \text{Eq. (39)}$$

Fifteen drugs were used in the development of the final model. The model's $R^2 = 82.89$ %, $R^2_{adjust.} = 81.57$ % , $R^2_{PRED} = 78.35$ %, S= 0.065

A 95 % confidence interval for log $K_{xm/a}$ is given by (-0.209, -0.120), t-statistic and standardised coefficient of log $K_{xm/a}$ are -7.935 ($p<0.05$) and -0.910 respectively

suggesting statistical significance of log $K_{xm/a}$ as a predictor. Also the F-ratio of the overall model is statistically significant, F= 62.96 and P value 0.000 ($p<0.05$).

Figure 160 shows no marked relationship between residuals and predicted values. Table 102 lists the experimental and predicted values of Caco-2 permeability coefficient while a plot of these values against each other is given by Figure 161.

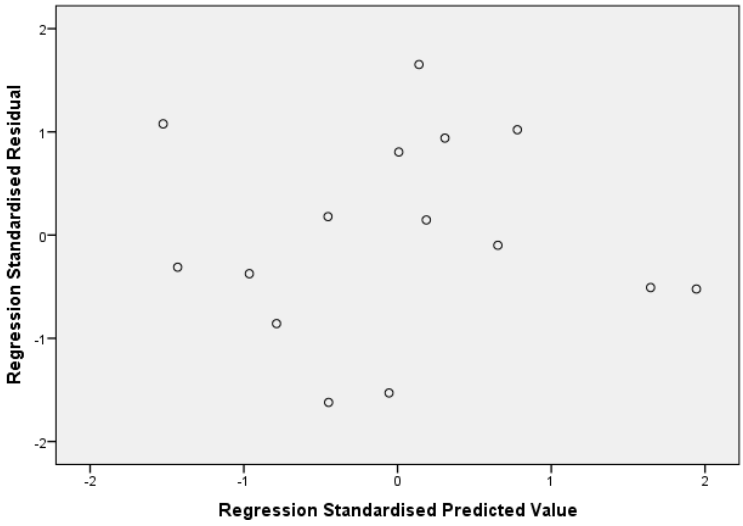

Figure 160: Residual plot for optimal Caco-2 regression model.

Table 102: Experimental and predicted values for Caco-2 log $P_{eff.}$.

Drug	Expt. Caco-2 log $P_{eff.}$	Pred. Caco-2 log $P_{eff.}$
Acetaminophen	-4.34[215]	-4.31
Caffeine	-4.30[277]	-4.27
Carbamazepine	-4.64[278]	-4.54
Diclofenac	-4.75[56]	-4.73
Fluconazole	-4.67[56, 217]	-4.74
Flurbiprofen	-4.70[230]	-4.64
Gemfibrozil	-4.41[246]	-4.51
Ibuprofen	-4.43[56, 277]	-4.49
Indomethacin	-4.69[277]	-4.67
Ketoprofen	-4.48[56]	-4.53
Lidocaine	-4.36[56]	-4.43
Meloxicam	-4.70[277]	-4.60
Naproxen	-4.58[56, 246]	-4.60
Piroxicam	-4.45[60]	-4.44
Quinine	-4.50[246]	-4.51

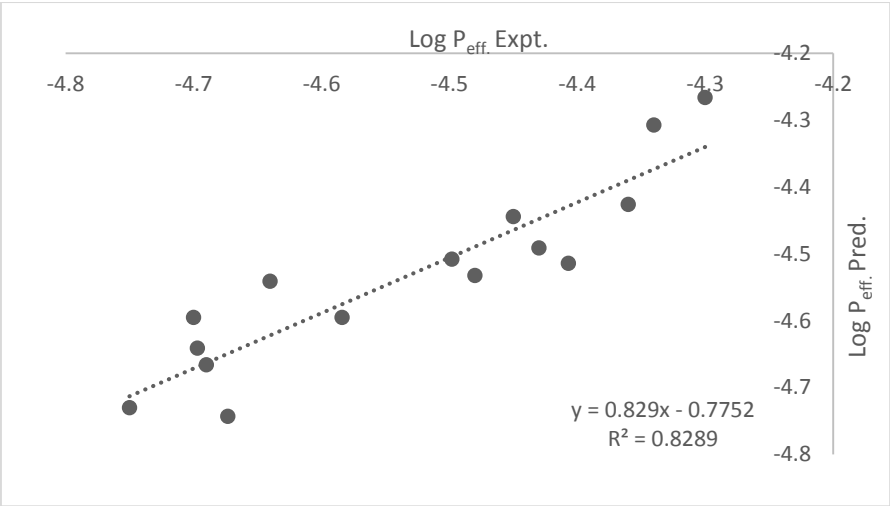

Figure 161: Plot of experimental vs predicted Caco-2 log $P_{eff.}$ values.

In summary, the predictive ability of the obtained models for the prediction of the *in vitro* permeability coefficients for PAMPA and Caco-2 methods was not as high as that of the obtained model for the prediction of human intestinal absorption (HIA) which showed that the method is more closely related to the physiological human intestinal environment. This is a very promising result, confirming the potential applicability of the micellar system.

Table 103: A summary of molecular descriptors for the selected drugs analysed by solubility method and the reported experimental values of %HIA and permeability coefficients of PAMPA and Caco-2 tests.

Drug	Log $K_{xm/a}$	LogP $_{o/w}$[184]	Mwt[218]	pK_a[184]	S_w [184]	HD[218]	HA[218]	RB[218]	PSA[219]	V_M[218]	Log P_o [215]	Log $P_{eff.}$	%HIA
Acetaminophen	3.16	0.46	151.20	9.9[220]	4.15	2	3	1	49.3	131.1	-5.81	-4.34[215]	80[205]
Acetylsalicylic acid	2.67	1.19	180.15	3.41	10[219]	1	4	3	63.6	139.6	-4.45	NI	68[245]
Alprenolol	3.71	3.10	249.35	9[279]	0.547	2	3	8	41.5	247.5	NI	NI	93[205]
Amitriptyline	5.45	4.92	277.40	9.4	0.00971	0	1	3	3.2	257.8	NI	NI	95[209]
Caffeine	2.92	-0.07	194.20	14[222]	11	0	6	0	58.4	133.4	-5.55	-4.30[277]	NI
Carbamazepine	4.59	2.45	236.36	13.9	0.0177	2	3	0	46.3	186.6	-3.73	-4.64[278]	97[243]
Cimetidine	2.92	0.40	252.34	6.8	9.38	3	6	8	114	198.2	-6.2	NI	68[244]
Diclofenac	5.74	4.51	296.20	4.15	0.00237	2	3	4	49.3	206.8	-1.37	-4.75[56]	99[208]
Diphenhydramine	3.75	3.27	255.36	8.98	3.06	0	2	6	12.5	249.2	NI	NI	72[207]
Fenoprofen	4.40	3.10	242.27	4.5	0.0811	1	3	4	46.5	204.7	NI	NI	85[206]
Fluconazole	5.82	0.40	306.27	12.71	0.001	1	7	5	81.6	205.3	NI	-4.673[56, 217]	97.5[205]
Flurbiprofen	5.20	4.16	244.26	4.42	0.008	1	2	3	37.3	203.6	-1.78	-4.697[230]	95[210]
Gemfibrozil	4.42	3.40	250.33	4.5[219]	0.0278	1	3	6	46.5	239.7	-1.59	-4.407[246]	95[207]
Ibuprofen	4.28	3.97	206.30	5.2[223]	0.0684	1	2	4	37.3	200.3	-2.11	-4.430[56, 277]	85[208, 275]
Indomethacin	5.35	4.27	357.79	4.5	0.000937	1	5	4	68.5	269.6	-1.65	-4.690[277]	100[205]
Ketoprofen	4.53	3.12	254.30	3.88	0.051	1	3	4	54.4	212.2	-2.67	-4.48[56]	95[205, 210]
Lidocaine	3.89	2.44	234.40	7.9[224]	4.1	1	3	5	32.3	238.8	-1.42	-4.36[56]	75[206, 207, 230]
Mannitol	1.56	-3.10	182.17	13.5	216	6	6	5	121	114.1	NI	NI	38.67[276]
Meloxicam	4.92	3.43	351.40	4.08	0.00715	2	7	2	136	220.3	-2.86	-4.70[277]	97[207]
Naproxen	4.92	3.18	230.26	4.15	0.0159	1	3	3	46.5	192.3	-2.3	-4.584[56, 246]	97.67[205]
Nicotinic acid	1.81	0.36	123.11	4.75	83.1	1	3	1	50.2	95.2	NI	NI	NI
phenylbutazone	3.99	3.16	308.37	4.4[225]	0.7[219]	0	4	5	40.6	262.8	-1.96	NI	90[245]
Piroxicam	4.00	3.06	331.35	6.3	0.023	2	7	2	108	222.8	-3.32	-4.450[60]	99[205]
Propranolol	4.39	3.48	259.34	9.5[226]	0.0617	2	3	6	41.5	237.2	NI	NI	95[205]
Quinine	4.38	3.44	324.42	9.05	0.5	1	4	4	45.6	266.4	-1.05	-4.498[246]	85[246]
Terbutaline	1.71	0.90	225.28	9.76	213	4	4	4	72.7	192.3	NI	NI	44[216, 275]

NI: value not included in training set.

4.A.3. Conclusion

Overall, the solubilisation method, i.e. using a simple NaDC micellar system in water, was successful in the development of a model predicting human intestinal absorption of compounds via calculation of the micelle/water partition coefficient. The obtained model has been shown to be reliable for the prediction of human intestinal absorption. This simple method is economic, robust and avoids the disadvantages of other methods using animals based experiments.

CHAPTER 4
Section (B)

Predicting Human Intestinal Absorption Using The Double Reciprocal method

Section (B): Predicting human intestinal absorption using the double reciprocal method

This section presents an alternative UV-based spectrophotometric method for the calculation of partition coefficients for a group of compounds via the determination and quantitation of spectroscopic changes induced in aqueous solutions of drugs, prepared at their minimal concentrations, when added to bile salt solutions of concentrations prepared around the CMC. Therefore, this method like the previously mentioned method in section A, is based on the effects of the bile salt monomers and micelles on the drug molecules present in solution.

4.B.1. Results and Discussion

4B.1.1. Double Reciprocal method

Using the double reciprocal approach presents two main benefits. Firstly there is no need for the physical separation of the aqueous and micellar phases and secondly, prevents changes of the equilibria in solution [110]. The method is based on the UV-spectrophotometric measurement of spectroscopic changes occurring for the studied drugs as a result of drug-NaDC (monomer and micelle) interactions upon the addition of the drug solutions to different NaDC solutions. These were prepared in a concentration range of (0.0005-0.0095 M) followed by incubation of the resulting solutions in the dark at 25 ^{o}C for 12 hours. The drug solutions were prepared at minimal concentrations to ensure that no self-micellisation of drugs took place.

The double reciprocal method was used in the calculation of partition coefficients of different compounds by fitting the following equation (Eq.(40)) to the experimental data [110].

$$(A_w - A_i)^{-1} = (A_w - A_m)^{-1} + \frac{1}{(A_w - A_m)K_p}\,[S_m]^{-1} \qquad \text{Eq. (40)}$$

Where:

A_i: Sum of absorbencies due to free and micelle bound forms of a drug.

A_w: The absorbance of the free form of a drug.

A_m: The absorbance of the micelle bound form of a drug.

K_p: Partition coefficient of the drug.

$[S_m]$: Micellar concentration which is equal to S_T – CMC (S_T: total concentration of a drug, CMC: critical micelle concentration of the surfactant used).

From the slope and intercept of the plots of $(A_w\text{-}A_i)^{-1}$ against $[S_m]^{-1}$ (Figures 162-166), Tables 104-108), partition coefficient (log K_p) was calculated where log K_p=log (intercept/slope).

According to this method, there was no change in the wavelength of maximum absorption of the studied drugs at NaDC concentrations higher than the CMC. However, the observed absorbance (A_i) was found to decrease as the bile salt concentration increased. At NaDC concentrations below the CMC, values of (A_i) were found to increase with the increase in NaDC concentration until reaching the CMC. This was found to take place for dihydroxy bile salts (NaDC) while no change in the value of A_i occurred for trihydroxy bile salts and was equal to that observed in the absence of bile salt. As a result, in this work using NaDC as a bile salt, the value of A_w used in Equation 40 was not the value of absorbance observed in the absence of NaDC but the value observed at the CMC. Therefore, the technique provided compensation for any alterations in the molar extinction coefficients (ε) because of the formed (1:1) complexes of drug/bile salt monomer therefore confirming that further alterations in ε above the CMC were related to effects resulting from incorporation or aggregation of drug in to the micelles.

Table 104: $[S_m]^{-1}$ and $(A_w\text{-}A_i)^{-1}$ values for amitriptyline.

$[S_m]^{-1}$	$(A_w\text{-}A_i)^{-1}$
500	7.605
400	7.458
333.3333	7.163
222.2222	6.400

Table 105: $[S_m]^{-1}$ and $(A_w\text{-}A_i)^{-1}$ values for phenylbutazone.

$[S_m]^{-1}$	$(A_w\text{-}A_i)^{-1}$
1000	25.158
500	18.848
400	15.947
333.3333	15.185
222.2222	15.150

Table 106: $[S_m]^{-1}$ and $(A_w\text{-}A_i)^{-1}$ values for lidocaine.

$[S_m]^{-1}$	$(A_w\text{-}A_i)^{-1}$
500	45.539
400	28.159
333.3333	26.208
222.2222	15.224

Table 107: $[S_m]^{-1}$ and $(A_w\text{-}A_i)^{-1}$ values for salicylic acid.

$[S_m]^{-1}$	$(A_w\text{-}A_i)^{-1}$
500	200.759
400	110.021
333.3333	85.149
222.2222	68.421

Table 108: $[S_m]^{-1}$ and $(A_w\text{-}A_i)^{-1}$ values for theophylline.

$[S_m]^{-1}$	$(A_w\text{-}A_i)^{-1}$
1000	148.152
500	59.769
400	48.214
333.3333	44.701
222.2222	68.421

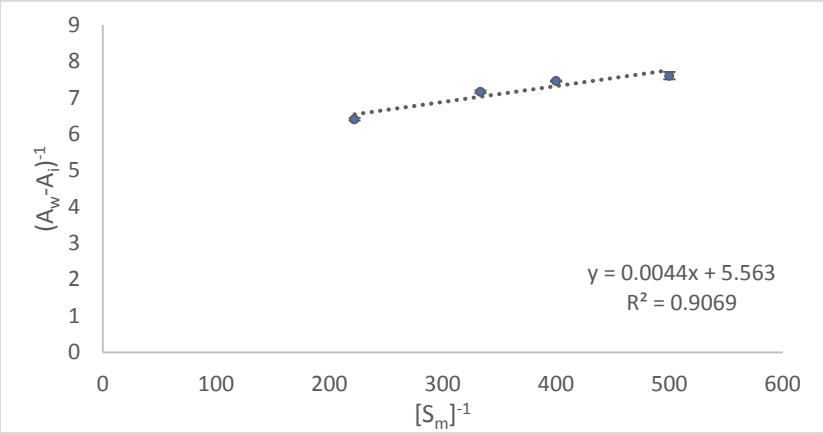

Figure 162: Double reciprocal plot for determination of K_p of amitriptyline.

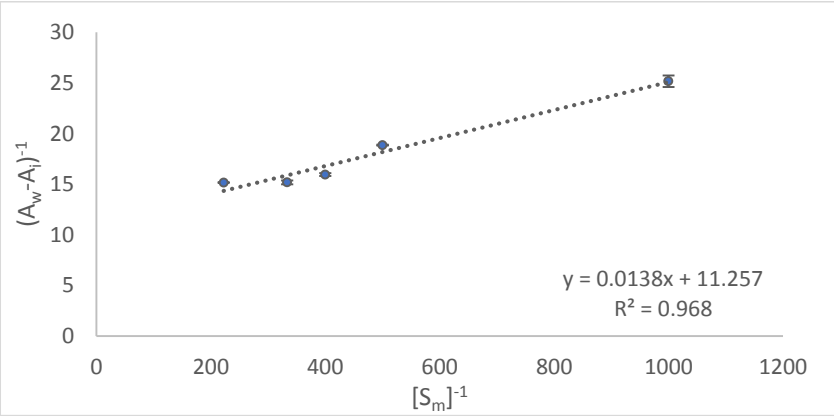

Figure 163: Double reciprocal plot for determination of K_p of phenylbutazone.

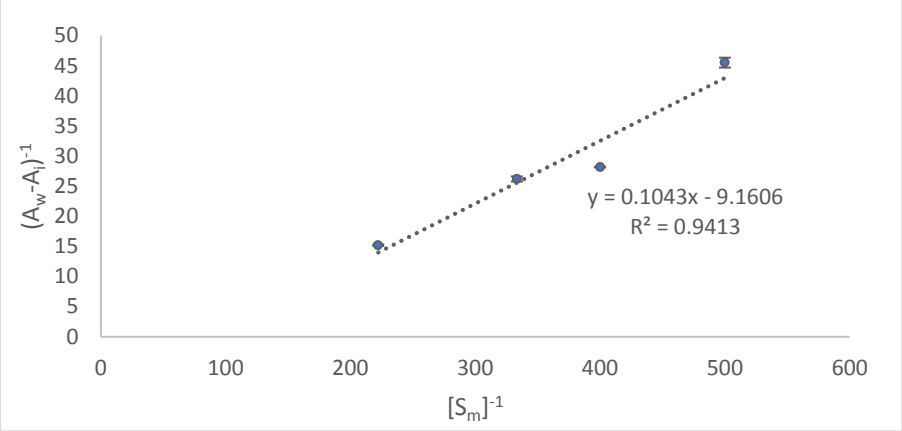

Figure 164: Double reciprocal plot for determination of K_p of lidocaine.

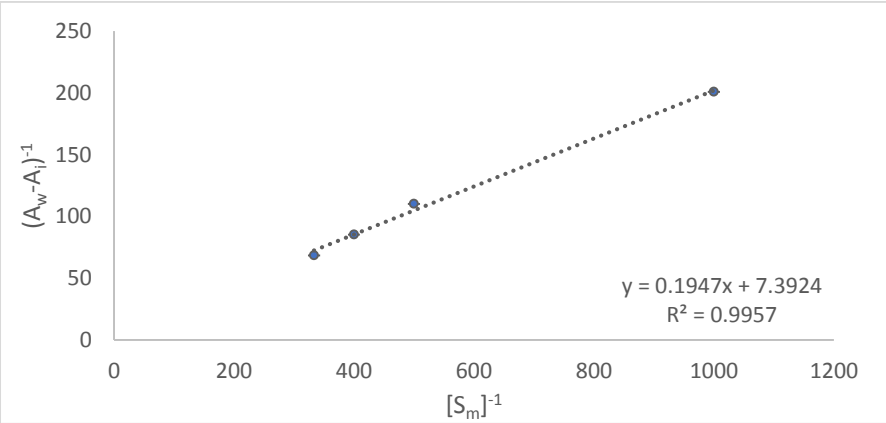

Figure 165: Double reciprocal plot for determination of K_p of salicylic acid.

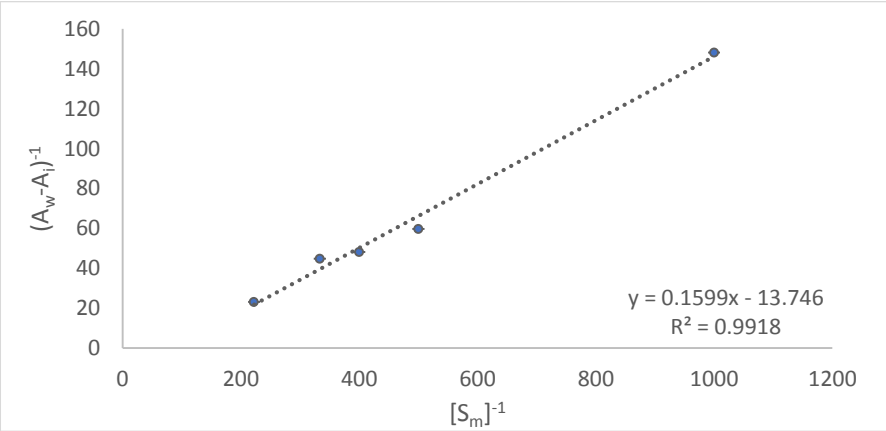

Figure 166: Double reciprocal plot for determination of K_p of theophylline.

Calculated values were considered along with values from the following sections, as summarised in Table 112. Overall, log K_p for most of the compounds was on the same order of magnitude as log $P_{o/w}$. However, the log K_p values of lipophilic compounds with a log $P_{o/w}$ in the range of 4.92-2.26, i.e. amitriptyline, propranolol, phenylbutazone, fenoprofen, piroxicam, carbamazepine, lidocaine, salicylic acid were found to increase with the increase in their log $P_{o/w}$ values. Conversely, some anionic lipophilic compounds of relatively high log $P_{o/w}$ (gemfibrozil, indomethacin, ibuprofen, diclofenac, meloxicam, ketoprofen, flurbiprofen and alprenolol) were found to have lower than expected log K_p values which could be attributed to strong repulsion forces between the negatively charged drug molecules and the negatively charged NaDC molecules. Diphenhydramine (a lipophilic compound) with a log $P_{o/w}$ value of 3.27 had a lower than expected log K_p value that might be attributed to the formation of stable (1:1) complexes with NaDC monomers by hydrophobic association and electrostatic attraction between the positively charged diphenhydramine molecules and the negatively charged NaDC monomers. The formed complex could be slowly breaking with the increase in NaDC concentration above the CMC. Generally, the log K_p of polar/hydrophilic compounds (theophylline, benzoic acid, cimetidine, fluconazole) was lower than that of lipophilic compounds. Moreover, some neutral poplar compounds had higher than expected log K_p values due to their low molecular weight (151.2, 123.1, 194.2 g/mol) for acetaminophen, nicotinic acid and caffeine respectively.

4.B.2. Statistical Modelling

A number of molecular descriptors such as molecular weight (Mwt), polar surface area (PSA), freely rotating bonds (FRB), molar volume (V_M), dissociation constant (pK_a), aqueous solubility (S_w), number of hydrogen bond donors (nHD) and number of hydrogen bond acceptors (nHA) were collected from literature and used alongside experimentally determined log K_p for the statistical modelling of human intestinal absorption (HIA) and permeability coefficients obtained by (PAMPA and Caco-2) *in vitro* methods.

4.B.2.1. Statistical Modelling of Human Intestinal absorption (HIA)

Experimentally obtained log K_p values, along with other molecular descriptors, were statistically analysed against the reported %HIA values to give a model for prediction of %HIA using multiple linear regression. Experimentally determined log K_p of the

studied compounds with their reported experimental values of %HIA are listed in Table 109.

The model obtained for the prediction of %HIA is shown in Equation 41:

$$\%HIA = 92.15 + 0.2295\ PSA - 5.88 \log K_p \qquad \text{Eq. (41)}$$

Sixteen drugs were used in the development of the final model. The model's $R^2 = 74.77$ %, $R^2_{adjust.} = 70.89$ % , $R^2_{PRED} = 61.90$ %, S= 2.413

A 95 % confidence interval for log K_p is given by (-9.91, -1.855), t-statistic and standardised coefficient of log K_p are -3.16 ($p<0.05$) and -0.455 respectively suggesting statistical significance of log K_p as a predictor. Also the F-ratio of the overall model is statistically significant, F= 19.28 and P value 0.000 ($p<0.05$). Absence of autocorrelation in the current regression model was proved by a Durbin- Watson statistic value of 2.062. Figure 167 shows no marked relationship between residuals and predicted values while Figure 168 summarises the model.

As shown in Table 109, eight compounds were used to test the model. The model was able to predict six of these within a range of 0.2 % - 8.36 % difference between their reported and predicted %HIA. However, two of the validation drugs were over predicted by the model (diphenhydramine and meloxicam) suggesting that the model is over predicting compounds where %HIA < 77 % or > 97 % which could be a limitation for the obtained model. A plot of literature %HIA values against the predicted values by the obtained model is shown in Figure 169.

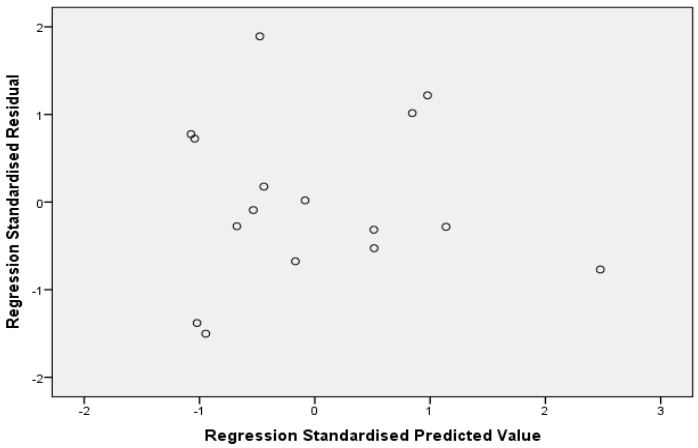

Figure 167: Residual plot for optimal %HIA regression model.

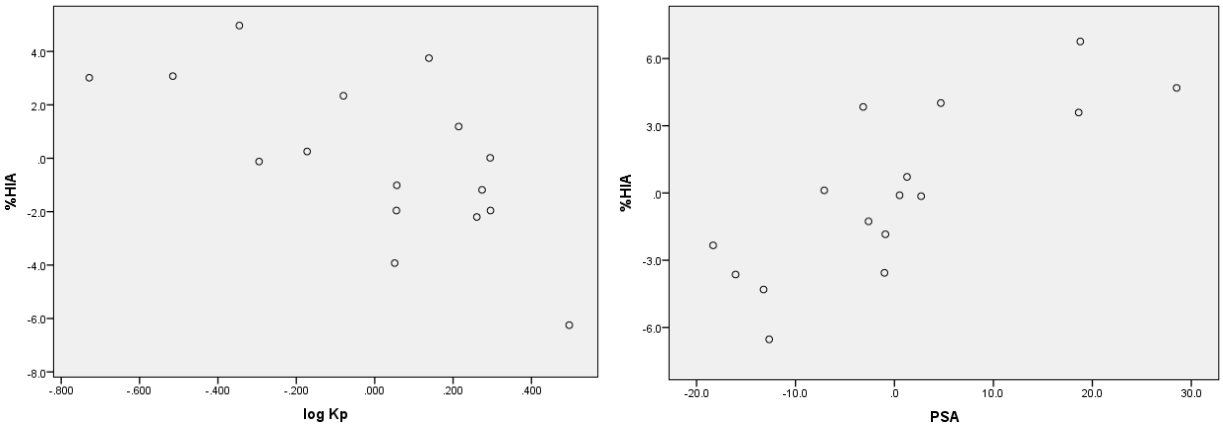

Figure 168: Partial regression plots of experimental %HIA values against log K_p and PSA.

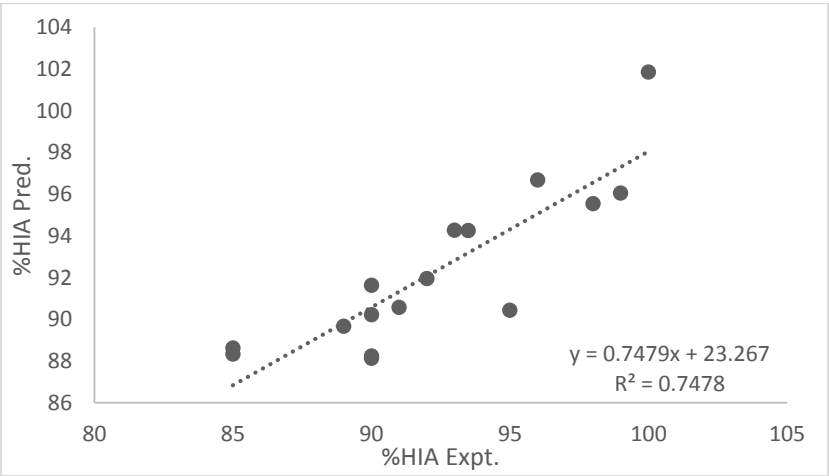

Figure 169: Regression plot of predicted %HIA values against literature %HIA.

Table 109: Experimental partition coefficient (log K_p), predicted %HIA (%$HIA_{pred.}$) and experimentally determined published literature %HIA (%$HIA_{Expt.}$) values for the compounds analysed including eight validation compounds (*).

Drug	%HIA Expt.	%HIA Pred.
Acetaminophen	90.00[205]	90.22
Acetylsalicylic acid*	95.00[33, 208]	94.80
Alprenolol	93.00[205]	94.27
Amitriptyline*	77.50[62, 210]	74.64
Caffeine*	99.00[230]	92.70
Carbamazepine	89.00[63, 67, 280]	89.67
Cimetidine*	100.00[246]	108.36
Diclofenac	90.00[210]	91.63
Diphenhydramine*	72.00[205]	90.35
Fenoprofen	85.00[206]	88.33
Fluconazole	100.00[205]	101.86
Flurbiprofen	92.00[247]	91.95
Gemfibrozil	95.00[207]	90.44
Ibuprofen	85.00[207]	88.62
Indomethacin	98.00[245]	95.55
Ketoprofen	93.50[63, 210, 280]	94.26
Lidocaine	90.00[210]	88.13
Meloxicam*	97.00[207]	111.74
Nicotinic acid	91.00[230]	90.57
Phenylbutazone*	90.00[245]	84.34
Piroxicam*	99.00[252]	103.52
Propranolol	90.00[205]	88.25
Salicylic acid	99.00[247]	96.06
Theophylline	96.00[231]	96.68

4.B.2.2. Modelling of permeability coefficients obtained from PAMPA

The model obtained for the prediction of PAMPA log P_o is shown in Equation 42:

$$\log P_o = 3.29 - 1.015\ HD - 1.98 \log K_p - 0.2091\ S_w \qquad \text{Eq. (42)}$$

Seventeen drugs were used in the development of the final model. The model's R^2 = 74.19 %, $R^2_{adjust.}$= 68.66 % , R^2_{PRED} = 55.11 %, S= 0.999

A 95 % confidence interval for log K_p is given by (-3.562, -0.399), t-statistic and standardised coefficient of log K_p are -2.69 ($p<0.05$) and -0.403 respectively suggesting statistical significance of log K_p as a predictor. Also the F-ratio of the overall model is statistically significant, F= 13.41 and P value 0.000 ($p<0.05$).

The close agreement of the values of $R^2_{adjust.}$ & R^2_{PRED} indicates that the model does not over-fit the data. The residual analysis did not detect any relationship between residuals and predicted values as shown in Figure 170. The model is shown in Figure 171. Experimental and predicted values of PAMPA permeability coefficients are given in Table 110. Also, the plot of these experimental values against their corresponding predicted values is shown in Figure 172.

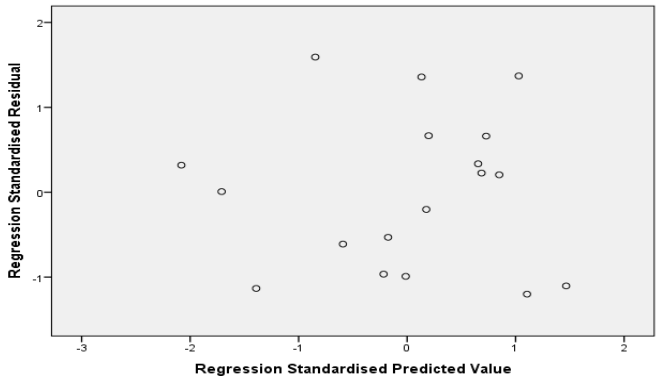

Figure 170: Residual plot for optimal PAMPA regression model.

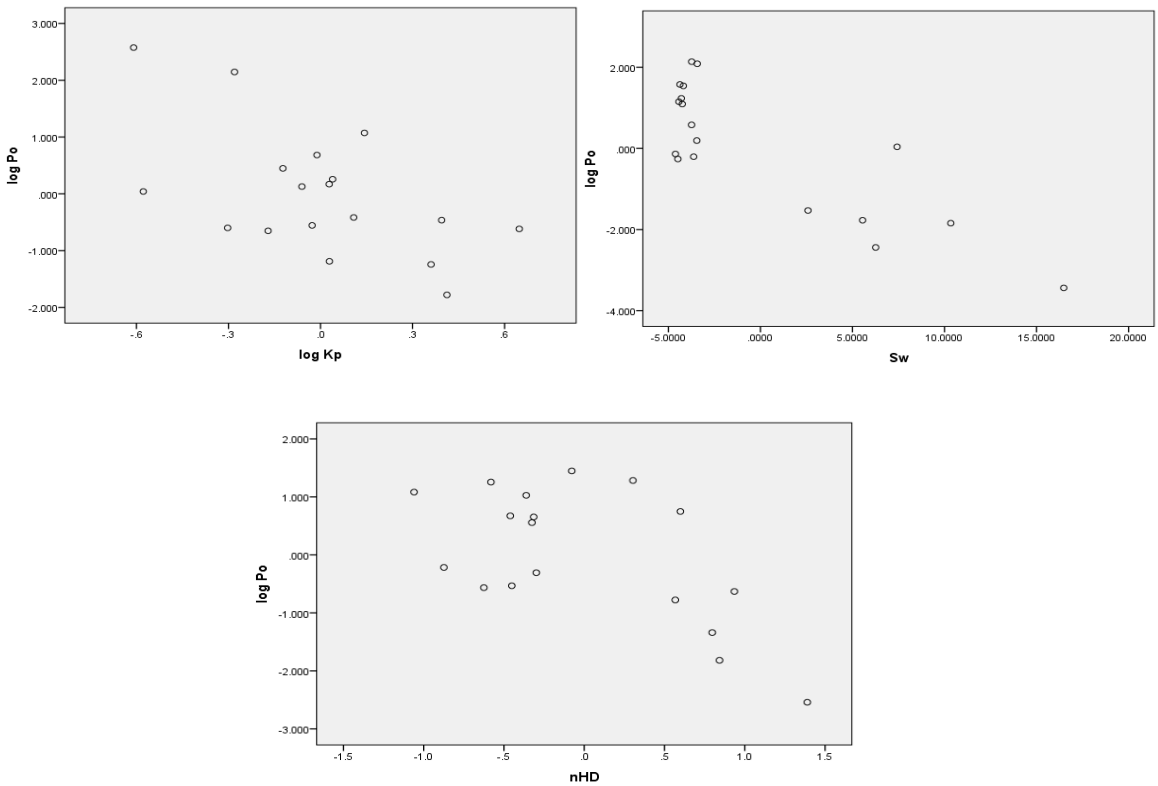

Figure 171: Partial regression plots of experimental PAMPA log P_o values against log K_p, S_w and HD.

Table 110: Experimental and predicted values for PAMPA logP_o.

Drug	Expt. PAMPA log P_o[215]	Pred. PAMPA log P_o
Acetaminophen	-5.81	-6.13
Acetylsalicylic acid	-4.45	-3.84
Alprenolol	0.02	-1.35
Benzoic acid	-3.94	-2.95
Caffeine	-5.55	-5.56
Carbamazepine	-3.73	-3.20
Cimetidine	-6.20	-5.07
Diclofenac	-1.37	-2.73
Flurbiprofen	-1.78	-0.68
Gemfibrozil	-1.59	-1.92
Ibuprofen	-1.15[64]	-1.81
Indomethacin	-1.65	-1.88
Ketoprofen	-2.43[64]	-1.23
Lidocaine	-1.42	-1.63
Meloxicam	-2.86	-2.66
Phenylbutazone	-1.96	-2.63
Piroxicam	-4.23[281]	-3.27
Salicylic acid	-2.64	-4.23

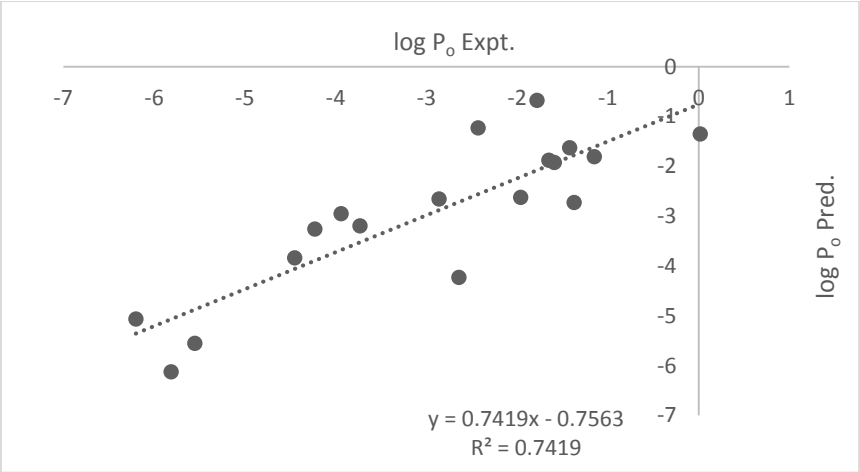

Figure 172: Plot of experimental vs. predicted log P_o values.

4.B.2.3. Modelling of permeability coefficients obtained from Caco-2 $P_{eff.}$

The model obtained for the prediction of Caco-2 $P_{eff.}$ is shown in Equation 43:

$$\log P_{eff.} = -5.301 + 0.3585 \log K_p + 0.003155\, V_M - 0.002148\, Mwt \qquad \text{Eq. (43)}$$

Seventeen drugs were used in the development of the final model. The model's R^2 = 85.27 %, $R^2_{adjust.}$= 81.25 % , R^2_{PRED} = 74.11 %, S= 0.059

A 95 % confidence interval for log K_p is given by (0.218, 0.499), t-statistic and standardised coefficient of log K_p are 5.62 ($p<0.05$) and 0.657 respectively suggesting

statistical significance of log K_p as a predictor. Also the F-ratio of the overall model is statistically significant, F=21.23 and P value 0.000 ($p<0.05$).

Figure 173 shows no marked relationship between residuals and predicted values while Figure 174 summarises the model. As shown in Table 111, two compounds were used to test the obtained model. The model was able to successfully predict Caco-2 log $P_{eff.}$ of the test compounds. Figure 175 shows a plot of literature values of Caco-2 permeability coefficients against their corresponding predicted values obtained by the model.

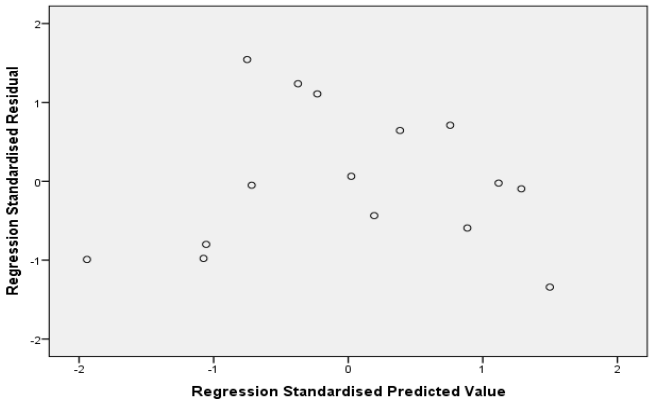

Figure 173: Residual plot for optimal Caco-2 regression model.

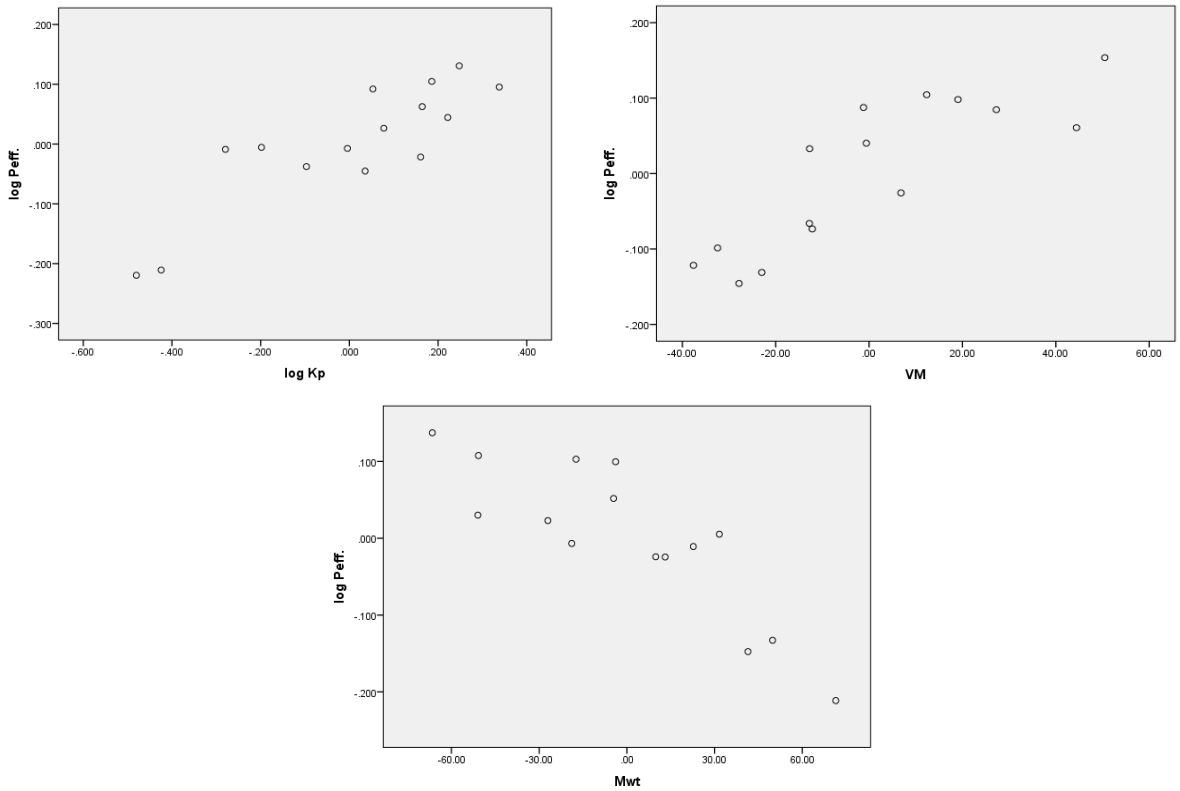

Figure 174: Partial regression plots of experimental Caco-2 log $P_{eff.}$ values against log K_p, V_M and Mwt.

Table 111: Experimental and predicted values for Caco-2 log $P_{eff.}$.

Drug	$logP_{eff.}$ Expt.	$logP_{eff.}$ Pred.
Acetaminophen	-4.44[56]	-4.41
Caffeine	-4.51[63]	-4.51
Carbamazepine	-4.38[56]	-4.42
Cimetidine	-4.52[249]	-4.61
Diclofenac	-4.491[56, 246]	-4.56
Fenoprofen*	-4.95[230]	-4.29
Fluconazole	-4.82[56]	-4.76
Flurbiprofen	-4.70[230]	-4.65
Gemfibrozil	-4.41[246]	-4.33
Ibuprofen	-4.38[246]	-4.38
Indomethacin	-4.43[246]	-4.47
Ketoprofen	-4.48[56]	-4.55
Lidocaine	-4.36[56]	-4.35
Meloxicam	-4.71[56]	-4.65
Phenylbutazone*	-5.00[250]	-4.09
Piroxicam	-4.52[246]	-4.49
Theophylline	-4.61[56]	-4.61

The asterisk (*) indicates the validation compounds.

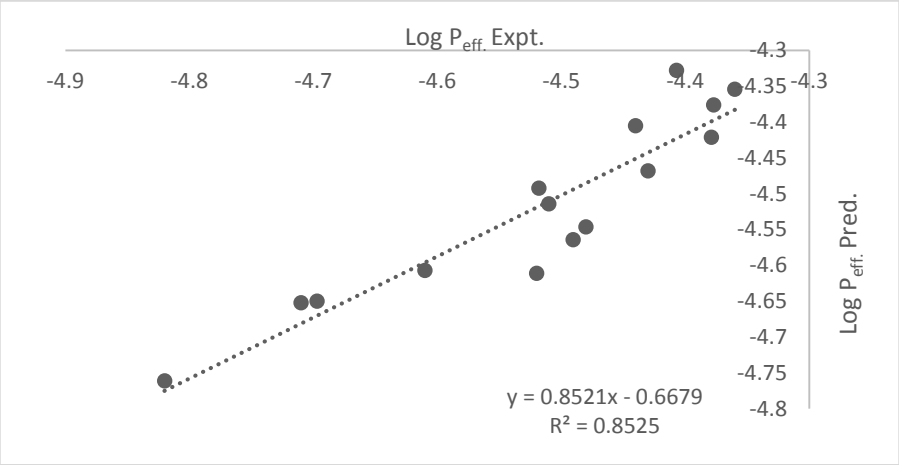

Figure 175: Plot of experimental vs predicted Caco-2 log $P_{eff.}$ values.

Table 112: A summary of molecular descriptors for the selected drugs analysed by double reciprocal method and the reported experimental values of %HIA and permeability coefficients of PAMPA and Caco-2 tests.

Drug	Log K_p	Log $P_{o/w}$[184]	Mwt[218]	pK_a [184]	S_w [184]	HD[218]	HA[218]	FRB[218]	PSA[219]	V_M[218]	log P_o[215]	Log $P_{eff.}$	%HIA
Acetaminophen	2.25	0.46	151.20	9.38	14	2	3	1	49.3	131.1	-5.81	-4.44[56]	90.00[205]
Acetylsalicylic acid	2.03	1.19	180.15	3.49	10[219]	1	4	3	63.6	139.6	-4.45	NI	95.00[33, 208]
Alprenolol	1.26	3.1	249.35	9[279]	0.547	2	3	8	41.5	247.5	0.02	NI	93.00[205]
Amitriptyline	3.10	4.92	277.40	9.4	0.00971	0	1	3	3.2	257.8	NI	NI	77.50[62, 210]
Benzoic acid	1.89	1.87	122.12	4.19	7.08	1	2	1	37.3	102.0	-3.94	NI	NI
Caffeine	2.19	-0.07	194.20	14[222]	21.6	0	6	0	58.4	133.4	-5.55	-4.51[63]	99.00[230]
Carbamazepine	2.23	2.45	236.36	13.9	0.21[184, 282]	2	3	0	46.3	186.6	-3.73	-4.379[56]	89.00[63, 67, 280]
Cimetidine	1.69	0.4	252.34	6.8	9.38	3	6	8	114	198.2	-6.2	-4.52[249]	100.00[246]
Diclofenac	2.01	4.51	296.20	4.15	0.00237	2	3	4	49.3	206.8	-1.37	-4.4905[56, 246]	90.00[210]
Diphenhydramine	0.79	3.27	255.36	8.98	3.06	0	2	6	12.5	249.2	NI	NI	72.00[205]
Fenoprofen	2.46	3.1	242.27	4.5	0.033[218]	1	3	4	46.5	204.7	NI	-4.947[230]	85.00[206]
Fluconazole	1.53	0.4	306.27	12.71	9[283]	1	7	5	81.6	205.3	NI	-4.82[56]	100.00[205]
Flurbiprofen	1.49	4.16	244.26	4.42	0.008	1	2	3	37.3	203.6	-1.78	-4.697[230]	92.00[247]
Gemfibrozil	2.11	3.4	250.33	4.5[219]	0.13[284]	1	3	6	46.5	239.7	-1.59	-4.407[246]	95.00[207]
Ibuprofen	2.06	3.97	206.30	4.91	0.0684	1	2	4	37.3	200.3	-1.15[64]	-4.377[246]	85.00[207]
Indomethacin	2.10	4.27	357.79	4.5	0.000937	1	5	4	68.5	269.6	-1.65	-4.430[246]	98.00[245]
Ketoprofen	1.76	3.12	254.30	4.45	0.051	1	3	4	54.4	212.2	-2.43[64]	-4.48[56]	93.50[63, 210, 280]
Lidocaine	1.94	2.44	234.40	8.01	0.2337[285]	1	3	5	32.3	238.8	-1.42	-4.36[56]	90.00[210]
Meloxicam	1.98	3.43	351.40	4.08	0.00715	2	7	2	136	220.3	-2.86	-4.71[56]	97.00[207]
Nicotinic acid	2.23	0.36	123.11	4.75	83.1	1	3	1	50.2	95.2	NI	NI	91.00[205, 230]
Phenylbutazone	2.91	3.16	308.37	4.5	0.7[219]	0	4	5	40.6	262.8	-1.96	-4.998[250]	90.00[245]
Piroxicam	2.28	3.06	331.35	6.3	0.023	2	7	2	108	222.8	-4.227[281]	-4.518[246]	99.00[252]
Propranolol	2.28	3.48	259.34	9.42	0.0617	2	3	6	41.5	237.2	NI	NI	90.00[205]
Salicylic acid	1.58	2.26	138.12	2.97	11.3	2	3	1	57.5	100.4	-2.64	NI	99.00[247]
Theophylline	1.93	-0.02	180.16	8.81	22.9	1	6	0	69.3	122.9	NI	-4.61[56]	96.00[231]

NI: value not included in training set.

4.B.3. Conclusion

In summary, the double reciprocal method is considered to be a simple, rapid and cost effective method for the determination of partition coefficients that could be used in the prediction of human intestinal absorption if may be more compounds were included in the model development. Also the models obtained from the partition coefficients calculated by this method were found to be good for prediction of the Caco-2 permeability coefficient and to a lesser extent predictive for PAMPA permeability coefficients. However, the main finding from this work is that the double reciprocal method can be considered a suitable *in vitro* system for predicting *in vivo* intestinal absorption.

CHAPTER 5

Predicting Human Intestinal Absorption Using bile salt hydrogels

Chapter 5: Predicting Human Intestinal Absorption Using bile salt hydrogels

5. Introduction

A branch of smart chemistry is supramolecular self-assembly which is concerned with chemical systems formed from a distinct number of assembled molecular subunits. Developing self-assembling small molecular hydrogels is considered an important example of supramolecular self-assembly which has been given significant attention by soft-material research because of their possible applications in a wide variety of fields such as drug delivery, pharmaceutical formulations, biomaterials, cosmetics and sensors.

Hydrogels consisting of biocompatible fragments including cholic acid derivatives, amino acid derivatives, peptides and carbohydrate systems have received special attention because they can be safely used in biomedical applications. One group of cholic acid derivatives are bile salts which are biosurfactants possessing an amphiphilic structure with steroidal backbone, a unique structure that distinguishes this class of surfactants from conventional synthetic surfactants. As a result of this unique structure, bile salts are known to self-assemble giving aggregates with characteristic properties having important biological functions such as cholesterol solubilisation, absorption of dietary fat and fat soluble vitamins in addition to removal of fatty acids resulting from pancreatic hydrolysis. There has been a growing interest in studying the physiological importance of bile salts reflected in a greater number of recent publications. It was found that certain bile salts such as NaDC, were able to self-assemble into gels in water which is a process that was found to be driven by the balance of van der Waals forces, H-bonding, hydrophobic interaction and steric effect. The hydrogels formed by bile salts are extremely different from polymeric gels which are basically formed as a result of chemical cross-linking. Bile salt hydrogels are formed through a network of intertwined fibrils developed by massive cycles of bile salt molecules brought together by noncovalent interactions particularly the H-bonds. NaCl is considered to have a pronounced influence on promoting the gelation of NaDC solutions forming supramolecular hydrogels with superior gelation capability and mechanical force due to the small radius of hydration of the ions of NaCl [286, 287].

Both the sodium and the chloride ions are believed to play an important role in the formation of the hydrogels by decreasing the electrostatic repulsion between the polar heads of NaDC molecules therefore contributing to the compression of the thickness of the electric double layer. Sodium ions form weak coordination bonds with carboxylate groups, stimulating connection of the polar head of carboxyl groups via H-bonding. This leads to the formation of a more regular crystalline interface thus shifting the growth of aggregates along one direction towards fibrous aggregate formation. Furthermore, the chloride ions play a role in the hydrogel formation as well as the weak electrostatic interaction which is thought to exist between the sodium salt anion (chloride ions) and the α-methylene attached to the carboxylate group of NaDC, as it is changed to a weak positive charge by the presence of cations [286]. NaDC solutions were reported to give highly viscous gels by the formation of polymer-like aggregates at pH values less than 7.8 but not above 8 [287, 288]. Figure 176 shows a schematic representation of the formed salt-induced NaDC gels.

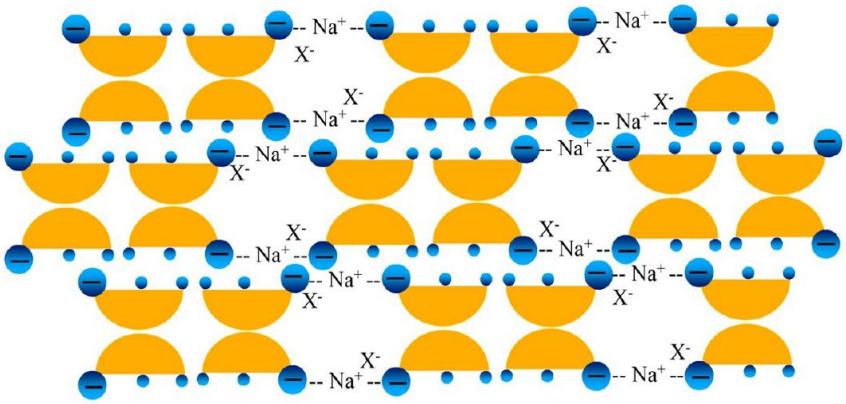

Figure 176: Schematic representation of the formed salt-induced NaDC gels.(reference [286])

Concept of the work

This work investigated bile salt based hydrogels as a permeation membrane by analysing drug permeation for a set of compounds. All experiments used a drug saturated hydrogel. Such a procedure was adopted to ensure uniform distribution of the drug within the gel thus, uniform permeation from all areas of the gel. The synthesised hydrogel was then used as a synthetic membrane in Franz diffusion cells and flow through cells, with completely permeable dialysis membrane used only as support for the gel to rest on, to determine the permeability coefficient (K_p) of the studied drugs. This was then statistically analysed for developing models for prediction

of human intestinal absorption and other *in vitro* permeability coefficients obtained from PAMPA and Caco-2 methods.

Diffusion cells

Diffusion cells have been one of the popular methods used in prediction of permeation of drugs and chemicals across the skin. They can be static, for example Franz cells or continuous flow (flow through) cells, both having acceptor and receiver compartments with a membrane placed in between and a water jacket surrounding them set at 37 ^{o}C.

A comparison of the two types of diffusion cells is summarised in Table 113.

Table 113: A comparison of the two types of diffusion cells.

Flow through cell	Franz cell
Sink conditions are maintained over the whole experiment period by the stirring resulting from the turbulence effect caused by the continuous flow of solvent to the receiver cell against the membrane lower surface. The flow carries the permeated drug to be collected as samples at predetermined time intervals [289].	Sink conditions are maintained by stirring of the receptor chamber fluid with a magnetic stirrer [289].
Receiver chamber size must be small (e.g. 0.5 mL) to allow complete and rapid flushing of the sample out during its collection [290].	Receiver chamber size is bigger (e.g. 5 mL) to prevent the accumulation of pronounced amounts of the sample inside it as the receiver solution is not being continuously replaced as in case of flow through cells [290, 291].
Samples are collected automatically [289].	Samples are collected manually through the sampling port [289].
More complex therefore more expensive [292].	Cheaper therefore its use is more common than flow through cells [292].

The two types of cells are illustrated in Figure 177.

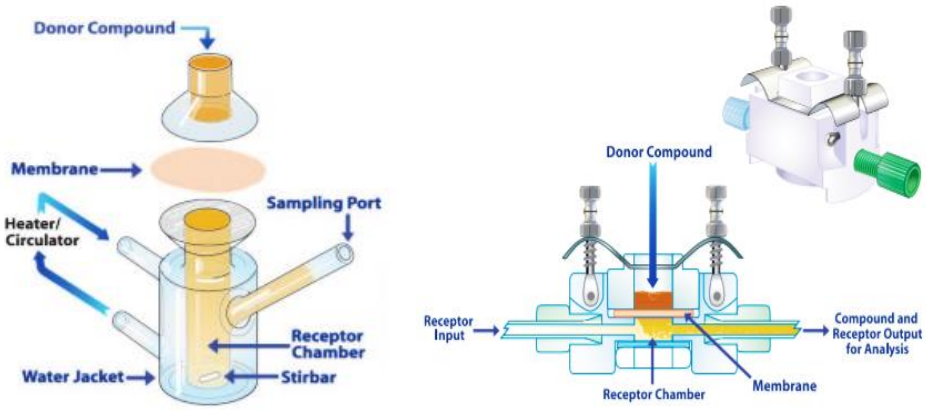

Figure 177: A diagrammatic representation of a static cell (left) and flow through cell (right) (reference [293]).

CHAPTER 5
Section (A)

Predicting Human Intestinal Absorption Using bile salt hydrogels:
"Use of flow through cells in determination of K_p "

Section (A): Use of flow through cells in determination of K_p.

This section involved the use of flow through cells for the study of the permeation of a group of studied drugs through the synthesised drug saturated NaDC hydrogels and determination of K_p. The data was used to evaluate whether the method could be used in the prediction of human intestinal absorption and the permeability coefficients of other *in vitro* methods.

5.A.1. Results and Discussion

5.A.1.1. Permeation study

Since the drug is added to the hydrogel in an infinite (saturated) dose, the permeability coefficient (K_p) can be calculated from the following relationship [293]:

$$K_p = Q/[A\,.\,t.\,(C_o - C_i)] \quad \text{Eq. (44)}$$

Where:

Q: the quantity of drug transported through the hydrogel in time t in (min).

C_o: the concentration of the drug in the donor chamber.

C_i: is the concentration of the drug in the receptor chamber.

A: the area of the exposed hydrogel in cm^2 which is 0.552 cm^2 in this work.

Since the drug was applied to the hydrogel in an infinite dose therefore C_i can be simplified to zero. K_p, which is defined as the permeant penetration rate per unit concentration is given in cm/min.

In this work K_p was first calculated for eight compounds for the determination of the best NaDC concentration to be used for the preparation of membrane-like hydrogel that would be used in the permeation studies of the rest of the compounds for prediction of human intestinal absorption and other *in vitro* permeability coefficients using the obtained K_p.

Table 114: A list of the obtained permeability coefficients (K_p) for eight drugs at different concentrations of NaDC solutions and hydrogels.

Drug	Acetaminophen	Carbamazepine	Fluconazole	Flurbiprofen	Gemfibrozil	Ibuprofen	Lidocaine	Piroxicam
K_p (cm/min)								
50 mM NaDC solution	20.98×10^{-4}	23.49×10^{-4}	25.77×10^{-4}	77.86×10^{-4}	152.25×10^{-4}	164.86×10^{-4}	20.03×10^{-4}	9.79×10^{-4}
70 mM NaDC solution	23.57×10^{-4}	31.69×10^{-4}	25.93×10^{-4}	53.10×10^{-4}	109.91×10^{-4}	282.34×10^{-4}	20.41×10^{-4}	10.48×10^{-4}
100 mM NaDC solution	18.10×10^{-4}	25.90×10^{-4}	19.89×10^{-4}	115.27×10^{-4}	194.43×10^{-4}	198.55×10^{-4}	15.1×10^{-4}	47.57×10^{-4}
K_p in different NaDC hydrogel								
50 mM NaDC hydrogel	29.10×10^{-4}	30.09×10^{-4}	0.87×10^{-4}	9.98×10^{-4}	8.42×10^{-4}	12.32×10^{-4}	6.20×10^{-4}	7.35×10^{-4}
60 mM NaDC hydrogel	20.59×10^{-4}	16.94×10^{-4}	7.00×10^{-4}	9.72×10^{-4}	7.96×10^{-4}	12.22×10^{-4}	11.78×10^{-4}	7.73×10^{-4}
70 mM NaDC hydrogel	36.58×10^{-4}	40.17×10^{-4}	15.93×10^{-4}	13.54×10^{-4}	8.65×10^{-4}	13.21×10^{-4}	17.57×10^{-4}	7.99×10^{-4}
80 mM NaDC hydrogel	20.97×10^{-4}	17.98×10^{-4}	12.45×10^{-4}	5.76×10^{-4}	7.37×10^{-4}	9.45×10^{-4}	16.01×10^{-4}	8.01×10^{-4}
100 mM NaDC hydrogel	23.82×10^{-4}	33.17×10^{-4}	2.74×10^{-4}	5.20×10^{-4}	8.24×10^{-4}	9.83×10^{-4}	2.82×10^{-4}	7.11×10^{-4}
K_p in zero mM NaDC (buffer only) i.e. 0 mM NaDC	29.14×10^{-4}	75.32×10^{-4}	32.22×10^{-4}	37.67×10^{-4}	27.75×10^{-4}	22.21×10^{-4}	16.96×10^{-4}	26.65×10^{-4}

Looking at Table 114, it can be seen that K_p values of neutral drugs (acetaminophen and fluconazole) with low lipophilicity were about 1.5 times higher in buffer pH 7.4 (no NaDC) than that in NaDC aqueous solutions. Also the K_p values of the neutral drug, carbamazepine, of relatively higher lipohiphilicity was about 3 times higher in buffer pH 7.4 than in NaDC aqueous solutions. Therefore, it can be concluded that the presence of neutral drugs in NaDC aqueous solution hinders their rate of permeation as the K_p obtained in these solutions were found to be 1.5 to 3 times less than the K_p obtained as a result of the permeation of these drugs from their buffered aqueous solutions free from NaDC. This could be attributed to the binding of these drugs to the NaDC micelles or their inclusion inside these micelles. On the other hand, three ionisable compounds (flurbiprofen, gemfibrozil and ibuprofen) showed lower values of K_p in buffer pH 7.4 than in NaDC aqueous solutions. Since flurbiprofen, gemfibrozil and ibuprofen have similar lipophilicities, pK_a values (4.42, 4.5 and 5.2 respectively) [184, 219, 223] and molecular weights (244.26, 250.33 and 206.3 g/mol respectively) [218], the higher K_p in NaDC aqueous solutions can be attributed to the ionisation of these anionic drugs in the NaDC solutions leading to strong repulsion forces between the negatively charged drugs and the negatively charged NaDC micelles forcing the ionised drug molecules to leave the donor solution to the receiver chamber and subsequently eluting out to be collected. The greatest increase in K_p was observed with ibuprofen as its K_p in NaDC was almost 10 times higher than its K_p in buffer while the K_p of gemfibrozil was almost 5 times higher and that of flurbiprofen was almost 3 times higher, this could be a result of the extent of ionisation being the highest in ibuprofen followed by gemfibrozil and flurbiprofen. Also, ibuprofen has the smallest molecular weight while gemfibrozil and flurbiprofen have higher molecular weights thus ibuprofen was the easiest to leave the donor solution to the receiver chamber after repelling from the NaDC micelles in the donor chamber. On the other hand, piroxicam, which is another anionic drug, showed higher K_p values in NaDC solution than in buffer at higher NaDC concentrations (100 mM) while at lower concentrations of NaDC in solution (50 and 70 mM) K_p was lower than that in buffer which could be due to partial ionisation of the drug (pK_a=6.3) [184] and its high molecular weight (331.35 g/mol) [218] which enables it to overcome repulsion forces with the negatively charged micelles at lower NaDC concentrations therefore staying in the donor solution while at higher NaDC concentration (100 mM) the drug experiences greater repulsion with the micelles forcing it to leave the donor solution to the receiver chamber. The

cationic drug lidocaine had a similar K_p in NaDC solutions and buffer. This could be due to neutralisation of the negatively charged NaDC micelles by the binding of the positively charged ionised lidocaine molecules forming uncharged drug-micelles complexes which can somewhat pass to the receiver chamber.

Comparing the K_p values of all drugs in buffer with those in NaDC hydrogels, it was observed that K_p was always higher in buffer than that in the hydrogels which could be attributed to the entrapment of the drug in the highly viscous gel matrix. Acetaminophen was an exception as its K_p in buffer was almost the same as its K_p in hydrogel. This was because acetaminophen was the only drug with significant aqueous solubility, a low molecular weight (151.2 g/mol) [218] and was the least lipophilic (log $P_{o/w}$ = 0.46) of all the drugs studied [184].

Comparing the K_p values of acetaminophen, carbamazepine, fluconazole, flurbiprofen, gemfibrozil, ibuprofen, lidocaine and piroxicam in NaDC hydrogels and NaDC aqueous solutions at the 3 concentrations (50, 70 and 100 mM) (Figures 178-180), it can be observed that there is a change in the permeation behaviour of almost all drugs at about 70 mM NaDC in solution or hydrogel matrix. The reason for such behaviour is assumed to be because as the NaDC concentration increases, the hydrogel formed becomes more compact. The microstructure of the hydrogel was investigated by SEM examination of a freeze-dried sample of a blank NaDC hydrogel (free from drug) which showed the hydrogel comprised of networks of characteristic thread-like shaped bundles of fibrils entangled and intertwined together with small hollow pockets in between (Figure 185). The microstructure of the NaDC hydrogel, observed by SEM, confirmed the previous assumption. The parabolic behaviour seen for most drugs in hydrogels can therefore be explained. Polar neutral drugs (acetaminophen and fluconazole), are forced to leave the increasingly hydrophobic environment in the donor solution with the increase in the NaDC concentration thus their K_p increases until a certain concentration is reached after which the gel matrix becomes compact enough to force these drugs to stay in the gel matrix in the donor chamber thus decreasing their K_p and creating the parabolic relation between the K_p of these drugs and the NaDC concentration in the hydrogel. Furthermore, carbamazepine which is a neutral lipophilic drug also showed a parabolic behaviour in hydrogel. This parabolic behaviour can be explained based on the increase in the hydrophobic interaction between the drug and the less compact NaDC polymer-like aggregates in the hydrogel as a result of the increase in the NaDC concentration. Also, the lipophilicity of

carbamazepine being the highest among the studied neutral drugs, having a log P value of 2.28 at pH 7.4 [218], makes the drug more capable of binding to the polymer-like aggregates forming highly lipophilic drug-NaDC aggregates which can rapidly cross over to the receiver chamber thus increasing the K_p value up to a certain concentration after which a drop in K_p occurs which is believed to be due to the inclusion of the drug itself in the more compact matrix structure. Then, at a higher concentration (100 mM) allows the drug to permeate out due to the replacement of the lipophilic drug in the matrix with the more lipophilic NaDC molecules which become more abundant at 100 mM causing a steric hindrance in the medium. By the examination of a freeze-dried sample of carbamazepine in 70 mM hydrogel using SEM it was observed that it has the same intertwined network of fibrils as that observed in the blank hydrogel but carbamazepine hydrogel had larger pockets which is consistent with the highest K_p reached at 70 mM thus confirming the theory. This idea assumes that the increase in K_p is attributed to the formation of highly lipophilic complexes of carbamazepine and the loose polymer-like aggregates in the gel matrix structure thus crossing to the receiver chamber while leaving large pockets behind in the gel matrix structure (Figure 186). Similarly, the same behaviour was observed for the neutral drugs (acetaminophen, carbamazepine and fluconazole) in aqueous solutions of NaDC which supports the assumption of polar drugs (acetaminophen and fluconazole) leaving the donor chamber as the hydrophobic environment increases with the increasing NaDC concentration. For these drugs, values of K_p increase until reaching a certain concentration after which the aggregates formed are large in number therefore, keeping the drug in the donor solution and so leading to a drop in K_p. Also carbamazepine showed an increase in K_p with increased NaDC concentration until 70 mM due to the solubilising effect of NaDC on carbamazepine which has poor aqueous solubility and the binding of the lipophilic neutral carbamazepine to NaDC micelles then after 70 mM the number of the formed NaDC aggregates is too large thus blocking the drug molecules passing to the donor chamber. On the other hand, ionisable drugs showed a difference in their permeation behaviour between their NaDC hydrogels and aqueous solutions. The ionisable drugs show a parabolic permeation behaviour in hydrogel except for gemfibrozil and piroxicam which appear to be not significantly affected by the change in the NaDC concentration in hydrogel. The parabolic behaviour for flurbiprofen and ibuprofen can be attributed to the ionisation of these drugs at pH 7.4. These are polar drugs with log P values of 0.68 and 0.45 respectively

[218] thus the drugs are expelled out of the donor to the receiver chamber then after a certain concentration the gel structure becomes too compact so entrapping the drugs inside. As for gemfibrozil, with a log P value of 1.58 at pH 7.4 [218] implies that the drug might have equal preference to aqueous medium and the hydrophobic hydrogel medium so it was not greatly affected by the increase in NaDC concentration in the hydrogel. Although piroxicam in hydrogel was expected to show a significant parabolic behaviour with a log P of 0.46 at pH 7.4 [218], it showed very weak parabolic behaviour suggesting almost no significant effect upon the change in the NaDC concentration in hydrogel. The reason could be that piroxicam has a high molecular weight (331.35 g/mol) [218] and poor aqueous solubility therefore resisting the effect of the low log P value at pH 7.4. An opposite permeation pattern for the two ionisable drugs (flurbiprofen and gemfibrozil) in the NaDC aqueous solutions was observed where they showed an opposite inverted parabolic behaviour where K_p values decreased until a certain concentration after which it started increasing again. This could be due to the ability of the drugs to overcome repulsion forces at lower concentrations of NaDC while at high concentration the ionised drug molecules were expelled out to the receiver chamber due to higher repulsion forces with NaDC micelles. The inverted parabolic permeation pattern in the case of gemfibrozil was found to be more prominent in NaDC aqueous solutions than in the hydrogels because of the drug's equal preference for NaDC polymeric aggregates and aqueous buffer solution. Ibuprofen, has a preference for NaDC micelles due to its lipophilicity (log $P_{o/w}$ = 3.97) [184] but it suffers from repulsion forces with the micelles carrying a negative charge thus forcing the small drug (206.3 g/mol) [218] to leave the donor chamber for the receiver chamber leading to an increase in K_p values until 70 mM of NaDC after which K_p starts decreasing. This could be attributed to the increase in the size of the formed aggregates through which the lipophilic drug can reside, overcoming repulsion forces, thus its K_p decreased. Furthermore, the ionisable drug; lidocaine in NaDC hydrogel showed a parabolic permeation behaviour which can be attributed to the binding of the drug to the NaDC loose polymer-like aggregates and thus permeating out to the receiver chamber. This occurs until reaching a certain NaDC concentration after which the drugs permeation started going down with the increase in the NaDC concentration because of the more compact structure of the NaDC polymer formed at high NaDC concentrations. On the other hand, lidocaine in NaDC aqueous solutions is ionised, carrying a positive charge, which neutralised the negative charge carried by the NaDC

micelles giving a neutral lipophilic drug-micelle complex which crossed easily to the receiver chamber. The permeation of these complexes appears not to be affected by the change in NaDC concentration from 50 and 70 mM to 100 mM, only a slight decrease in K_p at 100 mM was observed which could be due to the increase in size of these complexes. For piroxicam the change in NaDC concentration appears to have no effect on the formation of these complexes at low concentrations of NaDC (50 and 70 mM) but there was a great increase in K_p at 100 mM of NaDC which could be attributed to the high molecular weight of piroxicam (331.35 g/mol) [218], its poor aqueous solubility and partial ionisation. At low NaDC concentrations the drug is able to overcome the repulsion forces and remain in the donor solution while at high concentration the repulsion forces with the micelles become greater forcing it to leave the donor solution for the receiver chamber.

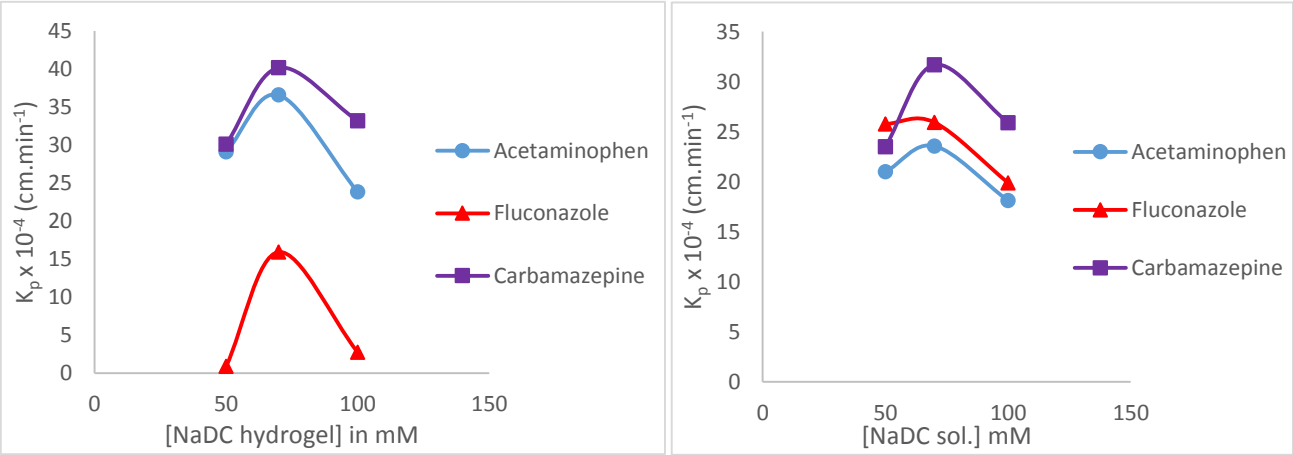

Figure 178: Permeability coefficients (K_p) of acetaminophen, fluconazole and carbamazepine at three different concentrations of NaDC hydrogels (left) and aqueous solutions (right).

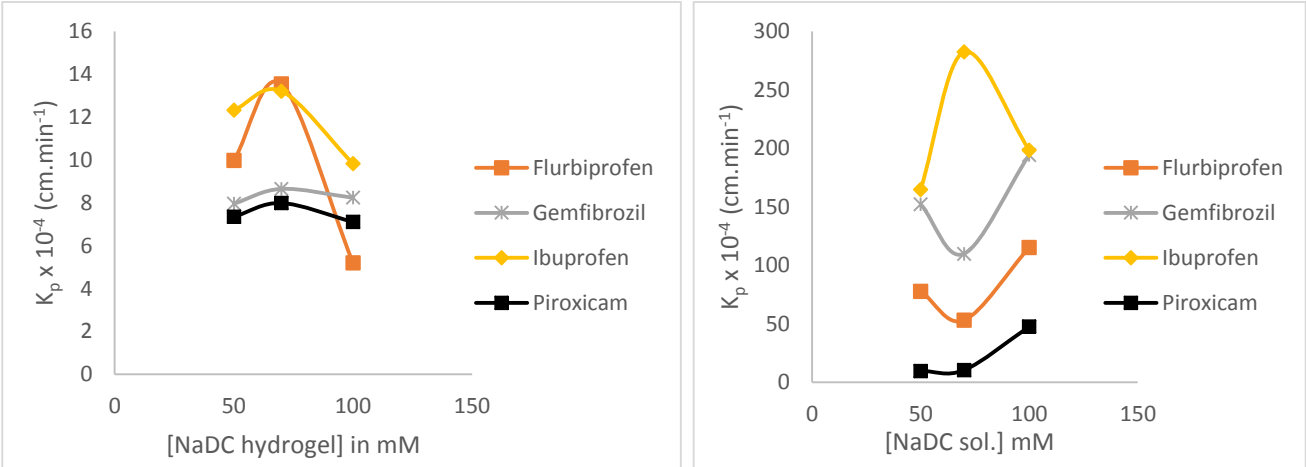

Figure 179: Permeability coefficients (K_p) of flurbiprofen, gemfibrozil, ibuprofen and piroxicam at three different concentrations of NaDC hydrogels (left) and aqueous solutions (right).

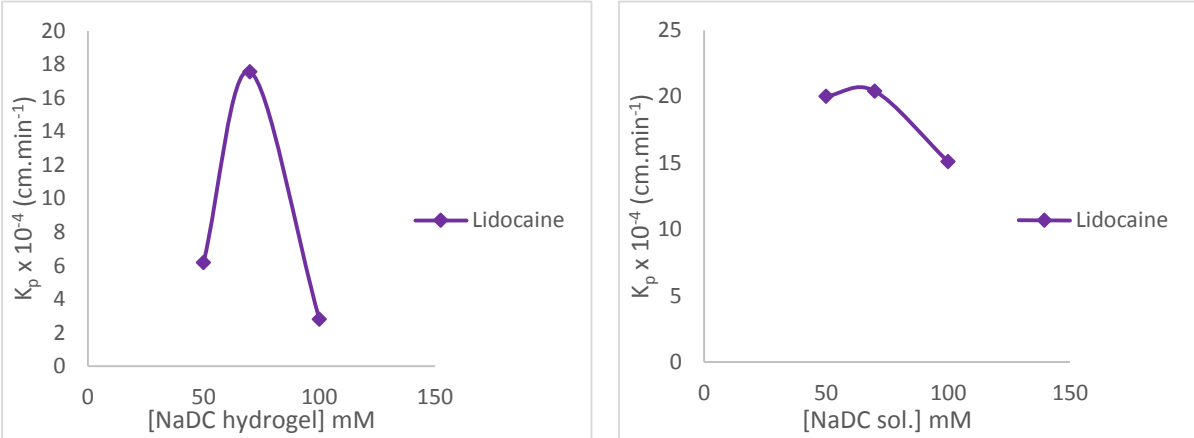

Figure 180: Permeability coefficients (K_p) of lidocaine at different concentrations of NaDC hydrogels (left) and aqueous solutions (right).

More data points were added to the studied NaDC concentration range used for the preparation of the hydrogels and their corresponding K_p values in order to confirm the parabolic permeation behaviour of the drugs under study. The further obtained data as shown in Figures (178-180) confirm the parabolic permeation behaviour of compounds over the studied NaDC increasing concentration range. In the carbamazepine plot, it is observed that the drug's K_p increased again after 80 mM which could be attributed to the lipophilic NaDC micelles bound to carbamazepine and escaping to the receiver chamber due to the increased repulsion between the NaDC micelles with the increase in NaDC concentration.

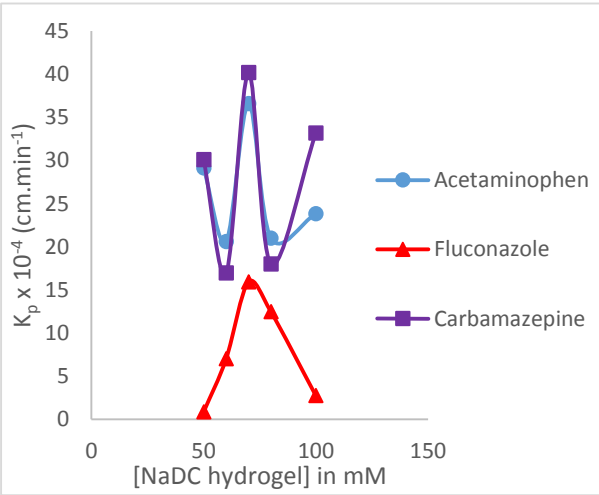

Figure 181: Permeability coefficients (K_p) of acetaminophen, fluconazole and carbamazepine at five different concentrations of NaDC hydrogels.

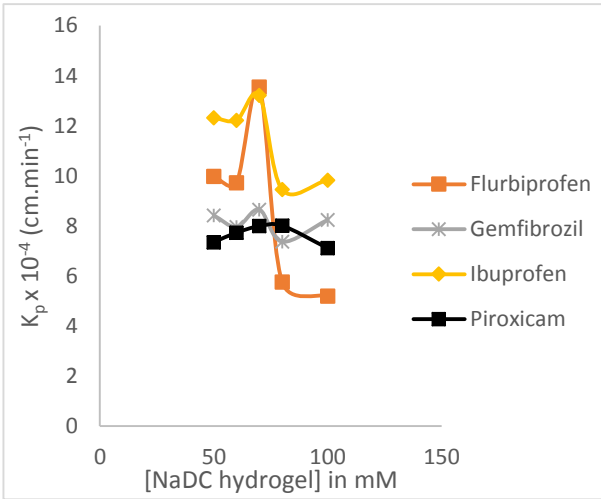

Figure 182: Permeability coefficients (K_p) of flurbiprofen, gemfibrozil, ibuprofen and piroxicam at five different concentrations of NaDC hydrogels.

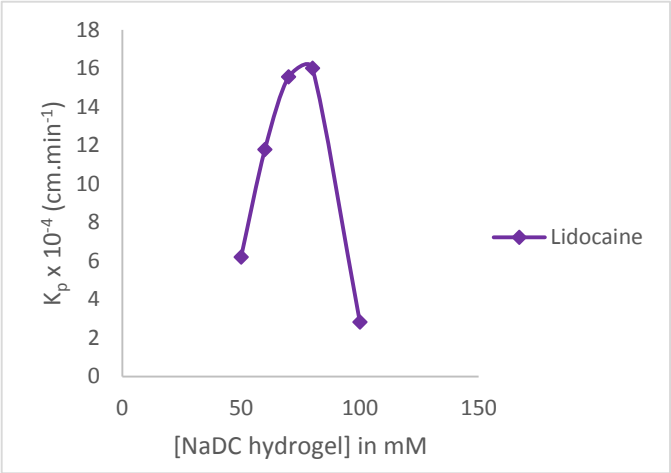

Figure 183: Permeability coefficients (K_p) of lidocaine at five different concentrations of NaDC hydrogels.

As a result of these findings, an NaDC concentration of 70 mM was selected to be used in a permeation study of twenty-five compounds. Calculated K_p values were then used in the statistical modelling of human intestinal absorption and other *in vitro* permeability coefficients. This exact concentration was selected because the highest permeation rate from the hydrogel was obtained at 70 mM for most drugs used. Using Equation (44), the permeability coefficient (K_p) for twenty-five compounds was calculated from the donor concentration (C_o) and the slopes of the plots of cumulative amount of drug permeated through the hydrogel (µg/cm^2) against time (min). Figure 184 shows the plots of cumulative permeated amount of eight selected representative compounds against time.

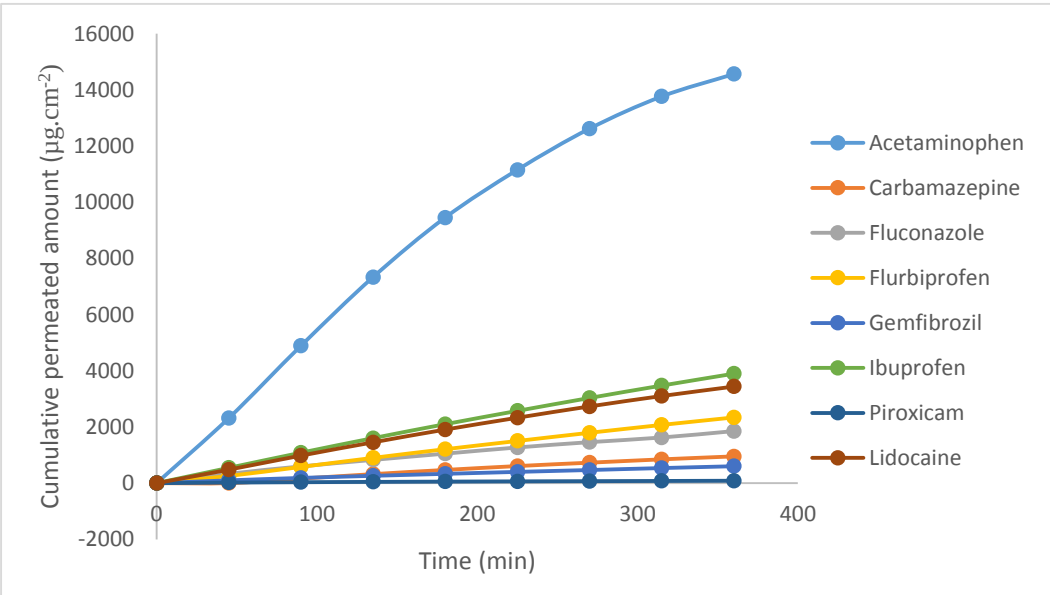

Figure 184: Plot of Cumulative permeated amount of different drugs against time.

5.A.1.2. Scanning Electron Microscopy (SEM)

In order to investigate the microstructures of the hydrogels formed by NaDC at pH 7.4, scanning of the freeze dried samples of blank NaDC hydrogel, as well as drug loaded NaDC hydrogel, using SEM was carried out. The results are summarised in Figure 185. The obtained SEM observations for the blank NaDC hydrogel freeze dried samples showed a network structure of intertwined fibrils with medium size pockets in between.

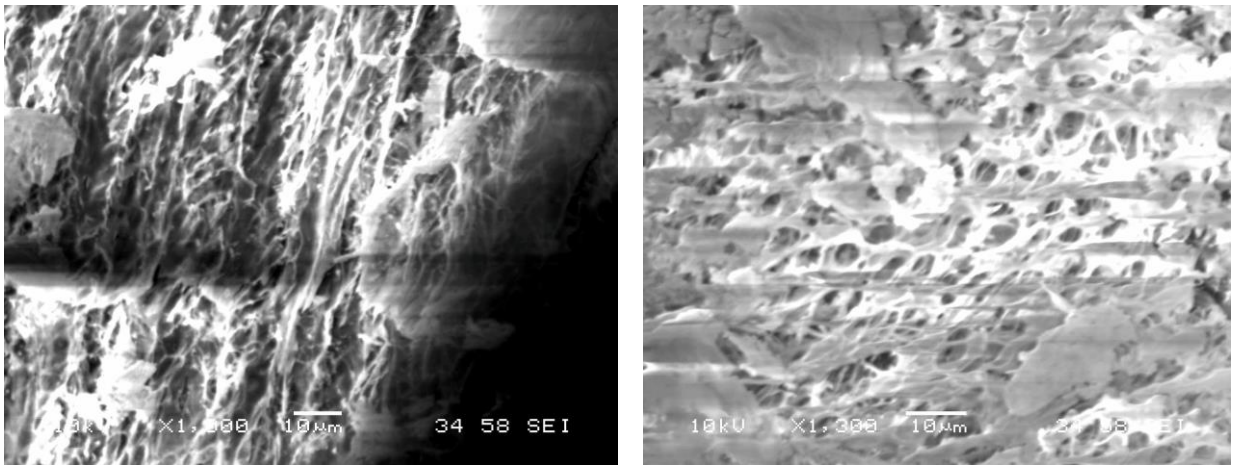

Figure 185: SEM images of gel formed by 70 mM NaDC of magnification power x1000 (left) and x1300 (right).

The microstructure of 70 mM NaDC hydrogels of two drugs (carbamazepine and meloxicam) was investigated. The SEM observations of the freeze dried samples of carbamazepine and meloxicam hydrogels showed the same network structure as the freeze dried sample of blank NaDC hydrogel but the carbamazepine showed a network structure with wider pockets than that of meloxicam hydrogel, i.e. a more compact network structure with narrow pockets in between (Figures 186-187). The difference in the structure of carbamazepine and meloxicam hydrogels could be attributed to carbamazepine being more hydrophobic than meloxicam where the log P of carbamazepine at pH 7.4 is 2.28 [218] while that of meloxicam at the same pH is 1.04. As a result, carbamazepine became more involved in the construction of the hydrogel network thus partially interrupting the crystalline like arrangement of NaDC molecules together in the gel and as a result wide pockets in the NaDC network structure are created. The anionic drug meloxicam is less hydrophobic (log P at pH 7.4=1.04) [218] and has a high molecular weight of 351.40 g/mol [218] so it is less involved in the main structure of hydrogel therefore, the network was more compact

with the presence of the drug entrapped inside the network structure. This was confirmed by the higher K_p value obtained for carbamazepine than that obtained for meloxicam which also confirms that the hydrophobic neutral carbamazepine was more solubilised in the network structure thus passing to the receptor chamber due to the hydrophobicity of the formed complex between the drug-polymer like aggregate of the hydrogel. The less hydrophobic, negatively charged, meloxicam with a higher molecular weight remained entrapped inside the network making the structure more compact with narrower pockets (Figures 186-187).

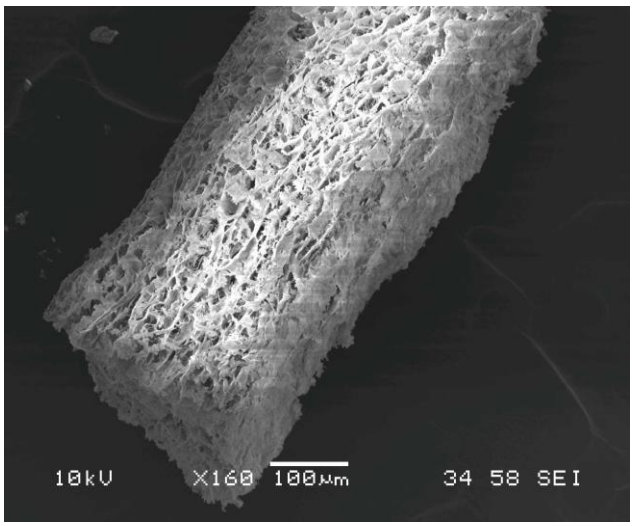

a)

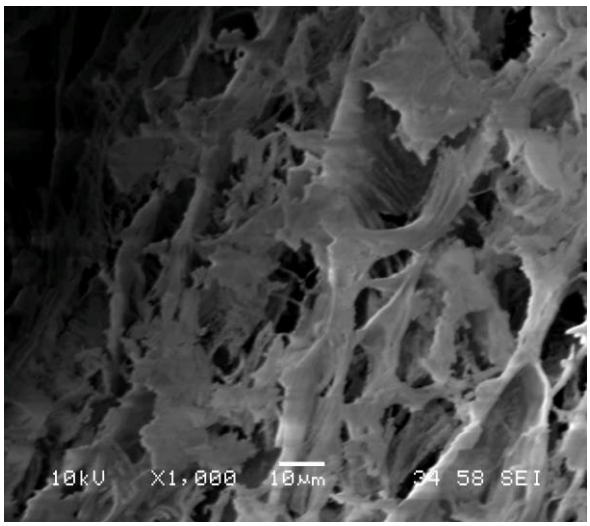

b)

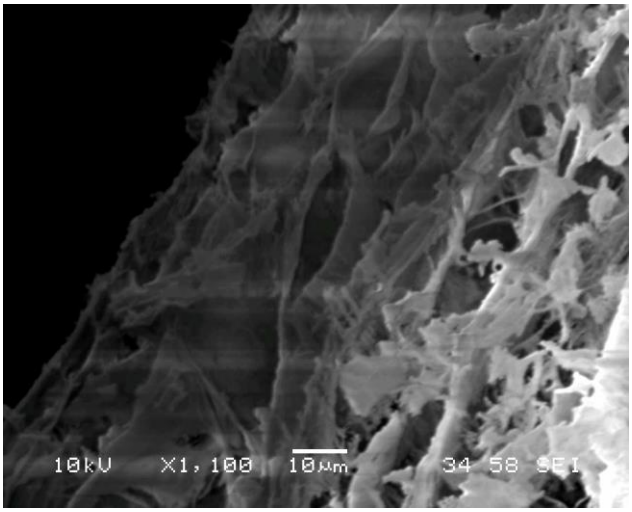

c)

Figure 186: SEM images for carbamazepine-70mM hydrogel of magnification power a) x160 b) x1000 c) x1100.

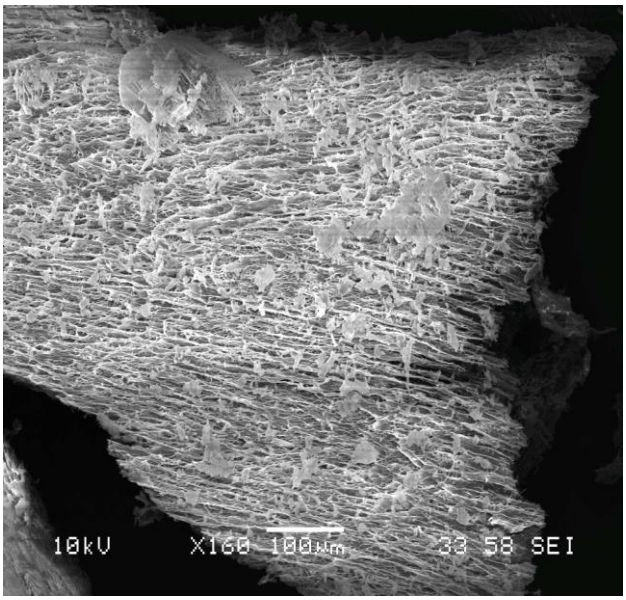

a)

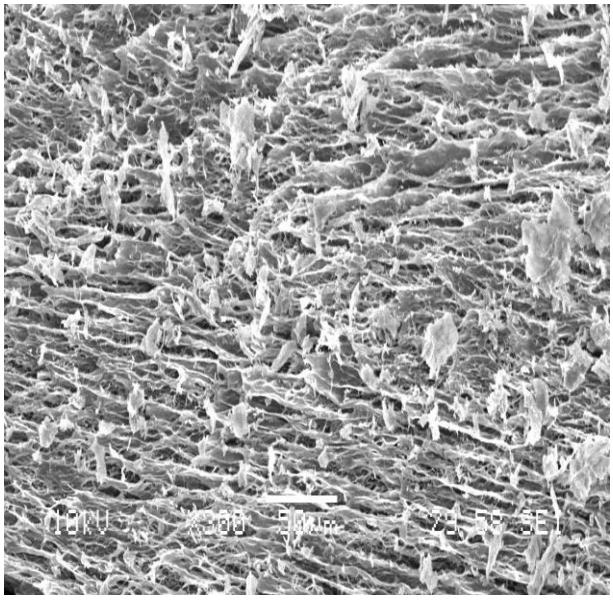

b)

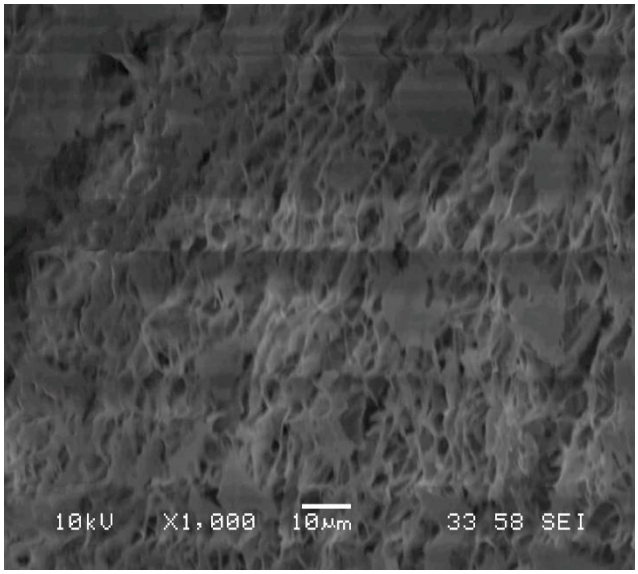

c)

Figure 187: SEM images for meloxicam-70mM hydrogel of magnification power a) x160 b) x300 c) x1000.

5.A.1.3. FT-IR analysis

FT-IR analysis of the hydrogels was carried out upon the drying of the sample to confirm the stability of the hydrogel upon addition of the drug where the blank hydrogel samples were analysed as well as samples of hydrogel containing the investigated drugs. This was to detect whether new characteristic peaks appeared or, if already existing peaks disappeared. All the drug containing hydrogels exhibited intense and continuous absorption peaks within the region 3500-1500 cm^{-1} in FT-IR spectra. A broad peak appeared at the range of 3350-3500 cm^{-1} which is known for antisymmetric and symmetric O-H stretching. Other peaks were seen in the regions 2928-2940 cm^{-1} and 2860-2865 cm^{-1} which are indicative for asymmetric and symmetric methylene stretching bands [286]. Furthermore, the peaks in the range 1552-1556 cm^{-1} can be related to N-H vibration [286]. In the range of 1644 and 1659 cm^{-1}, the stretching vibration can be correlated with carbonyl groups [286]. The peaks appearing at 1069-1098 cm^{-1} are consistent with the stretching vibration of the C-O bond [286]. These peaks are attributed to the asymmetric stretching vibration of COO^- in the crystallisation of NaDC indicating the combination of Na^+ ions and COO^- ions. This result proves that the behaviour of NaDC molecules in gels is similar to that in crystals. The results of the FT-IR analysis for a selection of drugs are shown in Figure 188.

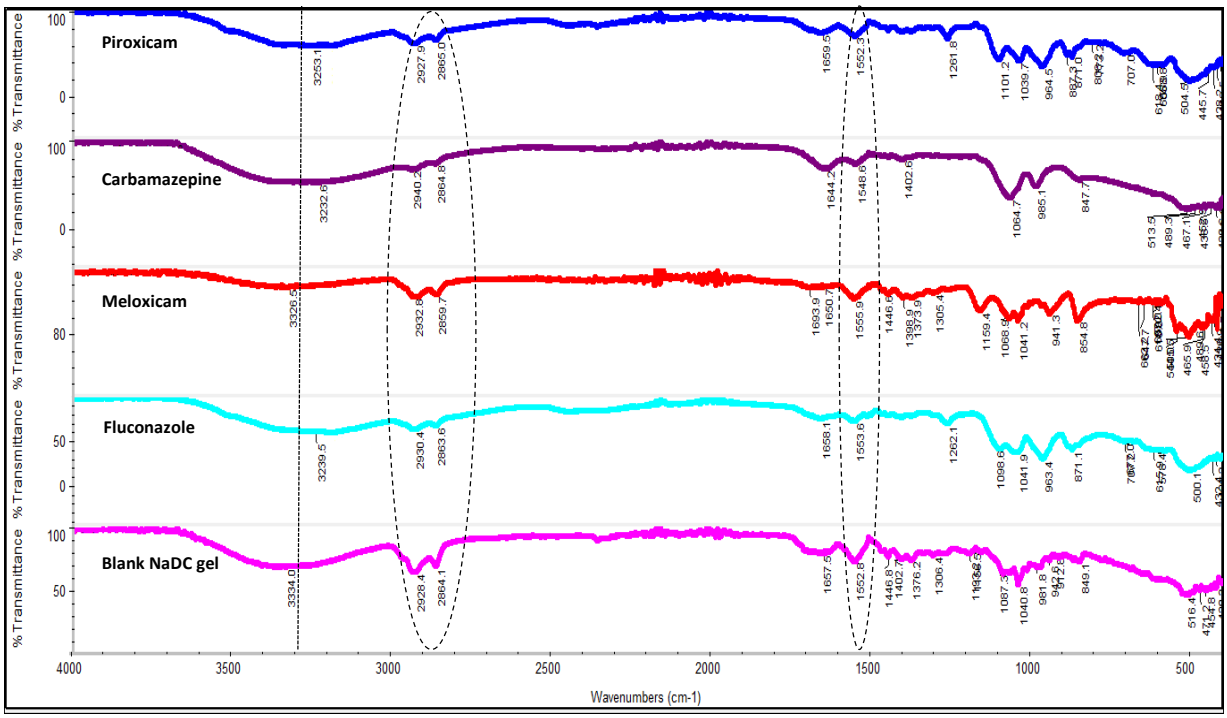

Figure 188: FTIR spectra of Blank NaDC hydrogel and of selected drugs (piroxicam, carbamazepine, meloxicam and fluconazole) in NaDC hydrogel.

As shown in Figure 188, it was observed that upon the inclusion of drugs to the NaDC hydrogel there was a decrease in the wave number of the O-H broad peak appearing at 3334 cm^{-1} for the blank NaDC hydrogel sample. This decrease shows destruction of H-bonding between the NaDC molecules and the formation of new H-bonding between the NaDC and each drug molecule [286]. The decrease was the highest in the case of carbamazepine (3233 cm^{-1}) indicating carbamazepine was more involved in the hydrogel structure confirming the previous SEM results for carbamazepine (Figure 186). While the decrease was the least in the case of meloxicam (3327 cm^{-1}) showing less inclusion of this drug in the NaDC hydrogel structure thus confirming the previous SEM results for meloxicam (Figure 187).

No appearance of new peaks or disappearance of existing peaks was observed suggesting no chemical interaction between the added drugs and NaDC gel suggesting NaDC gel as a safe carrier which is an advantage if such gel was considered as a carrier inside the human body, or if the gel was to be considered for analytical use.

5.A.2. Statistical Modelling

After measuring the permeation of a group of 25 drugs from the drug-loaded NaDC hydrogels and calculation of the permeability coefficients (K_p) of these drugs from the slopes of the plots of the cumulative permeated amount of each of the studied drugs against time, the obtained permeability coefficients (K_p) were statistically analysed alongside some molecular descriptors which were collected from literature such as molecular weight (Mwt), polar surface area (PSA), freely rotating bonds (FRB), molar volume(V_M), dissociation constant (pK_a), aqueous solubility (S_w), number of hydrogen bond donors (nHD) and number of hydrogen bond acceptors (nHA) using multiple linear regression for the prediction of human intestinal absorption (HIA) and permeability coefficients obtained by (PAMPA and Caco-2) in *vitro* methods. The obtained permeability coefficients (K_p) are listed with other molecular descriptors in Table 118.

5.A.2.1. Statistical Modelling of Human Intestinal absorption (HIA)

Analysing the obtained permeability coefficients, i.e. K_p values, alongside other molecular descriptors against the reported %HIA values enabled the application of multiple linear regression and therefore the successful inclusion of log K_p in a model equation with the logit form of %HIA experimental values for orally administered drugs

(as shown in Table 48) with other molecular descriptors (nHD and V_M) for the prediction of %HIA.

The model obtained for the prediction of %HIA is given by Equation 45:

$$\text{logit HIA} = -0.59 - 0.5522\ \text{nHD} - 0.006085\ V_M - 0.765 \log K_p \qquad \text{Eq. (45)}$$

Eighteen drugs were used in the development of the final model. The model's R^2 = 87.58 %, $R^2_{\text{adjust.}}$= 84.92 % , R^2_{PRED} = 79.80 %, S= 0.267

A 95 % confidence interval for log K_p is given by (-1.19, -0.34). t-statistic and standardised coefficient of log K_p are -3.86 ($p<0.05$) and -0.397 respectively suggesting the statistical significance of log K_p as a predictor. Also the F-ratio of the overall model is statistically significant, F=32.90 and P value 0.000 ($p<0.05$). Absence of autocorrelation in the current regression model was proved by a Durbin- Watson statistic value of 2.532. Figure 189 shows no marked relationship between residuals and predicted values while Figure 190 summarises the model. Seven compounds (carbamazepine, fenoprofen, linezolid, naproxen, piroxicam, quinine and zolmitriptan) were used for testing the obtained model as shown in Table 115. The model was able to successfully predict the %HIA for six compounds in the test set within a minimum of 0.29 % and a maximum of 10.97 % difference between the predicted %HIA and the published %HIA. The model underestimated the %HIA for piroxicam where its predicted value for human intestinal absorption was found to be 82.65 % against a literature value of 99 % experimentally obtained in humans. However, the obtained predicted value was found to be closer to a literature value of 89 % for piroxicam's intestinal absorption in dogs [294]. Figure 191 shows an overall close agreement between literature and predicted values of %HIA.

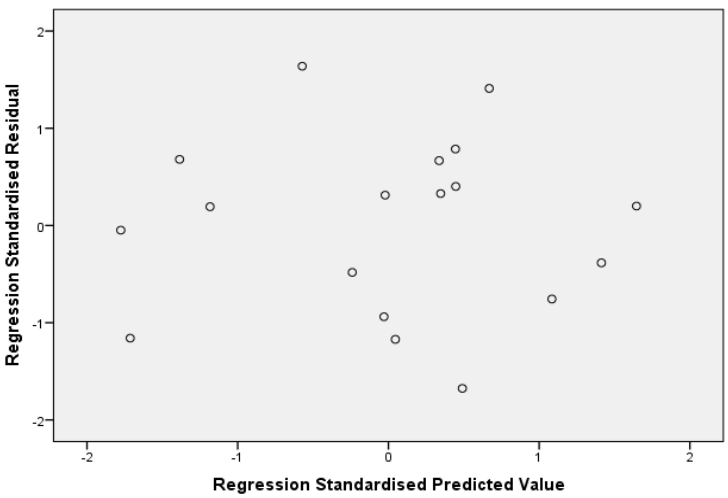

Figure 189: Residual plot for optimal HIA regression model.

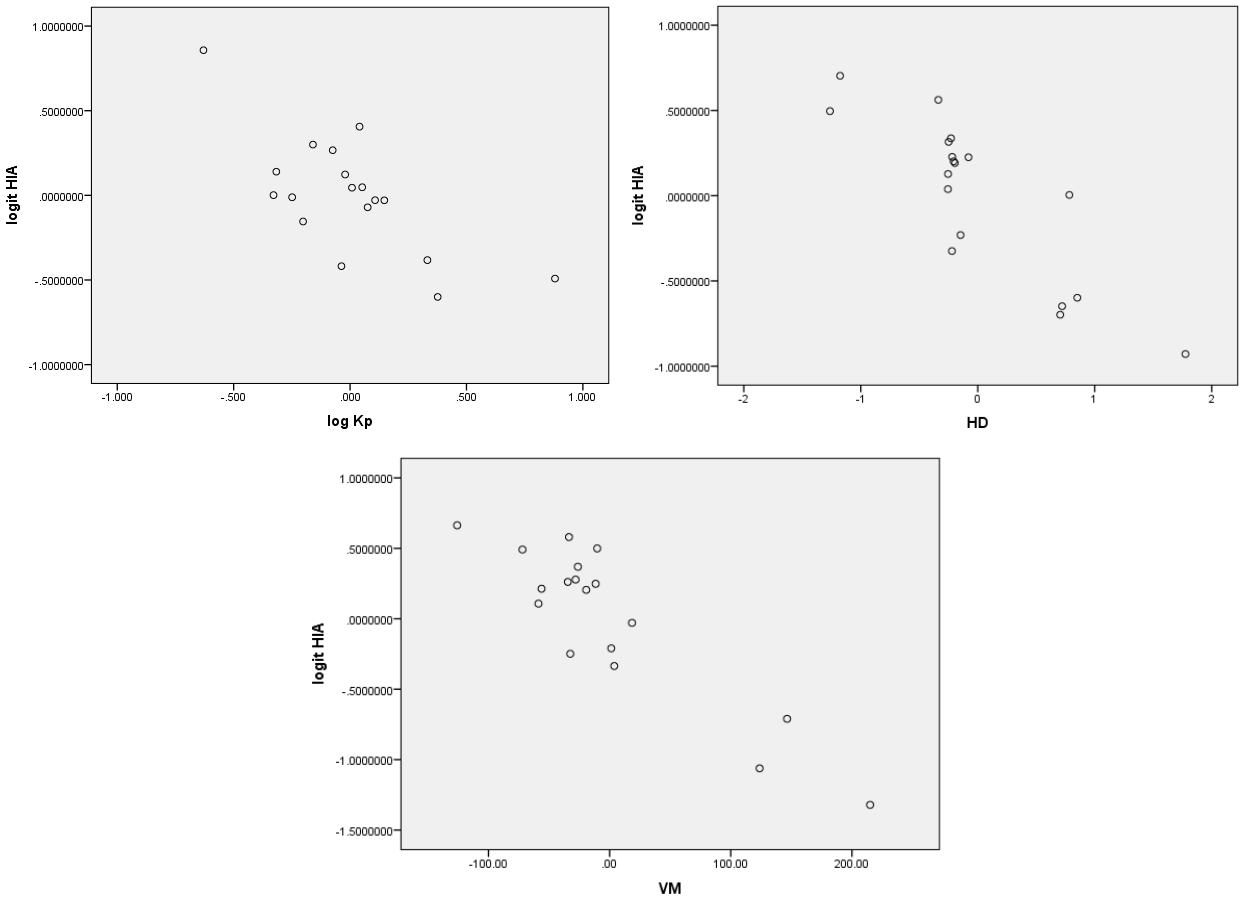

Figure 190: Partial regression plots of experimental logit HIA values against log K_p, nHD and V_M.

Table 115: Experimental permeability coefficient (log K_p), predicted %HIA (%HIA$_{pred.}$) and experimentally determined literature %HIA (% HIA$_{Expt.}$) values for the compounds analysed including seven validation compounds (*).

Drug	Expt. %HIA	Pred. %HIA
Acetaminophen	80.00[205]	84.32
Caffeine	99.00[230]	98.87
Carbamazepine*	70.00[209]	69.71
Cimetidine	60.00[205]	57.13
Diclofenac	80.50[206, 207]	88.02
Fenoprofen*	85.00[206]	95.97
Fluconazole	94.00[230]	92.76
Flurbiprofen	95.00[210]	93.69
Fosinopril	35.00[246]	35.68
Gemfibrozil	95.00[207]	92.66
Haloperidol	60.00[245]	49.70
Ibuprofen	85.00[207]	94.07
Indomethacin	98.00[245]	95.38
Ketoprofen	96.00[205]	93.67
Leflunomide	80.00[246]	89.14
Lidocaine	90.00[210]	88.14
Linezolid*	100.00[246]	91.16
Meloxicam	90.00[205]	76.70
Moexipril	23.00[246]	37.83
Naproxen*	94.00[205]	95.06
Phenylbutazone	96.00[230, 245, 252]	97.45
Piroxicam*	99.00[252]	82.65
Quinine*	95.00[210]	96.72
Theophylline	98.00[33]	98.41
Zolmitriptan*	70.25[246, 294]	68.01

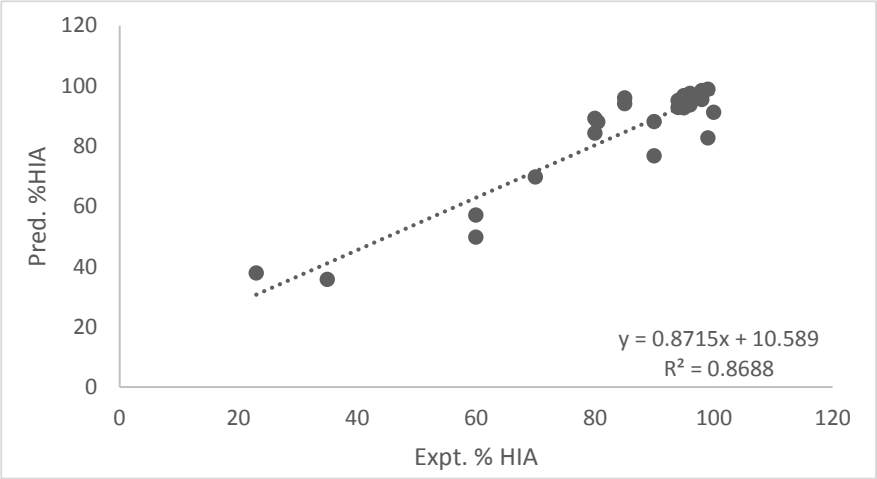

Figure 191: Regression plot of predicted %HIA values against literature %HIA.

5.A.2.2. Modelling of permeability coefficients obtained from PAMPA

The model obtained for the prediction of PAMPA log P_o is given by Equation 46:

$$\log P_o = -8.56 - 1.363 \log K_p - 0.1658\, S_w \qquad \text{Eq. (46)}$$

Seventeen drugs were used in the development of the final model. The model's R^2 = 83.81 %, $R^2_{adjust.}$= 81.49 % , R^2_{PRED} = 76.95 %, S= 0.708

A 95 % confidence interval for log K_p is given by (-2.488, -0.237). t-statistic and standardised coefficient of log K_p are -2.6 ($p<0.05$) and -0.292 respectively suggesting that its statistical significance of log K_p as a predictor. Also the F-ratio of the overall model is statistically significant, F= 36.23 and P value 0.000 ($p<0.05$).

The close agreement of the values of $R^2_{adjust.}$ & R^2_{PRED} indicates that the model does not over-fit the data. The residual analysis did not detect any relationship between residuals and predicted values as shown in Figure 192. The model is shown in Figure 193. As shown in Table 116 and Figure 194 the obtained model was found to have a good predictive ability for PAMPA permeability coefficient.

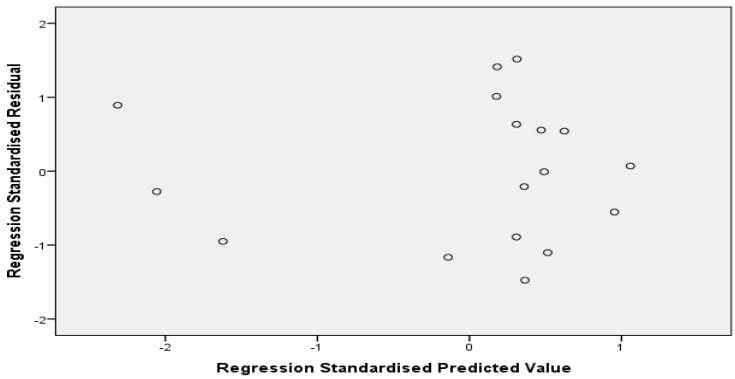

Figure 192: Residual plot for optimal PAMPA regression model.

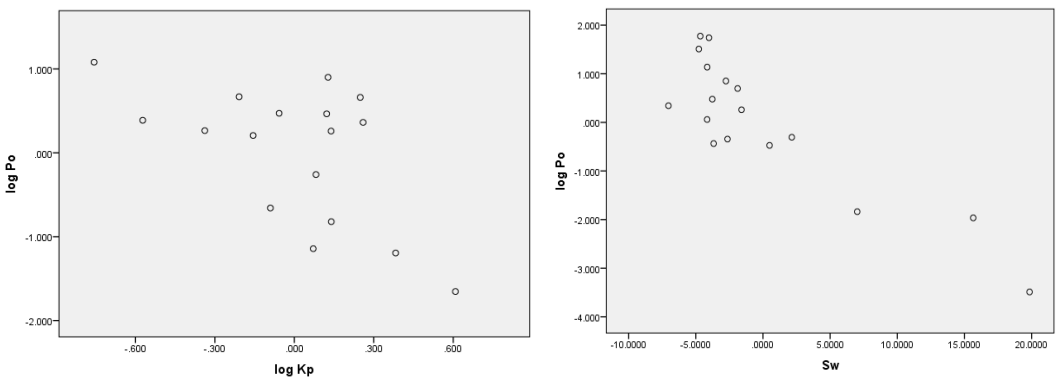

Figure 193: Partial regression plots of experimental PAMPA log P_o values against log K_p and S_w.

Table 116: Experimental and predicted values for PAMPA logP_o.

Drug	log P_o Expt. [215]	log P_o Pred.
Acetaminophen	-5.81	-5.14
Caffeine	-5.55	-6.18
Carbamazepine	-3.73	-2.91
Diclofenac	-1.37	-1.75
Flurbiprofen	-1.78	-2.23
Gemfibrozil	-1.59	-1.98
Ibuprofen	-1.15[64]	-2.22
Indomethacin	-1.65	-1.26
Ketoprofen	-3.19[64, 215, 281, 295]	-2.15
Lidocaine	-1.42	-2.42
Meloxicam	-2.86	-2.23
Naproxen	-2.3	-2.15
Phenylbutazone	-1.96	-1.95
Piroxicam	-2.70[64, 215]	-1.92
Quinine	-1.05	-1.1
Theophylline	-5.99	-5.79
Zolmitriptan	-1.71	-2.43

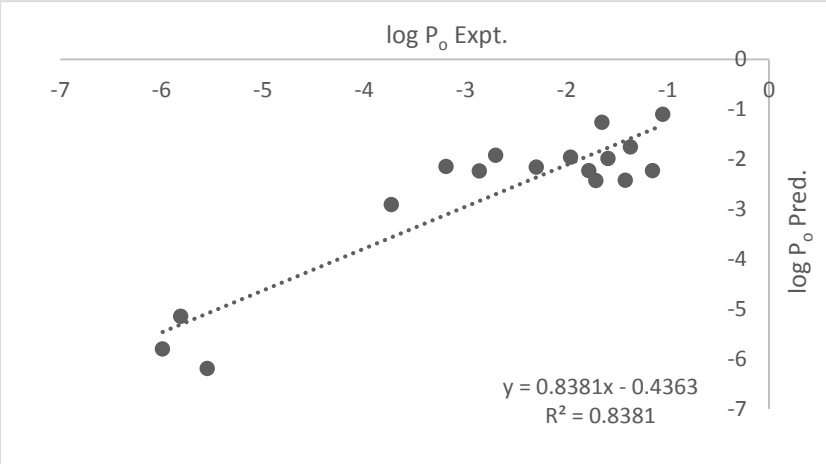

Figure 194: Plot of experimental vs. predicted log P_o values.

5.A.2.3. Modelling of permeability coefficients obtained from Caco-2 $P_{eff.}$

The model obtained for the prediction of Caco-2 $P_{eff.}$ is given by Equation 47:

$$\log P_{eff.} = -15.18 - 1.695 \log K_p + 0.00658\ Mwt + 0.1463\ pK_a \qquad \text{Eq. (47)}$$

Seventeen drugs were used in the development of the final model. The model's R^2 = 87.69 %, $R^2_{adjust.}$ = 84.85 % , R^2_{PRED} = 79.08 %, S= 0.289

A 95 % confidence interval for log K_p is given by (-2.155, -1.235). t-statistic and standardised coefficient of log K_p are -7.96 ($p<0.05$) and -0.926 respectively

suggesting that its statistical significance of log K_p as a predictor. Also the F-ratio of the overall model is statistically significant, F= 30.88 and P value 0.000 ($p<0.05$).

Figure 195 shows no marked relationship between residuals and predicted values while Figure 196 summarises the model. The model successfully predicted log $P_{eff.}$ for the five compounds (fluconazole, ibuprofen, lidocaine, phenylbutazone and piroxicam) which were used to test the obtained model. The literature and predicted values of Caco-2 permeability coefficients were found to be in close agreement as shown in Table 117 and Figure 197.

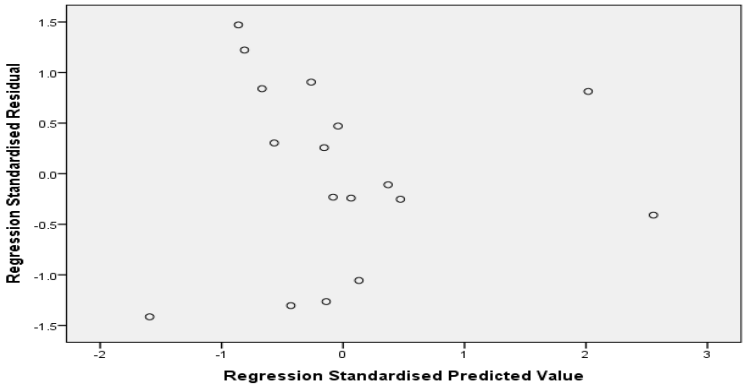

Figure 195: Residual plot for optimal Caco-2 regression model.

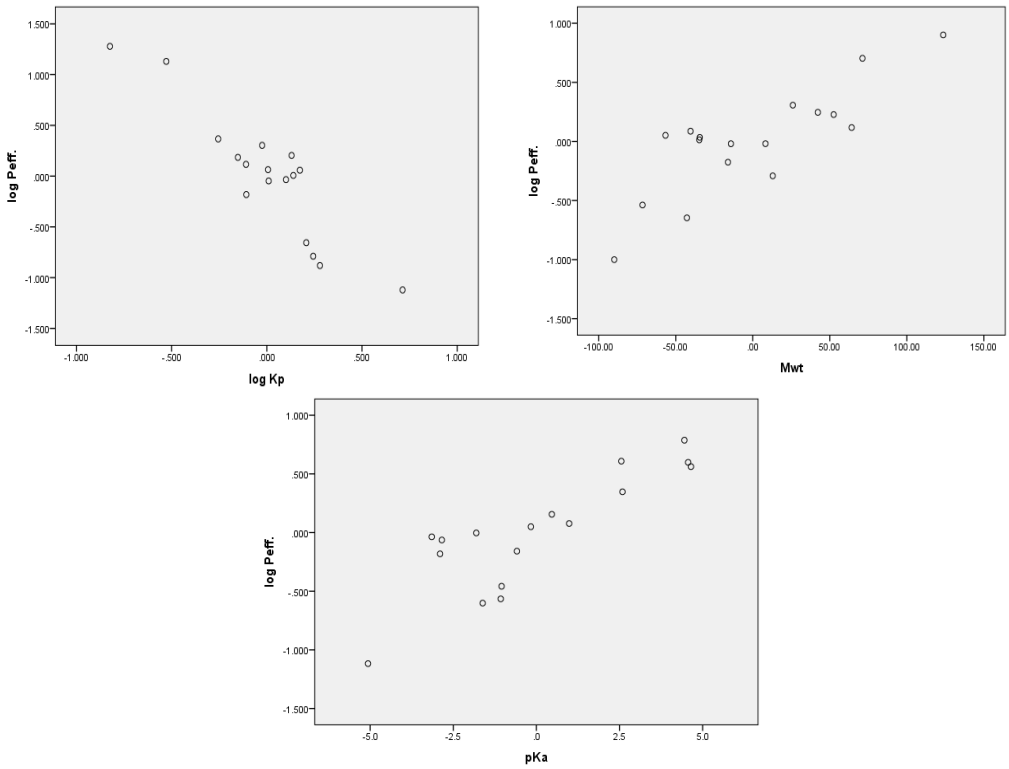

Figure 196: Partial regression plots of experimental Caco-2 log $P_{eff.}$ values against pK_a, Mwt and log K_p.

Table 117: Experimental and predicted values for Caco-2 log $P_{eff.}$.

Drug	log $P_{eff.}$ Expt.	log $P_{eff.}$ Pred.
Acetaminophen	-6.00[216]	-5.59
Caffeine	-4.51[63]	-4.44
Carbamazepine	-4.38[56]	-4.52
Cimetidine	-4.52[249]	-4.59
Diclofenac	-4.23[246]	-4.16
Fenoprofen	-4.94[230]	-4.58
Fluconazole*	-4.52[246]	-3.55
Flurbiprofen	-4.70[230]	-5.05
Gemfibrozil	-4.41[246]	-4.67
Haloperidol	-4.79[246]	-4.88
Ibuprofen*	-4.58[56]	-5.17
Indomethacin	-2.85[56, 215]	-3.09
Ketoprofen	-4.71[246]	-4.95
Lidocaine*	-4.36[56]	-4.8
Linezolid	-5.16[246]	-4.79
Meloxicam	-4.70[277]	-4.4
Naproxen	-4.66[56]	-5.08
Phenylbutazone*	-5.00[250]	-4.15
Piroxicam*	-3.26[215, 246]	-3.81
Quinine	-2.83[215]	-2.71
Theophylline	-4.61[56]	-4.54
Zolmitriptan	-4.26[215]	-4.23

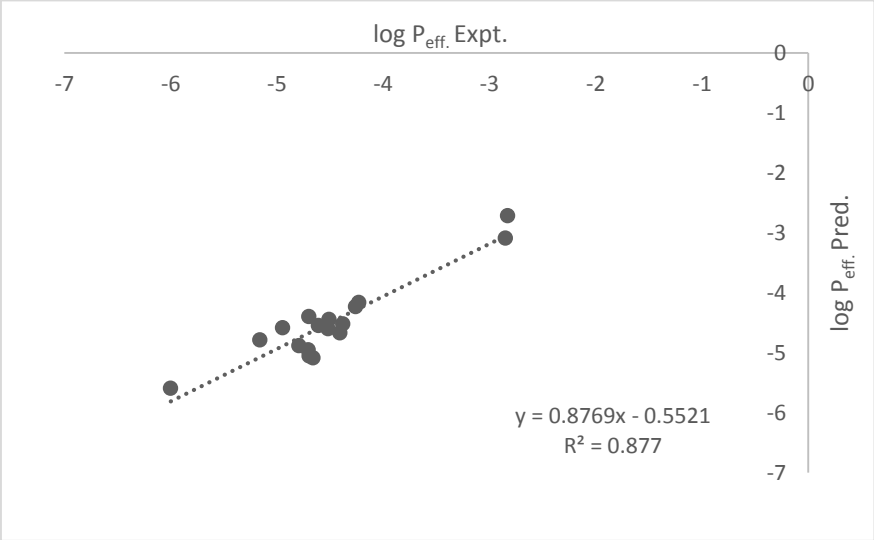

Figure 197: Plot of experimental vs predicted Caco-2 log $P_{eff.}$ values.

Table 118: A summary of molecular descriptors for the selected drugs analysed by permeation method using flow through cells and the reported experimental values of %HIA and permeability coefficients of PAMPA and Caco-2 tests.

Drug	log K_p*	Mwt[218]	pK_a[184]	S_w[184]	HD[218]	HA[218]	RB[218]	PSA[219]	V_M[218]	log P_o[215]	log $P_{eff.}$	%HIA
Acetaminophen	-4.21	151.20	9.9[220]	14	2	3	1	49.3	131.1	-5.81	-6.000[216]	80[205]
Caffeine	-4.37	194.20	14[222]	21.6	0	6	0	58.4	133.4	-5.55	-4.51[63]	99[230]
Carbamazepine	-4.17	236.36	13.9	0.21[184, 282]	2	3	0	46.3	186.6	-3.73	-4.379[56]	70[209]
Cimetidine	-4.68	252.34	6.8	9.38	3	6	8	114	198.2	NI	-4.52[249]	60[205]
Diclofenac	-4.99	296.20	4.15	0.00237	2	3	4	49.3	206.8	-1.37	-4.231[246]	80.5[206, 207]
Fenoprofen	-4.92	242.27	4.5	0.033[218]	1	3	4	46.5	204.7	NA	-4.947[230]	85[206]
Fluconazole	-4.58	306.27	12.71	9[283]	1	7	5	81.6	205.3	NA	-4.515[246]	94[230]
Flurbiprofen	-4.65	244.26	4.42	0.008	1	2	3	37.3	203.6	-1.78	-4.697[230]	95[210]
Fosinopril	-4.98	563.66	-4.4	0.00101	1	8	15	110	480.4	NA	NA	35[246]
Gemfibrozil	-4.84	250.33	4.5[219]	0.13[284]	1	3	6	46.5	239.7	-1.59	-4.407[246]	95[207]
Haloperidol	-3.90	375.86	8.3[296]	0.014	1	3	6	40.5	303.3	NI	-4.792[246]	60[245]
Ibuprofen	-4.66	206.30	5.2[223]	0.0684	1	2	4	37.3	200.3	-1.15[64]	-4.58[56]	85[207]
Indomethacin	-5.36	357.79	4.5	0.000937	1	5	4	68.5	269.6	-1.65	-2.85[56, 215]	98[245]
Ketoprofen	-4.71	254.30	3.88	0.051	1	3	4	54.4	212.2	-3.19[64, 215, 281, 295]	-4.707[246]	96[205]
Leflunomide	-4.23	270.21	-0.45	0.021	1	4	3	55.1	194.1	NA	NA	80[246]
Lidocaine	-4.53	234.40	7.9[224]	0.2337[285]	1	3	5	32.3	238.8	-1.42	-4.36[56]	90[210]
Linezolid	-4.88	337.35	-0.66	1.44	1	7	4	71.1	259.0	NA	-5.161[246]	100[246]
Meloxicam	-4.65	351.40	4.08	0.00715	2	7	2	136	220.3	-2.86	-4.7[277]	90[205]
Moexipril	-5.18	498.57	5.2	0.00585	2	9	12	114	408.1	NA	NA	23[246]
Naproxen	-4.70	230.26	4.15	0.0159	1	3	3	46.5	192.3	-2.3	-4.66[56]	94[205]
Phenylbutazone	-4.93	308.37	4.4[225]	0.7[219]	0	4	5	40.6	262.8	-1.96	-4.998[250]	96[230, 245, 252]
Piroxicam	-4.88	331.35	6.3	0.023	2	7	2	108	222.8	-2.70[64, 215]	-3.264[215,	99[252]
Quinine	-5.54	324.42	6.5	0.5	1	4	4	45.6	266.4	-1.05	-2.83[215]	95[210]
Theophylline	-4.82	180.16	8.8[228]	22.9	1	6	0	69.3	122.9	-5.99	-4.61[56]	98[33]
Zolmitriptan	-4.52	287.36	9.52[297]	0.19	2	5	5	57.4	236.1	-1.71	-4.26[215]	70.25[246, 294]

*The logarithm is taken for the K_p value (cm/sec), NA: no available data, NI: value not included in training set.

5.A.3. Conclusion

Using NaDC based supramolecular hydrogels in the presence of halide salts such as NaCl and also at a pH of 7.4, was achieved in this work by using phosphate buffer solution. Furthermore, determination of K_p from the permeation of a number of compounds from the prepared NaDC hydrogels using flow through cells was successful in the development of models of high predictive capabilities for human intestinal absorption and permeability coefficients of other *in vitro* methods such as PAMPA and Caco-2 by using the experimentally obtained K_p. NaDC, being a natural physiological surfactant and having gelation properties in the presence of certain factors, makes this method mimic the biological membrane and the absorption process inside the human intestine.

CHAPTER 5
Section (B)

Predicting Human Intestinal Absorption Using bile salt hydrogels:
"Use of Franz cells in determination of K_p "

Section (B): Use of Franz cells in determination of K_p.

This section reports the results of experiments using Franz cells for the study of the permeation of a group of studied drugs through the synthesised drug saturated NaDC hydrogels and determination of K_p of these drugs. Then the use of the obtained permeability coefficients (K_p) in the prediction of human intestinal absorption and the permeability coefficients of other *in vitro* methods. Two different pieces of apparatus (flow through and Franz cells) were used in the permeation study of the same group of compounds in order to detect which method would be the best for prediction of %HIA through the obtained permeability coefficients. In addition, it was a way of confirming the capability of using the proposed hydrogel as an intestinal membrane mimic for prediction of %HIA using different permeation apparatus.

5.B.1. Results and Discussion

A 70 mM hydrogel already loaded with an infinite (saturated) dose of the drug studied was used in all the permeation experiments carried out using Franz diffusion cells to investigate the permeation profile for a group of twenty-five compounds against time. Based on the same equation used in the previous section for calculation of permeability coefficient (K_p), calculations of the permeability coefficients (K_p) for the investigated twenty-five compounds in this section were carried out. A different area of exposed hydrogel was used (3.14 cm^2). K_p was determined from the donor concentration (C_o) and the slopes of the plots of cumulative amount of drug permeated through the hydrogel ($\mu g/cm^2$) against time (min) constructed from the permeation studies performed using Franz cells. For illustration, Figure 198 shows the plots of cumulative permeated amount of eight compounds against time.

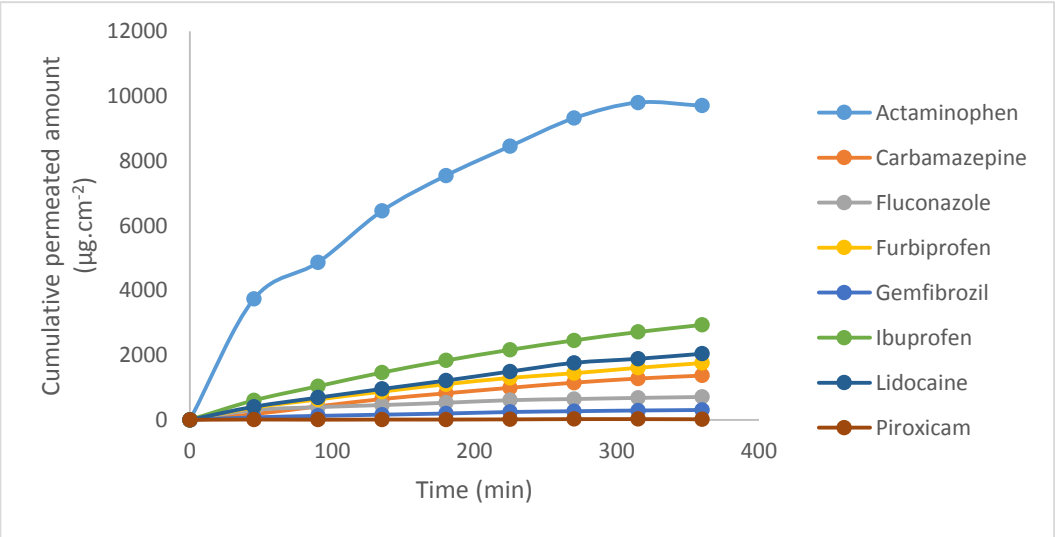

Figure 198: Plot of Cumulative permeated amount of different drugs against time.

From Figure 198, it can be seen that the drugs had similar patterns and similar rates of permeation to the rates they had using flow through cells. The exception was the lipophilic neutral drug carbamazepine which showed a higher K_p than that of fluconazole although when using flow through cells it had a lower K_p than that of fluconazole. This could be related to the greater area of hydrogel exposed when using Franz diffusion cells.

5.B.2. Statistical Modelling

For 25 drugs the obtained permeability coefficients (K_p) were statistically analysed alongside some molecular descriptors which were collected from literature such as molecular weight (Mwt), polar surface area (PSA), freely rotating bonds (FRB), molar volume(V_M), dissociation constant (pK_a), aqueous solubility (S_w), number of hydrogen bond donors (nHD) and number of hydrogen bond acceptors (nHA) using multiple linear regression for the prediction of human intestinal absorption (HIA) and permeability coefficients obtained by (PAMPA and Caco-2) in *vitro* methods. The obtained permeability coefficients (K_p) are listed with other molecular descriptors in Table 122.

5.B.2.1. Statistical Modelling of Human Intestinal absorption (HIA)

Analysing the obtained permeability coefficients K_p values alongside other molecular descriptors against the reported %HIA values enabled the application of multiple linear regression and therefore the successful inclusion of log K_p in a model equation with the logit form of %HIA experimental values for orally administered drugs (as shown in Table 122) with other molecular descriptors (nHD and V_M) for the prediction of %HIA. The model obtained for the prediction of %HIA is given by Equation 48:

$$\text{logit HIA} = 0.515 - 0.4294\ \text{nHD} - 0.006005\ V_M - 0.453 \log K_p \qquad \text{Eq. (48)}$$

Eighteen drugs were used in the development of the final model. The model's R^2 = 86.61 %, $R^2_{adjust.}$= 83.74 % , R^2_{PRED} = 79.67 %, S= 0.253

A 95 % confidence interval for log K_p is given by (-0.874, -0.031). t-statistic and standardised coefficient of log K_p are -2.3 ($p<0.05$) and -0.261 respectively suggesting the statistical significance of log K_p as a predictor. Also the F-ratio of the overall model is statistically significant, F= 30.19 and P value 0.000 ($p<0.05$). Absence of autocorrelation in the current regression model was proved by a Durbin- Watson statistic value of 2.105. Figure 199 shows no marked relationship between residuals

and predicted values while Figure 200 summarises the model. Seven compounds (carbamazepine, fenoprofen, indomethacin, linezolid, piroxicam, quinine and zolmitriptan) were used for testing the obtained model. As shown in Table 119, the model was able to successfully predict the %HIA for six compounds in the test set within a minimum of 0.6 % and a maximum of 12.60 % difference between the predicted %HIA and the published %HIA. The model underestimated the %HIA for piroxicam where its predicted value for %HIA was found to be 80.73 % against a literature value of 99 % experimentally obtained in humans. However, the obtained predicted value was found to be closer to a literature value of 89 % for piroxicam's intestinal absorption in dogs [294]. The model's good predictive power is shown in Figure 201.

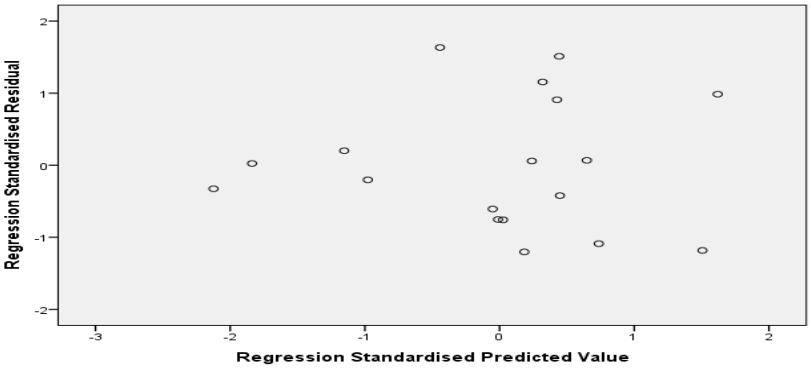

Figure 199: Residual plot for optimal HIA regression model.

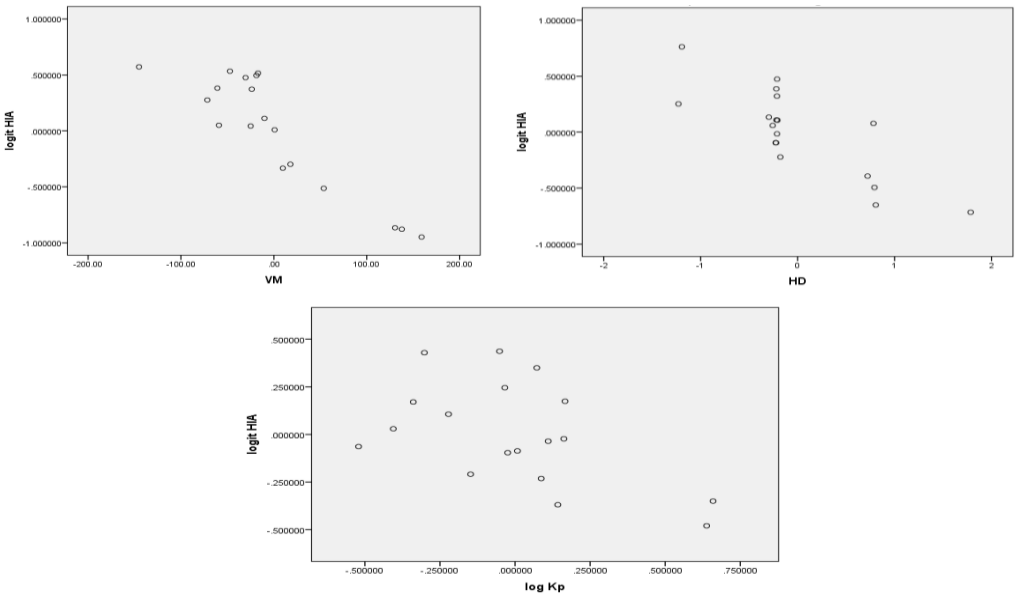

Figure 200: Partial regression plots of experimental logit HIA values against log K_p, nHD and V_M.

Table 119: Experimental permeability coefficient (log K_p), predicted %HIA (%HIA$_{pred.}$) and experimentally determined literature %HIA (%HIA$_{Expt.}$) values for the compounds analysed including seven validation compounds (*).

Drug	%HIA Expt.	%HIA Pred.
Acetaminophen	80.00[205]	88.97
Caffeine	99.00[230]	98.24
Carbamazepine*	70.00[209]	70.60
Cimetidine	60.00[205]	57.16
Diclofenac	80.50[206, 207]	85.47
Fenoprofen*	85.00[206]	92.37
Fluconazole	94.00[230]	93.77
Flurbiprofen	95.00[210]	91.79
Fosinopril	35.00[246]	34.68
Gemfibrozil	95.00[207]	90.64
Haloperidol	60.00[245]	62.80
Ibuprofen	90.00[207, 231]	92.01
Indomethacin*	98.00[245]	86.36
Ketoprofen	90.00[210]	89.69
leflunomide	80.00[246]	86.12
Lidocaine	80.75[209, 210, 230, 252]	86.71
Linezolid*	100.00[246]	87.40
Meloxicam	90.00[205]	77.64
Moexipril	23.00[246]	26.55
Naproxen	96.50[205, 210]	91.95
Phenylbutazone	90.00[245]	94.44
Piroxicam*	99.00[252]	80.73
Quinine*	95.00[210]	93.94
Theophylline	96.00[231]	97.95
Zolmitriptan*	70.25[246, 294]	70.94

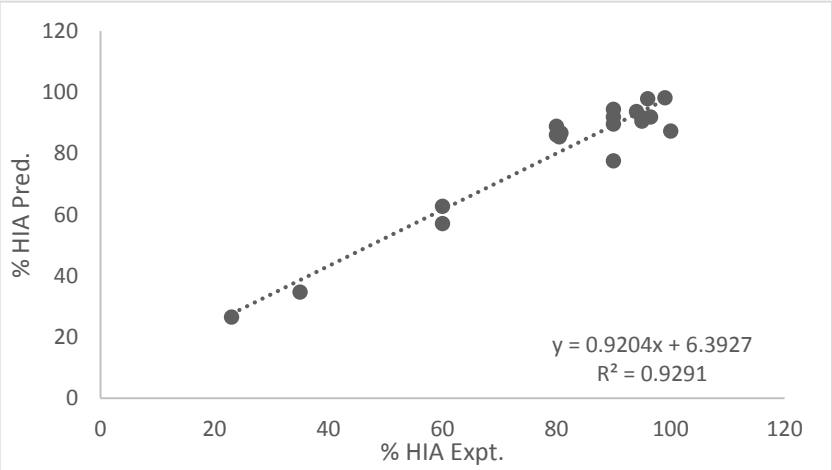

Figure 201: Regression plot of predicted %HIA values against literature %HIA.

5.B.2.2. Modelling of permeability coefficients obtained from PAMPA

The model obtained for the prediction of PAMPA log P_o is given by Equation 49:

$$\log P_o = -7.66 - 1.297 \log K_p - 0.1879\, S_w - 0.685\, nHD \qquad \text{Eq. (49)}$$

Seventeen drugs were used in the development of the final model. The model's R^2 = 86.75 %, $R^2_{adjust.}$= 83.91 % , R^2_{PRED} = 78.63 %, S= 0.721

A 95 % confidence interval for log K_p is given by (-2.254, -0.340). t-statistic and standardised coefficient of log K_p are -2.91 ($p<0.05$) and -0.289 respectively suggesting that its statistical significance of log K_p as a predictor. Also the F-ratio of the overall model is statistically significant, F= 30.56 and P value 0.000 ($p<0.05$).

The close agreement of the values of $R^2_{adjust.}$ & R^2_{PRED} indicates that the model does not over-fit the data. The residual analysis did not detect any relationship between residuals and predicted values as shown in Figure 202. The model is shown in Figure 203. The literature and predicted values of PAMPA permeability coefficients were found to be in agreement (Table 120 and Figure 204).

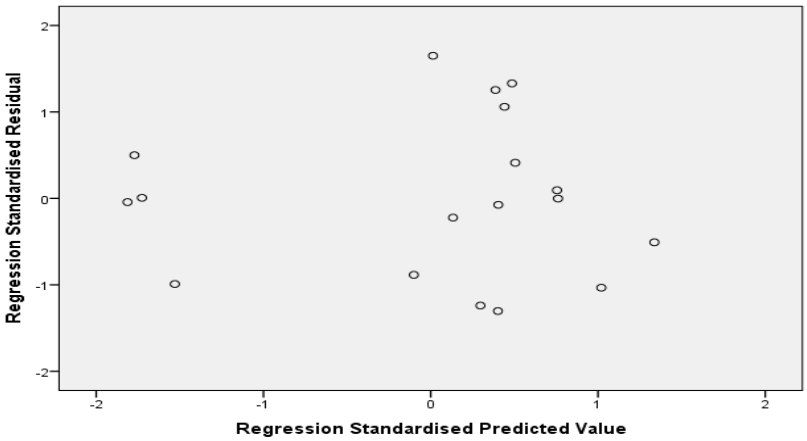

Figure 202: Residual plot for optimal PAMPA regression model.

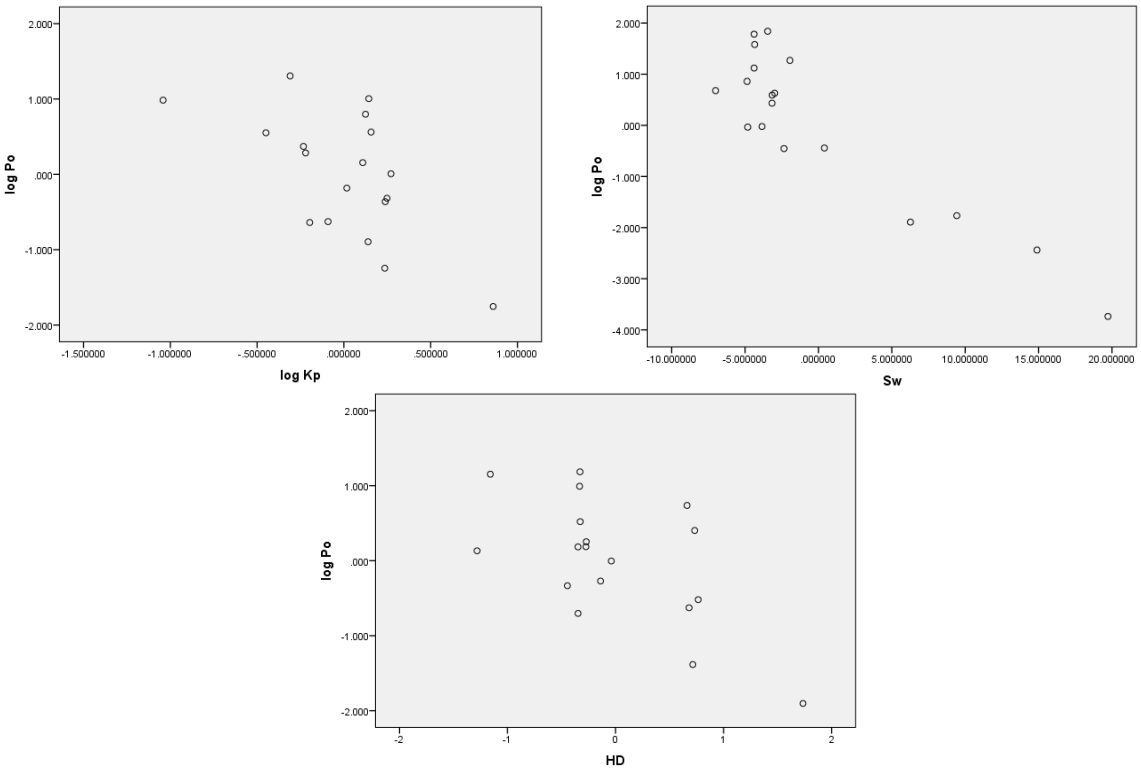

Figure 203: Partial regression plots of experimental PAMPA log P_o values against log K_p, S_w and nHD.

Table 120: Experimental and predicted values for PAMPA logP_o.

Drug	log P_o Expt. [215]	log P_o Pred.
Acetaminophen	-5.81	-5.82
Caffeine	-5.53	-5.89
Carbamazepine	-3.73	-3.09
Cimetidine	-6.2	-5.49
Diclofenac	-1.37	-2.28
Flurbiprofen	-1.78	-2.08
Gemfibrozil	-1.59	-1.66
Ibuprofen	-1.15[64]	-2.11
Indomethacin	-1.65	-1.65
Ketoprofen	-3.19[64, 215, 281, 295]	-2.25
Lidocaine	-1.42	-2.18
Meloxicam	-2.86	-2.70
Naproxen	-2.3	-2.25
Phenylbutazone	-1.96	-1.22
Piroxicam	-3.32	-2.43
Quinine	-1.05	-0.68
Theophylline	-5.99	-5.96
Zolmitriptan	-1.71	-2.90

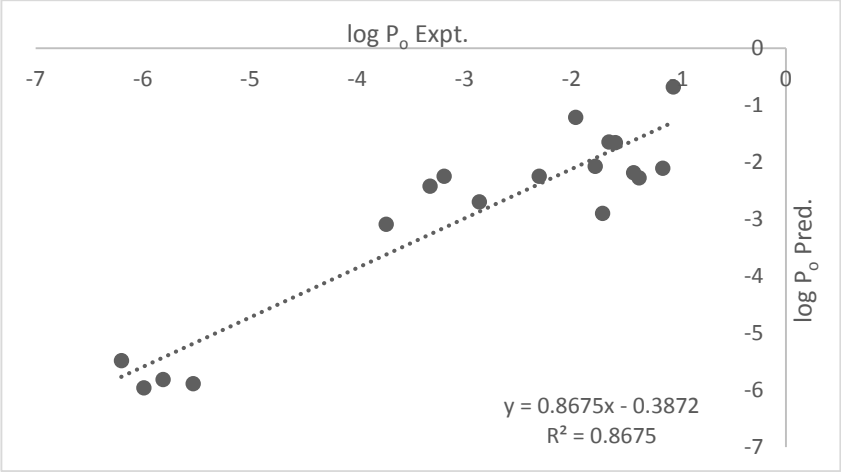

Figure 204: Plot of experimental vs. predicted log P_o values.

5.B.2.3. Modelling of permeability coefficients obtained from Caco-2 $P_{eff.}$

The model obtained for the prediction of Caco-2 $P_{eff.}$ is given by Equation 50:

$$\log P_{eff.} = -5.996 - 0.2882 \log K_p - 0.001507\ Mwt + 0.06532\ pK_a \qquad \text{Eq. (50)}$$

Seventeen drugs were used in the development of the final model. The model's R^2 = 88.73 %, $R^2_{adjust.}$= 86.13 % , R^2_{PRED} = 82.03 %, S= 0.103

A 95 % confidence interval for log K_p is given by (-0.451, -0.125). t-statistic and standardised coefficient of log K_p are -3.81 ($p<0.05$) and -0.442 respectively suggesting that its statistical significance of log K_p as a predictor. Also the F-ratio of the overall model is statistically significant, F= 34.13 and P value 0.000 ($p<0.05$).

Figure 205 shows no marked relationship between residuals and predicted values while Figure 206 summarises the model. The model successfully predicted log $P_{eff.}$ for the five compounds (fluconazole, fenoprofen, gemfibrozil, phenylbutazone and piroxicam) which were used to test the obtained model. The good predictive power of the obtained model was shown in Table 121 and Figure 207.

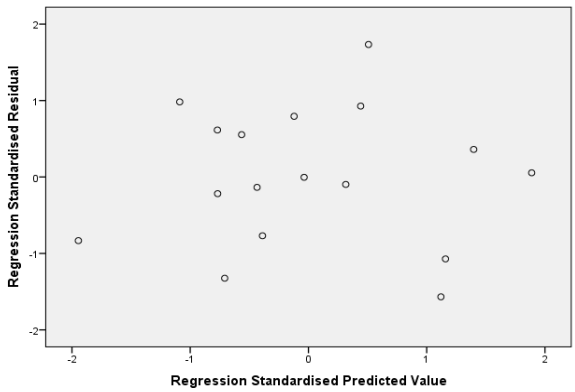

Figure 205: Residual plot for optimal Caco-2 regression model.

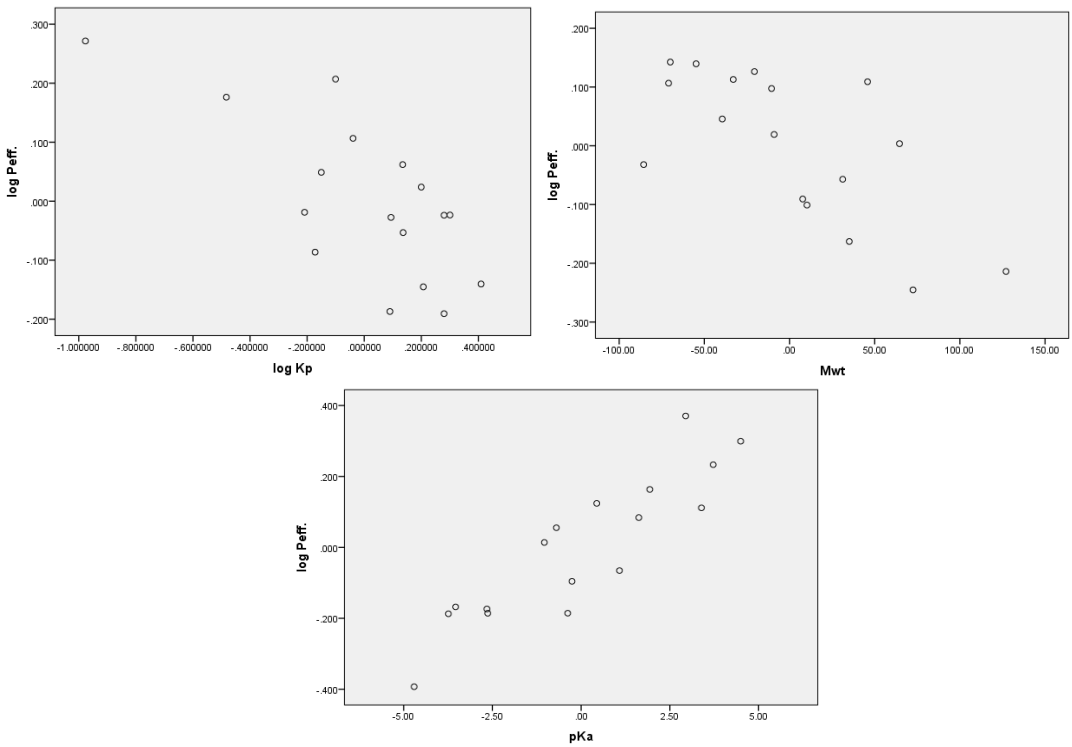

Figure 206: Partial regression plots of experimental Caco-2 log $P_{eff.}$ values against log K_p, Mwt and pK_a.

Table 121: Experimental and predicted values for Caco-2 log $P_{eff.}$.

Drug	log $P_{eff.}$ Expt.	log $P_{eff.}$ Pred.
Acetaminophen	-4.44[56]	-4.08
Caffeine	-4.07[216]	-4.28
Carbamazepine	-4.38[56]	-4.27
Cimetidine	-4.52[249]	-4.60
Diclofenac	-4.75[56]	-4.67
Fenoprofen*	-4.95[230]	-4.65
Fluconazole*	-4.52[246]	-4.15
Flurbiprofen	-4.70[230]	-4.68
Gemfibrozil*	-4.41[246]	-4.59
Haloperidol	-4.79[246]	-4.77
Ibuprofen	-4.58[56]	-4.58
Indomethacin	-4.89[56]	-4.75
Ketoprofen	-4.71[246]	-4.77
Lidocaine	-4.36[56]	-4.46
Linezolid	-5.16[246]	-5.08
Meloxicam	-4.75[246]	-4.85
Naproxen	-4.66[56]	-4.72
Phenylbutazone*	-5.00[250]	-4.71
Piroxicam*	-4.52[246]	-4.62
Quinine	-4.50[246]	-4.488
Theophylline	-4.17[215]	-4.21
Zolmitriptan	-4.26[215]	-4.44

The asterisk (*) indicates the validation compounds.

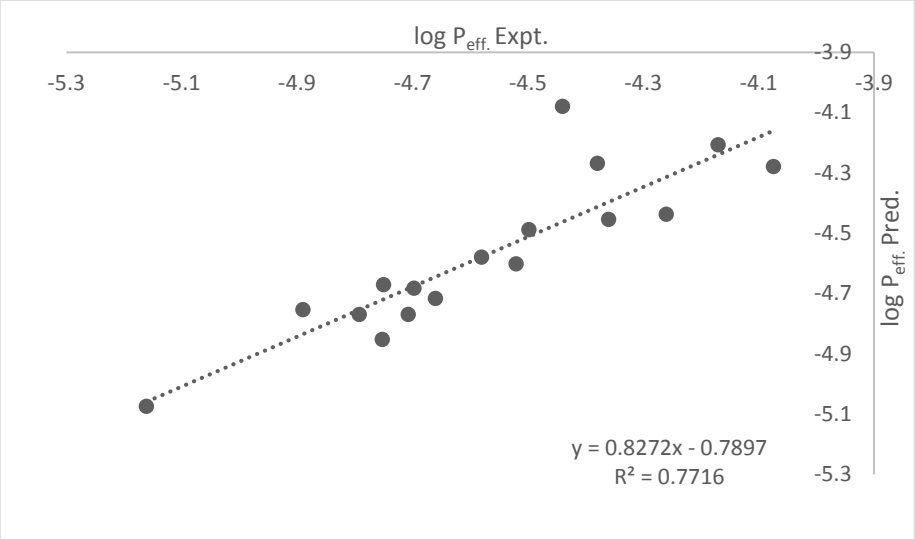

Figure 207: Plot of experimental vs predicted Caco-2 log $P_{eff.}$ values.

Table 122: A summary of molecular descriptors for the selected drugs analysed by permeation method using Franz diffusion cells and the reported experimental values of %HIA and permeability coefficients of PAMPA and Caco-2 tests.

Drug	log K_p*	Mwt[218]	pK_a[184]	S_w[184]	HD[218]	HA[218]	RB[218]	V_M[218]	Log P_o[215]	log $P_{eff.}$	%HIA
Acetaminophen	-4.50	151.20	9.9[220]	14	2	3	1	131.1	-5.81	-4.44[56]	80[205]
Caffeine	-4.49	194.20	14[222]	21.6	0	6	0	133.4	-5.53[298]	-4.074[216]	99[230]
Carbamazepine	-4.08	236.36	13.9	0.21[184, 282]	1[184]	3	0	186.6	-3.73	-4.379[56]	70[209]
Cimetidine	-4.62	252.34	6.8	9.38	3	6	8	198.2	-6.2	-4.52[249]	60[205]
Diclofenac	-5.20	296.20	4.15	0.00237	2	3	4	206.8	-1.37	-4.75[56]	80.5[206, 207]
Fenoprofen	-4.92	242.27	4.5	0.033[218]	1	3	4	204.7	NA	-4.947[230]	85[206]
Fluconazole	-5.14	306.27	12.71	9[283]	1	7	5	205.3	NA	-4.515[246]	94[230]
Flurbiprofen	-4.83	244.26	4.42	0.008	1	2	3	203.6	-1.78	-4.697[230]	95[210]
Fosinopril	-5.58	563.66	-4.4	0.00101	1	8	15	480.4	NA	NA	35[246]
Gemfibrozil	-5.17	250.33	4.5[219]	0.13[284]	1	3	6	239.7	-1.59	-4.407[246]	95[207]
Haloperidol	-4.34	375.86	8.3[296]	0.014	1	3	6	303.3	NI	-4.792[246]	60[245]
Ibuprofen	-4.81	206.30	5.2[223]	0.0684	1	2	4	200.3	-1.15[64]	-4.58[56]	90[207, 231]
Indomethacin	-5.16	357.79	4.5	0.000937	1	5	4	269.6	-1.65	-4.89[56]	98[245]
Ketoprofen	-4.70	254.30	3.88	0.051	1	3	4	212.2	-3.19[64, 215, 281, 295]	-4.707[246]	90[210]
Leflunomide	-4.14	270.21	-0.45	0.021	1	4	3	194.1	NA	NA	80[246]
Lidocaine	-4.78	234.40	7.9[224]	0.2337[285]	1	3	5	238.8	-1.42	-4.36[56]	80.75[209, 210, 230, 252]
Linezolid	-5.11	337.35	-0.66	1.44	1	7	4	259.0	NA	-5.161[246]	100[246]
Meloxicam	-4.88	351.40	4.08	0.00715	2	7	2	220.3	-2.86	-4.752[246]	90[205]
Moexipril	-5.20	498.57	5.2	0.00585	2	9	12	408.1	NA	NA	23[246]
Naproxen	-4.70	230.26	4.15	0.0159	1	3	3	192.3	-2.3	-4.66[56]	96.5[205, 210]
Phenylbutazone	-5.07	308.37	4.4[225]	0.7[219]	0	4	5	262.8	-1.96	-4.998[250]	90[245]
Piroxicam	-5.09	331.35	6.3	0.023	2	7	2	222.8	-3.32	-4.518[246]	99[252]
Quinine	-5.98	324.42	4.2	0.5	1	4	4	266.4	-1.05	-4.498[246]	95[210]
Theophylline	-5.15	180.16	8.8[228]	22.9	1	6	0	122.9	-5.99	-4.17[215]	96[231]
Zolmitriptan	-4.75	287.36	9.52[297]	0.19	2	5	5	236.1	-1.71	-4.26[215]	70.25[246, 294]

*The logarithm is taken for the K_p value (cm/sec), NA: no available data, NI: value not included in training set.

5.B.3. Conclusion

Determination of K_p from the permeation of a number of compounds using Franz diffusion cells was found to be a successful method for prediction of human intestinal absorption and permeability coefficients obtained from other *in vitro* methods. Overall, the two permeation methods yielded highly predictive models for both the *in vivo* %HIA and *in vitro* Caco-2 and PAMPA permeability coefficients. Although Franz cells presented a cheaper option, flow through cells could be considered as a better method as it requires less volumes of buffer solution and tested samples in addition to the easier sample collection.

CHAPTER 6

Conclusions & Future Work

Chapter 6: Conclusions and future work

The aims of the work carried out in this thesis can be summarised as follows:

a) **The first aim** was to develop an MLC method for the determination of log P_{mw} for a set of compounds using biosurfactants such as bile salts, which are unlike conventional synthetic surfactants, in order to mimic the physiological conditions in the intestine to predict human intestinal absorption and other related permeability coefficients obtained from *in vitro* methods such as Caco-2 and PAMPA.

This aim was achieved in Chapter 3 (section A, B, C and E) where different MLC methods were developed using different types of bile salts. The use of different bile salts led to obtaining different patterns of binding of the analysed compounds to the bile salt formed micelles which could be as a result of their different structures and hydropohobocities which affect their micellisation and the way they behave in the presence of some of the analysed compounds in the medium. The different MLC methods that were developed in this work have successfully led to the development of models useful in the prediction of human intestinal absorption (%HIA) and permeability coefficients in Caco-2 and PAMPA. These developed MLC methods are very useful in acting as a replacement for the use of animals in experiments performed for determination of compounds' absorption in the intestine where animals have always been considered to be the best mimics for humans in such experiments. Also it saves time and money as it can be used in preformulation studies for determination of the absorption of new drug entities (NDE) before getting to the clinical stage. This would otherwise waste a lot of money if the drug entered the clinical stage and turned out not to be suitable for oral administration because of poor oral absorption. After using a single component bile salt system as a mobile phase in MLC, such as the individual use of NADC, NATDC and NaC as a mobile phase, an attempt to investigate the use of a multiple component bile salt system with lecithin included in the system was carried out. This was because of the similarity to the intestinal membrane bilayer due to the formation of mixed micelles with a larger diameter and fluidic core capable of incorporating and solubilising compounds inside even if it was of opposite charge to that of the mixed micelles where the net surface charge on these micelles was much less than that of the simple micelles. Using the mixed micellar system provided a better

mimic to the physiological conditions inside the intestine therefore providing better prediction of %HIA. The use of such a system led to a change for most drugs to the binding behaviour, confirming better solubilisation of drugs in the core of the mixed micelles.

b) **The second aim** was to investigate the effect of using another type of chromatographic column such as an amino column on the partitioning of the analysed compounds.

The aim was achieved by the developed method using NaDC as a mobile phase and the amino column used as a stationary phase that led to a change in the binding behaviour of some of the analysed compounds. This was mostly to antibinding behaviour because of the special interaction between the micelles and the column that led to the formation of a bilayer like network of bile salts on the surface of the column. A reliable model capable of predicting HIA was obtained using the log P_{mw} calculated from this method.

c) **The third aim** was to study the thermodynamics of NaDC binding to the analysed compounds with the change in temperature.

The result of the study was interesting as the nonlinear vant's Hoff plots proved that the micellar interaction with the analysed compounds and their partitioning into the micelles was a complex process due to the natural source of the bile salt surfactants which confirms the need to further investigate the nature of the thermodynamic interaction between the bile salt micelles and the analysed compounds, also to investigate such interaction in the mixed micellar systems as well.

d) **The fourth aim** was to develop a simple spectrophotometric method using a simple NaDC micellar system for determination of micelle-water partition coefficients and their use in the prediction of %HIA.

This aim was achieved where two spectrophotometric methods were developed depending on the use of the solubilising capacity of NaDC micelles and also the binding of NaDC micelles to the analysed compounds. The developed solubilisation spectrophotometric method was more successful than the double reciprocal method in the prediction of %HIA. This method can play an important role in reducing or even replacing the use of animals in experiments for the determination of a drugs absorption properties.

e) **The fifth aim** was to develop permeation methods using Franz and flow through cells with a prepared NaDC hydrogel as a membrane to determine the

permeability coefficient (K_p) for a series of compounds and their use in prediction of %HIA.

The aim was achieved by the use of NaDC hydrogel of optimum concentration which led to developing models for prediction of %HIA with high predictability. This method is the first method to use bile salt hydrogels and also Franz and flow through cells in the prediction of intestinal absorption. Like the other developed methods in this thesis it is considered a simple, rapid and cost effective method that can contribute to the reduction of the use of animals in experimentation.

All the obtained models with a good predictive ability were found to cover compounds with a wide variety of physicochemical properties, which reflects that these models can be applied to a wide range of compounds. However, most of the compounds included in the development of these models were found to be of relatively low aqueous solubility, especially those involved in the solubilisation method.

It was observed that compounds of relatively higher aqueous solubility, for example salicylic acid, caffeine and nicotinic acid, were excluded from the development of most prediction models because they were considered as outliers although these compounds were included in the development of some prediction models. This could be a result of compounds behaving differently in each experimental method, such as the use of different bile salts which exhibit different characteristics, such as solubilising capacities, as discussed in Chapter 3 (sections A-D). Further analysis was undertaken to investigate alternative potential relationships yet none of significance could be found. Therefore, it can be concluded that the developed predictive models worked well for specific groups of compounds yet there was not one specific overall model that could be applied to encompass all compounds considered.

In summary, all the aims of the thesis were successfully fulfilled by providing promising and reliable replacement methods to animal testing that can save time and money.

Future work

The overall aim of this project was to develop an *in vitro* method to predict human intestinal absorption.

Although many of the methods developed show a promise (and have the potential to be adopted by industry to replace animal testing), more research is still required. In order of priority, the six main avenues for future research are:

- Investigating the use of other types of columns (monolithic, HILIC and polymeric) for the determination of log P_{mw} of compounds using micellar liquid chromatography could be useful in detecting other patterns of binding of compounds to micelles and the column and its effect on the determination of human intestinal absorption.
- Expanding the applications of MLC to the prediction of other pharmacokinetic parameters by using other biologically relevant compounds such as using the physiological surfactant system found in human lungs for prediction of pulmonary absorption of drugs administered through the pulmonary route.
- Using other types of bile salts in the prediction of human intestinal absorption such as chenodeoxycholate, glycochenodeoxycholate and lithocholate.
- Use of isothermal calorimetry (ITC) to further study the binding of compounds to bile salt micelles and to provide a better understanding of the characteristic micellisation behaviour of bile salts.
- Further studying of the thermodynamics of compounds binding to bile salt micelles in MLC using a larger set of compounds and wider range of temperatures such as expanding to the range of temperatures less than 25 ºC taking in to consideration not to go below the Krafft temperature of the studied bile salt.
- Studying the permeation of drugs available on the market through prepared bile salt hydrogels using diffusion cells and its correlation with the already developed method.

References

References

1. Prentis, R., Y. Lis, and S. Walker, *Pharmaceutical innovation by the seven UK-owned pharmaceutical companies (1964-1985).* British journal of clinical pharmacology, 1988. **25**(3): p. 387-396.
2. Kennedy, T., *Managing the drug discovery/development interface.* Drug discovery today, 1997. **2**(10): p. 436-444.
3. Venkatesh, S. and R.A. Lipper, *Role of the development scientist in compound lead selection and optimization.* Journal of pharmaceutical sciences, 2000. **89**(2): p. 145-154.
4. Arlington, S., *Pharma 2005-An industrial revolution in R&D.* Pharmaceutical Executive, 2000. **20**(1): p. 74-85.
5. Testa, B. and J. Caldwell, *Prodrugs revisited: the "ad hoc" approach as a complement to ligand design.* Medicinal research reviews, 1996. **16**(3): p. 233-241.
6. Amidon, G.L., H. Lennernäs, V.P. Shah, and J.R. Crison, *A theoretical basis for a biopharmaceutic drug classification: the correlation of in vitro drug product dissolution and in vivo bioavailability.* Pharmaceutical research, 1995. **12**(3): p. 413-420.
7. Johnson, K.C. and A.C. Swindell, *Guidance in the setting of drug particle size specifications to minimize variability in absorption.* Pharmaceutical research, 1996. **13**(12): p. 1795-1798.
8. Norris, D., G. Leesman, P. Sinko, and G. Grass, *Development of predictive pharmacokinetic simulation models for drug discovery.* Journal of controlled release, 2000. **65**(1): p. 55-62.
9. Mishra, A. and G.K. Makharia, *Techniques of functional and motility test: how to perform and interpret intestinal permeability.* J Neurogastroenterol Motil, 2012. **18**(4): p. 443-447.
10. Singer, S. and G.L. Nicolson, *The fluid mosaic model of the structure of cell membranes.* Membranes and Viruses in Immunopathology; Day, SB, Good, RA, Eds, 1972: p. 7-47.
11. Gorter, E. and F. Grendel, *On bimolecular layers of lipoids on the chromocytes of the blood.* The Journal of experimental medicine, 1925. **41**(4): p. 439.
12. https://en.wikipedia.org/wiki/Cell_membrane, 3 April, 2017.
13. Muranishi, S., *Absorption enhancers.* Critical reviews in therapeutic drug carrier systems, 1989. **7**(1): p. 1-33.
14. Stenberg, P., K. Luthman, and P. Artursson, *Virtual screening of intestinal drug permeability.* Journal of Controlled Release, 2000. **65**(1): p. 231-243.
15. Krämer, S.D., *Absorption prediction from physicochemical parameters.* Pharmaceutical science & technology today, 1999. **2**(9): p. 373-380.
16. Clark, D.E. and S.D. Pickett, *Computational methods for the prediction of 'drug-likeness'.* Drug discovery today, 2000. **5**(2): p. 49-58.
17. Pappenheimer, J. and K.Z. Reiss, *Contribution of solvent drag through intercellular junctions to absorption of nutrients by the small intestine of the rat.* Journal of Membrane Biology, 1987. **100**(1): p. 123-136.
18. Nellans, H.N., *(B) Mechanisms of peptide and protein absorption:(1) Paracellular intestinal transport: modulation of absorption.* Advanced drug delivery reviews, 1991. **7**(3): p. 339-364.
19. Diamond, J.M., *Twenty-first Bowditch lecture.* The epithelial junction: bridge, gate, and fence. Physiologist20, 1977: p. 10-18.
20. Madara, J.L., *Loosening tight junctions. Lessons from the intestine.* Journal of Clinical Investigation, 1989. **83**(4): p. 1089.
21. Tanaka, H., K.i. Miyamoto, K. Morita, H. Haga, H. Segawa, T. Shiraga, A. Fujioka, T. Kouda, Y. Taketani, and S. Hisano, *Regulation of the PepT1 peptide transporter in the*

rat small intestine in response to 5-fluorouracil–induced injury. Gastroenterology, 1998. **114**(4): p. 714-723.
22. Swaan, P.W., *Recent advances in intestinal macromolecular drug delivery via receptor-mediated transport pathways.* Pharmaceutical research, 1998. **15**(6): p. 826-834.
23. Hunter, J. and B.H. Hirst, *Intestinal secretion of drugs. The role of P-glycoprotein and related drug efflux systems in limiting oral drug absorption.* Advanced drug delivery reviews, 1997. **25**(2): p. 129-157.
24. Borst, P., R. Evers, M. Kool, and J. Wijnholds, *A family of drug transporters: the multidrug resistance-associated proteins.* Journal of the National Cancer Institute, 2000. **92**(16): p. 1295-1302.
25. Suzuki, H. and Y. Sugiyama, *Role of metabolic enzymes and efflux transporters in the absorption of drugs from the small intestine.* European journal of pharmaceutical sciences, 2000. **12**(1): p. 3-12.
26. Ambudkar, S.V., S. Dey, C.A. Hrycyna, M. Ramachandra, I. Pastan, and M.M. Gottesman, *Biochemical, cellular, and pharmacological aspects of the multidrug transporter 1.* Annual review of pharmacology and toxicology, 1999. **39**(1): p. 361-398.
27. Brandl, M., G. Eide Flaten, and A. Bauer-Brandl, *Passive diffusion across membranes.* Wiley Encyclopedia of Chemical Biology, 2009.
28. Stenberg, P., *Computational models for the prediction of intestinal membrane permeability*. 2001, Acta Universitatis Upsaliensis.
29. Balimane, P.V., Y.-H. Han, and S. Chong, *Current industrial practices of assessing permeability and P-glycoprotein interaction.* The AAPS journal, 2006. **8**(1): p. E1-E13.
30. Deferme, S., P. Annaert, and P. Augustijns, *In vitro screening models to assess intestinal drug absorption and metabolism*, in *Drug absorption studies*. 2008, Springer. p. 182-215.
31. Erlejman, A., C. Fraga, and P.I. Oteiza. *CACO-2 Cells and Their Uses*. in *Nova Science Publishers, Inc.* 2011.
32. Le Ferrec, E., C. Chesne, P. Artusson, D. Brayden, G. Fabre, P. Gires, F. Guillou, M. Rousset, W. Rubas, and M.-L. Scarino, *In vitro models of the intestinal barrier.* Atla, 2001. **29**: p. 649-668.
33. Kansy, M., F. Senner, and K. Gubernator, *Physicochemical high throughput screening: parallel artificial membrane permeation assay in the description of passive absorption processes.* Journal of medicinal chemistry, 1998. **41**(7): p. 1007-1010.
34. Thompson, M., U. Krull, and P. Worsfold, *The structure and electrochemical properties of a polymer-supported lipid biosensor.* Analytica Chimica Acta, 1980. **117**: p. 133-145.
35. http://pharmacokinetics.wixsite.com/paba/research-areas, 9th April, 2017.
36. Ussing, H.H. and K. Zerahn, *Active Transport of Sodium as the Source of Electric Current in the Short-circuited Isolated Frog Skin.* Acta Physiologica, 1951. **23**(2-3): p. 110-127.
37. Grass, G.M. and S.A. Sweetana, *In vitro measurement of gastrointestinal tissue permeability using a new diffusion cell.* Pharmaceutical research, 1988. **5**(6): p. 372-376.
38. Ungell, A.-L., *In vitro absorption studies and their relevance to absorption from the GI tract.* Drug development and industrial pharmacy, 1997. **23**(9): p. 879-892.
39. Deferme, S., R. Mols, W.V. Driessche, and P. Augustijns, *Apricot extract inhibits the P-gp–mediated efflux of talinolol.* Journal of pharmaceutical sciences, 2002. **91**(12): p. 2539-2548.
40. Larsson, J., N. Pantzar, J. Permert, and G. Olaison, *Integrity and metabolism of human ileal mucosa in vitro in the Ussing chamber.* Acta Physiol. Scand, 1998. **162**: p. 47-56.
41. Neirinckx, E., *Towards a veterinary biopharmaceutics classification system: oral bioavailability and ex vivo intestinal permeability studies of paracetamol and ketoprofen in different animal species*. 2010, Ghent University.

42. Rogers, S.M., D. Back, and M. Orme, *Intestinal metabolism of ethinyloestradiol and paracetamol in vitro: studies using Ussing chambers.* British journal of clinical pharmacology, 1987. **23**(6): p. 727-734.
43. Smith, P., C. Mirabelli, J. Fondacaro, F. Ryan, and J. Dent, *Intestinal 5-fluorouracil absorption: Use of Ussing chambers to assess transport and metabolism.* Pharmaceutical research, 1988. **5**(9): p. 598-603.
44. Annaert, P., J.J. Tukker, J. Van Gelder, L. Naesens, E. De Clercq, G. Van den Mooter, R. Kinget, and P. Augustijns, *In vitro, ex vivo, and in situ intestinal absorption characteristics of the antiviral ester prodrug adefovir dipivoxil.* Journal of pharmaceutical sciences, 2000. **89**(8): p. 1054-1062.
45. Araya, H., M. Tomita, and M. Hayashi, *The novel formulation design of self-emulsifying drug delivery systems (SEDDS) type O/W microemulsion III: the permeation mechanism of a poorly water soluble drug entrapped O/W microemulsion in rat isolated intestinal membrane by the Ussing chamber method.* Drug metabolism and pharmacokinetics, 2006. **21**(1): p. 45-53.
46. Koga, K., S. Kawashima, and M. Murakami, *In vitro and in situ evidence for the contribution of Labrasol® and Gelucire 44/14 on transport of cephalexin and cefoperazone by rat intestine.* European Journal of Pharmaceutics and Biopharmaceutics, 2002. **54**(3): p. 311-318.
47. Shen, Q., Y. Lin, T. Handa, M. Doi, M. Sugie, K. Wakayama, N. Okada, T. Fujita, and A. Yamamoto, *Modulation of intestinal P-glycoprotein function by polyethylene glycols and their derivatives by in vitro transport and in situ absorption studies.* International journal of pharmaceutics, 2006. **313**(1): p. 49-56.
48. Söderholm, J.D., K.H. Peterson, G. Olaison, L.E. Franzén, B. Weström, K.-E. Magnusson, and R. Sjödahl, *Epithelial permeability to proteins in the noninflamed ileum of Crohn's disease?* Gastroenterology, 1999. **117**(1): p. 65-72.
49. Ungell, A., *Transport studies using intestinal tissue ex-vivo*, in *Cell culture models of biological barriers: In vitro test systems for drug absorption and delivery*. 2002, Taylor & Francis, New York. p. 164-188.
50. Yamashita, S., Y. Tanaka, Y. Endoh, Y. Taki, T. Sakane, T. Nadai, and H. Sezaki, *Analysis of drug permeation across Caco-2 monolayer: implication for predicting in vivo drug absorption.* Pharmaceutical research, 1997. **14**(4): p. 486-491.
51. Lennernäs, H., *Human intestinal permeability.* Journal of pharmaceutical sciences, 1998. **87**(4): p. 403-410.
52. Yuasa, H., K. Matsuda, and J. Watanabe, *Influence of anesthetic regimens on intestinal absorption in rats.* Pharmaceutical research, 1993. **10**(6): p. 884-888.
53. Balimane, P.V., S. Chong, and R.A. Morrison, *Current methodologies used for evaluation of intestinal permeability and absorption.* Journal of pharmacological and toxicological methods, 2000. **44**(1): p. 301-312.
54. Barthe, L., J. Woodley, and G. Houin, *Gastrointestinal absorption of drugs: methods and studies.* Fundamental & clinical pharmacology, 1999. **13**(2): p. 154-168.
55. Alam, M.A., F.I. Al-Jenoobi, and A.M. Al-mohizea, *Everted gut sac model as a tool in pharmaceutical research: limitations and applications.* Journal of Pharmacy and Pharmacology, 2012. **64**(3): p. 326-336.
56. Paixão, P., L.F. Gouveia, and J.A. Morais, *Prediction of the in vitro permeability determined in Caco-2 cells by using artificial neural networks.* European Journal of Pharmaceutical Sciences, 2010. **41**(1): p. 107-117.
57. Thomas, S., F. Brightman, H. Gill, S. Lee, and B. Pufong, *Simulation modelling of human intestinal absorption using Caco-2 permeability and kinetic solubility data for early drug discovery.* Journal of pharmaceutical sciences, 2008. **97**(10): p. 4557-4574.
58. Camenisch, G., G. Folkers, and H. van de Waterbeemd, *Comparison of passive drug transport through Caco-2 cells and artificial membranes.* International journal of pharmaceutics, 1997. **147**(1): p. 61-70.

59. Subramanian, G. and D.B. Kitchen, *Computational approaches for modeling human intestinal absorption and permeability.* Journal of molecular modeling, 2006. **12**(5): p. 577.
60. Hou, T., W. Zhang, K. Xia, X. Qiao, and X. Xu, *ADME evaluation in drug discovery. 5. Correlation of Caco-2 permeation with simple molecular properties.* Journal of chemical information and computer sciences, 2004. **44**(5): p. 1585-1600.
61. Reynolds, D.P., K. Lanevskij, P. Japertas, R. Didziapetris, and A. Petrauskas, *Ionization-specific analysis of human intestinal absorption.* Journal of pharmaceutical sciences, 2009. **98**(11): p. 4039-4054.
62. Bujard, A., M. Sol, P.-A. Carrupt, and S. Martel, *Predicting both passive intestinal absorption and the dissociation constant toward albumin using the PAMPA technique.* European Journal of Pharmaceutical Sciences, 2014. **63**: p. 36-44.
63. Zhu, C., L. Jiang, T.-M. Chen, and K.-K. Hwang, *A comparative study of artificial membrane permeability assay for high throughput profiling of drug absorption potential.* European journal of medicinal chemistry, 2002. **37**(5): p. 399-407.
64. Akamatsu, M., M. Fujikawa, K. Nakao, and R. Shimizu, *In silico prediction of human oral absorption based on QSAR analyses of PAMPA permeability.* Chemistry & biodiversity, 2009. **6**(11): p. 1845-1866.
65. Nielsen, P.E. and A. Avdeef, *PAMPA—a drug absorption in vitro model: 8. Apparent filter porosity and the unstirred water layer.* European journal of pharmaceutical sciences, 2004. **22**(1): p. 33-41.
66. Kim, J.-S., S. Mitchell, P. Kijek, Y. Tsume, J. Hilfinger, and G.L. Amidon, *The suitability of an in situ perfusion model for permeability determinations: utility for BCS class I biowaiver requests.* Molecular pharmaceutics, 2006. **3**(6): p. 686-694.
67. Zakeri-Milani, P., H. Valizadeh, H. Tajerzadeh, Y. Azarmi, Z. Islambolchilar, S. Barzegar, and M. Barzegar-Jalali, *Predicting human intestinal permeability using single-pass intestinal perfusion in rat.* J Pharm Pharm Sci, 2007. **10**(3): p. 368-379.
68. Sun, L., X. Liu, R. Xiang, C. Wu, Y. Wang, Y. Sun, J. Sun, and Z. He, *Structure-based prediction of human intestinal membrane permeability for rapid in silico BCS classification.* Biopharmaceutics & drug disposition, 2013. **34**(6): p. 321-335.
69. Ekins, S., J. Mestres, and B. Testa, *In silico pharmacology for drug discovery: applications to targets and beyond.* British journal of pharmacology, 2007. **152**(1): p. 21-37.
70. Sahitya, G., B. Krishnamoorthy, and M. Muthukumaran, *Importance of preformulation studies in designing formulations for sustained release dosage forms.* International Journal Of Pharmacy&Technology, 2013. **4**(4): p. 2311-2331.
71. Guy, R.H., J. Hadgraft, and D.A. Bucks, *Transdermal drug delivery and cutaneous metabolism.* Xenobiotica, 1987. **17**(3): p. 325-343.
72. Rutkowska, E., K. PajIk, and K. Jóźwiak, *Lipophilicity methods of determination and its role in medicinal chemistry.* Acta poloniae pharmaceutica, 2012. **70**(1): p. 3-18.
73. Scott, D.C. and J.W. Clymer, *Estimation of Distribution Coefficients from the Partition Coefficient and pKa.* Pharmaceutical technology, 2002: p. 30-40.
74. Lipinski, C.A., F. Lombardo, B.W. Dominy, and P.J. Feeney, *Experimental and computational approaches to estimate solubility and permeability in drug discovery and development settings.* Adv Drug Deliv Rev, 2001. **46**(1-3): p. 3-26.
75. Scherrer, R.A. and S.M. Howard, *Use of distribution coefficients in quantitative structure-activity relations.* Journal of medicinal chemistry, 1977. **20**(1): p. 53-58.
76. Sangster, J., *Octanol-water partition coefficients of simple organic compounds.* Journal of Physical and Chemical Reference Data, 1989. **18**(3): p. 1111-1229.
77. Lyman, W.J., *Octanol/water partition coefficient.* IN: Handbook of Chemical Property Estimation Methods: Environmental Behavior of Organic Compounds. American Chemical Society, Washington, DC. 1990. p 1. 1-1. 54. 1 fig, 11 tab, 48 ref., 1990.
78. Berthod, A. and S. Carda-Broch, *Determination of liquid–liquid partition coefficients by separation methods.* Journal of Chromatography A, 2004. **1037**(1-2): p. 3-14.

79. Saghaie, L. and R.C.H.S.A. Mostafavi, *Comparison of automated continuous flow method with shake-flask method in determining partition coefficients of bidentate hydroxypyridinone ligands.* DARU Journal of Pharmaceutical Sciences, 2003. **11**(2): p. 38-46.
80. Brooke, D., A. Dobbs, and N. Williams, *Octanol: water partition coefficients (P): measurement, estimation, and interpretation, particularly for chemicals with P greater than 10 (5).* Ecotoxicology and environmental safety, 1986. **11**(3): p. 251.
81. De Bruijn, J., F. Busser, W. Seinen, and J. Hermens, *Determination of octanol/water partition coefficients for hydrophobic organic chemicals with the "slow-stirring" method.* Environmental Toxicology and Chemistry, 1989. **8**(6): p. 499-512.
82. DeVito, S.C. and C.A. Farris, *Premanufacture Notification: Chemistry Assistance for Submitters*. 1997: John Wiley & Sons. 53-54.
83. Doucette, W.J. and A.W. Andren, *Correlation of octanol/water partition coefficients and total molecular surface area for highly hydrophobic aromatic compounds.* Environmental science & technology, 1987. **21**(8): p. 821-824.
84. Doucette, W. and A. Andren, *Estimation of octanol/water partition coefficients: Evaluation of six methods for highly hydrophobic aromatic hydrocarbons.* Chemosphere, 1988. **17**(2): p. 345-359.
85. Shiu, W.Y., W. Doucette, F.A. Gobas, A. Andren, and D. Mackay, *Physical-chemical properties of chlorinated dibenzo-p-dioxins.* Environmental science & technology, 1988. **22**(6): p. 651-658.
86. Comer, J., K. Tam, B. Testa, H. van de Waterbeemd, G. Folkers, and R. Guy, *Pharmacokinetic optimization in drug research: Biological, physicochemical, and computational strategies.* Switzerland: Wiley-VCH, 2001: p. 275-304.
87. Avdeef, A., *Absorption and drug development: solubility, permeability and charge state.* 2003: p. 55-58.
88. Berthod, A. and S. Carda-Broch, *Determination of liquid–liquid partition coefficients by separation methods.* Journal of Chromatography A, 2004. **1037**(1): p. 3-14.
89. Leo, A.J. and C. Hansch, *Role of hydrophobic effects in mechanistic QSAR.* Perspectives in Drug Discovery and Design, 1999. **17**(1): p. 1-25.
90. Hansch, C. and A. Leo, *Exploring QSAR, Fundamentals and Applications in Chemistry and Biology. 1995.* ACS, Washington, USA: p. 392-403.
91. Van de Waterbeemd, H. and E. Gifford, *ADMET in silico modelling: towards prediction paradise?* Nature reviews Drug discovery, 2003. **2**(3): p. 192-204.
92. Wildman, S.A. and G.M. Crippen, *Prediction of physicochemical parameters by atomic contributions.* Journal of chemical information and computer sciences, 1999. **39**(5): p. 868-873.
93. Mannhold, R., G.I. Poda, C. Ostermann, and I.V. Tetko, *Calculation of molecular lipophilicity: state-of-the-art and comparison of log P methods on more than 96,000 compounds.* Journal of pharmaceutical sciences, 2009. **98**(3): p. 861-893.
94. Xie, X., *Molecular modeling and in silico drug design.* et al., Foye's Principles of Medicinal Chemistry, Lippincott Williams & Wilkins, Philadelphia, 2008: p. 79.
95. Hansch, C., A. Leo, and D. Hoekman, *Exploring QSAR: Volume 2: Hydrophobic, Electronic, And Steric Constants (Hydrophobic, Electronic & Steric Constants).* 1995.
96. Hansch, C. and A. Leo, *Substituent constants for correlation analysis in chemistry and biology*. 1979: Wiley.
97. Cheng, T., Y. Zhao, X. Li, F. Lin, Y. Xu, X. Zhang, Y. Li, R. Wang, and L. Lai, *Computation of octanol-water partition coefficients by guiding an additive model with knowledge.* Journal of chemical information and modeling, 2007. **47**(6): p. 2140-2148.
98. Mannhold, R. and A. Petrauskas, *Substructure versus whole-molecule approaches for calculating log P.* QSAR & Combinatorial Science, 2003. **22**(4): p. 466-475.
99. Viswanadhan, V.N., A.K. Ghose, and J.J. Wendoloski, *Estimating aqueous solvation and lipophilicity of small organic molecules: A comparative overview of atom/group contribution methods.* Perspectives in drug discovery and design, 2000. **19**(1): p. 85-98.

100. Poole, S.K. and C.F. Poole, *Separation methods for estimating octanol–water partition coefficients.* Journal of Chromatography B, 2003. **797**(1): p. 3-19.
101. Müller, L., P. Bednář, P. Barták, K. Lemr, and J. Ševčík, *Estimation of partition coefficients by MEKC Part 2: Anthocyanins.* Journal of separation science, 2005. **28**(12): p. 1285-1290.
102. Gavenda, A., P. Bednář, P. Barták, P. Adamovský, J. Ševčík, P. Tzoumas, and J. Ulrichová, *Estimation of partition coefficients by MEKC Part I: Potential pharmaceuticals based on 2-quinolone and 2-indolone.* Journal of separation science, 2001. **24**(9): p. 723-728.
103. Ibrahim, W.A.W., D. Hermawan, M.N. Hasan, H.Y.A. Enein, and M.M. Sanagi, *Rapid Estimation of Octanol–Water Partition Coefficient for Triazole Fungicides by MEKC with Sodium Deoxycholate as Surfactant.* Chromatographia, 2008. **68**(5-6): p. 415-419.
104. Poole, S.K., D. Durham, and C. Kibbey, *Rapid method for estimating the octanol–water partition coefficient (log Pow) by microemulsion electrokinetic chromatography.* Journal of Chromatography B: Biomedical Sciences and Applications, 2000. **745**(1): p. 117-126.
105. Poole, S.K., S. Patel, K. Dehring, H. Workman, and J. Dong, *Estimation of octanol–water partition coefficients for neutral and weakly acidic compounds by microemulsion electrokinetic chromatography using dynamically coated capillary columns.* Journal of Chromatography B, 2003. **793**(2): p. 265-274.
106. Jia, Z., L. Mei, F. Lin, S. Huang, and R.B. Killion, *Screening of octanol–water partition coefficients for pharmaceuticals by pressure-assisted microemulsion electrokinetic chromatography.* Journal of Chromatography A, 2003. **1007**(1–2): p. 203-208.
107. Ishihama, Y., Y. Oda, K. Uchikawa, and N. Asakawa, *Evaluation of solute hydrophobicity by microemulsion electrokinetic chromatography.* Analytical Chemistry, 1995. **67**(9): p. 1588-1595.
108. Schmitt-Kopplin, P., *Capillary electrophoresis: methods and protocols*. Vol. 384. 2008: Springer.
109. de Castro, B., P. Gameiro, C. Guimarães, J.L. Lima, and S. Reis, *Study of partition of nitrazepam in bile salt micelles and the role of lecithin.* Journal of pharmaceutical and biomedical analysis, 2001. **24**(4): p. 595-602.
110. de Castro, B., P. Gameiro, C. Guimarães, J.L. Lima, and S. Reis, *Partition coefficients of β-blockers in bile salt/lecithin micelles as a tool to assess the role of mixed micelles in gastrointestinal absorption.* Biophysical chemistry, 2001. **90**(1): p. 31-43.
111. Kleyle, R.M., D. Nurok, A.D. Kossoy, and S.C. Burris, *Novel computational methods for the determination of partition coefficients by planar chromatography.* Journal of Chromatography A, 1996. **749**(1): p. 211-217.
112. Biagi, G., A. Barbaro, A. Sapone, and M. Recanatini, *Determination of lipophilicity by means of reversed-phase thin-layer chromatography: II. Influence of the organic modifier on the slope of the thin-layer chromatographic equation.* Journal of Chromatography A, 1994. **669**(1): p. 246-253.
113. Biagi, G., A. Barbaro, A. Sapone, and M. Recanatini, *Determination of lipophilicity by means of reversed-phase thin-layer chromatography: I. Basic aspects and relationship between slope and intercept of TLC equations.* Journal of Chromatography A, 1994. **662**(2): p. 341-361.
114. Wang, Q., L. Zhang, H. Yang, and H. Liu, *Lipophilicity determination of some potential photosystem ii inhibitors on reversed-phase high-performance thin-layer chromatography.* Journal of chromatographic science, 1999. **37**(2): p. 41-44.
115. Ong, S., H. Liu, and C. Pidgeon, *Immobilized-artificial-membrane chromatography: measurements of membrane partition coefficient and predicting drug membrane permeability.* Journal of Chromatography A, 1996. **728**(1): p. 113-128.
116. Pidgeon, C., S. Ong, H. Liu, X. Qiu, M. Pidgeon, A.H. Dantzig, J. Munroe, W.J. Hornback, and J.S. Kasher, *IAM chromatography: an in vitro screen for predicting drug membrane permeability.* Journal of Medicinal Chemistry, 1995. **38**(4): p. 590-594.

117. Genty, M., G. Gonzalez, C. Clere, V. Desangle-Gouty, and J.-Y. Legendre, *Determination of the passive absorption through the rat intestine using chromatographic indices and molar volume.* European journal of pharmaceutical sciences, 2001. **12**(3): p. 223-229.
118. Ducarme, A., M. Neuwels, S. Goldstein, and R. Massingham, *IAM retention and blood brain barrier penetration.* European journal of medicinal chemistry, 1998. **33**(3): p. 215-223.
119. Reichel, A. and D.J. Begley, *Potential of immobilized artificial membranes for predicting drug penetration across the blood− brain barrier.* Pharmaceutical research, 1998. **15**(8): p. 1270-1274.
120. Nasal, A., M. Sznitowska, A. Buciński, and R. Kaliszan, *Hydrophobicity parameter from high-performance liquid chromatography on an immobilized artificial membrane column and its relationship to bioactivity.* Journal of Chromatography A, 1995. **692**(1): p. 83-89.
121. Barbato, F., B. Cappello, A. Miro, M. La Rotonda, and F. Quaglia, *Chromatographic indexes on immobilized artificial membranes for the prediction of transdermal transport of drugs.* Il Farmaco, 1998. **53**(10): p. 655-661.
122. Stewart, B.H. and O. Helen Chan, *Use of immobilized artificial membrane chromatography for drug transport applications.* Journal of pharmaceutical sciences, 1998. **87**(12): p. 1471-1478.
123. Pidgeon, C. and U. Venkataram, *Immobilized artificial membrane chromatography: supports composed of membrane lipids.* Analytical biochemistry, 1989. **176**(1): p. 36-47.
124. Chan, E., W. Tan, P. Ho, and L. Fang, *Modeling Caco-2 permeability of drugs using immobilized artificial membrane chromatography and physicochemical descriptors.* Journal of Chromatography A, 2005. **1072**(2): p. 159-168.
125. Liu, X.-Y., C. Nakamura, Q. Yang, N. Kamo, and J. Miyake, *Immobilized liposome chromatography to study drug–membrane interactions: correlation with drug absorption in humans.* Journal of Chromatography A, 2002. **961**(1): p. 113-118.
126. Ong, S., H. Liu, X. Qiu, G. Bhat, and C. Pidgeon, *Membrane partition coefficients chromatographically measured using immobilized artificial membrane surfaces.* Analytical chemistry, 1995. **67**(4): p. 755-762.
127. Thurnhofer, H., J. Schnabel, M. Betz, G. Lipka, C. Pidgeon, and H. Hauser, *Cholesterol-transfer protein located in the intestinal brush-border membrane. Partial purification and characterization.* Biochimica et Biophysica Acta (BBA)-Biomembranes, 1991. **1064**(2): p. 275-286.
128. Pidgeon, C., S.J. Cai, and C. Bernal, *Mobile phase effects on membrane protein elution during immobilized artificial membrane chromatography.* Journal of Chromatography A, 1996. **721**(2): p. 213-230.
129. OTTO, S., C. MARCUS, C. PIDGEON, and C. JEFCOATE, *A Novel Adrenocorticotropin-Inducible Cytochrome P450 from Rat Adrenal Microsomes Catalyzes Polycylic Aromatic Hydrocarbon Metabolism*.* Endocrinology, 1991. **129**(2): p. 970-982.
130. Pidgeon, C., J. Stevens, S. Otto, C. Jefcoate, and C. Marcus, *Immobilized artificial membrane chromatography: rapid purification of functional membrane proteins.* Analytical biochemistry, 1991. **194**(1): p. 163-173.
131. Chui, W.-K. and I.W. Wainer, *Enzyme-based high-performance liquid chromatography supports as probes of enzyme activity and inhibition: the immobilization of trypsin and α-chymotrypsin on an immobilized artificial membrane high-performance liquid chromatography support.* Analytical biochemistry, 1992. **201**(2): p. 237-245.
132. Xiao-Ming, Z. and I.W. Wainer, *On-line determination of lipase activity and enantioselectivity using an immobilized enzyme reactor coupled to a chiral stationary phase.* Tetrahedron letters, 1993. **34**(30): p. 4731-4734.

133. Kallury, K.M.R., W.E. Lee, and M. Thompson, *Enhancement of the thermal and storage stability of urease by covalent attachment to phospholipid-bound silica.* Analytical Chemistry, 1992. **64**(9): p. 1062-1068.
134. Rutkowska, E., K. Pajak, and K. Jóźwiak, *Lipophilicity--methods of determination and its role in medicinal chemistry.* Acta poloniae pharmaceutica, 2012. **70**(1): p. 3-18.
135. Rutkowska, E., K. PajIk, and K. Jóźwiak, *Lipophilicity--methods of determination and its role in medicinal chemistry.* Acta poloniae pharmaceutica, 2012. **70**(1): p. 3-18.
136. Lundahl, P. and F. Beigi, *Immobilized liposome chromatography of drugs for model analysis of drug-membrane interactions.* Advanced drug delivery reviews, 1997. **23**(1): p. 221-227.
137. Berthod, A. and C. Garcia-Alvarez-Coque, *Micellar liquid chromatography*. 2000: CRC Press.
138. Hernández, M.J.M. and M.C.G. Alvarez-Coque, *Solute–mobile phase and solute–stationary phase interactions in micellar liquid chromatography. A review.* Analyst, 1992. **117**(5): p. 831-837.
139. Kanakaiah, B., *Micellar Liquid Chromatography.* International Journal of Bio-Pharma Research, 2013. **2**(04): p. 117-122.
140. López-Grío, S., J. Baeza-Baeza, and M. Garcia-Alvarez-Coque, *Influence of the addition of modifiers on solute-micelle interaction in hybrid micellar liquid chromatography.* Chromatographia, 1998. **48**(9-10): p. 655-663.
141. Murray, R. and G. Hartley, *Equilibrium between micelles and simple ions, with particular reference to the solubility of long-chain salts.* Trans. Faraday Soc., 1935. **31**: p. 183-189.
142. Mittal, K.L., *Solution chemistry of surfactants*. Vol. 1. 1979: Plenum Press New York.
143. Ruiz-Ángel, M., J.R. Torres-Lapasió, M. García-Álvarez-Coque, and S. Carda-Broch, *Submicellar and micellar reversed-phase liquid chromatographic modes applied to the separation of β-blockers.* Journal of Chromatography A, 2009. **1216**(15): p. 3199-3209.
144. Tehrani-Bagha, A.R. and K. Holmberg, *Solubilization of hydrophobic dyes in surfactant solutions.* Materials, 2013. **6**(2): p. 580-608.
145. Marina, M. and M. Garcia, *Micellar liquid chromatography.* Encyclopedia of separation science. Level II. Methods and instrumentation.–Elsevier, 2000: p. 729-737.
146. Rambla-Alegre, M., *Basic principles of MLC.* Chromatography Research International, 2012. **2012**.
147. Kalyankar, T., P. Kulkarni, S. Wadher, and S. Pekamwar, *Applications of Micellar Liquid Chromatography in Bioanalysis: A Review.* Journal of Applied Pharmaceutical Science, 2014. **4**(1).
148. Armstrong, D.W. and F. Nome, *Partitioning behavior of solutes eluted with micellar mobile phases in liquid chromatography.* Analytical Chemistry, 1981. **53**(11): p. 1662-1666.
149. Borgerding, M.F. and W.L. Hinze, *Characterization and evaluation of the use of nonionic polyoxyethylene (23) dodecanol micellar mobile phases in reversed-phase high-performance liquid chromatography.* Analytical Chemistry, 1985. **57**(12): p. 2183-2190.
150. Sehgal, P. and D.E. Otzen, *Thermodynamics of unfolding of an integral membrane protein in mixed micelles.* Protein science, 2006. **15**(4): p. 890-899.
151. Marina, M., O. Jimenez, M. García, and S. Vera, *Study of the separation selectivity of a group of benzene and naphthalene derivatives in micellar liquid chromatography.* Microchemical journal, 1996. **53**(2): p. 215-224.
152. Ruiz-Angel, M., S. Carda-Broch, J.R. Torres-Lapasió, and M. García-Álvarez-Coque, *Retention mechanisms in micellar liquid chromatography.* Journal of Chromatography A, 2009. **1216**(10): p. 1798-1814.
153. Garcia-Alvarez-Coque, M., J. Torres-Lapasió, and J. Baeza-Baeza, *Modelling of retention behaviour of solutes in micellar liquid chromatography.* Journal of Chromatography A, 1997. **780**(1): p. 129-148.

154. Arunyanart, M. and L.C. Love, *Model for micellar effects on liquid chromatography capacity factors and for determination of micelle-solute equilibrium constants.* Analytical Chemistry, 1984. **56**(9): p. 1557-1561.
155. Armstrong, D.W., *Micelles in separations: practical and theoretical review.* Separation and purification methods, 1985. **14**(2): p. 213-304.
156. Hinze, W.L. and D.W. Armstrong, *Ordered media in chemical separations.* 1987.
157. Dorsey, J.G., *Micellar liquid chromatography.* Adv. Chromatogr, 1987. **27**: p. 167-214.
158. Berthod, A. and J. Dorsey, *Micelles in mobile phases.* Analusis, 1988. **16**(2): p. 75-89.
159. Khaledi, M.G., *Micelles as separation media in high-performance liquid chromatography and high-performance capillary electrophoresis: overview and perspective.* Journal of Chromatography A, 1997. **780**(1): p. 3-40.
160. Okada, T., *Micellar chromatography of inorganic compounds.* Journal of Chromatography A, 1997. **780**(1): p. 343-360.
161. Ruiz-Ángel, M.J., M.C. García-Álvarez-Coque, and A. Berthod, *New insights and recent developments in micellar liquid chromatography.* Separation & Purification Reviews, 2009. **38**(1): p. 45-96.
162. He, Z., J. Sun, X. Wu, R. Lu, J. Liu, and Y. Wang, *Profiling drug membrane permeability and activity via biopartitioning chromatography.* Current drug metabolism, 2008. **9**(2): p. 152-166.
163. Escuder-Gilabert, L., M. Molero-Monfort, R. Villanueva-Camañas, S. Sagrado, and M. Medina-Hernández, *Potential of biopartitioning micellar chromatography as an in vitro technique for predicting drug penetration across the blood–brain barrier.* Journal of Chromatography B, 2004. **807**(2): p. 193-201.
164. Martın-Biosca, Y., M. Molero-Monfort, S. Sagrado, R. Villanueva-Camañas, and M. Medina-Hernández, *Rapid in vitro test to predict ocular tissue permeability based on biopartitioning micellar chromatography.* European journal of pharmaceutical sciences, 2003. **20**(2): p. 209-216.
165. Martínez-Pla, J., Y. Martín-Biosca, S. Sagrado, R. Villanueva-Camañas, and M. Medina-Hernández, *Biopartitioning micellar chromatography to predict skin permeability.* Biomedical Chromatography, 2003. **17**(8): p. 530-537.
166. Molero-Monfort, M., Y. Martín-Biosca, S. Sagrado, R. Villanueva-Camañas, and M. Medina-Hernández, *Micellar liquid chromatography for prediction of drug transport.* Journal of Chromatography A, 2000. **870**(1): p. 1-11.
167. Torres-Cartas, S., Y. Martín-Biosca, R. Villanueva-Camañas, S. Sagrado, and M. Medina-Hernández, *Biopartitioning micellar chromatography to predict mutagenicity of aromatic amines.* European journal of medicinal chemistry, 2007. **42**(11): p. 1396-1402.
168. Waters, L.J., Y. Shahzad, and J. Stephenson, *Modelling skin permeability with micellar liquid chromatography.* European Journal of Pharmaceutical Sciences, 2013. **50**(3): p. 335-340.
169. Escuder-Gilabert, L., J. Martınez-Pla, S. Sagrado, R. Villanueva-Camañas, and M. Medina-Hernández, *Biopartitioning micellar separation methods: modelling drug absorption.* Journal of Chromatography B, 2003. **797**(1): p. 21-35.
170. Dorsey, J.G., M.T. DeEchegaray, and J.S. Landy, *Efficiency enhancement in micellar liquid chromatography.* Analytical Chemistry, 1983. **55**(6): p. 924-928.
171. Lavine, B.K. and S. Hendayana, *Band broadening in micellar liquid chromatography.* Journal of Liquid Chromatography & Related Technologies, 1996. **19**(1): p. 101-123.
172. Borgerding, M.F., W.L. Hinze, L.D. Stafford, G.W. Fulp Jr, and W.C. Hamlin Jr, *Investigations of stationary phase modification by the mobile phase surfactant in micellar liquid chromatography.* Analytical Chemistry, 1989. **61**(13): p. 1353-1358.
173. Armstrong, D.W. and T.J. Ward, *Micellar effects on molecular diffusion: theoretical and chromatographic considerations.* Analytical Chemistry, 1986. **58**(3): p. 579-582.
174. Berthod, A. and A. Roussel, *The rôle of the stationary phase in micellar liquid chromatography: Adsorption and efficiency.* Journal of Chromatography A, 1988. **449**: p. 349-360.

175. Yarmchuk, P., R. Weinberger, R.F. Hirsch, and L. Cline Love, *Effects of restricted mass transfer on the efficiency of micellar chromatography.* Journal of Chromatography A, 1984. **283**: p. 47-60.
176. Madenci, D. and S. Egelhaaf, *Self-assembly in aqueous bile salt solutions.* Current Opinion in Colloid & Interface Science, 2010. **15**(1): p. 109-115.
177. Radulescu, M., V. Voicu, A. Medvedovici, and V. David, *Retention study of some cation-type compounds using bile acid sodium salts as ion pairing agents in liquid chromatography.* Biomedical Chromatography, 2011. **25**(8): p. 873-878.
178. Verde, A.V. and D. Frenkel, *Simulation study of micelle formation by bile salts.* Soft Matter, 2010. **6**(16): p. 3815-3825.
179. Takeuchi, T., J. Chu, and T. Miwa, *Bile acids as stationary phase in liquid chromatography.* Chromatographia, 1998. **47**(3-4): p. 183-188.
180. Carey, M.C. and D.M. Small, *Micelle formation by bile salts: physical-chemical and thermodynamic considerations.* Archives of internal medicine, 1972. **130**(4): p. 506-527.
181. Oakenfull, D. and L. Fisher, *The role of hydrogen bonding in the formation of bile salt micelles.* The Journal of Physical Chemistry, 1977. **81**(19): p. 1838-1841.
182. Kawamura, H., Y. Murata, T. Yamaguchi, H. Igimi, M. Tanaka, G. Sugihara, and J.P. Kratohvil, *Spin-label studies of bile salt micelles.* Journal of Physical Chemistry, 1989. **93**(8): p. 3321-3326.
183. Warren, D.B., D.K. Chalmers, K. Hutchison, W. Dang, and C.W. Pouton, *Molecular dynamics simulations of spontaneous bile salt aggregation.* Colloids and Surfaces A: Physicochemical and Engineering Aspects, 2006. **280**(1): p. 182-193.
184. http://www.drugbank.ca/, December, 2014.
185. Pyell, U., *Electrokinetic chromatography: theory, instrumentation and applications*. 2007: John Wiley & Sons.
186. Vadnere, M. and S. Lindenbaum, *Distribution of bile salts between 1-octanol and aqueous buffer.* Journal of pharmaceutical sciences, 1982. **71**(8): p. 875-881.
187. Deutscher, M.P., *Guide to protein purification*. Vol. 182. 1990: Gulf Professional Publishing.
188. Hélix-Nielsen, C., *Biomimetic membranes for sensor and separation applications*. 2012: Springer Science & Business Media.
189. Armarego, W.L., *Purification of laboratory chemicals*. 2017: Butterworth-Heinemann.
190. Frazier, R.A., H. Nursten, and J.M. Ames, *Capillary electrophoresis for food analysis: method development*. 2000: Royal Society of Chemistry.
191. Nair, P., D. Kritchevsky, and K. Setchell, *The bile acids: chemistry, physiology and metabolism.* 1971: p. 317.
192. Reis, S., C.G. Moutinho, C. Matos, B. de Castro, P. Gameiro, and J.L. Lima, *Noninvasive methods to determine the critical micelle concentration of some bile acid salts.* Analytical biochemistry, 2004. **334**(1): p. 117-126.
193. Moffat, A.C., M.D. Osselton, B. Widdop, and J. Watts, *Clarke's analysis of drugs and poisons*. 2011: Pharmaceutical Press.
194. Pramauro, E., C. Minero, G. Saini, R. Graglia, and E. Pelizzetti, *Partition equilibria of phenols between water and anionic micelles: Correlation with the octanol/water system.* Analytica Chimica Acta, 1988. **212**: p. 171-180.
195. Khaledi, M.G., *Hydrophobic selectivity in micellar and hydro-organic reversed-phase liquid chromatography.* Analytical Chemistry, 1988. **60**(9): p. 876-887.
196. Khaledi, M.G., E. Peuler, and J. Ngeh-Ngwainbi, *Retention behavior of homologous series in reversed-phase liquid chromatography using micellar, hydro organic, and hybrid mobile phases.* Analytical Chemistry, 1987. **59**(23): p. 2738-2747.
197. Torres-Lapasió, J., J. Baeza-Baeza, and M. Garcia-Alvarez-Coque, *On the measurement of dead time in micellar liquid chromatography.* Journal of liquid chromatography & related technologies, 1996. **19**(8): p. 1205-1228.

198. Lavine, B.K., S. Hendayana, Y. He, and W.T. Cooper, *Solid-state NMR studies of ionic surfactants adsorbed on cyanopropyl bonded phases: implications for micellar liquid chromatography.* Journal of colloid and interface science, 1996. **179**(2): p. 341-349.
199. Waters, L.J. and B. Kasprzyk-Hordern, *Micellar chromatographic determination of partition coefficients and associated thermodynamic data for pharmaceutical compounds.* Journal of thermal analysis and calorimetry, 2010. **102**(1): p. 343-347.
200. Olesen, N.E., P. Westh, and R. Holm, *Determination of thermodynamic potentials and the aggregation number for micelles with the mass-action model by isothermal titration calorimetry: A case study on bile salts.* Journal of colloid and interface science, 2015. **453**: p. 79-89.
201. Armstrong, D.W. and F. Nome, *Partitioning behavior of solutes eluted with micellar mobile phases in liquid chromatography.* Anal. Chem, 1981. **53**(11): p. 1662-1666.
202. Arunyanart, M. and L.C. Love, *Determination of drugs in untreated body fluids by micellar chromatography with fluorescence detection.* Journal of Chromatography B: Biomedical Sciences and Applications, 1985. **342**: p. 293-301.
203. Atwood, D. and A. Florence, *Surfactant systems.* Surfactant Systems, 1983: p. 698.
204. Olejnik, A., R. Marecik, M. Skrzypczak, K. Czaczyk, and W. Grajek, *Application of rapid Caco-2 cell culture system in the studies on the bacterial adhesion and transepithelial transport.* Polish Journal of Food and Nutrition Sciences, 2008. **58**(3).
205. Castillo-Garit, J., Y. Cañizares-Carmenate, Y. Marrero-Ponce, C. Abad, and F. Torrens, *Prediction of ADME properties, part 1: classification models to predict Caco-2 cell permeability using atom-based bilinear indices.* Afinidad, 2014. **71**(566).
206. Hou, T., J. Wang, W. Zhang, and X. Xu, *ADME evaluation in drug discovery. 7. Prediction of oral absorption by correlation and classification.* Journal of chemical information and modeling, 2007. **47**(1): p. 208-218.
207. Paixão, P., L.F. Gouveia, and J.A. Morais, *Prediction of the human oral bioavailability by using in vitro and in silico drug related parameters in a physiologically based absorption model.* International journal of pharmaceutics, 2012. **429**(1): p. 84-98.
208. Balon, K., B. Riebesehl, and B. Müller, *Drug liposome partitioning as a tool for the prediction of human passive intestinal absorption.* Pharmaceutical research, 1999. **16**(6): p. 882-888.
209. Varma, M.V., K. Sateesh, and R. Panchagnula, *Functional role of P-glycoprotein in limiting intestinal absorption of drugs: contribution of passive permeability to P-glycoprotein mediated efflux transport.* Molecular pharmaceutics, 2005. **2**(1): p. 12-21.
210. Molero-Monfort, M., L. Escuder-Gilabert, R. Villanueva-Camanas, S. Sagrado, and M. Medina-Hernández, *Biopartitioning micellar chromatography: an in vitro technique for predicting human drug absorption.* Journal of Chromatography B: Biomedical Sciences and Applications, 2001. **753**(2): p. 225-236.
211. Norinder, U., T. Österberg, and P. Artursson, *Theoretical calculation and prediction of intestinal absorption of drugs in humans using MolSurf parametrization and PLS statistics.* European journal of pharmaceutical sciences, 1999. **8**(1): p. 49-56.
212. Raevsky, O.A., V.I. Fetisov, E.P. Trepalina, J.W. McFarland, and K.J. Schaper, *Quantitative Estimation of Drug Absorption in Humans for Passively Transported Compounds on the Basis of Their Physico-chemical Parameters.* Quantitative Structure-Activity Relationships, 2000. **19**(4): p. 366-374.
213. Zhao, Y.H., M.H. Abraham, J. Le, A. Hersey, C.N. Luscombe, G. Beck, B. Sherborne, and I. Cooper, *Rate-limited steps of human oral absorption and QSAR studies.* Pharmaceutical research, 2002. **19**(10): p. 1446-1457.
214. Stępnik, K.E., I. Malinowska, and E. Rój, *in vitro and in silico determination of oral, jejunum and Caco-2 human absorption of fatty acids and polyphenols. Micellar liquid chromatography.* Talanta, 2014. **130**: p. 265-273.
215. Avdeef, A., *Absorption and drug development: solubility, permeability, and charge state*. 2012: John Wiley & Sons.

216. Subramanian, G. and D.B. Kitchen, *Computational approaches for modeling human intestinal absorption and permeability.* Journal of molecular modeling, 2006. **12**(5): p. 577-589.
217. Ponce, Y.M., M.A.C. Pérez, V.R. Zaldivar, E. Ofori, and L.A. Montero, *Total and local quadratic indices of the "molecular pseudograph's atom adjacency matrix". application to prediction of caco-2 permeability of drugs.* International Journal of Molecular Sciences, 2003. **4**(8): p. 512-536.
218. http://www.chemspider.com/, December, 2014.
219. https://pubchem.ncbi.nlm.nih.gov/, December, 2014.
220. Rhodes, H., J. DeNardo, D. Bode, and M. Blake, *Differentiating nonaqueous titration of aspirin, acetaminophen, and salicylamide mixtures.* Journal of pharmaceutical sciences, 1975. **64**(8): p. 1386-1388.
221. Schanker, L.S., P.A. Shore, B.B. Brodie, and C.A.M. Hogben, *Absorption of drugs from the stomach I. The rat.* Journal of Pharmacology and Experimental Therapeutics, 1957. **120**(4): p. 528-539.
222. Martin, A., *Physical pharmacy: Physical chemical principles in the pharmaceutical sciences*. 2nd ed. ed. 1969, Philadelphia: Lea & Febiger.
223. information, U.p., 1975.
224. NARAHASHI, T., D.T. FRAZIER, and M. YAMADA, *The site of action and active form of local anesthetics. I. Theory and pH experiments with tertiary compounds.* Journal of Pharmacology and Experimental Therapeutics, 1970. **171**(1): p. 32-44.
225. Stella, V. and J. Pipkin, *Phenylbutazone ionization kinetics.* Journal of pharmaceutical sciences, 1976. **65**(8): p. 1161-1165.
226. Kim, C.-j., *Advanced pharmaceutics: physicochemical principles*. 2004: CRC Press.
227. Kolthoff, I.M. and V.A. Stenger, *Volumetric Analysis Vol 1: With 31 Illustrations Vol-1*. 1942: Interscience Publishers; New York.
228. Ballard, B.E. and E. Nelson, *Physicochemical properties of drugs that control absorption rate after subcutaneous implantation.* Journal of Pharmacology and Experimental Therapeutics, 1962. **135**(1): p. 120-127.
229. Helenius, A. and K. Simons, *Solubilization of membranes by detergents.* Biochimica et Biophysica Acta (BBA)-Reviews on Biomembranes, 1975. **415**(1): p. 29-79.
230. Yan, A., Z. Wang, and Z. Cai, *Prediction of human intestinal absorption by GA feature selection and support vector machine regression.* International journal of molecular sciences, 2008. **9**(10): p. 1961-1976.
231. Deconinck, E., H. Ates, N. Callebaut, E. Van Gyseghem, and Y. Vander Heyden, *Evaluation of chromatographic descriptors for the prediction of gastro-intestinal absorption of drugs.* Journal of Chromatography A, 2007. **1138**(1): p. 190-202.
232. Patist, A., S. Bhagwat, K. Penfield, P. Aikens, and D. Shah, *On the measurement of critical micelle concentrations of pure and technical-grade nonionic surfactants.* Journal of Surfactants and Detergents, 2000. **3**(1): p. 53-58.
233. Zhang, X., J.K. Jackson, and H.M. Burt, *Determination of surfactant critical micelle concentration by a novel fluorescence depolarization technique.* Journal of biochemical and biophysical methods, 1996. **31**(3): p. 145-150.
234. Sakhawat, S.S., *Effect of Temperature and Aprotic Solvents on the CMC of Sodium Dodecyl Sulphate*, in *Interactions of Water in Ionic and Nonionic Hydrates*. 1987, Springer. p. 251-255.
235. Bjergegaard, C., S. Michaelsen, P. Møller, and H. Sørensen, *Separation of desulphoglucosinolates by micellar electrokinetic capillary chromatography based on a bile salt.* Journal of Chromatography A, 1995. **717**(1-2): p. 325-333.
236. Willmann, S., W. Schmitt, J. Keldenich, J. Lippert, and J.B. Dressman, *A physiological model for the estimation of the fraction dose absorbed in humans.* Journal of medicinal chemistry, 2004. **47**(16): p. 4022-4031.
237. Monograph, P., *Diflucan (fluconazole).* Pfizer Canada Inc, 2004.

238. Roda, A., A.F. Hofmann, and K.J. Mysels, *The influence of bile salt structure on self-association in aqueous solutions.* Journal of Biological Chemistry, 1983. **258**(10): p. 6362-6370.
239. Natalini, B., R. Sardella, A. Gioiello, F. Ianni, A. Di Michele, and M. Marinozzi, *Determination of bile salt critical micellization concentration on the road to drug discovery.* Journal of pharmaceutical and biomedical analysis, 2014. **87**: p. 62-81.
240. Wiedmann, T.S., W. Liang, and L. Kamel, *Solubilization of drugs by physiological mixtures of bile salts.* Pharmaceutical research, 2002. **19**(8): p. 1203-1208.
241. Cheng, C.-Y., H. Oh, T.-Y. Wang, S.R. Raghavan, and S.-H. Tung, *Mixtures of lecithin and bile salt can form highly viscous wormlike micellar solutions in water.* Langmuir, 2014. **30**(34): p. 10221-10230.
242. Malik, N.A., *Solubilization and Interaction Studies of Bile Salts with Surfactants and Drugs: a Review.* Applied biochemistry and biotechnology, 2016. **179**(2): p. 179-201.
243. Dressman, J., G. Amidon, and D. Fleisher, *Absorption potential: estimating the fraction absorbed for orally administered compounds.* Journal of pharmaceutical sciences, 1985. **74**(5): p. 588-589.
244. Linnankoski, J., J.M. Mäkelä, V.-P. Ranta, A. Urtti, and M. Yliperttula, *Computational prediction of oral drug absorption based on absorption rate constants in humans.* Journal of medicinal chemistry, 2006. **49**(12): p. 3674-3681.
245. Veber, D.F., S.R. Johnson, H.-Y. Cheng, B.R. Smith, K.W. Ward, and K.D. Kopple, *Molecular properties that influence the oral bioavailability of drug candidates.* Journal of medicinal chemistry, 2002. **45**(12): p. 2615-2623.
246. Newby, D., A.A. Freitas, and T. Ghafourian, *Decision trees to characterise the roles of permeability and solubility on the prediction of oral absorption.* European journal of medicinal chemistry, 2015. **90**: p. 751-765.
247. Raevsky, O.A., *Physicochemical descriptors in property-based drug design.* Mini reviews in medicinal chemistry, 2004. **4**(10): p. 1041-1052.
248. Grès, M.-C., B. Julian, M. Bourrié, V. Meunier, C. Roques, M. Berger, X. Boulenc, Y. Berger, and G. Fabre, *Correlation between oral drug absorption in humans, and apparent drug permeability in TC-7 cells, a human epithelial intestinal cell line: comparison with the parental Caco-2 cell line.* Pharmaceutical research, 1998. **15**(5): p. 726-733.
249. Obata, K., K. Sugano, R. Saitoh, A. Higashida, Y. Nabuchi, M. Machida, and Y. Aso, *Prediction of oral drug absorption in humans by theoretical passive absorption model.* International journal of pharmaceutics, 2005. **293**(1): p. 183-192.
250. Newby, D.A., *Data mining methods for the prediction of intestinal absorption using QSAR*. 2014, University of Kent, University of Greenwich. Retrieved from https://kar. kent. ac. uk/47600/1/DNEWBY_Thesis_FINAL_Nov14. pdf.
251. Anslyn, E.V. and D.A. Dougherty, *Modern physical organic chemistry*. 2006: University Science Books.
252. Chu, K.A., *Predicting Passive Intestinal Drug Absorption: An Interesting Relationship between Fraction Absorbed and Melting Point.* 2009.
253. Bui, H.H., *Thermodynamic Study and Prediction of Solute Partitioning into Micelles and Liposomes Using Electrokinetic Chromatography.* 2004.
254. Chester, T.L. and J.W. Coym, *Effect of phase ratio on van't Hoff analysis in reversed-phase liquid chromatography, and phase-ratio-independent estimation of transfer enthalpy.* Journal of Chromatography A, 2003. **1003**(1): p. 101-111.
255. Knox, J.H. and G. Vasvari, *The performance of packings in high-speed liquid chromatography: III. Chemically bonded pellicular materials.* Journal of Chromatography A, 1973. **83**: p. 181-194.
256. Quach, V., *Evaluation of polar-embedded reversed-phase liquid chromatography columns and the temperature dependence of the phase ratio*. 2009: THE FLORIDA STATE UNIVERSITY.

257. Melander, W., D.E. Campbell, and C. Horváth, *Enthalpy—entropy compensation in reversed-phase chromatography.* Journal of Chromatography A, 1978. **158**: p. 215-225.
258. Waters, L., S. Leharne, J. Mitchell, and J. Hanrahan, *Determination of micelle/water partition coefficients and associated thermodynamic data for dialkyl phthalate esters.* Journal of Thermal Analysis and Calorimetry, 2007. **90**(1): p. 283-288.
259. Berthod, A., I. Girard, and C. Gonnet, *Micellar liquid chromatography, adsorption isotherms of two ionic surfactants on five stationary phases.* Analytical Chemistry, 1986. **58**(7): p. 1356-1358.
260. Cole, L.A. and J.G. Dorsey, *Temperature dependence of retention in reversed-phase liquid chromatography. 1. Stationary-phase considerations.* Analytical chemistry, 1992. **64**(13): p. 1317-1323.
261. Gill, S., N. Nichols, and I. Wadsö, *Calorimetric determination of enthalpies of solution of slightly soluble liquids II. Enthalpy of solution of some hydrocarbons in water and their use in establishing the temperature dependence of their solubilities.* The Journal of Chemical Thermodynamics, 1976. **8**(5): p. 445-452.
262. Liu, Y., N. Grinberg, K. Thompson, R. Wenslow, U. Neue, D. Morrison, T. Walter, J. O'Gara, and K. Wyndham, *Evaluation of a C18 hybrid stationary phase using high-temperature chromatography.* Analytica chimica acta, 2005. **554**(1): p. 144-151.
263. Bidlingmeyer, B.A. and J. Henderson, *Investigation of retention on bare silica using reversed-phase mobile phases at elevated temperatures.* Journal of Chromatography A, 2004. **1060**(1): p. 187-193.
264. Taft, R. and M.J. Kamlet, *The solvatochromic comparison method. 2. The. alpha.-scale of solvent hydrogen-bond donor (HBD) acidities.* Journal of the American Chemical Society, 1976. **98**(10): p. 2886-2894.
265. Vitha, M.F., J.D. Weckwerth, K. Odland, V. Dema, and P.W. Carr, *Study of the Polarity and Hydrogen Bond Ability of Sodium Dodecyl Sulfate Micelles by the Kamlet− Taft Solvatochromic Comparison Method.* The Journal of Physical Chemistry, 1996. **100**(48): p. 18823-18828.
266. Vitha, M.F. and P.W. Carr, *Study of the Polarity and Hydrogen-Bond Ability of Dodecyltrimethylammonium Bromide Micelles by the Kamlet− Taft Solvatochromic Comparison Method.* The Journal of Physical Chemistry B, 1998. **102**(11): p. 1888-1895.
267. Boysen, R.I., A.J. Jong, J.A. Wilce, G.F. King, and M.T. Hearn, *Role of interfacial hydrophobic residues in the stabilization of the leucine zipper structures of the transcription factors c-Fos and c-Jun.* Journal of Biological Chemistry, 2002. **277**(1): p. 23-31.
268. Fisicaro, E., C. Compari, E. Duce, M. Biemmi, M. Peroni, and A. Braibanti, *Thermodynamics of micelle formation in water, hydrophobic processes and surfactant self-assemblies.* Physical Chemistry Chemical Physics, 2008. **10**(26): p. 3903-3914.
269. Lee, H.K. and N.E. Hoffman, *Effect of temperature on the retention of simple organic compounds in ion-exchange HPLC.* Journal of chromatographic science, 1994. **32**(3): p. 97-101.
270. Akamatsu, M., Y. Yoshida, H. Nakamura, M. Asao, H. Iwamura, and T. Fujita, *Hydrophobicity of Di-and Tripeptides Having Unionizable Side Chains and Correlation with Substituent and Structural Parameters.* Molecular Informatics, 1989. **8**(3): p. 195-203.
271. Mithani, S.D., V. Bakatselou, C.N. TenHoor, and J.B. Dressman, *Estimation of the increase in solubility of drugs as a function of bile salt concentration.* Pharmaceutical research, 1996. **13**(1): p. 163-167.
272. Pedersen, B.L., H. Brøndsted, H. Lennernäs, F.N. Christensen, A. Müllertz, and H.G. Kristensen, *Dissolution of hydrocortisone in human and simulated intestinal fluids.* Pharmaceutical research, 2000. **17**(2): p. 183-189.

273. Pedersen, B.L., A. Müllertz, H. Brøndsted, and H.G. Kristensen, *A comparison of the solubility of danazol in human and simulated gastrointestinal fluids.* Pharmaceutical research, 2000. **17**(7): p. 891-894.
274. Casabianca, L.B. and A.C. de Dios, *13C NMR study of the self-association of chloroquine, amodiaquine, and quinine.* The Journal of Physical Chemistry A, 2004. **108**(40): p. 8505-8513.
275. Sanghvi, T., N. Ni, M. Mayersohn, and S.H. Yalkowsky, *Predicting passive intestinal absorption using a single parameter.* QSAR & Combinatorial Science, 2003. **22**(2): p. 247-257.
276. Palm, K., P. Stenberg, K. Luthman, and P. Artursson, *Polar molecular surface properties predict the intestinal absorption of drugs in humans.* Pharmaceutical Research, 1997. **14**(5): p. 568-571.
277. Castillo-Garit, J.A., Y. Marrero-Ponce, F. Torrens, and R. García-Domenech, *Estimation of ADME properties in drug discovery: Predicting Caco-2 cell permeability using atom-based stochastic and non-stochastic linear indices.* Journal of pharmaceutical sciences, 2008. **97**(5): p. 1946-1976.
278. Mandagere, A.K., T.N. Thompson, and K.-K. Hwang, *Graphical model for estimating oral bioavailability of drugs in humans and other species from their Caco-2 permeability and in vitro liver enzyme metabolic stability rates.* Journal of medicinal chemistry, 2002. **45**(2): p. 304-311.
279. Kazakevich, Y.V. and R. Lobrutto, *HPLC for pharmaceutical scientists*. 2007: John Wiley & Sons.
280. Parrott, N. and T. Lavé, *Prediction of intestinal absorption: comparative assessment of gastroplus™ and idea™.* European journal of pharmaceutical sciences, 2002. **17**(1): p. 51-61.
281. Sugano, K., Y. Nabuchi, M. Machida, and Y. Aso, *Prediction of human intestinal permeability using artificial membrane permeability.* International journal of pharmaceutics, 2003. **257**(1): p. 245-251.
282. Shayanfar, A., S. Velaga, and A. Jouyban, *Solubility of carbamazepine, nicotinamide and carbamazepine–nicotinamide cocrystal in ethanol–water mixtures.* Fluid Phase Equilibria, 2014. **363**: p. 97-105.
283. http://www.pharminfotech.co.nz/manual/Formulation/mixtures/fluconazole.html, April, 2015.
284. http://www.chemicalbook.com/ProductMSDSDetailCB9154247_EN.htm, April, 2015.
285. https://comptox.epa.gov/dashboard/dsstoxdb/results?search=DTXSID1045166#toxval, April, 2015.
286. Sun, X., X. Xin, N. Tang, L. Guo, L. Wang, and G. Xu, *Manipulation of the gel behavior of biological surfactant sodium deoxycholate by amino acids.* The Journal of Physical Chemistry B, 2014. **118**(3): p. 824-832.
287. Murata, Y., G. Sugihara, K. Fukushima, M. Tanaka, and K. Matsushita, *Study of the micelle formation of sodium deoxycholate. Concentration dependence of carbon-13 nuclear magnetic resonance chemical shift.* The Journal of Physical Chemistry, 1982. **86**(24): p. 4690-4694.
288. Yan, Q., *Membrane transporters: methods and protocols*. Vol. 227. 2003: Springer Science & Business Media.
289. Addicks, W.J., G.L. Flynn, and N. Weiner, *Validation of a flow-through diffusion cell for use in transdermal research.* Pharmaceutical research, 1987. **4**(4): p. 337-341.
290. Shah, V.P., H.I. Maibach, and J. Jenner, *Topical drug bioavailability, bioequivalence, and penetration*. 1993: Springer.
291. Rosen, M., *Delivery system handbook for personal care and cosmetic products: technology, applications and formulations*. 2005: William Andrew.
292. Moss, G.P., D.R. Gullick, and S.C. Wilkinson, *Predictive Methods in Percutaneous Absorption*. 2015: Springer.
293. Inc., P. *Diffusion Testing Fundamentals*.

294. Musther, H., A. Olivares-Morales, O.J. Hatley, B. Liu, and A.R. Hodjegan, *Animal versus human oral drug bioavailability: Do they correlate?* European Journal of Pharmaceutical Sciences, 2014. **57**: p. 280-291.
295. Sinkó, B., T.M. Garrigues, G.T. Balogh, Z.K. Nagy, O. Tsinman, A. Avdeef, and K. Takács-Novák, *Skin–PAMPA: A new method for fast prediction of skin penetration.* European Journal of Pharmaceutical Sciences, 2012. **45**(5): p. 698-707.
296. Janssen, P.A., C. Van De Westeringh, A.H. Jageneau, P.J. Demoen, B.K. Hermans, G.H. Van Daele, K.H. Schellekens, C.A. Van Der Eycken, and C.J. Niemegeers, *Chemistry and pharmacology of CNS depressants related to 4-(4-hydroxy-4-phenylpiperidino) butyrophenone. Part I: Synthesis and screening data in mice.* J. med. pharm. Chem, 1959. **1**: p. 281-297.
297. Patel, S.R., H. Zhong, A. Sharma, and Y.N. Kalia, *Controlled non-invasive transdermal iontophoretic delivery of zolmitriptan hydrochloride in vitro and in vivo.* European Journal of Pharmaceutics and Biopharmaceutics, 2009. **72**(2): p. 304-309.
298. Mensch, J., A. Melis, C. Mackie, G. Verreck, M.E. Brewster, and P. Augustijns, *Evaluation of various PAMPA models to identify the most discriminating method for the prediction of BBB permeability.* European Journal of Pharmaceutics and Biopharmaceutics, 2010. **74**(3): p. 495-502.

Appendix A

Appendix A

Peer reviewed publications

1- Predicting human intestinal absorption in the presence of bile salt with micellar liquid chromatography.
Laura J. Waters, Dina S. Shokry and Gareth M. B. Parkes, Journal of Biomedical Chromatography, 30(10): 1618-1624, 2016.

2- The use of bile salt micelles for the prediction of human intestinal absorption.
Laura J. Waters, Dina S. Shokry, Gareth M.B. Parkes, John C. Mitchell, Journal of Pharmaceutical Sciences, 105: 3611-3614, 2016.

3- Formation of bile salt gel and permeation analysis to predict human intestinal absorption.
Laura J. Waters, Dina S. Shokry and Gareth M. B. Parkes. (In preparation).

4- Incorporating physiologically relevant mobile phases in micellar liquid chromatography for the prediction of human intestinal absorption.
Laura J. Waters, Dina S. Shokry and Gareth M. B. Parkes. (In preparation).

Oral presentations

1- A novel analytical technique for prediction of human intestinal, APS UKPharmSci (7th - 9th September 2015), East Midlands Conference Centre, University of Nottingham, UK.

2- Bile salt: a biosurfactant or a pharmacokinetic predictive tool?, World congress on Chromatography (7th – 9th August 2017), Rome, Italy.

Poster presentations

1- A novel analytical technique for prediction of human intestinal, APS UKPharmSci (7th - 9th September 2015), East Midlands Conference Centre, University of Nottingham, UK.

2- Micellar liquid chromatography as an alternative for *in vivo* and expensive *in vitro* tests commonly used in prediction of human intestinal absorption, 19th European Congress on Alternatives to Animal Testing & 16th Annual Congress of EUSAAT (2015), Linz, Austria.

3- Expansion of micellar liquid chromatography: from transdermal permeability to bile salts studies, 54th Annual Eastern Analytical Symposium, (16-18 Nov, 2015), Somerset, New Jersey.

4- MLC and spectrophotometry as an effective tool in the prediction of human intestinal absorption, World Congress on Chromatography (2016), Hoofdorpp, Netherlands.
5- MLC: An effective tool for prediction of human intestinal absorption, University of Huddersfield PGR conference (2016), University of Huddersfield, Huddersfield, UK.

Research article

Biomedical Chromatography

Received: 1 December 2015, Revised: 22 February 2016, Accepted: 29 March 2016 Published online in Wiley Online Library

(wileyonlinelibrary.com) DOI 10.1002/bmc.3731

Predicting human intestinal absorption in the presence of bile salt with micellar liquid chromatography

Laura J. Waters*, Dina S. Shokry and Gareth M.B. Parkes

ABSTRACT: Understanding intestinal absorption for pharmaceutical compounds is vital to estimate the bioavailability and therefore the *in vivo* potential of a drug. This study considers the application of micellar liquid chromatography (MLC) to predict passive intestinal absorption with a selection of model compounds. MLC is already known to aid prediction of absorption using simple surfactant systems; however, with this study the focus was on the presence of a more complex, bile salt surfactant, as would be encountered in the *in vivo* environment. As a result, MLC using a specific bile salt has been confirmed as an ideal *in vitro* system to predict the intestinal permeability for a wide range of drugs, through the development of a quantitative partition–absorption relationship. MLC offers many benefits including environmental, economic, time-saving and ethical advantages compared with the traditional techniques employed to obtain passive intestinal absorption values. Copyright © 2016 John Wiley & Sons, Ltd.

Keywords: intestinal absorption; chromatography; MLC; micellar; bile salts

Introduction

The most favourable option for drug administration is the oral route, accounting for the majority of pharmaceutical formulations on the market. A large percentage of these products are absorbed within the gastrointestinal (GI) tract, thus it is essential to quantify the extent of absorption to predict bioavailability. Most new chemical entities intended for oral administration are within Class II or IV of the Biopharmaceutics Classification System, that is, of low aqueous solubility (Williams *et al.*, 2013). As a result these compounds tend to exhibit poor bioavailability which can be problematic for development. Facilitating the prediction of drug absorption is therefore fundamental to maximize potential bioavailability, and consequently, efficacy of a new chemical entity.

Traditionally, *in vivo* performance following oral administration has been predicted using animal models. In recent years this has been less favourable for reasons including interspecies variability (Martignoni *et al.*, 2006), substantial economic costs and ethical considerations (Zurlo and Hutchinson, 2014). For these reasons research has focused on the development of alternatives to such models. One of the most widely researched *in vitro* methods to simulate *in vivo* performance is the application of dissolution studies in biorelevant media (Berthelsen *et al.*, 2014). It is believed that the use of physiologically relevant media is crucial as the components present, for example bile salts, are present in intestinal fluids, allowing a closer replication of the *in vivo* scenario (Tomaszewska *et al.*, 2013). The composition of GI fluids is well characterized with respect to pH, buffer capacity, osmolarity, surface tension and lipid concentration under fasted and fed conditions. Numerous studies have confirmed the relationship between the impact of these properties through preformulation studies, allowing an estimation of the fraction of drug absorbed *in vivo* for orally administered compounds (Bergström *et al.*, 2014). However, some researchers have found that dissolution testing by itself may not be adequate and it may be more beneficial to undertake the simultaneous assessment of dissolution and permeation (Sugano *et al.*, 2010).

Another technique to predict *in vivo* permeability is the parallel artificial membrane permeability assay, also known as PAMPA. This assay has been used previously to predict permeability through a range of biological environments including skin (Ottaviani *et al.*, 2006), the blood–brain barrier (Di *et al.*, 2003) and the GI tract (Bujard *et al.*, 2014). Although it has been shown to be useful for *in vivo* prediction, PAMPA does have some limitations, for example unpredictable drug retention for highly lipophilic drugs (Bendels *et al.*, 2006) and a significant unstirred water layer (Avdeef *et al.*, 2004; Ruell *et al.*, 2003). Some of these challenges have been investigated in an attempt to overcome these difficulties to improve accuracy and precision with a degree of success in certain aspects (Buckley *et al.*, 2012).

Many researchers consider the 'gold standard' for predicting intestinal absorption to be the Caco-2 model (Wuyts *et al.*, 2015). This is a cell culture model consisting of monolayers cultivated on permeable growth inserts. Such models exhibit structural and biological properties similar to those *in vivo* with the expression of appropriate enzymes, conferring their suitability as a model system. However, cellular models are renowned for their limited reproducibility, extensive culturing requirements and economic cost (Buckley *et al.*, 2012). Some research has attempted to enhance the biorelevance of permeability data, for example by using

* Correspondence to: L. J. Waters, School of Applied Sciences, University of Huddersfield, Queensgate, Huddersfield, HD1 3DH, UK. Email: l.waters@hud.ac.uk

School of Applied Sciences, University of Huddersfield, Queensgate, Huddersfield HD1 3DH, UK

Abbreviations used: CMC, critical micellar concentration; GI, gastrointestinal; HIA%, human intestinal absorption values; MLC, micellar liquid chromatography; NaDC, sodium deoxycholate

Journal of Pharmaceutical Sciences 105 (2016) 3611-3614

Contents lists available at ScienceDirect

Journal of Pharmaceutical Sciences

journal homepage: www.jpharmsci.org

Pharmaceutics, Drug Delivery and Pharmaceutical Technology

The Use of Bile Salt Micelles for the Prediction of Human Intestinal Absorption

Laura J. Waters [1,*], Dina S. Shokry [1], Gareth M.B. Parkes [1], John C. Mitchell [2]

[1] School of Applied Sciences, University of Huddersfield, Queensgate, Huddersfield HD1 3DH, UK
[2] Faculty of Engineering and Science, Medway Centre for Formulation Science, University of Greenwich, Chatham, Kent ME4 4TB, UK

ARTICLE INFO

Article history:
Received 11 August 2016
Revised 12 September 2016
Accepted 12 September 2016
Available online 21 October 2016

Keywords:
human intestinal absorption
HIA
solubilization
UV
bile salts

ABSTRACT

Human intestinal absorption (HIA) will dictate biopharmaceutical performance through its influence on absorption, distribution, metabolism, and elimination and can vary significantly depending upon the nature of the compound under consideration. In this study, an *in vitro* assay method is proposed for the prediction of HIA through the measurement of drug solubility in an aqueous phase containing micellar bile salt, namely sodium deoxycholate. A series of twenty compounds, displaying a range of physicochemical properties and known HIA values, were analyzed using UV spectroscopy to determine a solubilization ratio for each compound. A micelle/water partition coefficient ($K_{xm/a}$) was calculated and then used to develop an equation through simple linear regression; logit HIA $= -0.919 + 0.4618 \log K_{xm/a}$ ($R^2 = 0.85$). From this equation, a value for % HIA was determined which compared well with literature. Furthermore, 4 additional drugs were then analyzed using the developed equation and found to match well with literature, confirming the suitability of the method. Using a simple, economic, and robust UV bile salt assay allows prediction of HIA and avoids many of the disadvantages of other techniques, such as animal-based methods.

Introduction

Human intestinal absorption (HIA) is the mechanism through which drugs traverse from the intestine into the bloodstream. The vast majority of active pharmaceutical ingredients are administered orally; thus, it is essential that they are absorbed within the intestine to reach the intended site of action. Although it is possible to measure the percent HIA (% HIA) during clinical studies, it is far more useful to be able to predict the value much earlier on during drug development. It is for this reason that a significant amount of research has been undertaken in an attempt to develop a reliable, robust, and accurate method to predict % HIA.

Several different predictive approaches have been undertaken, including computational (*in silico*) methods,[1,2] such as quantitative structure-activity relationships[3,4] and physiologically based pharmacokinetic modelling.[5] These techniques have a clear advantage in that they remove the need for costly laboratory-based experimental measurement yet their predictive ability can be limited.

In vitro models for the prediction of absorption include the application of dissolution analysis,[6] chromatographic analysis,[7] and dynamic gastric models.[8] Many of these *in vitro* models have included the presence of physiologically relevant solvent compositions, mainly because it is known that solvent composition dictates intestinal drug solubility which, in turn, is an important factor in determining the rate, and extent, of absorption.[9] The specific components within human intestinal fluids that dramatically alter drug solubility are bile salts. The main biological function of bile salts is to solubilize lipids and vitamins in the intestine with a similar effect encountered for orally administered drugs. For a full review of the absorption-enhancing effects of bile salts.[10]

In humans, the composition of bile salts is rather complex and for the purposes of this study was simplified to consider 1 bile salt in particular, namely sodium deoxycholate (NaDC). NaDC is a well-characterized amphiphilic molecule which can undergo micellar aggregation,[11,12] stabilized by polar interactions,[13] with comparatively small aggregation numbers as a result of the rigid molecular structure.[14] Previous research within our group has shown that NaDC, when in the presence of drugs, will exhibit modified physicochemical properties, for example, a variable (drug-specific) reduction in critical micellar concentration.[15]

When quantifying (or comparing) enhancement in solubility for a specific drug, or series of drugs, it is possible to evaluate the solubilization ratio (SR), where SR is equal to the moles of drug solubilized per mole of bile salt. One study in particular calculated

* *Correspondence to:* Laura J. Waters (Telephone: 01484 472190).
E-mail address: l.waters@hud.ac.uk (L.J. Waters).

http://dx.doi.org/10.1016/j.xphs.2016.09.007
0022-3549/